EVERTON GERALDO DE MORAIS

BIOCHAR AND HUMIC SUBSTANCES-BASED FERTILIZERS: SYNTHESIS, CHARACTERIZATION AND AGRONOMIC USE

LAVRAS-MG
2022

EVERTON GERALDO DE MORAIS

BIOCHAR AND HUMIC SUBSTANCES-BASED FERTILIZERS: SYNTHESIS, CHARACTERIZATION AND AGRONOMIC USE

Thesis presented to the Federal University of Lavras, as part of the requirements of the Graduate Program in Soil Science, area of concentration in Soil Fertility and Plant Mineral Nutrition, to obtain the title of Doctor.

Carlos Alberto Silva, PhD
Advisor

Henrique José Guimarães Moreiral Maluf, PhD
Co-Advisor

LAVRAS-MG
2022

Ficha catalográfica elaborada pelo Sistema de Geração de Ficha Catalográfica da Biblioteca Universitária da UFLA, com dados informados pelo(a) próprio(a) autor(a).

Morais, Everton Geraldo de.
Biochar and humic substances-based fertilizers: Synthesis,characterization and agronomic use / Everton Geraldo de Morais. - 2022.
301 p. : il.

Orientador(a): Carlos Alberto Silva.

Tese (doutorado) - Universidade Federal de Lavras, 2022.
Bibliografia.

1. Fertilizantes. 2. Fertilidade do solo. 3. Nutrição de plantas. I. Silva, Carlos Alberto. II. Título.

EVERTON GERALDO DE MORAIS

BIOCHAR AND HUMIC SUBSTANCES-BASED FERTILIZERS: SYNTHESIS, CHARACTERIZATION AND AGRONOMIC USE

FERTILIZANTES A BASE DE BIOCARVÃO E SUBSTÂNCIAS HÚMICAS: SÍNTESE, CARACTERIZAÇÃO E USO AGRONÔMICO

Thesis presented to the Federal University of Lavras, as part of the requirements of the Graduate Program in Soil Science, area of concentration in Soil Fertility and Plant Mineral Nutrition, to obtain the title of Doctor.

APPROVED on July 26, 2022.

Dr. Cícero Célio Figueiredo	UnB
Dr. Guilherme Lopes	UFLA
Dr. Jader Galba Busato	UnB
Dr. Keiji Jindo	Wangeningen University

Carlos Alberto Silva, PhD
Advisor

Henrique José Guimarães Moreiral Maluf, PhD
Co-Advisor

LAVRAS-MG
2022

I dedicate the thesis to Jesus Christ for his sacrifice on the cross

ACKNOWLEDGMENTS

Firstly, I would like to thank God for everything in my life and Jesus Christ for his life ministryand sacrifice on the cross; without these, I would be a sheep without a fold.

I am thankful:

To my wife Débora, who, with much patience, sometimes stress, love, care and wisdom have always been and is by my side. I am very grateful to God for her life.

To my beloved children, Letícia and Levi, who teach me how to be a father. Beings so small but capable of occupying an ample space in my heart and life, I understand the meaning of sacrificial love.

To my parents, Baltazar and Ilma, for being my base during my life, people who shaped my character. I especially thank you for always believing in the potential of your children's education; without you getting here would not be possible. I extend this thanks to my brothers Herivelto, Wellington and Wanderson, who have been by my side on this journey.

To my church Vide-community of Faith, and especially to my friend and Pastor Davi.

To my advisor, Professor Carlos Alberto Silva, for the receptivity of this master's degree, partnership in so many works and the guidance and advice on our journey together.

To colleagues from the Laboratory for the Study of Soil Organic Matter (LEMOS-UFLA), Otávio, Murilo, Rimena, Igor, Gabrielly and Loren; especially to those closest to me during my journey in LEMOS-UFLA, Marina, Sara and Bruno; and to my personal friend Henrique, thank you for the conversations, partnerships in experiments, criticism, suggestions and teachings since the master's degree.

To the Coordenação de Aperfeiçoamento de Pessoal de Nível Superior (CAPES), the Conselho Nacional de Desenvolvimento Científico e Tecnológico (CNPq) (303899/2015-8 and 461935/2014-7 grants), and Fundação de Amparo à pesquisa de Minas Gerais (FAPEMIG) for granting a scholarship and funding for the Doctor's study.

To the Department of Soil Science at UFLA (DCS-UFLA). To the professors, laboratory technicians and employees for their help and other contributions to carrying out this work, especially to Geila, Dirce, José Roberto (Pezão), Lívia and Mariene.

To all those who, in some way, contributed to the completion of this work.

This study was financed in part by the Coordenação de Aperfeiçoamento de Pessoal de Nível Superior – Brasil (CAPES) – Finance Code 001"

THANK YOU!!!

For from him and through him and for him are all things. To him be the glory forever! Amen.

Romans 11:36

RESUMO GERAL

Fertilizantes organominerais (FOMs), comparado a fertilizantes minerais, podem ter maior valor agronômico para o cultivo de plantas em Latossolos. Várias rotas e matrizes podem ser utilizadas para sintetizar FOMs, incluindo o uso de ácidos húmicos (AH), compostos e biocarvão (pirólise). Análises químicas e espectroscópicas podem acessar formas e quantidades de nutrientes nos FOMs, e técnicas espectroscópicas, como a espectroscopia de infravermelho (IV), podem predizer os valores quantificados em análises químicas. Assim, o presente estudo usou diferentes rotas na síntese de FOMs, com base em Zn-AH, NPK-composto produzido por compostagem e NPK-biocarvão com maior valor agronômico comparado a fertilizantes minerais, e além disso usou o IV para predizer propriedades, formas e quantidades de nutrientes em NPK-FOMs. No primeiro estudo, a mistura de Zn e AH promoveu a complexação do Zn pelo AH; quando essas moléculas foram aplicadas via solo, em relação ao sulfato de Zn, houve aumento do Zn na solução do solo e aumento no crescimento e nutrição do milho seguido do cultivo de brachiaria em Latossolos. No segundo estudo, utilizando diferentes rotas foram sintetizados Zn-FOMs à base de AH com liberação gradual do Zn o que modificou a dinâmica do Zn liberado no solo, aumentando a eficiência de uso do Zn em uma sequência do cultivo milho-braquiária. No terceiro estudo, diferentes FOMs foram produzidos a partir da compostagem de diferentes proporções entre fontes de P, casca de café e esterco de galinha; entre os FOMs produzidos, aqueles que incluíam fosfato de amônio (MAP) tiveram o maior valor agronômico. Por meio da análise de IV, foi possível predizer as propriedades e as quantidades de nutrientes nos FOMs. Em um quarto estudo, os FOMs sintetizados a partir de MAP na etapa 3 foram testados em dois Latossolos contrastantes, e observou-se que os FOMs tiveram uma liberação gradual de P contribuindo para a redução do P inicial na solução do solo, aumento da biomassa e nutrição do milho comparado ao uso exclusivo de MAP. No quinto estudo, FOMs foram sintetizados a partir da acidulação do fosfato natural de Araxá (FA) e sua mistura com resíduo da pós-colheita de café antes da pirólise. A produção de FOMs à base de biochar promoveram uma liberação gradual de P, e a produção e nutrição em uma sequência de cultivo de milho-braquiária dependeu da proporção de P solúvel em citrato neutro de amônio mais água dos FOMs. O sexto estudo foi desenvolvido com base nos resultados do quinto estudo avaliando novas rotas envolvendo a acidulação do FA, com mistura subsequente de biocarvão produzido a partir de resíduo da pós-colheita de café. Os novos FOMs sintetizados tiveram altos teores de NPK, e o P dos FOMs foi liberado de forma gradual indicado por estudos de cinética de liberação e pelos teores de P na solução do solo para o milho cultivado em Latossolo. A liberação gradual de P na solução do solo correlacionou-se positivamente com o acúmulo de P na parte aérea do milho, o que aumentou a biomassa em relação ao uso de fertilizantes minerais.

Palavras-chave: Ácidos Húmicos. Biocarvão. Compostagem. Latossolo. Solução do Solo.

GENERAL ABSTRACT

Organomineral fertilizers (OMFs) over mineral fertilizers may have higher agronomic value for growing plants in Oxisols. Several routes and matrices can be used to synthesize OMFs, including humic acid (HA), composts, and biochar (pyrolysis). Chemical and spectroscopic analyses can access nutrient forms and pools in OMFs, and spectroscopic techniques such as infrared analysis can predict the values quantified in chemical analyses. Thus, the present study aims to use different routes in the synthesis of OMFs, based on Zn-AH, NPK-compost produced by composting, and NPK-biochar with higher agronomic value over mineral fertilizers and use infrared spectroscopy to predict properties and nutrient pools in NPK-OMFs. In the first study, the mixture of Zn and HA promoted the complexation of Zn by the HA structure; when these molecules were applied via soil, compared to Zn sulfate, there was an increase of Zn in soil solution, and growth and nutrition of maize plants followed by the cultivation of brachiaria in Oxisols. In the second study, using different synthesis routes of OMFs, Zn-OMFs based on HA were synthesized with the aim to gradually release Zn that modified the dynamics of Zn released in the whole soil and its solution, increasing the use efficiency of Zn in the sequence of maize-brachiaria cultivation. In the third study, different OMFs were produced by composting different mixtures between sources of P, coffee husk, and chicken manure; among the OMFs produced, those that included monoammonium phosphate (MAP) in the composted mixtures had the highest agronomic value. Through infrared analysis, it was possible to predict the properties and nutrient pools in the OMFs. In a fourth study, the OMFs synthesized based on MAP in step 3 were tested in two contrasting Oxisols, and it was observed that the synthesized OMFs had a gradual release of P, which contributes to the reduction of the initial contents of P in soil solution, increasing the maize biomass and nutrition over the exclusive use of MAP. In the fifth study, OMFs were synthesized based on the acidulation of Araxá phosphate rock (APR) and in its mixture with coffee post-harvest residue before pyrolysis. Production of OMFs based on biochar promoted a gradual release of P, and the production and nutrition in a maize-brachiaria crop sequence depended on the proportion of P soluble in neutral ammonium citrate plus water in the OMFs. The sixth study was developed based on the outputs of the fifth study evaluating new routes involving the acidulation of APR, a subsequent mixture of biochar produced from coffee post-harvest residues. The new synthesized OMFs had high levels of NPK, and the P from the OMFs was released gradually, either in studies of kinetics release in water or citric acid or by evaluating the P contents in the soil solution during maize cultivation in a medium textured Oxisol. This gradual release of P in soil solution correlated positively with P accumulated in the maize shoot, which increased the biomass over soluble mineral NPK-fertilizers.

Keywords: Humic Acid. Biochar. Composting. Oxisol. Soil Solution.

SUMMARY

FIRST PART

1 GENERAL INTRODUCTION

Tropical soils have low pH and low nutrient availability, mainly P (phosphorus), under natural conditions; thus, the use of fertilizers and liming are necessary to increase soil nutrient availability and, consequently, to improve crop yield (FAO, 2017; LOPES; GUILHERME, 2016; MONTALVO *et al.*, 2016; WITHERS *et al.*, 2018). In addition, in tropical soils, there is a predominance in the solid phase of iron (Fe) and aluminium (Al) oxides, and low-activity mineral colloids, such as kaolinite, which are matrices prone to adsorb P in stable bonds, which consequently reduce the efficiency of phosphate fertilization (FINK *et al.*, 2016; LOPES; GUILHERME, 2016; MCLAUGHLIN *et al.*, 2011). Different factors, including the increase in soil pH to 5.5-6.5 promoted by liming and soils with higher soil organic matter (SOM) contents, can increase fertilization efficiency (FINK *et al.*, 2016; MCLAUGHLIN *et al.*, 2011; MONTALVO *et al.*, 2016). SOM through different mechanisms increase the availability of the nutrients such as nitrogen (N), P, potassium (K) and metallic micronutrients such as zinc (Zn), blocking adsorption sites, complexing nutrients, reducing nutrient leaching and through the mineralization process (DHALIWAL *et al.*, 2019; FINK *et al.*, 2016; NOVAIS *et al.*, 2007). However, due to intense weathering, increasing SOM levels in tropical soils is an enormous challenge achieved in the long term (FINK *et al.*, 2016; MCLAUGHLIN *et al.*, 2011).

Soluble mineral fertilizers with a high concentration of nutrients are generally used in Oxisols. Considering the main properties of these soils, mineral fertilizers generally have low agronomic value due to free and highly soluble nutrients release by mineral fertilizers that strongly interact with soil components and colloids (JOHAN *et al.*, 2021; MCLAUGHLIN *et al.*, 2011; WITHERS *et al.*, 2018). Organic fertilizers have nutrients in organic and mineral forms; these nutrient-available forms interact positively with the organic matrix, increasing crop nutrient use efficiency (MUMBACH *et al.*, 2020). Despite these benefits, organic fertilizers are characterized by low nutrient concentrations, which require high rates to adequately nourish plants, restricting the use of organic residues to places close to the site of organic residues production (MUMBACH *et al.*, 2020).

One way to reconcile higher concentrations of nutrients with the interaction of these nutrients with the organic matrix is the synthesis of organomineral fertilizers (OMFs) (ERRO *et al.*, 2012; KOMINKO; GORAZDA; WZOREK, 2017; SÁ *et al.*, 2017). OMFs generally have a higher agronomic value than mineral sources due to the presence of mineral and organic

forms, compared to the predominance of readily available nutrients in mineral fertilizers (ERRO *et al.*, 2012; SÁ *et al.*, 2017; SAKURADA *et al.*, 2016). OMFs can be produced through different routes, mineral nutrient sources and organic matrices. Among the routes and materials used in the synthesis of OMFs, three OMF routes of synthesis stand out: the use of humic substances such as humic acid (HA), the use of composted matrices derived from animal manures and plant residues, and pyrolysis of manure and plant residues, and subsequent use of biochar (BARBOSA *et al.*, 2022; ERRO *et al.*, 2012; FRAZÃO *et al.*, 2021; LUSTOSA FILHO *et al.*, 2017; MALUF *et al.*, 2018; SANTOS *et al.*, 2018).

The extraction of HA from organic waste is a laborious process, and a low proportion of HA is recovered in relation to the total material mass, which makes this synthesis route of OMFs more expensive (SWIFT, 1996). Thus, the use of HA in OMFs synthesis has a higher potential to micronutrient-based OMFs since the amounts applied are lower than those required for NPK fertilizers (MARSCHNER, 2012; ROSE *et al.*, 2014; SANTOS *et al.*, 2018). Among the micronutrients, the metallic ones have a higher beneficial interaction with HA, such as Zn (BOGUTA; SOKOŁOWSKA, 2016; MORAIS; SILVA; JINDO, 2021; SANTOS *et al.*, 2018). The interaction between HA and Zn involves different mechanisms and processes, including ionic or uncoordinated forms, unidentate complexes, bidentate chelates, and coordination chemistry bidentate bridging ligands, as well as the interaction and complexation between organic molecules and Zn shown by infrared spectroscopy (BOGUTA; SOKOŁOWSKA, 2016; JUSTI *et al.*, 2021; OSTE *et al.*, 2002; SANTOS *et al.*, 2018). HA, when mixed with mineral fertilizers containing Zn, promote the HA-Zn interaction, and when these forms are applied via soil, the use efficiency of Zn by plants grown in Oxisols increased over Zn mineral sources (MORAIS; SILVA; JINDO, 2021).

The composting process in the synthesis of OMFs is cheaper than the synthesis of OMFs based on HA. The use of compost to promote the interaction of mineral fertilizers with organic residues requires fewer steps than the use do HA, with a high potential to be used in the synthesis of NPK-OMFs on a large scale (MALUF *et al.*, 2018). Mineral fertilizers can be added either before or after composting to increase the concentration of one or more nutrients, which consequently increases the agronomic value of the OMFs produced (FRAZÃO *et al.*, 2019, 2021; MALUF *et al.*, 2018; SÁ *et al.*, 2017). During composting, nutrients added via mineral fertilizers interact with the organic matrix, modifying nutrient forms, contents and availability, and their kinetics release, thus, properties that truly regulate the OMF agronomic value (CRUSCIOL *et al.*, 2020; MALUF *et al.*, 2018).

When monoammonium phosphate, coffee husk and chicken manure are mixed before composting, P availability is improved since forms of P soluble in water and readily available for plants are reduced, though P available in the long-term for plants is maintained, a factor that may improve the agronomic performance of OMFs over P mineral fertilizers (MALUF *et al.*, 2018). Furthermore, in compost-based OMFs, there are mineral and organic forms of N, which contribute to a more synchronized N release with crop nutritional demand, as the N-mineral can be rapidly released and used in the early stages of plant growth, while organic N in OMF is mineralized and released during plant growth cycle (ANTILLE; SAKRABANI; GODWIN, 2014; GROHSKOPF *et al.*, 2020).

Despite being a viable process to produce OMFs fertilizers containing NPK, composting takes a long time to generate stable composts due to the high time for organic residue decomposition and the maturation (humification) process completed (MALUF *et al.*, 2018; MENGQI *et al.*, 2021). Pyrolysis is a faster process than composting and with a high potential to produce OMFs containing NPK, thus, generating biochar-based fertilizers (BBFs) (AN *et al.*, 2021; GWENZI *et al.*, 2018; LUSTOSA FILHO *et al.*, 2017; PIASH; IWABUCHI; ITOH, 2022). In the production of BBFs, animal and crop residues waste are subjected to pyrolysis, which is a process whose feedstocks are charred at high temperatures (300-750°C) under oxygen-limited conditions (SINGH; CAMPS-ARBESTAIN; LEHMANN, 2017). As in the composting process, during BBFs synthesis, mineral fertilizers can be added either in processes before or after pyrolysis (LUSTOSA FILHO *et al.*, 2017; MATOSO *et al.*, 2019; PIASH; IWABUCHI; ITOH, 2022). In the addition of materials in the process prior to pyrolysis, the mixture between poorly soluble rock phosphate (Dorowa phosphate rock) and maize residues did not promote significant gains in the agronomic value of the produced BBFs compared to low-grade rock phosphate (TUMBURE *et al.*, 2020). Thus, in routes involving the synthesis of BBFs from poorly soluble phosphate rocks, the apatite acidulation process must be used in a previous pyrolysis step, resembling the process used in the synthesis of P mineral fertilizers (UNIDO; IFDC, 1998).

The use of different fertilizer routes, the modifications within each route, and the use of different mineral or organic materials result in the synthesis of OMFs with different chemical properties and nutrient pools, and these properties determine the agronomic value of the carbon-fertilizers (CARNEIRO *et al.*, 2022; ERRO *et al.*, 2012; FRAZÃO *et al.*, 2021; LUSTOSA FILHO *et al.*, 2017; MALUF *et al.*, 2018; SANTOS *et al.*, 2018). The main properties that differentiate organomineral fertilizers over mineral fertilizers are the presence of organic and mineral nutrient forms in OMFs, complexation of nutrients by OMF organic matrix and

functional radicals, retention of cationic nutrients in negative changes generate in the surface of OMF organic matrix, and presence of C organic compounds capable of blocking adsorption sites of nutrients, mainly phosphate, in soil, presence of organic compounds with the capacity of plant biostimulants, and gradual release of nutrients as well (CARNEIRO *et al.*, 2022; ERRO *et al.*, 2012; FACHINI; FIGUEIREDO; VALE, 2022; FINK *et al.*, 2016; FRAZÃO *et al.*, 2019; GHODSZAD *et al.*, 2021; JING *et al.*, 2022; KABIRI *et al.*, 2017; LUSTOSA FILHO *et al.*, 2017). These properties mentioned above and nutrients pools in OMFs assessed by different analytical methods affect the availability of nutrients in the whole soil and its solution, consequently improving crop nutrition and production (AN *et al.*, 2021; GHODSZAD *et al.*, 2021; ROSE *et al.*, 2019; SHI *et al.*, 2020; WANG et al., 2012). Thus, the effects on these nutrient compartments must be evaluated when OMFs are used to fertilize different crops and investigate residual nutrient effects for subsequent crops.

Forms and availability of nutrients in OMFs can be evaluated through different methods, such as the determination of organic and mineral forms of nutrients, availability of nutrients in different extractors, such as in water, citric acid, neutral ammonium citrate plus water, and formic acid, the kinetics of nutrient release, cultivation of crops to evaluate the availability of nutrients in the whole soil and its solution, and its relationship with plant nutrition and biomass production; use of infrared spectroscopy (BARBOSA *et al.*, 2022; CARNEIRO *et al.*, 2021; LÓPEZ-RAYO *et al.*, 2017; LUSTOSA FILHO *et al.*, 2017; MALUF *et al.*, 2018; SHI *et al.*, 2020). Through infrared analysis, it is possible to identify functional groups and specific nutrient bonds in OMFs (BARBOSA *et al.*, 2022; CHEN *et al.*, 2018; LUSTOSA FILHO *et al.*, 2017; MALUF *et al.*, 2018; SHI *et al.*, 2020); thus, it is expected that the compatibility of this method and chemical quantification methods commonly used in the characterization of OMFs, as was already observed the prediction of properties and the availability of P through the spectroscopic signature of OMFs (LU *et al.*, 2019; RUANGRATANAKORN *et al.*, 2020; WANG *et al.*, 2019).

Due to the gradual release of nutrients from OMFs, compared to mineral fertilizers, OMFs may have a higher residual effect after the application to supply nutrients in a first crop, which makes it necessary to evaluate theses effects in subsequent crops (CARNEIRO *et al.*, 2021; MARTINS *et al.*, 2017; SAKURADA *et al.*, 2019). In addition, the efficiency of the application of OMFs has a higher relationship with soil properties, and in soils with higher levels of SOM, the effects of OMFs may be smaller due to the natural effect observed by SOM (ANTILLE *et al.*, 2017; BORGES *et al.*, 2019; DUBOC *et al.*, 2022; ERRO *et al.*, 2012; FRAZÃO *et al.*, 2019; SÁ *et al.*, 2017).

Thus, this study had the following aims: i) to use different synthesis routes in the production of OMFs with higher agronomic value than mineral sources; for the HA route, Zn was used as a nutrient target, for composting and pyrolysis, NPK was used as target nutrients, with a greater focus on P; ii) Use infrared analysis to predict nutrient properties and pools in different compost-based OMFs. Thus, the thesis is structured in six chapters with the respective specific aims of each chapter as follows:

- Chapter 1: Humic acid interaction with Zn, increasing the efficiency of Zn fertilization for maize and brachiaria successively grown in Oxisols with contrasting SOM content and texture;
- Chapter 2: Synthesis of Zn-OMFs using different HA produces fertilizers with different rates of Zn release and with higher agronomic value for maize and brachiaria successively grown in Oxisols with contrasting SOM content and texture;
- Chapter 3: Use of infrared spectroscopy to predict properties and nutrient pools in NPK-OMFs-derived compost produced through the mixing of chicken manure, coffee husk and low-grade and soluble P sources;
- Chapter 4: Evaluate the agronomic value of OMFs with a gradual P release produced by composting of monoammonium phosphate, chicken manure and coffee husk for maize cultivation in Oxisols with contrasting SOM content and texture, and to evaluate the residual effect of NPK-OMF fertilization as well;
- Chapter 5: Synthesize different BBFs containing NPK from the acidulation of Araxá phosphate rock (APR), using different inorganic acids and mixing them with coffee post- harvest residues, with the subsequent characterization of OMFs regarding nutrient pools, the kinetics of P release, and their agronomic value for the successive growth of maize followed by brachiaria in Oxisols with contrasting SOM content and texture;
- Chapter 6: Synthesize new BBFs containing NPK from new routes involving APR acidulation and the used inorganic acid in different stoichiometric ratios and with subsequent incorporation of biochar with gradual release of NPK, mainly P; testing OMF agronomic value for maize growth in a Sandy Loam Oxisol.

REFERENCES

AN, X.; WU, Z.; LIU, X.; SHI, W.; TIAN, F.; YU, B. A new class of biochar-based slow-release phosphorus fertilizers with high water retention based on integrated co-pyrolysis and co-polymerization. **Chemosphere**, Oxford, v. 285, p. 131481, 2021.

ANTILLE, D. L.; GODWIN, R. J.; SAKRABANI, R.; SENEWEERA, S.; TYRREL, S. F.; JOHNSTON, A. E. Field-scale evaluation of biosolids-derived organomineral fertilizers applied to winter wheat in England. **Agronomy Journal**, Madinson, v. 109, p. 654-674, 2017.

ANTILLE, D. L.; SAKRABANI, R.; GODWIN, R. J. nitrogen release characteristics from biosolids-derived organomineral fertilizers. **Communications in Soil Science and Plant Analysis**, London, v. 45, p. 1687-1698, 2014.

BARBOSA, C. F.; CORREA, D. A.; CARNEIRO, J. S. DA S.; MELO, L. C. A. Biochar phosphate fertilizer loaded with urea preserves available nitrogen longer than conventional urea. **Sustainability**, Toroton, v. 14, p. 686, 2022.

BOGUTA, P.; SOKOŁOWSKA, Z. Interactions of Zn(II) ions with humic acids isolated from various type of soils. Effect of pH, Zn concentrations and humic acids chemical properties. **PLoS ONE**, San Franscico, v. 11, p. 1–20, 2016.

BORGES, B. M. M. N.; ABDALA, D. B.; SOUZA, M. F. DE; VIGLIO, L. M.; COELHO, M. J. A.; PAVINATO, P. S.; FRANCO, H. C. J. Organomineral phosphate fertilizer from sugarcane byproduct and its effects on soil phosphorus availability and sugarcane yield. **Geoderma**, Amsterdam, v. 339, p. 20-30, 2019.

CARNEIRO, J. S. DA S.; LEITE, D. A. DA C.; CASTRO, G. M. DE; FRANCA, J. R.; BOTELHO, L.; SOARES, J. R.; OLIVEIRA, J. E. DE; MELO, L. C. A. Biochar-graphene oxide composite is efficient to adsorb and deliver copper and zinc in tropical soil. **Journal of Cleaner Production**, Oxford, v. 360, p. 132170, 2022.

CARNEIRO, J. S. S.; ANDRADE RIBEIRO, I. C.; NARDIS, B. O.; BARBOSA, C. F.; LUSTOSA FILHO, J. F.; AZEVEDO MELO, L. C. Long-term effect of biochar-based fertilizers application in tropical soil: Agronomic efficiency and phosphorus availability. **Science of Total Environment**, Amsterdam, v. 760, p. 143955, 2021.

CHEN, L.; CHEN, Q.; RAO, P.; YAN, L.; SHAKIB, A.; SHEN, G. Formulating and optimizing a novel biochar-based fertilizer for simultaneous slow-release of nitrogen and immobilization of cadmium. **Sustainability**, Toronto, v. 10, p. 2740, 2018.

CRUSCIOL, C. A. C.; CAMPOS, M. DE; MARTELLO, J. M.; ALVES, C. J.; NASCIMENTO, C. A. C.; PEREIRA, J. C. DOS R.; CANTARELLA, H. Organomineral fertilizer as source of P and K for sugarcane. **Scientific Reports**, Berlin, v. 10, p. 1-11, 2020.

DHALIWAL, S. S.; NARESH, R. K.; MANDAL, A.; SINGH, R.; DHALIWAL, M. K. Dynamics and transformations of micronutrients in agricultural soils as influenced by organic matter build-up: A review. **Environmental and Sustainability Indicators**, Amsterdam, v. 1-2, p. 100007, 2019.

DUBOC, O.; HERNANDEZ-MORA, A.; WENZEL, W. W.; SANTNER, J. Improving the prediction of fertilizer phosphorus availability to plants with simple, but non-standardized extraction techniques. **Science of The Total Environment**, Amsterdam, v. 806, p. 150486, 2022.

ERRO, J.; URRUTIA, O.; BAIGORRI, R.; APARICIO-TEJO, P.; IRIGOYEN, I.; TORINO, F.; MANDADO, M.; YVIN, J. C.; GARCIA-MINA, J. M. organic complexed superphosphates (CSP): Physicochemical characterization and agronomical properties. **Journal of Agricultural and Food Chemistry**, Washington, v. 60, p. 2008-2017, 2012.

FACHINI, J.; FIGUEIREDO, C. C. DE; VALE, A. T. DO. Assessing potassium release in natural silica sand from novel K-enriched sewage sludge biochar fertilizers. **Journal of Environmental Management**, London, v. 314, p. 115080, 2022.

FAO. **World fertilizer trends and outlook to 2020: Summary report**. Food and Agriculture Organization of United Nations. 2017.

FINK, J. R.; INDA, A. V.; TIECHER, T.; BARRÓN, V. Iron oxides and organic matter on soil phosphorus availability. **Ciência e Agrotecnologia**, Lavras, v. 40, p. 369-379, 2016.

FRAZÃO, J. J.; BENITES, V. D. M.; PIEROBON, V. M.; RIBEIRO, S. A poultry litter-derived organomineral phosphate fertilizer has higher agronomic effectiveness than conventional phosphate fertilizer applied to field-grown maize and soybean. **Sustainability**, Toronto, v. 13, p. 11635, 2021.

FRAZÃO, J. J.; BENITES, V. DE M.; RIBEIRO, J. V. S.; PIEROBON, V. M.; LAVRES, J. Agronomic effectiveness of a granular poultry litter-derived organomineral phosphate fertilizer in tropical soils: Soil phosphorus fractionation and plant responses. **Geoderma**, Amsterdma, v. 337, p. 582-593, 2019.

GHODSZAD, L.; REYHANITABAR, A.; MAGHSOODI, M. R.; ASGARI LAJAYER, B.; CHANG, S. X. Biochar affects the fate of phosphorus in soil and water: A critical review. **Chemosphere**, Oxford, v. 283, p. 131176, 2021.

GROHSKOPF, M. A.; CORRÊA, J. C.; FERNANDES, D. M.; TEIXEIRA, P. C.; MOTA, S. C. A. Mobility of nitrogen in the soil due to the use of organomineral fertilizers with different concentrations of phosphorus. **Communications in Soil Science and Plant Analysis**, London, v. 51, p. 208-220, 2020.

GWENZI, W.; NYAMBISHI, T. J.; CHAUKURA, N.; MAPOPE, N. Synthesis and nutrient release patterns of a biochar-based N–P–K slow-release fertilizer. **International Journal of Environmental Science and Technology**, New York, v. 15, p. 405-414, 2018.

JING, J.; ZHANG, S.; YUAN, L.; LI, Y.; CHEN, C.; ZHAO, B. Humic acid modified by being incorporated into phosphate fertilizer increases its potency in stimulating maize growth and nutrient absorption. **Frontiers in Plant Science**, Lausanne, v. 13, p. 885156, 2022.

JOHAN, P. D.; AHMED, O. H.; OMAR, L.; HASBULLAH, N. A. Phosphorus transformation in soils following co-application of charcoal and wood ash. **Agronomy**, Basel, v. 11, p. 2010, 2021.

JUSTI, M.; FREITAS, M. P. DE; SILLA, J. M.; NUNES, C. A.; SILVA, C. A. Molecular structure features and fast identification of chemical properties of metal carboxylate complexes by FTIR and partial least square regression. **Journal of Molecular Structure**, Amsterdam, v. 1237, p. 130405, 2021.

KABIRI, S.; DEGRYSE, F.; TRAN, D. N. H.; SILVA, R. C. DA; MCLAUGHLIN, M. J.; LOSIC, D. Graphene oxide: A new carrier for slow release of plant micronutrients. **ACS Applied Materials & Interfaces**, Washington, v. 9, p. 43325-43335, 2017.

KOMINKO, H.; GORAZDA, K.; WZOREK, Z. The possibility of organo-mineral fertilizer production from sewage sludge. **Waste and Biomass Valorization**, Dordrecht, v. 8, p. 1781-1791, 2017.

LOPES, A. S.; GUILHERME, L. R. G. A career perspective on soil management in the Cerrado region of Brazil. **Advances in Agronomy**, v. 137, p. 1-72, 2016.

LÓPEZ-RAYO, S.; IMRAN, A.; BRUUN HANSEN, H. C.; SCHJOERRING, J. K.; MAGID, J. Layered double hydroxides: Potential release-on-demand fertilizers for plant zinc nutrition. **Journal of Agricultural and Food Chemistry**, Washington, v. 65, p. 8779-8789, 2017.

LU, B.; LIU, N.; LI, H.; YANG, K.; HU, C.; WANG, X.; LI, Z.; SHEN, Z.; TANG, X. Quantitative determination and characteristic wavelength selection of available nitrogen in coco-peat by NIR spectroscopy. **Soil and Tillage Research**, Amsterdam, v. 191, p. 266-274, 2019.

LUSTOSA FILHO, J. F.; PENIDO, E. S.; CASTRO, P. P.; SILVA, C. A.; MELO, L. C. A. Co-pyrolysis of poultry litter and phosphate and magnesium generates alternative slow-release fertilizer suitable for tropical soils. **ACS Sustainable Chemistry & Engineering**, Washington, v. 5, p. 9043-9052, 2017.

MALUF, H. J. G. M.; SILVA, C. A.; MORAIS, E. G. DE; PAULA, L. H. D. DE. Is composting a route to solubilize low-grade phosphate rocks and improve map-based composts? **Revista Brasileira de Ciência do Solo**, Viçosa, v. 42, p. e0170079. 2018.

MARSCHNER, P. **Marschner's mineral nutrition of higher plants**. Oxford: Elsevier, 2012.

MARTINS, D. C.; RESENDE, Á. V. DE; GALVÃO, J. C. C.; SIMÃO, E. D. P.; FERREIRA, J. P. D. C.; ALMEIDA, G. D. O. Organomineral phosphorus fertilization in the production of corn, soybean and bean cultivated in succession. **American Journal of Plant Sciences**, New York, v. 8, p. 2407-2421, 2017.

MATOSO, S. C. G.; WADT, P. G. S.; SOUZA JÚNIOR, V. S. DE; PÉREZ, X. L. O. Synthesis of enriched biochar as a vehicle for phosphorus in tropical soils. **Acta Amazonica**, Manaus, v. 49, p. 268-276, 2019.

MCLAUGHLIN, M. J.; MCBEATH, T. M.; SMERNIK, R.; STACEY, S. P.; AJIBOYE, B.; GUPPY, C. The chemical nature of P accumulation in agricultural soils-implications for fertiliser management and design: An Australian perspective. **Plant and Soil**, Dordrecht, v. 349, p. 69-87, 2011.

MENGQI, Z.; SHI, A.; AJMAL, M.; YE, L.; AWAIS, M. Comprehensive review on agricultural waste utilization and high-temperature fermentation and composting. **Biomass Conversion and Biorefinery**, Heidelberg, b. 2021, p. 1-24, 2021.

MONTALVO, D.; DEGRYSE, F.; SILVA, R. C. DA; BAIRD, R.; MCLAUGHLIN, M. J. Agronomic effectiveness of zinc sources as micronutrient fertilizer. **Advances in agronomy**, v. 139, p. 215-267, 2016.

MORAIS, E. G. DE; SILVA, C. A.; JINDO, K. Humic acid improves Zn fertilization in oxisols successively cultivated with maize–brachiaria. **Molecules**, Basel, v. 26, p. 4588, 2021.

MUMBACH, G. L.; GATIBONI, L. C.; BONA, F. D. DE; SCHMITT, D. E.; CORRÊA, J. C.; GABRIEL, C. A.; DALL'ORSOLETTA, D. J.; IOCHIMS, D. A. Agronomic efficiency of organomineral fertilizer in sequential grain crops in southern Brazil. **Agronomy Journal**, Madinson, v. 112, p. 3037-3049, 2020.

NOVAIS, R. F.; ALVAREZ V., V. H.; BARROS, N. F.; FONTES, R. L. F.; CANTARUTTI, R. B.; LIMA, J. C. (eds.). **Fertilidade do solo**. Viçosa-MG: Sociedade Brasileira de Ciência do Solo, 2007.

OSTE, L. A.; TEMMINGHOFF, E. J. M.; LEXMOND, T. M.; RIEMSDIJK, W. H. VAN. Measuring and modeling zinc and cadmium binding by humic acid. **Analytical Chemistry**, Washington, v. 74, p. 856-862, 2002.

PIASH, M. I.; IWABUCHI, K.; ITOH, T. Synthesizing biochar-based fertilizer with sustained phosphorus and potassium release: Co-pyrolysis of nutrient-rich chicken manure and Ca-bentonite. **Science of The Total Environment**, Amsterdam, v. 822, p. 153509, 2022.

ROSE, M. T.; PATTI, A. F.; LITTLE, K. R.; BROWN, A. L.; JACKSON, W. R.; CAVAGNARO, T. R. A meta-analysis and review of plant-growth response to humic substances. **Advances in agronomy**, v. 124, p. 37-89, 2014.

ROSE, T. J.; SCHEFE, C.; WENG, Z. (HAN); ROSE, M. T.; ZWIETEN, L. VAN; LIU, L.; ROSE, A. L. Phosphorus speciation and bioavailability in diverse biochars. **Plant and Soil**, Dordrecht, v. 443, p. 233-244, 2019.

RUANGRATANAKORN, J.; SUWONSICHON, T.; KASEMSUMRAN, S.; THANAPASE, W. Installation design of on-line near infrared spectroscopy for the production of compound fertilizer. **Vibrational Spectroscopy**, Amsterdam, v. 106, p. 103008, 2020.

SÁ, J. M.; JANTALIA, C. P.; TEIXEIRA, P. C.; POLIDORO, J. C.; BENITES, V. DE M.; ARAÚJO, A. P. Agronomic and P recovery efficiency of organomineral phosphate fertilizer from poultry litter in sandy and clayey soils. **Pesquisa Agropecuaria Brasileira**, Brasília, v. 52, p. 786-793, 2017.

SAKURADA, R. L.; MUNIZ, A. S.; SATO, F.; INOUE, T. T.; NETO, A. M.; BATISTA, M. A. Chemical, thermal, and spectroscopic analysis of organomineral fertilizer residue recovered from an oxisol. **Soil Science Society of America Journal**, Hoboken, v. 83, p. 409-418, 2019.

SAKURADA, R.; BATISTA, L. M. A.; INOUE, T. T.; MUNIZ, A. S.; PAGLIAR, P. H. Organomineral phosphate fertilizers: Agronomic efficiency and residual effect on initial corn development. **Agronomy Journal**, Madinson, v. 108, p. 2050-2059, 2016.

SANTOS, A. M. P.; BERTOLI, A. C.; BORGES, A. C. C. P.; GOMES, R. A. B.; GARCIA, J. S.; TREVISAN, M. G. New Organomineral complex from humic substances extracted from poultry wastes: Synthesis, characterization and controlled release study. **Journal of the Brazilian Chemical Society**, São Paulo, v. 29, p. 140-150, 2018.

SHI, W.; JU, Y.; BIAN, R.; LI, L.; JOSEPH, S.; MITCHELL, D. R. G.; MUNROE, P.; TAHERYMOOSAVI, S.; PAN, G. Biochar bound urea boosts plant growth and reduces nitrogen leaching. **Science of The Total Environment**, Amsterdam, v. 701, p. 134424, 2020.

SINGH, B; CAMPS-ARBESTAIN, M.; LEHMANN, J. **Biochar: a guide to analytical methods.** Clayton: Csiro Publishing, 2017.

SWIFT, R. S. Organic Matter Characterization. In: SPARKS, D. L.; PAGE, A. L.; HELMKE, P.A.; LOEPPERT, R. H.; SOLTANPOUR, P. N.; TABATABAI, M. A.; JOHNSTON, C. T.; SUMNER, M. E. **Methods of soil analysis**: Part 3 chemical methods. New Jersey: John Wiley & Sons, 1996, p. 1011–1069.

TUMBURE, A.; BISHOP, P.; BRETHERTON, M.; HEDLEY, M. Co-pyrolysis of maize stover and igneous phosphate rock to produce potential biochar-based phosphate fertilizer with improved carbon retention and liming value. **ACS Sustainable Chemistry and Engineering**, Washington, v. 8, p. 4178-4184, 2020.

UNIDO; IFDC. **Fertilizer manual**. 1. ed. Dordrecht: Kluwer Academic Publishers, 1998.

WANG, L. S.; WANG, R. J.; LU, C. P.; WANG, J.; HUANG, W.; JIAN, Q.; WANG, Y. B.; LIN, L. Z.; SONG, L. T. Quantitative analysis of total nitrogen content in monoammonium phosphate fertilizer using visible-near infrared spectroscopy and least squares support vector machine. **Journal of Applied Spectroscopy**, New York, v. 86, p. 465-469, 2019.

WANG, T.; CAMPS-ARBESTAIN, M.; HEDLEY, M.; BISHOP, P. Predicting phosphorus bioavailability from high-ash biochars. **Plant and Soil**, Dordrecht, v. 357, p. 173-187, 2012.

WITHERS, P. J. A.; RODRIGUES, M.; Soltangheisi, A.; CARVALHO, T. S.; GUILHERME, L. R. G.; BENITES, V. M.; GATIBONI, L. C.; SOUSA, D. M. G.; NUNES, R. S.; ROSOLEM, C. A.; ANDREOTE, F. D.; OLIVEIRA JR, A. O.; COUTINHO, L. M.; PAVINATO, P. S. Transitions to sustainable management of phosphorus in Brazilian agriculture. **Scientific Reports**, Berlin, v. 8, p. 2537, 2018.

SECOND PART – MANUSCRIPTS

Manuscript 1 - Humic acid improves Zn fertilization in Oxisols successively cultivated with maize–brachiaria (*Paper published at Molecules Journal* (DOI: doi.org/10.3390/molecules26154588)

Manuscript 2 - Synthesis of slow-release humic acid-based zinc organomineral fertilizers and their agronomic value for successively grown maize and brachiaria in contrasting Oxisols (*Manuscript edited following the rules of ACS Agricultural Science & Technology Journal* (ISSN: 2692-1952))

Manuscript 3 - PLS regression based on ATR-FTIR to predict organomineral fertilizers properties and nutrient pools (*Manuscript edited following the rules of Communications in Soil Science and Plant Analysis Journal* (ISSN: 1532-2416))

Manuscript 4 - Effects of compost-based organomineral fertilizers on the kinetics of NPK release and maize growth in contrasting Oxisols (*Manuscript edited following the rules of Waste and Biomass Valorization Journal* (ISSN: 1877-265X))

Manuscript 5 - Biochar-based phosphate fertilizers: synthesis, properties, kinetics of P release, and recommendation basis for successively grown maize and brachiaria in contrasting Oxisols (*Manuscript edited following the rules of Science of The Total Environment Journal* (ISSN: 0048-9697))

Manuscript 6 - Novel NPK-slow release biochar-based fertilizer produced from the coffee post-harvest residues-derived biochar and acidulated low-grade phosphate rock (*Manuscript edited following the rules of Science of The Total Environment Journal* (ISSN: 0048-9697))

Manuscript published in Molecules Journal (DOI: doi.org/10.3390/molecules26154588)

Humic Acid Improves Zn Fertilization in Oxisols Successive ly Cultivated with Maize–Brachiaria

Everton Geraldo de Morais [1], Carlos Alberto Silva[1,*] and Keiji Jindo[2,*]

[1]Soil Science Department, Federal University of Lavras, Lavras, Minas Gerais, 37200-000, Brazil; evertonmoraislp@gmail.com

[2]Agrosystems Research, Wageningen University & Research, P.O. Box 16, 6700 AA, Wageningen, The Netherlands

[*]Correspondence: csilva@ufla.br (C.A.S.); keiji.jindo@wur.nl (K.J.)

Abstract: Zinc (Zn) is a micronutrient for plant growth, and Zn deficiency is a global issue, especially in tropical soils. This study aimed to investigate the effects of humic acid (HA) and the Zn addition (Zn sulfate + HA) on the growth of maize and brachiaria in two contrasting Oxisols. The potential complexation of Zn sulfate by HA was evaluated by Fourier-transform infrared (FTIR) spectroscopy analysis. Zinc content and its availability in solution and the shoot and root biomass of maize and brachiaria were determined. FTIR spectroscopy revealed the complexation of Zn sulfate by HA through its S and C functional groups. In both Oxisols, solution Zn increased due to the combined use of Zn and HA. In a soil type-dependent manner, maize biomass and Zn in its shoots were affected only by the exclusive use of Zn fertilization. In the Yellow Oxisol, brachiaria growth and Zn accumulated in its shoot were positively

affected by the combined use of Zn fertilization with HA. In the Oxisol with lower organic matter content, HA can assure adequate supplying of residual Zn, while increasing growth of brachiaria cultivated in sequence to maize.

Keywords: organometallic complexes; tropical soils; humic fertilization; residual zinc

1. Introduction

Zinc (Zn) plays a role in plant metabolism, acting as catalytic and structural components of proteins, tryptophan, carbohydrate metabolism, and indoleacetic acid synthesis, while maintaining cell membrane integrity and increasing lipid peroxidation [1]. Regarding tolerance to Zn, maize (Zea mays) is highly sensitive, while some grass plants such as brachiaria are less affected by low levels of Zn in the growth media [2]. The maize–brachiaria cultivation sequence is adopted in many Brazilian cropping areas [3]. The efficient use and adequate Zn fertilization are key issues to increase food production in Brazilian soils [2]. The Zn deficiency in soils is a global concern [2,4], mainly in tropical soils such as the Brazilian soils where parent material and intense weathering are key processes decreasing Zn availability in cerrado soils [2,4,5]. In addition, the acidic conditions, low pH, and reduced P availability in the Brazilian soils require other agronomic practices to improve crop production; liming and phosphate fertilization are frequently used to correct acidity and increase soil available P levels though these practices aggravate Zn deficiency in poor Zn fertilized cerrado soils [1,4].

In soil, Zn availability is controlled by the intensity of adsorption and precipitation reactions [4]. Zn sorption increases as the soil pH is higher due to the rise of negative charges on soil colloid surfaces and the increased presence of adsorbed and precipitated Zn forms in

soil [4]. Organic matter (OM) content controls the magnitude of Zn sorption in soil [4]. OM is composed of different fractions, including humic (HA) and fulvic acids, which are OM pools characterized by low isoelectric points; thus, even at low soil pH levels, negative charges prevail on the surface of organic colloids [6]. The increase of OM and soil pH augment Zn adsorption due to the higher amount of organic ligands and the increase of density of charges in these organic ligands, besides the increased stability of organic complexes with HA, as the pH is increased [4,7]. An increase in clay content is a key factor to increase Zn adsorption in soils. However, the density of negative charges in tropical clay minerals and Al and Fe oxides is lower than those in organic colloids [1,2,4]. Moreover, Zn availability to plants is controlled by soil type, minerals associated with clay and Fe and Al oxides, soil parent material, total Zn content, soil pH, concentrations of organic matter, Ca, calcite, bicarbonate, and phosphate found in the soil, solution or in labile forms prone to be solubilized and to react with zinc with subsequent formation of precipitates and high-stability organometallic complexes [1,2,4,7].

In Brazilian cropland areas, the increase of OM and humic substances stored in the soil is not a simple task, even in no-tillage and conservative cropland fields. This is why the soil amendment with exogenous OM such as humic acid should be tested to reduce specific Zn adsorption into soil mineral colloids while improving Zn uptake by crops. Humic acid, a pool of humic substances (HS), is prone to form complexes with Zn. However, the stability and solubility of complexes formed depend on the Zn–HA stoichiometry, plant type, HA rate added to soil, growing medium properties, and soil type [7–11]. Therefore, depending on the combination of the factors mentioned above and soil management practices adopted, Zn uptake by crops may be improved or diminished [8,9,11]. In combination with Zn, HA addition to soil improves nutrient uptake and plant growth through direct and indirect effects of HS [9,11]. Direct effects occur when HA is in contact with the plant cell membrane and tissues, stimulating several plant chemical, physiological, and biochemical processes [11–14]. The action of HS on

plant tissues includes the stimulation of root proliferation, enhancement of H^+-ATPase activity in the cell membrane, and changes in the magnitude of nutrient uptake, assimilation, and use efficiency [8,9,11–13,15,16].

Indirect effects of HS are related to the modifications in the growing medium in response to humic fertilization [11,12]. In soil, HA may complex Zn [7], improving Zn nutrition and plant growth [17]. Complexation of Zn by organic ligands is relevant to improve Zn uptake by plants, considering that the organometallic complexes increase Zn content in soil solution and Zn diffusion from solution to cell root surface as well [4,7,10,14]. Even though the Zn concentration in solution is only a tiny fraction of soil total Zn content, Zn dissolved in the soil liquid phase is a readily available Zn pool for plants [4]. Therefore, it is expected that HA has organic radicals in its structure capable of complexing the Zn in soluble forms. Even at high soil pH conditions (pH 7.2), the HA uses efficiently increased the Zn content in solution [10].

When present in soil solution, HA is also capable of buffering soil acidity, keeping the pH in the optimum range required for plentiful nutrient supplying to crops, mainly of Zn, whose availability is reduced as the soil pH is increased [1,2,4]. The HA effect on soil acidity buffering is highlighted primarily in soils with low clay and organic matter contents. In less buffered soils, pH oscillation is more frequent, and, when pH is within the alkaline range, less dissolved Zn is found in soils, while low insoluble forms ($ZnOH^+$ and $ZnOH_2$) are formed in the whole soil [2,4]. When present in the growing medium, HA is capable of buffering soil acidity, avoiding oscillations in soil reaction [14,18], which, consequently, favours the formation of soluble Zn^{2+} free hydrated forms, as well as soluble Zn-organic complexes [4].

Humic acid effects on plants also rely on the properties of HA's structure-organic functional groups-function [15,17]. The positive effects of humic acid on maize or brachiaria were already reported, as well as the residual effects of humic fertilization on brachiaria after successive cuttings [8,19]. In tropical soils, Zn is prone to be immobilized in the soil mineral

phase, but little is known regarding the humic fertilization–Zn interaction on plant nutrition and growth. Additionally, in the large area of Brazilian integrated crop-livestock systems, maize and brachiaria are simultaneously cultivated [3], and both crops show different responses to HA application and Zn fertilization [2,4,8].

The direct and indirect effects of HA occur simultaneously [9,11], and are linked to the type and concentration of oxygen-, nitrogen-, and sulfur-containing functional groups in the HA structure [14,15,20]. Infrared spectroscopy is a suitable technique to reveal the functional groups and specific bonds formed between the metals and HA [6,7,14]. The use of infrared to evaluate the chemical complexation was proved when $ZnCl_2$ was mixed with HA, considering that the OH-stretching at 3290 cm^{-1} increased when Zn was complexed by HA [7]. Other bonds are involved in Zn complexation through organic molecules, such as the FTIR peak at 1075 cm^{-1} related to the formation of organic-SO_4^{-2}–metal complexes [21], reflecting the role played by HA sulfur groups in complexing Zn [20]. When organic matrices and metal are mixed, HA acts both as a source of complexed metal to plants and bioactive molecules capable of improving plant nutrition, physiology, and growth [20]. Some functional groups found in the HA structure are positively related to HA bioactivity [14]. Besides, the peaks related to the C-H_3 bending, C=C (aromatic-C), and aliphatic C–H stretching recorded in HA infrared spectra contribute to improving plant growth medium capacity to buffer acidity [14,18].

This work is the first attempt to study the HA-Zn interaction in contrasting Brazilian soils. HA is not supposed to play a role in plant growth and soil Zn chemistry, forms, and availability in OM-enriched soils. In less-buffered soils, HA is prone to act as a buffer for acidity, which may improve brachiara's nutrition and growth, which is more adapted than maize to acidic soil growth.

Zinc is prone to be adsorbed in Brazilian soils enriched with clay and Al and Fe Oxides. However, in sandy soils, the simultaneous reduction of Zn adsorption, and the formation of Zn–

HA complexes should act positively on soil Zn availability to crops, mainly for brachiaria, which is not fertilized in most Brazilian pasture areas. The use of Zn in combination with HA is a promising strategy to decrease Zn adsorption and precipitation while increasing the formation of soluble Zn–HA complexes that are prone to nourish or to be acquired by roots. When combined with HA, Zn is supposed to prevail in soils in soluble forms, thus increasing its residual effect on brachiaria plants. In Brazil, the supply of Zn relies only on the Zn fertilization of previous crops (maize) in rotation. Thus, it is interesting to investigate how soil type influences Zn fertilization's efficiency and the magnitude of HA action on plant and Zn supplying to maize and brachiaria.

We hypothesized that when Zn sulfate ($ZnSO_4$) (the main source of Zn for plants [4]) is mixed with HA, there are modifications in the HA structure due to the formation of Zn–HA complexes. Some organic functional groups of HA can act by complexing with Zn, playing a positive role in the efficiency of Zn fertilization for the maize–brachiaria rotation in a soil type-dependent manner. The aims of the study were: (1) To demonstrate the formation of Zn–HA complexes through the use of FTIR spectroscopy analysis; (2) To study the capacity of HA in increasing the effects of Zn fertilization on the nutrition and growth of brachiaria following maize cultivation; (3) To evaluate the effects of HA on the Zn availability in soil and solution, and soil residual Zn to brachiaria plants; (4) to verify if the combination of Zn–HA is effective in improving plant growth in the two constrasting Oxisols.

2. Results

2.1. Maize Growth

The addition of HA and/or Zn did not significantly affect soil pH, as well as solution pH (Figure 1a,b). YO had higher soil and solution pH values than RO. The soil–Zn DTPA increased in response to Zn fertilization over control (no Zn added to the soil), regardless of the

HA application (Figure 1c). Soil Zn-DTPA contents in the YO are significantly higher than RO. In addition, it shows that RO had a higher soluble Zn content than YO (Figure 1d). For both Oxisols, the Zn fertilization increased the solution Zn content over control. When HA was combined with Zn, the solution Zn was more significant than the single-use of Zn fertilization (Figure 1d).

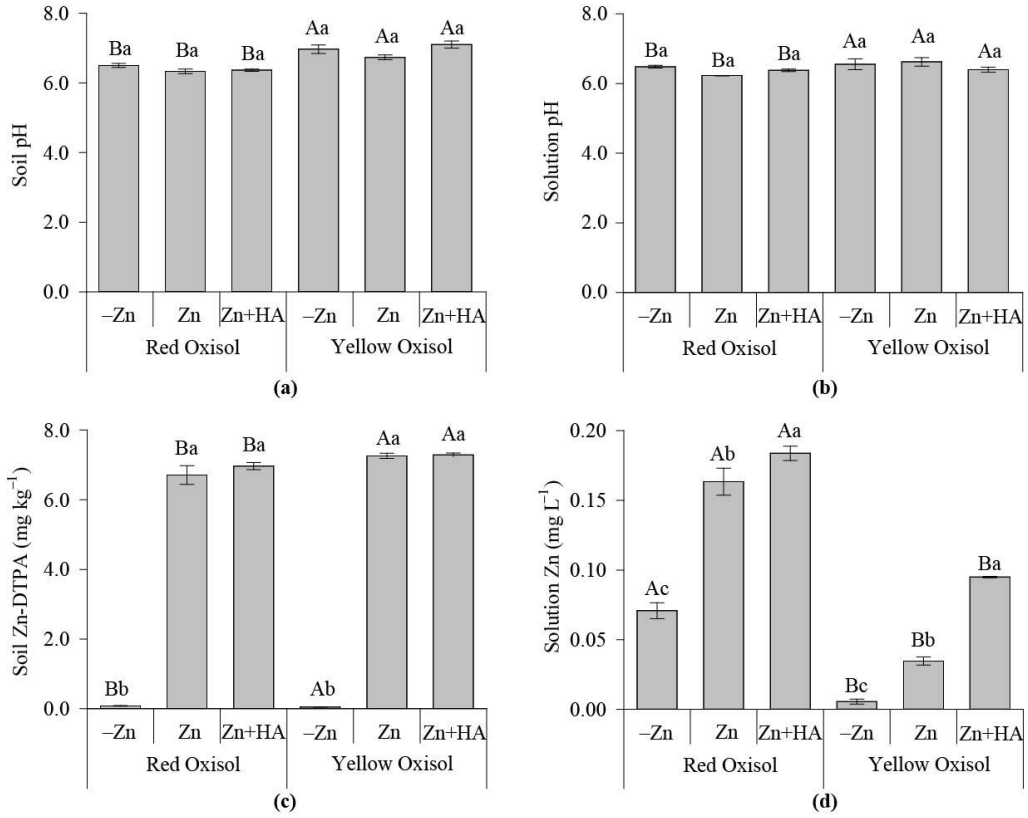

Figure 1. Effects of Zn fertilization and humic acid (HA) on soil pH and Zn availability in contrasting Oxisols cultivated with maize. Soil pH (**a**); soil solution pH (**b**); soil available Zn by the DTPA method (**c**); Zn in soil solution (**d**). Bars followed by the same capital letter means that the soil type properties differ regarding the Zn fertilization strategies studied according to the Tukey test ($p < 0.05$). Bars followed by the same lowercase letter mean that crop traits do not differ regarding the Zn fertilization strategies adopted, again, according to the Tukey test ($p < 0.05$), within each soil type. -Zn: no-Zn fertilization; Zn: Zn fertilization; Zn + HA: Zn fertilization combined with HA application.

In RO, the SDM, RDM, and TDM increased in response to Zn fertilization, and maize biomass production with HA combined with Zn was slightly greater in comparison to the single use of Zn (Figure 2a). SDM and TDM increased due to Zn fertilization over control,

independent of the HA use in YO (Figure 2a). However, the RDM decreased in response to HA added in combination with Zn (Figure 2a). When Zn was applied to soil, maize growth is more prominent in RO over YO, mirrored by a greater SDM, RDM and TDM. YO has a significantly higher maize root: shoot ratio than RO. Root: shoot ratio reduced due to the HA application compared to the single-use of Zn fertilization in YO (Figure2b). Zinc accumulated in maize shoot increased in response to Zn fertilization, regardless of the HA use, with higher amounts of Zn in maize shoots cultivated in YO over the plants grown in RO (Figure 2c).

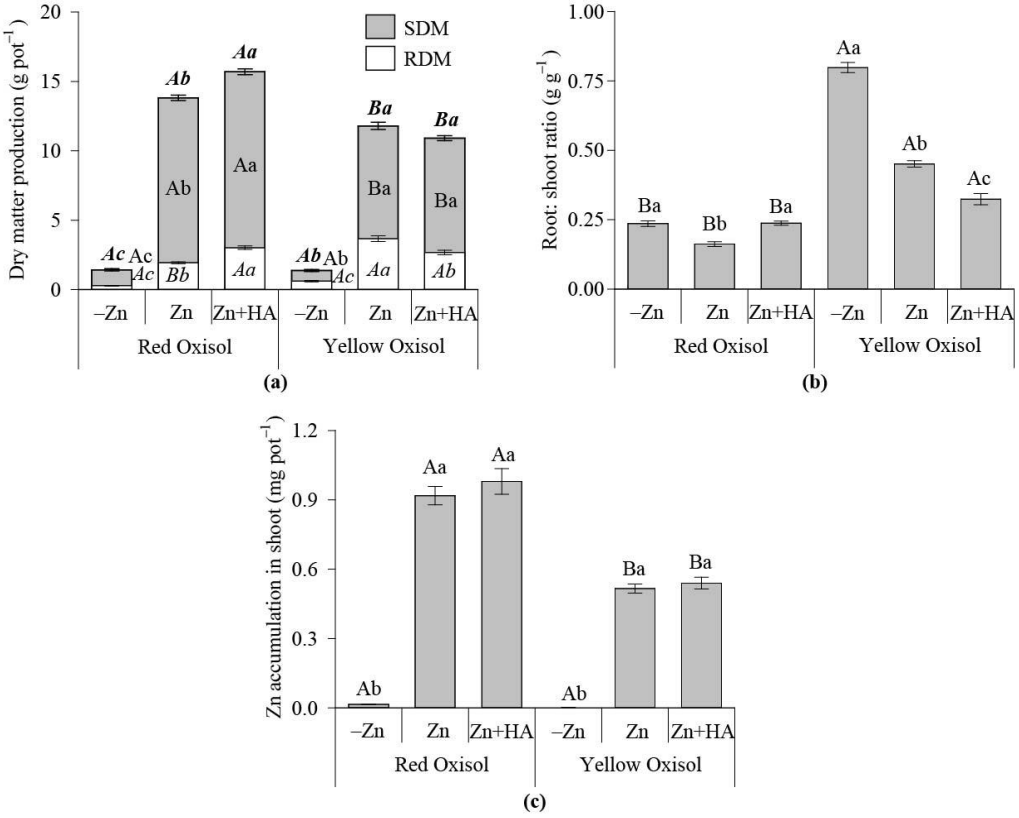

Figure 2. Effect of Zn fertilization and humic acid (HA) application on Zn nutrition and maize growth in contrasting Oxisols. Dry matter production (**a**); Root: shoot ratio (**b**); Zn accumulated in maize shoot (**c**). SDM: shoot dry matter; RDM: root dry matter; full bar in the biomass graph represents the total dry matter production (TDM). Bars followed by the same capital letter do not differentiate the soil types regarding the Zn fertilization strategies studied, according to the Tukey test ($p < 0.05$). Bars followed by the same lowercase letter do not differentiate the Zn fertilization strategies adopted within each soil type by the Tukey test ($p < 0.05$). The combined use of bold-italic letters compare TDM means in response to treatments; the use of italics compared RDM means in response to treatments. -Zn: no-Zn fertilization; Zn: Zn fertilization; Zn + HA: Zn fertilization combined with HA application.

2.2. Brachiaria Growth

When brachiaria was grown in sequence to maize, the soil pH was higher in YO than RO (Figure 3a). Solution pH was similar in both Oxisoils when Zn fertilization was combined with HA (Zn + HA); without HA application, YO had a greater solution pH than RO (Figure 3b). HA significantly reduced the solution pH in YO (Figure 3b). Soil Zn-DTPA content was higher in RO over YO, regardless of the use of Zn and HA. (Figure 3c). Zinc fertilization increased the soil Zn-DTPA content, independent of soil type and HA application (Figure 3c). The solution Zn was higher in RO over YO, and HA applied together with $ZnSO_4$ increased the solution Zn in both Oxisols (Figure 3d).

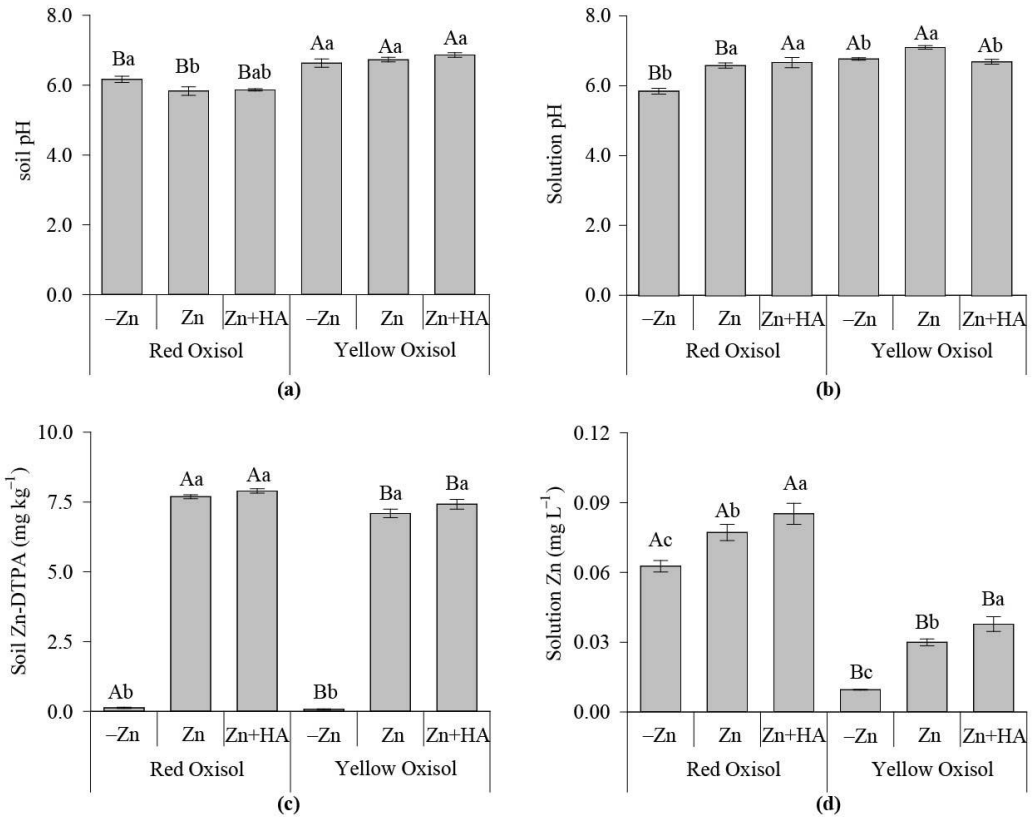

Figure 3. Effect of Zn fertilization and humic acid (HA) on soil pH and available DTPA Zn in contrasting Oxisols cultivated with brachiaria. Soil pH (**a**); soil solution pH (**b**); Zn available through the DTPA soil test (**c**); Zn in soil solution (**d**). Bars followed by the same capital letter mean that the soil attributes did not differ in terms of the Zn fertilization strategies adopted, according to the Tukey test ($p < 0.05$). Bars followed by the same lowercase letter mean that the soil attribute means do not differ regarding response to Zn fertilization strategies within each soil type, according to the Tukey test ($p < 0.05$). -Zn: no-Zn fertilization; Zn: Zn fertilization; Zn + HA: Zn fertilization combined with HA application.

The treatment of Zn+HA significantly increased SDM and TDM over control (-Zn) in RO, mainly affected by the increased RDM in response to HA combined with Zn fertilization (Figure 4a). In YO, the SDM, RDM, and TDM increased due to Zn fertilization over control (no Zn addition), and HA acts in synergy with Zn fertilization considering that HA promoted a higher SDM, RDM and TDM over the exclusive use of Zn in maize fertilization (Figure 4a). In the absence of HA, the RO over YO produced a higher maize SDM, RDM and TDM. In the presence of HA, YO over RO had a greater maize SDM and TDM (Figure 4a. In RO, HA application increased the root: shoot ratio compared to the single-use of Zn. In YO, the HA use decreased the root: shoot ratio compared to the exclusive use of Zn. Zinc accumulated in maize shoot grown in RO increased due to Zn fertilization, but it was not influenced by HA (Figure 4c). In YO, the positive effect of Zn use on Zn in maize shoot was magnified when HA was combined with Zn sulfate (Figure 4c). When compared, the plants grown in the RO over the YO had a greater Zn accumulation in the shoots in response to the single use of Zn fertilization. On the contrary, Zn fertilization in combination with HA assured the highest accumulation of Zn in maize plants grown in YO (Figure 4c).

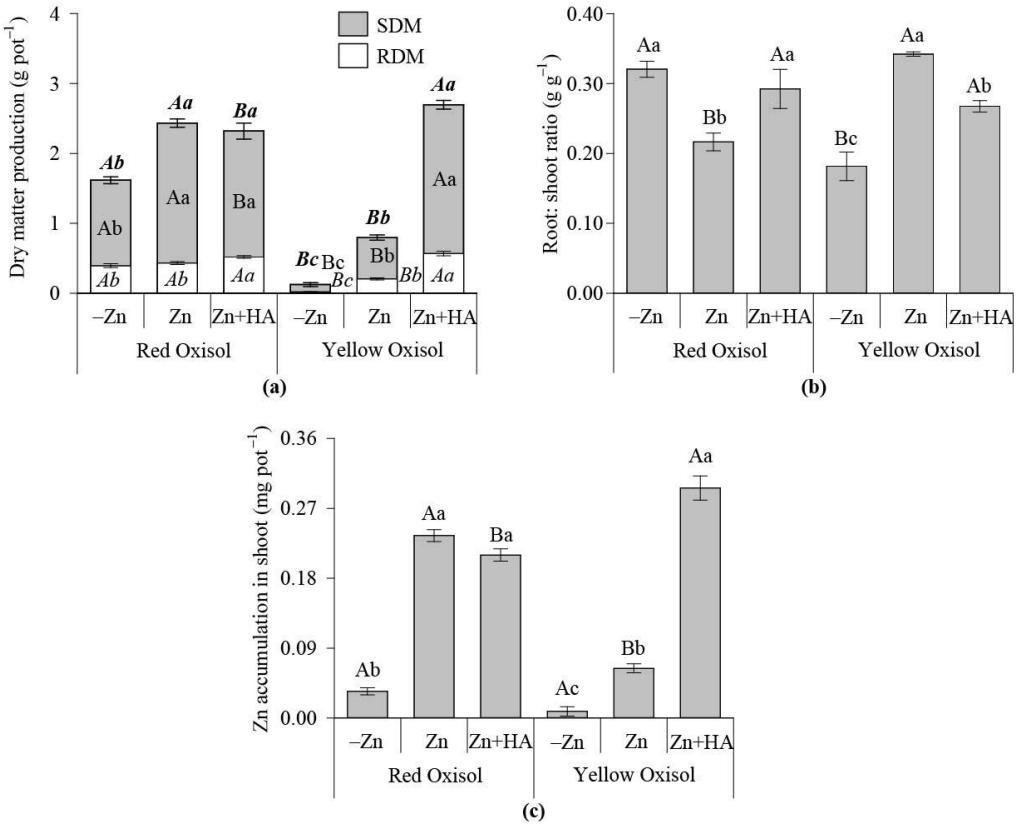

Figure 4. Effect of Zn fertilization and humic acid (HA) application on brachiaria growth traits and Zn nutrition of plants grown in contrasting Oxisols. Dry matter production (**a**); Root: shoot ratio (**b**); Zn accumulated in brachiaria shoot (**c**). SDM: shoot dry matter production; RDM: root dry matter production; full bar in the biomass graph represents the total dry matter production (TDM). Bars followed by the same capital letter do not differentiate the soil types according to the Zn fertilization strategies studied by the Tukey test ($p < 0.05$). Bars followed by the same lowercase letter do not differentiate the Zn fertilization system adopted to each soil type according to the Tukey test ($p < 0.05$). The combined use of bold-italic letters was used to compare TDM treatment means; the use of italics compared the values of RDM across the treatments. -Zn: no-Zn fertilization; Zn: Zn fertilization; Zn+HA: Zn fertilization combined with HA application.

2.3. Principal Component Analysis

By reducing dimensionality, PCA is a multivariate analysis capable of identifying potential correlations, dependencies, and features of the main clusters of a dataset in response to Zn treatments investigated. When maize and soil attributes were analyzed, 87.1% of the covariances can be explained by the PC1 and PC2 axes, while for the brachiaria experiment, 87.6% (Figure 5a) of the variations were explained. For the maize experiment, PCA showed that the solution pH and soil pH are favoured by the absence of HA in YO. Soil pH and solution pH are negatively related to solution Zn, Zn accumulated in shoot, SDM and TDM.

On the contrary, plant traits are favoured by the Zn fertilization combined with HA. The solution pH is positively related to RDM and root: shoot ratio for the maize trial. The significance of some correlations aforementioned was confirmed by the Pearson's linear correlation matrix ($p < 0.05$) (Supplementary Material 1, maize experiment). Thus, soil solution pH was negatively correlated with soluble Zn, Zn in shoot, positively associated to RDM and root: shoot ratio (Supplementary Material 1); soil pH negatively correlated with soluble Zn, SDM, TDM and Zn in a shoot, and positively correlated with the root: shoot ratio. Soluble Zn is directly linked to SDM, TDM, Zn shoot accumulation and negatively related to RDM and shoot: root ratio. The root: shoot ratio is negatively correlated with SDM, TDM and Zn accumulated in maize shoots.

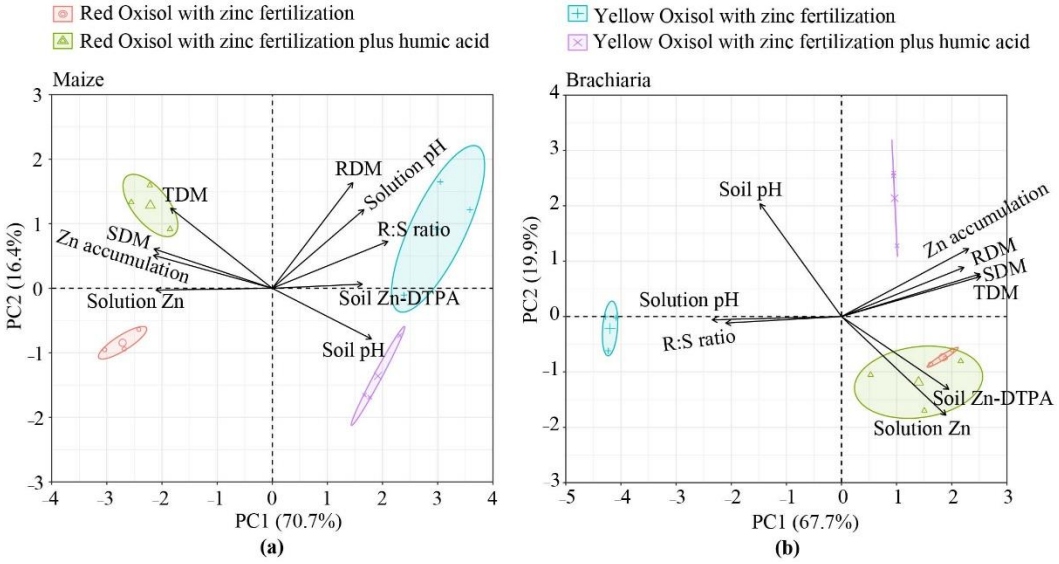

Figure 5. Biplot of principal component analysis (PCA) separated according to the crop grown in pot Oxisols. The main clusters of plant traits and soil attributes in response to Zn with/without humic acid (HA) use are shown in PCA graphs. The maize experiment variables (**a**); brachiaria experiment variables (**b**); SDM, RDM and TDM: shoot, root and total dry matter production, respectively; R:S ratio: ratio between shoot (SDM) and root (RDM) biomasses; Zn accumulation: Zn accumulated in shoots.

As outcomes of PCA for the brachiaria experiment, it was verified that Zn accumulated in shoots, and the RDM, SDM and TDM were favoured by the addition of Zn+HA in the case of YO. Plant variables are negatively related to solution pH and root: shoot ratio (Figure 5b).

The solution Zn and soil Zn-DTPA were related to each other and negatively associated with soil pH. To check the statistical significance and association degree of the relationships as mentioned above, Pearson's linear correlation matrix analysis ($p < 0.05$) was performed (Supplementary Material 2). With Pearson's linear correlation analysis, a negative correlation between soil pH and soluble Zn and soil-Zn DTPA was confirmed. The solution pH was negatively correlated with soluble Zn, SDM, RDM, TDM, and Zn accumulated in brachiaria shoot, and positively associated with root: shoot ratio. Root: shoot ratio also was negatively correlated with SDM, TDM, and Zn in brachiaria shoots.

2.4. Infrared Spectroscopy

FTIR-ATR peaks (Figure 6) in HA spectra at 3290 cm^{-1} are related to OH stretching, at 2915 and 2845 cm^{-1} to aliphatic CH groups, at 1560 cm^{-1} is assigned to C=C stretching in aromatic rings, while at 1365 cm^{-1} is related to C-CH_3 groups bending [7,18]. Spectra of the zinc sulfate revealed peaks at 3170 cm^{-1} related to OH stretching, at 1640 cm^{-1} assigned to water, and at 1060 and 980 cm^{-1} linked to SO_4^- stretching (free sulfate groups) [22,23]. When $ZnSO_4$ was mixed with HA, the peaks assigned to OH stretching (3290 and 3170 cm^{-1}), aliphatic CH groups (2915 and 2845 cm^{-1}), water (1640 cm^{-1}), aromatic-C (1560 cm^{-1}), C-CH_3 groups bending (1365 cm^{-1}), and SO_4^- free groups (980 cm^{-1}) were the main features recorded in the HA-Zn spectra [7,22,23]. Additionally, for the $ZnSO_4$+HA mixture, new peaks at 1315 and 815 cm^{-1} were related to SO_2 stretching (sulfone) and, at 715 cm^{-1}, to C-S stretching (Methyl sulfone-CH_3-SO_2) [21]. The infrared peak at 1060 cm^{-1} related to SO_4^- stretching (free sulfate groups) from $ZnSO_4$ mixed with HA shifted to 1075 cm^{-1}, which is assigned for SO_2 stretching (alkyl sulfate salts), indicating the formation of $RSO_4^-M^+$, where R is the humic organic radical bonded to M $(Zn^{2+})^+$, the complexed metal [21].

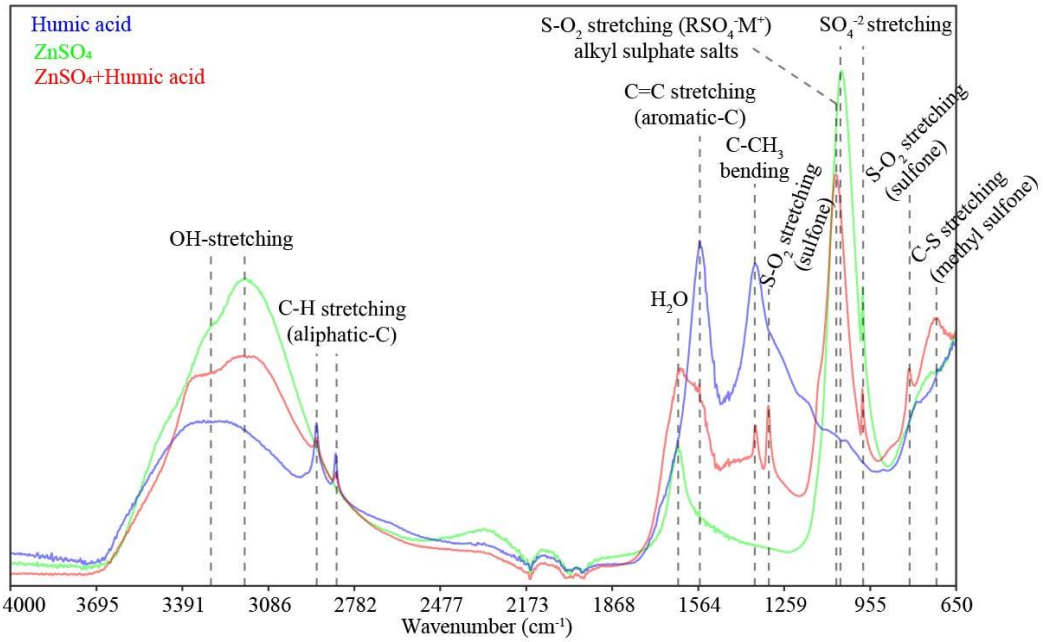

Figure 6. Peaks and the main features of chemical groups recorded by the Fourier-transform infrared spectroscopy analysis with attenuated total reflectance (FTIR–ATR). FTIR bands were assigned for pure samples of $ZnSO_4$ (Heptahydrate zinc sulfate), humic acid and the mixture of $ZnSO_4$ with humic acid.

3. Materials and Methods

3.1. Maize–Brachiaria Growth Conditions

3.1.1. Treatments and Growing Conditions

Effects of Zn fertilization, combined or not with HA, were tested on a sequence of maize–brachiaria grown in greenhouse conditions. The HA used in the experiment was extracted from Leonardite through a 0.05 mol L^{-1} KOH solution [24]. The main HA properties are described as follows: pH: 9.7, E4/E6 ratio: 4.84, C: 354.9 g kg^{-1}, N: 5.3 g kg^{-1}, Zn: 76.3 mg kg^{-1} [10,17]. The Zn source was the heptahydrate zinc sulfate ($ZnSO_4.7H_2O$) *pure per analysis* reagent [p.a.]). HA and Zn were added to Oxisols (two) with clay and organic matter (OM) contrasting contents. Plants were grown in pots filled with 1.8 kg Oxisol samples. In the Red Oxisol (RO), liming was performed to increase Ca and Mg optimum levels for maize-brachiara and raise pH to 6.0. Soil samples were incubated for 30 days with $CaCO_3$ and $MgCO_3$ (p.a.) at the 4:1 ratio, keeping the soil moisture close to 70% of soil maximum water-holding capacity (MWHC). In the Yellow Oxisol (YO), the soil pH and Ca content were already in levels

considered optimum for both maize and brachiaria plentiful growth; thus, liming was not performed, and only 15 mg kg^{-1} Mg was provided to maize at the sowing fertilization through the $MgSO_4.7H_2O$ p.a salt. After soil acidity correction, soil samples were dried and passed through a 2 mm sieve and used in the lab to determine the main physical and physicochemical properties of Oxisols (Table 1).

Table 1. Main chemical and physicochemical properties of Oxisols in which maize and brachiaria were cultivated.

Oxisol	pH	C(g kg^{-1})	Clay (g kg^{-1})	Silt (g kg^{-1})	Sand (g kg^{-1})	Available Zn (DTPA) (mg kg^{-1})
Red (RO)	6.4	19.8	770	100	130	0.93
Yellow (YO)	6.2	4.49	460	85	455	0.60

pH was determined in water at a ratio of 1:2.5 (*w/v*); C–total C determined (dry combustion) in an automatic TOC analyzer., silt and sand were determined by the Boyoucos method; Zn was determined by ICP-OES after extraction of Zn from the soil through the use of the DTPA extraction method.

Treatments were displaced in pots using a complete randomized design with three replicates in a 2 × 3 factorial scheme; thus, the first factor is related to soil type (RO and YO), while the second one is related to Zn fertilization strategies as follows: no-Zn fertilization and no-HA addition to Oxisols (1), only Zn fertilization (2), and Zn fertilization combined with HA application (3). Oxisols were treated with 20 mg kg^{-1} Zn and 50 mg kg^{-1} C-HA was added to soils when Zn was combined with HA. The rate of HA added to soils was based on previous studies carried out to set the optimum HA level to plentiful plant growth [9,25]. Treatments were homogeneously mixed with the whole soil mass at the beginning of maize cultivation.

At the maize sowing, nutrients were supplied to plants at the following concentrations: 135, 300, 100, 40, 0.81, 1.33, 3.66, 0.15, and 1.55 mg kg^{-1}, respectively, N, P, K, S, B, Cu, Mn, Mo, and Fe, using, respectively, the following sources: $NH_4H_2PO_4$, K_2SO_4, H_3BO_3, $CuSO_4.5H_2O$, $MnCl_2.4H_2O$, $(NH_4)6Mo_7O_{24}.4H_2O$ and $FeCl_3.6H_2O$ p.a. In sequence, the soil

moisture was kept at ~70% MWHC, then, five maize seeds were sowed per pot. Ten days after maize planting, thinning was performed, and two plants were left in each pot. The top-dressing fertilization was carried out at 15 and 20 days after maize planting, adding to soil 100 mg kg^{-1} N, which was provided as NH_4NO_3 p.a. Maize plants were grown in greenhouse conditions for 30 days.

To evaluate the Zn fertilization residual effect after the maize cultivation, ten seeds of *Brachiaria brizantha* cv. Paiaguás were planted in the same pot used to grow maize. Ten days after planting, thinning was done, and two brachiaria plants remained in each pot. The brachiaria planting fertilization was carried out by adding to soil 100 mg kg^{-1} N and 100 mg kg^{-1} K, respectively, supplied through the NH_4NO_3 and KCl p.a. salts. The top-dressing fertilization of brachiaria was carried out at 15, 25, and 35 days after planting, using 100 mg kg^{-1} N, which provided to plants as NH_4NO_3 p.a. in each top-dressing fertilization. The brachiaria was grown for 45 days, and Zn was only furnished to maize plants; thus, brachiaria was nourished only with the residual Zn found soils previously cultivated with maize.

3.1.2. Soil and Solution Analysis

At the beginning of each cultivation, after 12 h of planting and keeping the soil moisture at ~70% MWHC, an aliquot of the soil solution (20 mL) was collected using the Suolo Acqua® sampler [26]. The soil solution sampler was inserted in the middle of the pot during its filling with soil. Soil solution samples were filtered through a 0.45 µm membrane, and their pH values were determined through a Mettler Toledo bench pH meter. Zn content in soil solution (soluble Zn) was determined by inductively coupled plasma optical emission spectroscopy (ICP-OES). After 18 h of planting, it was collected 30 g of soil in each experimental unit, then the soil samples were dried and sieved (2 mm). The pH of soil samples were determined in a suspension of 1 g soil plus 2.5 mL water. Available Zn content in soil (soil Zn-DTPA) was extracted by

the DTPA soil test [27], and Zn was determined in an ICP-OES machine. A sampling of solution and the whole soil was carried out for each experimental unit, thus, totaling three replicates for each treatment investigated.

3.1.3. Biomass Production and Zn in Shoot

At the end of maize or brachiaria cultivation, plants were harvested, separated into shoot and root, and dried in an oven with air circulation at 60 °C until constant weight. The dried biomass was weighed, and shoot (SDM) and root (RDM) dry matter production was determined. The total dry matter was obtained by summing SDM plus RDM. The root: shoot ratio was calculated by dividing SDM by RDM. The shoot dried biomass was sieved (1-mm) and digested in a mixture of nitric and perchloric acids at a 4:1 ratio [28], and Zn content in the shoot was, in sequence, determined in an ICP-OES machine. Based on the SDM and Zn content in a shoot of each experimental unit, Zn accumulation was calculated, as follows: ZnAc (mg pot^{-1}) = SDM (g pot^{-1}) × ZnC (mg g^{-1}), in which ZnAc is the Zn accumulated in shoot; and ZnC is the Zn content in maize or brachiaria shoots.

3.2. Infrared Spectroscopy

The spectra of HA and $ZnSO_4.7H_2O$ samples were recorded by Fourier transform infrared spectroscopy (FTIR) with attenuated total reflectance. The same proportion of HA and $ZnSO_4.7H_2O$ used to treat maize plants was dissolved in water; in sequence, the mixture was dried at 60ºC until constant weight, then, the FTIR analysis was performed. FTIR was performed in an Agilent® Cary 630 spectrometer with a ZnSe crystal. The measurements were performed in the wavenumber range of 4000 to 650 cm^{-1} with a resolution of 4 cm^{-1}. The FTIR spectra dataset was pre-processed using the background correction and dataset normalization procedures [29].

3.3. Statistical Analysis

All statistical analysis was carried out using the base, stats, agricolae, corrplot, factoextra and FactoMineR packages of the R software [30–35]. Effects of treatment on plant and soil means were compared through the Tukey test ($p < 0.05$) after the assumptions of analysis variance (ANOVA) were attended ($p < 0.05$). Before the ANOVA test, we assessed the normality distribution (Shapiro–Wilk's Test), homogeneity (Bartlett's Test), and independence of the observations and residuals (Durblin–Watson's test). Principal component analysis (PCA) was performed after removing the no-Zn fertilization data from the whole dataset due to the high negative influence of the absence and severe deficiency of Zn on plant growth (biomass). In sequence, the dataset originating from the maize or brachiaria experiments was staggered separately, and PCA was performed for the dataset of each crop grown in both Oxisols. The Pearson's linear correlation matrix ($p < 0.05$) was also carried out, aiming to validate clusters and potential relationships of soil and plant attributes as outcomes of PCA (Supplementary Materials 1 and 2). Before PCA and correlation analysis, each variable from the dataset was tested regarding its normality through the Shapiro–Wilk test, and once the normality was confirmed, the analysis was performed.

4. Discussion

When Zn is mixed with HA, free sulfates were kept in the complex formed (SO_4^{2-} stretching at 980 cm^{-1}) (Figure 6). Additionally, bonds related to sulfone groups ($S\text{-}O_2$ stretching and C-S methyl sulfone) are formed, which is indicative of the interaction of HA-with $ZnSO_4$ and synthesis of Zn–HA complexes. Sulfur groups present in the mixture of HA+$ZnSO_4$ are indicative of Zn–HA complexation. This was possibly due to the presence of oxygen-, nitrogen-, and sulfur-containing functional groups in the HA structure [15,20]. Another peak indicating the Zn complexation with HA is recorded at 1075 cm^{-1}, which is an

FTIR band related to the formation of a new spectral signature related to $RSO_4^-M^+$ groups, where R is the C-humic functional group and M^+ is the complexed metal [21]. FTIR bands indicated that Zn from sulfate was complexed into the humic matrix. The peak recorded at 3290 cm^{-1} and related to OH stretching is more pronounced when $ZnSO_4$ is mixed with HA, compared to the intact HA spectral signature, indicating the increase of hydration and production of Zn aqueous complexes [7]. Hydroxide ions (OH^-) found in carboxylic and phenolic groups and aliphatic domains of HA play a key role in forming soluble metal complexes [15], resembling the spectral signature of the Zn--humic acid complex synthesized in this study.

The specific spectral signature of Zn_complexes demonstrated the potential of FTIR spectroscopy in identifying Zn sulfate bonded to HA, compared to the over bands recorded for the intact HA. The interaction of HA with Zn was relevant to show changes in functional groups of the new configuration and spectral signature of HA as an organic ligand for Zn, as well as to indicate and changes in the intensity of FTIR bands' shift [7]. The mechanisms and processes of Zn interaction with HA included ionic or uncoordinated forms, unidentate complexes, bidentate chelates, and bidentate bridging coordination bonds [7]. The interaction of organic ligands with Zn is beneficial to Zn supplying to plants, considering that free Zn ions are prone to react with soil components through sorption and precipitation, which are the main processes regulating Zn availability in soils [4,11,16].

Zn deficiency is a global issue [2,4] and is frequently reported in tropical soils [5]. Plants have different sensitivities to Zn deficiency in the soil. While maize (*Zea mays*) has a high sensitivity, grass such as *Brachiaria brizantha* is known to tolerate Zn deficiency [2]. The natural deficiency of Zn in tropical soil limits crop production, as occurred in this study. Both maize and brachiaria growth were hampered by the limited supply of Zn in both Oxisols with contrasting OM and clay contents. Thus, regardless of the Oxisol cultivation, the maize and

brachiaria biomasses are sharply reduced when the supply of Zn is restricted in both highly weathered soils (Figures 2 and 4).

Zn deficiency is frequently reported in other studies conducted in low pH tropical soils with reduced P availability [5]. Zn is prone to interact with the surface of minerals found in soil colloids negatively charged, which reduces its availability to crops; liming increases the adsorption of Zn into soil colloids due to the increased density of negative charges on the surface of clay minerals and Fe and Al (hydro) oxides [2,10].

In this study, the reduction of soil Zn deficiency by Zn fertilization was followed by the significant effect of solution pH on solution Zn. Thus, changes in Zn availability affected SDM, TDM, and the accumulation of Zn in shoots (Figure 5a,b, Supplementary Material 1 and 2). A negative correlation between the pH and solution Zn verified in the study was aligned with results reported in other work relating Zn supplying to coffee plants treated with variable rates of HA [10]. Another factor regulating Zn availability in soils is the OM and its pools; Zn interacts with organic radicals present in the OM structure, forming stable complexes capable of reducing Zn availability in soil [2].

However, the OM is also a source of soluble organic compounds capable of binding micronutrients through the formation of soluble organo-metal complexes [36]. In this study, RO, which had a higher OM content than YO, presented a lower soil Zn-DTPA content (maize experiment). However, RO had a greater Zn-DTPA content (Figure 1c) and produced a higher maize biomass and Zn in the shoots than the plants grown in YO (Figure 2). Thus, soil type is a key issue influencing the magnitude of plant response to Zn fertilization [2,4], as well as the role played by HA on plant nutrition and growth [8].

Regarding the soil's physical and physicochemical properties, the texture (clay content), OM, and pH were the factors that sharply influenced soil Zn availability. Soil properties are capable of modulating Zn interaction, adsorption, and precipitation with soil

components, including organic matter pools [1,2,4]. When associated with organic ligands, the Zn availability to crops relies on the chemical stability, solubility, and reactivity of the bonds formed between the humic matrix and the metal in the complexes formed [7,8]. Thus, RO, the soil with the highest OM and clay contents and the lowest pH is initially more prone to adsorb Zn than YO (Figure 1).

However, soluble Zn and maize biomass production were higher in RO over YO, signaling the possible formation of soluble to complexes with natural OM fractions present in RO, a key issue to be considered to supply Zn to plants in cultivation conditions where HA and Zn are simultaneously added to the soil (Figure 1). A low supply of soluble Zn affects plant growth, mirrored by the increased root: shoot ratio of maize plants grown in the soil with low Zn contents in solution (Figure 1, 2, and 6a). Humic acid acts to relieve the stress of low contents of readily available Zn in YO, and reduces the maize root: shoot ratio, which is a signal of suitable conditions for plentiful plant growth.

An increase of the root: shoot ratio is strongly related to the capacity of the growth medium (soil) to nourish plants. In low-fertility soils, plants promote a greater release of C-exudates for root elongation, thus consuming energy that could be eventually driven to increase shoot biomass [37,38]. Increased root proliferation at the expense of shoot could result in a decrease in the plant above biomass. It is reported that an increase in the root: shoot ratio resembles the low levels of soluble Zn in the growth medium [38]. In this study, the negative correlation between soluble Zn and the root: shoot ratio was confirmed in the maize experiment (Figure 5, Supplementary Material 1), though the main factor of stress to plants was the increase of solution pH, followed by an increased root: shoot ratio, and reduced maize and brachiaria biomass production (Figure 5, Supplementary Materials 1 and 2).

Contrary to the maize experiment, even with a higher maize biomass production and Zn accumulation in RO over YO, the conditions of YO soil solution were essential to improve

brachiaria growth (brachiaria) (Figures 3 and 4). However, the soil Zn-DTPA was higher in RO over YO (Figure 3), indicating that the organic-Zn complexes in RO, naturally richer in OM than YO, possibly reduced the soil Zn-DTPA in the maize experiment; thus, less residual Zn was thought to be supplied to brachiaria plants. The effect aforementioned signals that the initial formation of Zn complexes with natural OM pools of RO is less stable over time, thus not suitable to attend Zn plant demand in the long term.

In the brachiaria experiment, the soil type effect on plants relies on HA application (Figures 3 and 4). Despite the higher soil and solution pH of RO over YO, when brachiaria was cultivated in sequence to maize, the HA application reduced the solution pH in YO, with values similar to RO (Figure 3). This effect possibly eliminated the formation of insoluble forms of Zn as the soil pH was increased [4].

In addition to the soil type effect, HA increased the soluble Zn contents in the two Oxisols in both maize and brachiaria experiments, besides increasing soil Zn-DTPA contents (Figures 1 and 3). The stoichiometry of the reaction between HA and Zn is an important factor regulating the amount of soluble Zn in Zn–HA complexes [7]. When Zn was added to soil at low concentration (5 mg kg^{-1}), mainly in soils with low OM contents, the use of 50 mg kg^{-1} C as HA reduced Zn in soil solution, which was mainly due to the specific adsorption and formation of Zn–HA complexes of high stability, reducing Zn uptake by crops [9]. However, in this study, with an adequate concentration of Zn (20 mg kg^{-1}) added to soil, it was demonstrated that HA acts positively on Zn contents in soil solution, as well as on crop Zn nutrition (Figures 1 and 3).

In solution, the main forms of Zn found are free hydrated $Zn(6H_2O)^{2+}$ and soluble organic complexes. When HA is applied together with Zn sulfate, Zn free ions become partially complexed by HA radicals, as observed by the FTIR spectra, which demonstrated the production of aqueous Zn-complexes and the formation of $RSO_4^-M^+$ bonds (Figure 6). The

aforementioned factors contribute to an increase in the Zn content in the soil solutions of both Oxisols due to Zn's bond to organic molecules such as Has, thus contributing to the improvement of Zn availability in soil [4,8,15]. When Zn interacts with organic molecules, there are new forms of Zn capable of generating in soil-soluble Zn chemical species, which improve Zn diffusion from solution to plant roots [4]. The increased release of Zn from the solid phase to soil solution in response to HA application was already demonstrated elsewhere [9]. Although the Zn in the soil solution is a small fraction of soil total Zn, this is the Zn pool readily available to plants; thus, Zn in soil solution is a key issue regulating Zn uptake by crops [1,4,26].

The role played by HA on soil physicochemical properties and nutrient available contents are claimed as indirect effects of HS on plants. Humic acid changes the growing medium in a way that plant growth is positively affected [8,9,11,15,16]. Besides the indirect effect, in contact with plant tissues, HA plays a positive role in crop nutrition and growth [11,12]. The direct effects of HS on plants include increased H^+-ATPase membrane activity, improved cell plasmatic membrane permeability, regulation of the levels and activity of reactive oxygen species (ROS), increased activity of nutrient transporters, control of nutrient translocation, and regulation of several plant physiological processes [8,9,11–13,15,16].

Recently, it was demonstrated that metal-HA complexes are a source of readily available nutrients, besides increasing the bioactivity of humic molecules on plants [20]. Thus, the direct and indirect effects of HA occur simultaneously, improving plant nutrition, growth, and yield [9,11,15,20]. In this study, the potential direct effects of HA on plants are indicated by the presence of peaks at 2915, 2845, 1560, and 1365 cm^{-1} in the FTIR spectra when HA was mixed with $ZnSO_4$ (Figure 4). These FTIR spectral bands are indices of HA bioactivity on plants, considering that these FTIR spectral fingerprints were positively related to improved lateral root emergence in maize plants [14].

When HA was combined with Zn fertilization in RO, the maize biomass production was improved and positively related to Zn contents in soil solution. However, Zn in maize shoot was not augmented (Figures 1 and 2). Despite the indirect effect of HA on soil solution attributes, both direct and indirect (soil) effects of HA on plants occurred simultaneously, considering that the increased availability of Zn in soil solution did no improve plant Zn uptake, even with the increase in maize biomass production. HA positively affected brachiaria growth in RO, improving root proliferation and Zn uptake (Figures 3 and 4). When HA was added to YO, the brachiaria biomass increased, and plant Zn nutrition was improved (Figure 4). This effect of HA on plants is more pronounced in YO over RO (Figure 4).

The results reported in this study showed that HA promoted positives effects on maize, and guaranteed a residual Zn for brachiaria plants grown in sequence to maize, in a soil type-dependent way. However, maize–brachiaria cultivated in a sequence is widely performed in Brazilian cropping areas [3]; there is no study reporting how HA-Zn interaction exerts influence on the brachiaria cultivated in sequence to maize. Evaluating only the effect of HA-Zn interaction in single cultivation of coffee seedlings, Just et al. [10] reported that the application of 50 mg kg^{-1} C-HA increased the solution Zn in alkalinized soils (pH > 7.2), probably due to the Zn–HA complexation. In this study, the main and residual effects of Zn fertilization+HA are related to the increase in the solution Zn contents. In addition, in the soil with the lower OM content (YO), HA acted as a buffer for soil acidification, thus, favoring Zn acquisition and growth of brachiaria cultivated in sequence to maize.

The results of this study showed that humic increased the release of Zn from Oxisols, mainly to soil solution, increased Zn availability, transport and uptake by crops. Release of Zn relies on HA concentration, solution pH, and soil types, all of which influenced the degree of Zn complexation, precipitation, and amount of Zn moving from solid to liquid soil phase [39]. Overall, precipitation reactions, formation of Zn–HA complexes, and adsorption of humic acid

to soil components reduce the amount of Zn released from soil [39]. Parent materials of highly weathered Brazilian soils are poor natural sources of Zn. Thus, both under natural vegetation and cultivation conditions, the Brazilian tropical soils are limited in their capacity to nourish grasses (high-demanding Zn crops) with adequate Zn levels. Even in enriched OM soils, organic compounds are chemically stabilized or bonded to clay and Fe and Al oxides in tropical soils. Thus, it is suitable to add some exogenous humic materials to improve Zn nutritional status and growth of maize-brachiara in Brazilian crop fields. Successive cultivation of maize–brachiaria is very common in the large area of crop-livestock integrated systems established in Brazil, and brachiaria usually is supposed to cope with the residual Zn derived from the fertilization of the first crop of rotation. In this study, it was demonstrated that the Zn soil chemistry and forms are affected by the presence of Zn–HA complexes in highly weathered soils, with a positive effect on Zn uptake and growth of maize and brachiaria. In line with Boguta et al. (6), in a soil type-dependent way, the understanding of Zn–HA interactions is the first step to improve Zn fertilization in tropical soils and a suitable strategy to be used in the synthesis of Zn–HA fertilizers.

5. Conclusions

FTIR spectroscopy revealed the complexation of Zn sulfate by HA through sulfone and carbon functional groups. A significant portion of Zn fertilizer applied to Oxisols is not available for the first crop (maize), but it is prone to be acquired by brachiaria plants. It was demonstrated that Zn in solution is sharply increased by the combined use of Zn sulfate and HA. The humic acid that complexed to $ZnSO_4$ increased Zn contents in Oxisols solution while reducing the negative reactions (e.g., adsorption and precipitation) of Zn in the whole soil. In the lower organic matter Oxisol, the use of HA is capable of assuring adequate supplying of residual Zn and increasing growth of brachiaria grown in sequence to maize. Oxisol organic

matter content is a key factor regulating the action of HA on soil Zn availability and plant growth.

Supplementary Materials: The following are available online. Supplementary Material 1: The Pearson's linear correlation matrix for soil attributes and maize traits. * and ** significant correlation of soil and plant attributes at $p < 0.05$ and $p < 0.01$, respectively; blue ellipse with right sloping top: positive correlation; red ellipse with left sloping top: negative correlation. SDM, RDM and TDM: shoot, root and total dry matter production, respectively; R:S ratio: ratio of shoot over proportion between the production of (SDM) over root dry matter in relation to R(RDM); Zn accumulation: Zn accumulated in maize shoots. Supplementary Material 2 The Pearson's linear correlation matrix for soil attributes and brachiaria traits. * and ** significant relationships between soil and plant traits at $p < 0.05$ and $p < 0.01$, respectively; blue ellipse with right sloping top: positive correlation; red ellipse with left sloping top: negative correlation. SDM, RDM and TDM: brachiaria shoot, root and total dry matter production, respectively; R:S ratio: ratio of shoot (SDM) over root dry matter (RDM); Zn accumulation: Zn accumulated in brachiaria shoots.

Author Contributions: Conceptualization, E.G.M., C.A.S. and K.J.; methodology, E.G.M. and C.A.S.; software, E.G.M.; validation, E.G.M. and C.A.S.; formal analysis, E.G.M.; investigation, E.G.M. and C.A.S.; resources, E.G.M., C.A.S. and K.J.; data curation, E.G.M.; writing—original draft preparation, E.G.M., C.A.S. and K.J.; writing—review and editing, E.G.M., C.A.S. and K.J.; visualization, E.G.M; supervision, C.A.S. and K.J.; project administration, C.A.S.; funding acquisition, C.A.S. and K.J. All authors have read and agreed to the published version of the manuscript.

Funding: This research was funded by the Coordination For The Improvement Of Higher Education Personnel (CAPES), grant number CAPES-PROEX/AUXPE 593/2018, the National Council For Scientific And Technological Development (CNPq), grant numbers 303899/2015-8 and 307447/2019-7, and the Foundation For Research Of The State Of Minas Gerais (FAPEMIG). The Federal University Of Lavras (UFLA) is an equal opportunity provider and employer. Keiji Jindo wishes to acknowledge financial support (grant #3710473400-1).

Institutional Review Board Statement: Not applicable.

Informed Consent Statement: Not applicable.

Data Availability Statement: Not applicable

Acknowledgments: Many thanks to the Coordination for the Improvement of Higher Education Personnel (CAPES) (CAPES-PROEX/AUXPE 593/2018), the National Council for Scientific and Technological Development (CNPq) (303899/2015-8 and 307447/2019-7 grants), and the Foundation for Research of the State of Minas Gerais (FAPEMIG) for the financial support and scholarships. UFLA is an equal opportunity provider and employer. Keiji Jindo wish to acknowledge financial support (3710473400-1).

Conflicts of Interest: The authors declare no conflicts of interest.

Sample Availability: Samples of humic acid, $ZnSO_4.7H_2O$ and the mixture of humic acid with $ZnSO_4.7H_2O$ are available from the authors.

References

1. Broadley, M.; Brown, P.; Cakmak, I.; Rengel, Z.; Zhao, F. Function of nutrients: micronutrients. In: Marschner H.Mineral nutrition of higher plants; Elsevier: Amsterdam, The Netherlands, 2012; pp. 191–248.
2. Alloway, B.J. Soil factors associated with zinc deficiency in crops and humans. Environ. Geochem. Health 2009, 31, 537–548, doi:10.1007/s10653-009-9255-4.
3. Anghinoni, G.; Tormena, C.A.; Lal, R.; Zancanaro, L.; Kappes, C. Enhancing soil physical quality and cotton yields through diversification of agricultural practices in central <scp>Brazil</scp>. L. Degrad. Dev. 2019, 30, 788–798, doi:10.1002/ldr.3267.
4. Montalvo, D.; Degryse, F.; da Silva, R.C.; Baird, R.; McLaughlin, M.J. Agronomic Effectiveness of Zinc Sources as Micronutrient Fertilizer; Elsevier Inc.: Amsterdam, The Netherlands, 2016; vol. 139; ISBN 9780128047736.
5. Lopes, A.S.; Guimarães Guilherme, L.R. A career perspective on soil management in the Cerrado region of Brazil; Advances in Agronomy, 2016; vol. 137; ISBN 9780128046920.
6. Stevenson, F.J. Humus chemistry: genesis, composition, reactions; John Wiley and Sons: New York, NY, USA, 1994; ISBN 978-0-471-59474-1.
7. Boguta, P.; Sokołowska, Z. Interactions of Zn (II) Ions with Humic Acids Isolated from Various Type of Soils. Effect of pH, Zn Concentrations and Humic Acids Chemical Properties. PLoS One 2016, 11, 1–20, doi:10.1371/journal.pone.0153626.
8. Rose, M.T.; Patti, A.F.; Little, K.R.; Brown, A.L.; Jackson, W.R.; Cavagnaro, T.R. A Meta-Analysis and Review of Plant-Growth Response to Humic Substances. Advances in Agronomy; 2014; pp. 37–89 ISBN 0065-2113.
9. Morais, E.G.; Silva, C.A.; Maluf, H.J.G.M. Soaking of Seedlings Roots in Humic Acid as an Effective Practice to Improve Eucalyptus Nutrition and Growth. Commun. Soil Sci. Plant Anal. 2021, 1–17, doi:10.1080/00103624.2021.1885686.
10. Justi, M.; Morais, E.G.; Silva, C.A. Fulvic acid in foliar spray is more effective than humic acid via soil in improving coffee seedlings growth. Arch. Agron. Soil Sci. 2019, doi:10.1080/03650340.2019.1584396.
11. Olaetxea, M.; De Hita, D.; Garcia, C.A.; Fuentes, M.; Baigorri, R.; Mora, V.; Garnica, M.; Urrutia, O.; Erro, J.; Zamarreño, A.M. Hypothetical framework integrating the main mechanisms involved in the promoting action of rhizospheric humic substances on plant root- and shoot-growth. Appl. Soil Ecol. 2018, 123, 521–537, doi:10.1016/j.apsoil.2017.06.007.
12. Tavares, O.C.H.; Santos, L.A.; Ferreira, L.M.; Sperandio, M.V.L.; da Rocha, J.G.; García, A.C.; Dobbss, L.B.; Berbara, R.L.L.; de Souza, S.R.; Fernandes, M.S. Humic acid differentially improves nitrate kinetics under low- and high-affinity systems and alters the expression of plasma membrane H + -ATPases and nitrate transporters in rice. Ann. Appl. Biol. 2017, 170, 89–103, doi:10.1111/aab.12317.
13. Jindo, K.; Martim, S.A.; Navarro, E.C.; Pérez-Alfocea, F.; Hernandez, T.; Garcia, C.; Aguiar, N.O.; Canellas, L.P. Root growth promotion by humic acids from composted and non-composted urban organic wastes. Plant Soil 2012, 353, 209–220, doi:10.1007/s11104-011-1024-3.
14. Aguiar, N.O.; Novotny, E.H.; Oliveira, A.L.; Rumjanek, V.M.; Olivares, F.L.; Canellas, L.P. Prediction of humic acids bioactivity using spectroscopy and multivariate analysis. J. Geochemical Explor. 2013, 129, 95–102, doi:10.1016/j.gexplo.2012.10.005.
15. Nardi, S.; Schiavon, M.; Francioso, O. Chemical structure and biological activity of humic substances define their role as plant growth promoters. Molecules 2021, 26, doi:10.3390/molecules26082256.

16. Shah, Z.H.; Rehman, H.M.; Akhtar, T.; Alsamadany, H.; Hamooh, B.T.; Mujtaba, T.; Daur, I.; Al Zahrani, Y.; Alzahrani, H.A.S.; Ali, S.; et al. Humic substances: Determining potential molecular regulatory processes in plants. Front. Plant Sci. 2018, 9, 1–12, doi:10.3389/fpls.2018.00263.
17. Morais, E.G.; Silva, C.A.; Rosa, S.D. Nutrient acquisition and eucalyptus growth affected by humic acid sources and concentrations. Semin. Agrar. 2018, 39, 1417–1435, doi:10.5433/1679-0359.2018v39n4p1417.
18. Rosa, S.D.; Silva, C.A.; Maluf, H.J.G.M. Wheat nutrition and growth as affected by humic acid-phosphate interaction. J. Plant Nutr. Soil Sci. 2018, 181, 870–877, doi:10.1002/jpln.201700532.
19. Pinheiro, P.L.; Passos, R.R.; Peçanha, A.L.; Canellas, L.P.; Olivares, F.L.; de Sá Mendonça, E.S. Promoting the growth of Brachiaria decumbens by humic acids (HAs). Aust. J. Crop Sci. 2018, 12, 1114–1121, doi:10.21475/ajcs.18.12.07.PNE1038.
20. Zanin, L.; Tomasi, N.; Cesco, S.; Varanini, Z.; Pinton, R. Humic substances contribute to plant iron nutrition acting as chelators and biostimulants. Front. Plant Sci. 2019, 10, 1–10, doi:10.3389/fpls.2019.00675.
21. Socrates, G. Infrared and Raman characteristic group frequencies: tables and charts; John Wiley and Sons, Ltd,: Chichester, UK 2004; ISBN 978-0-470-09307-8.
22. Sadeek, S.A. Preparation, infrared spectrum and thermal studies of [Zn2(H2O)4(SO4)2] complex formed by the reaction of urea with zinc (II) sulphate. J. Phys. Chem. Solids 1993, 54, 919–922, doi:10.1016/0022-3697(93)90219-H.
23. Saha, J.; Podder, J. Crystallization Of Zinc Sulphate Single Crystals And Its Structural, Thermal And Optical Characterization. J. Bangladesh Acad. Sci. 2011, 35, 203–210, doi:10.3329/jbas.v35i2.9426.
24. Swift, R.S. Organic Matter Characterization. In Methods of Soil Analysis: Part 3 Chemical Methods; Soil Science Society of America: Madinson, USA, 1996; pp. 1011–1069.
25. Alvarez, J.M. Influence of soil type on the mobility and bioavailability of chelated zinc. J. Agric. Food Chem. 2007, 55, 3568–3576, doi:10.1021/jf063236g.
26. Carmo, D.L. do; Silva, C.A.; Lima, J.M. de; Pinheiro, G.L. Electrical Conductivity and Chemical Composition of Soil Solution: Comparison of Solution Samplers in Tropical Soils. Rev. Bras. Ciência do Solo 2016, 40, doi:10.1590/18069657rbcs20140795.
27. Brown, A.L.; Quick, J.; Eddings, J.L. A comparison of analytical methods for soil zinc. Soil Sci. Soc. Am. J. 1971, 35, 105–107.
28. Kalra, Y. Handbook of reference methods for plant analysis; CRC press: Boca Raton, FL, USA 1997; ISBN 9780367448004.
29. Gautam, R.; Vanga, S.; Ariese, F.; Umapathy, S. Review of multidimensional data processing approaches for Raman and infrared spectroscopy. EPJ Tech. Instrum. 2015, 2, doi:10.1140/epjti/s40485-015-0018-6.
30. Mendiburu, F. *Agricolae: Statistical Procedures for Agricultural Research*; 2020.
31. R Core Team R: *A Language and Environment for Statistical Computing;* 2020.
32. Wickham, H.; Averick, M.; Bryan, J.; Chang, W.; McGowan, L.; François, R.; Grolemund, G.; Hayes, A.; Henry, L.; Hester, J.; et al. Welcome to the Tidyverse. J. Open Source Softw. 2019, 4, 1686, doi:10.21105/joss.01686.
33. Wei, T.; Simko, V. R package "corrplot": Visualization of a Correlation Matrix 2017.
34. Kassambara, A.; Mundt, F. factoextra: Extract and Visualize the Results of Multivariate Data Analyses 2020.
35. Lê, S.; Josse, J.; Husson, F. FactoMineR : An R Package for Multivariate Analysis. J. Stat. Softw. 2008, 25, doi:10.18637/jss.v025.i01.
36. Wang, K.; Xing, B. Structural and Sorption Characteristics of Adsorbed Humic Acid on Clay Minerals. J. Environ. Qual. 2005, 34, 342–349, doi:10.2134/jeq2005.0342.
37. Ikka, T.; Ogawa, T.; Li, D.; Hiradate, S.; Morita, A. Effect of aluminum on metabolism of organic acids and chemical forms of aluminum in root tips of Eucalyptus camaldulensis Dehnh. Phytochemistry 2013, 94, 142–147, doi:10.1016/j.phytochem.2013.06.016.

38. Morais, E.; Silva, C.A.; Maluf, H.J.G.M. UV-visible Spectroscopy as a New Tool to Predict the Bioactivity of Humic Fragments Induced by Citric / Oxalic Acids on Eucalyptus Nutrition and Growth. Commun. Soil Sci. Plant Anal. 2020, 00, 1–16, doi:10.1080/00103624.2020.1849266.
39. Güngör, E.B.Ö.; Bekbölet, M. Zinc release by humic and fulvic acid as influenced by pH, complexation and DOC sorption. Geoderma 2010, 159, 131–138, doi:10.1016/j.geoderma.2010.07.004.

Supplementary material

Article

Humic Acid Improves Zn Fertilization in Oxisols Successive ly Cultivated with Maize–Brachiaria

Everton Geraldo de Morais [1], Carlos Alberto Silva[1,*] and Keiji Jindo[2,*]

[1]Soil Science Department, Federal University of Lavras, Lavras, Minas Gerais, 37200-000, Brazil; evertonmoraislp@gmail.com

[2]Agrosystems Research, Wageningen University & Research, P.O. Box 16, 6700 AA, Wageningen, The Netherlands

[*]Correspondence: csilva@ufla.br (C.A.S.); keiji.jindo@wur.nl (K.J.)

Supplementary material 1. The Pearson's linear correlation matrix for soil attributes and maize traits. * and ** significant relationship of soil and plant attributes at $p<0.05$ and $p<0.01$, respectively; blue ellipse with right sloping top: positive relationship; red ellipse with left sloping top: negative correlation. SDM, RDM and TDM: shoot, root and total dry matter production, respectively; R:S ratio: ratio of shoot over (SDM) over root dry matter (RDM); Zn accumulation: Zn accumulated in maize shoots.

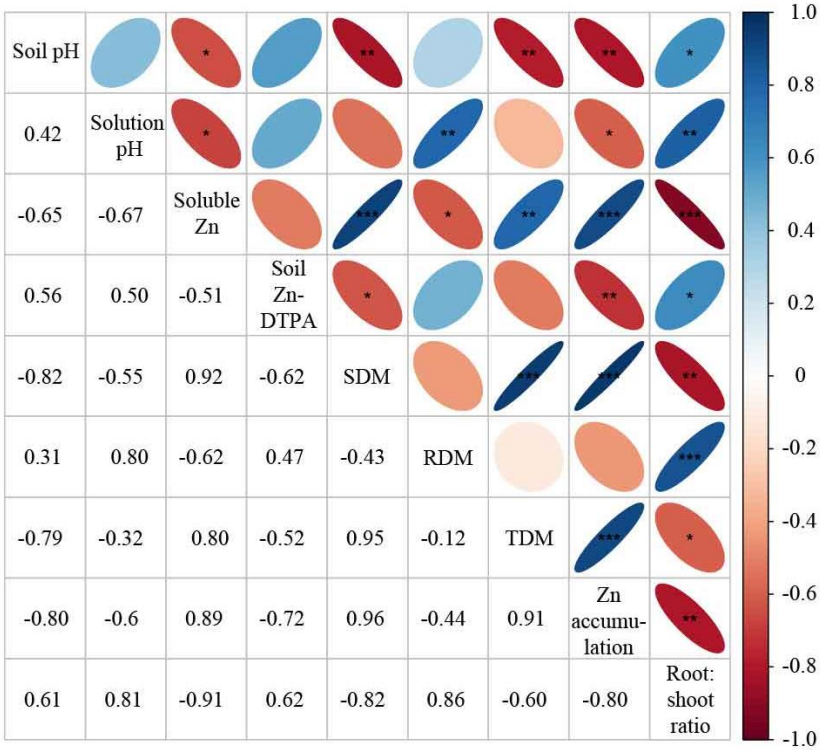

Supplementary material 2. The Pearson's linear correlation matrix for soil attributes and brachiaria traits. * and ** significant relationhips between soil and plant traits at $p<0.05$ and $p<0.01$, respectively; blue ellipse with right sloping top: positive correlationship; red ellipse with left sloping top: negative correlationship. SDM, RDM and TDM: brachiaria shoot, root and total dry matter production, respectively; R:S ratio: ratio of shoot (SDM) over root dry matter (RDM); Zn accumulation: Zn accumulated in brachiaria shoots.

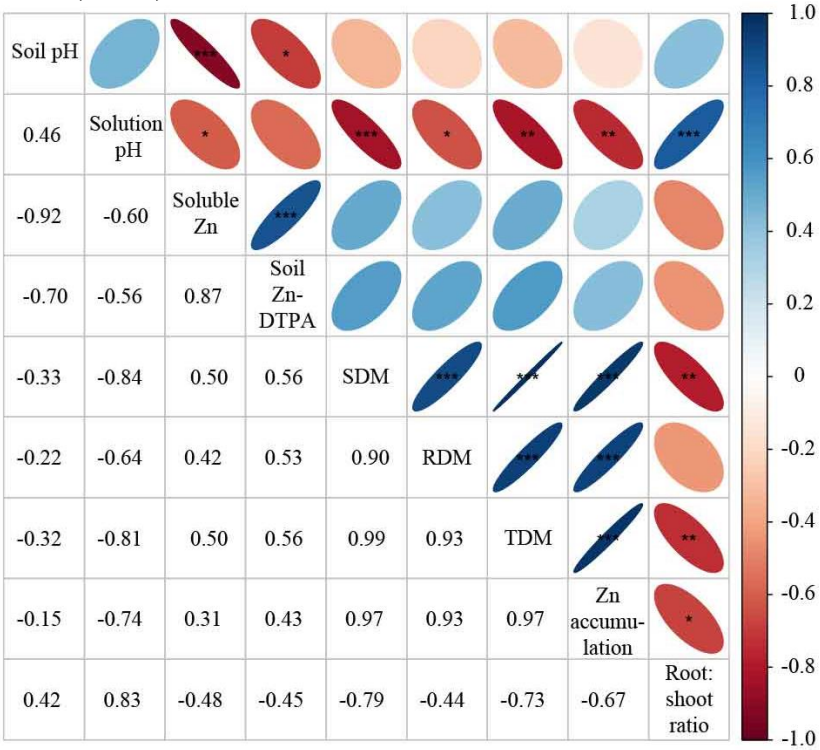

Preliminary version of manuscript edited following the rules of ACS Agricultural Science & Technology Journal

Synthesis of slow-release humic acid-based zinc organomineral fertilizers and their agronomic value for successively grown maize and brachiaria in contrasting Oxisols

Everton G. Morais[†*], Carlos A. Silva[†] and Henrique J. G. M. Maluf[‡]

[†] Departament of Soil Science, Federal University of Lavras, Av. Doutor Sylvio Menicucci 1001, zip code: 37200-900, Lavras-Minas Gerais, Brazil.

[‡]Galvani Fertilizantes, Avenida Luís Eduardo Magalhães, 2071, Jardim das Acácias, 47.850-000, Luís Eduardo Magalhães-Bahia, Brazil.

[*] Corresponding author: evertonmoraislp@yahoo.com.br

Abstract: Zinc (Zn) organomineral fertilizers (OMFs) contain Zn complexes less prone to react with soil components. However, there are few synthesis routes of Zn-OMFs promoting Zn complexation with a slow Zn release and sustained delivery of Zn for plants successively grown in contrasting Oxisols. This study aimed to synthesize and characterize four Zn-OMFs based on humic acid, indicate Zn complexation through infrared spectroscopy and evaluate the features and patterns of OMFs over zinc sulfate ($ZnSO_4$) on the kinetics of Zn release from fertilizer, diffusion essays in Oxisols and biomass production and Zn and P accumulated in the shoot for successively grown of maize and brachiaria in two Oxisols with texture and soil organic matter constrasting. Infrared analysis indicated that Zn was complexed in OMFs through S and C groups. Zinc complexed in OMFs was gradually released; consequently, Zn diffusion was reduced in both Oxisols. OMFs initially reduced the Zn content in soil solution. At least one of the OMFs over $ZnSO_4$ increased the maize biomass production, and Zn accumulated in the shoot during the first cultivation. The OMFs over $ZnSO_4$ may have a higher

Zn residual effect in Oxisols for brachiaria grown cultivated after maize, thus, increasing the brachiaria biomass production and Zn accumulated in the shoot in effect depending on OMFs properties controlled by their synthesis route interacting with Oxisol properties. At least one OMFs with Zn complexed by organic molecules increased the P availability in the soil and P uptake by maize and brachiaria plants. Overall, maize and brachiaria growth and Zn and P nutrition were improved by at least one of the OMFs synthetized over $ZnSO_4$ due to Zn complexed by organic molecules from humic acid promoting a slow Zn release from OMFs.

Keywords: organometallic complexes, residual Zn; zinc-humic acid synergy, tropical soils, ATR-FTIR groups.

Graphical Abstract

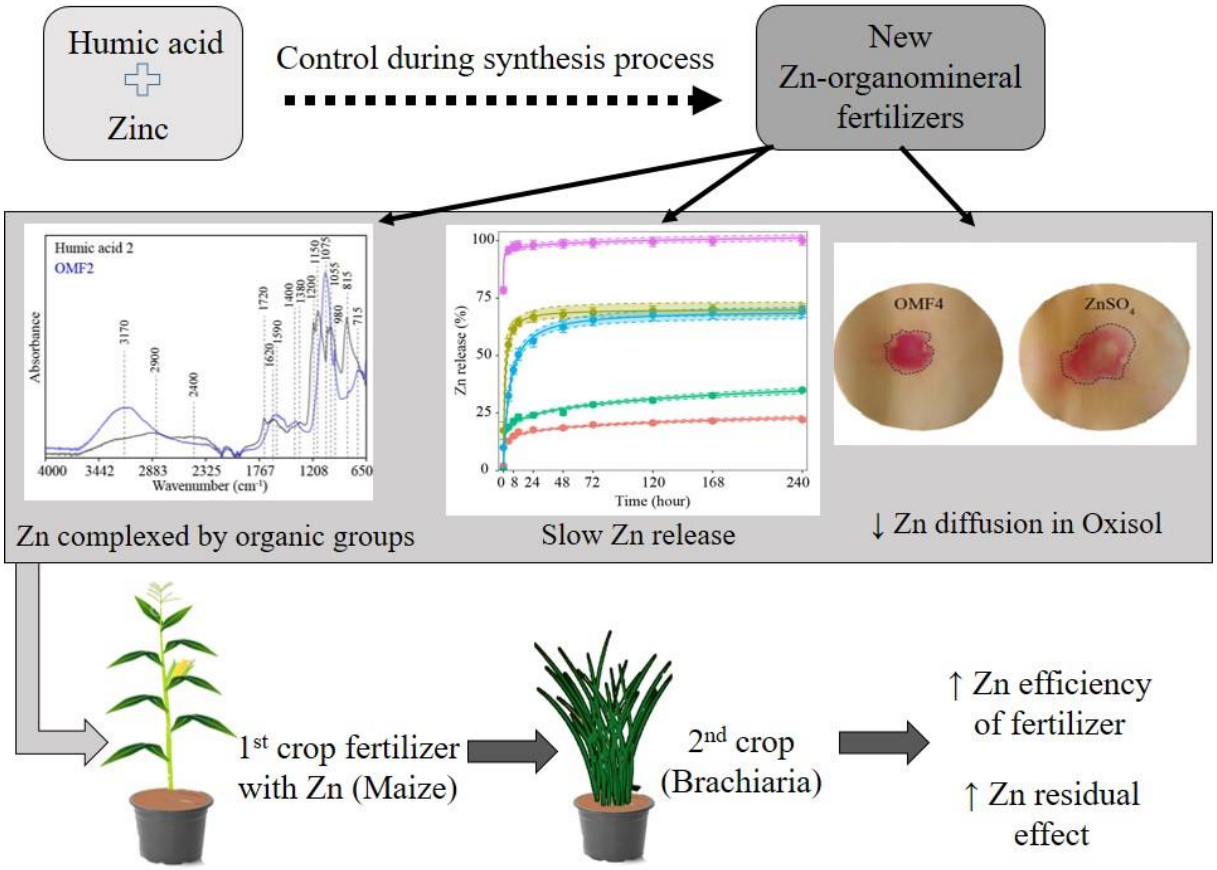

1 Introduction

Zinc (Zn) is a component of several molecules and plays a role in many biochemical and physiological plant processes[1]. Zinc deficiency in plants and humans is spread worldwide[2]. The soil or foliar Zn fertilization is a sustainable strategy for correcting Zn deficiency in plants enhancing plant Zn nutrition and yield[2]. In plants, Zn deficiency is due to Zn deficiency in the soil, occurring in alkaline and tropical soils[2]. In tropical soils, the Zn deficiency in soil occurs due to intense weathering that results in Zn leaching from soil parent material and due to high oxide mineral content where Zn strongly interacts with Fe and Al (hydro)oxides; thus, high-energy bonds are formed after Zn adsorption in mineral colloids[2–4]. In addition to Zn deficiency in tropical soils, low P availability and pH have been verified, conditions inadequate for plentiful plant growth[4]. Agronomic management, such as liming to increase soil pH and high P fertilization rates to correct P deficiency are necessary for tropical soils; however, these managements exacerbate Zn deficiency in soils, increasing Zn precipitation and adsorption[2,3,5]. Thus, Zn fertilization needs to be carefully planned due to the specifics managements required of tropical soils.

Overall, Zn availability in the soil is affected by several factors: mineralogy, texture, soil parent material, Zn fertilizer sources, soil organic matter (OM) content, and interaction of Zn with organic molecules[1,5,6]. The Zn can be supplied through fertilization in different ways, as a single nutrient or as a nutrient incorporated in macronutrient fertilizers[2,7]. Zn sources used include inorganic compounds, synthetic chelates, and natural organic and inorganic[2,7]. Inorganic compounds such as sulfate ($ZnSO_4$) and oxide (ZnO) are most commonly used fertilizers, and sulfate ($ZnSO_4.xH_2O$) is the main source used to nourish plants and correct Zn levels in soils[2,5]. The Zn from sulfate is in soluble free forms resulting in Zn being highly soluble with quick dissolution in the soil, which consequently can promote the formation of insoluble

Zn precipitates and increase the Zn adsorption in the soil; besides, a rapid release of Zn from $ZnSO_4$ is incompatible with the stages of higher demand of Zn for plants[2,5,7].

In Oxisols successively grown with maize and brachiaria, when $ZnSO_4$ was mixed with humic acid (HA) over isolated $ZnSO_4$ soil application, the agronomic performance of Zn fertilization improved, increasing the Zn uptake and biomass production by maize and brachiaria, in part due to complexation of Zn in organic molecules from HA[6]. Thus, the Zn-HA interaction has high potential in synthesizing enhanced-efficiency organomineral fertilizers; however, there is a lack of these fertilizers for soil application. The main organic groups involved in Zn-HA interactions are related to oxygen, nitrogen, and sulfur functional groups present in the HA structure[6,8,9]. The Zn-HA interaction and its effects on Zn forms present in fertilizers are ruled by different mechanisms and processes, including ionic or uncoordinated forms, unidentate complexes, bidentate chelates, and coordination chemistry bidentate bridging ligands[10].

The infrared spectrum is a tool that indicates Zn complexation by organic molecules[6,9–12]. The infrared analysis has limitations, and the technique such as metal speciation in synchrotron base X-ray absorption spectroscopy is used in a more detailed speciation configuration of the Zn complex, involving Zn forms, coordination chemistry, monodentate or bidentate linkages and distance of linkages[13,14]. However, the interaction between HA and Zn verified by infrared spectroscopy indicates the complexation degree, solubility and stability of formed organomineral complexes (OMCs) explained by changes in absorbance intensity and formation of new peaks as OMCs fingerprint in infrared spectra[6,9–12]. When compared to HA precursor, the mixture between HA and Zn forming HA-Zn complexes increases the absorbance intensity at 3425-3450 cm^{-1} related to OH-stretching, indicating the formation of metal aqua-complexes; and reduces absorbance intensity at ~1710 cm^{-1} (asymmetric COOH) and 1210-1267 cm^{-1} (symmetric COOH) related to the formation of HA-Zn(II) complexes in carboxylic

groups[10]. In addition, when $ZnSO_4$ is mixed with HA compared to only $ZnSO_4$, the change from the peak at 1060 cm^{-1} (SO_4^{2-}) to the peak at 1075-1080 cm^{-1} indicates the interaction of sulfate with a humic matrix, forming HA-alkyl sulfate salt with zinc (HA-SO_4-Zn), where S groups complex the Zn[6]. The formation of complexes between organic acids and Zn is also verified by reducing absorbance intensity in carboxylate bands in infrared analysis, thus, confirming the interaction of metals with carboxyl oxygen[12]. Thus, infrared analysis is a potential tool to indicate the metal complexation in organomineral fertilizers based on HA.

In contrast to mineral sources, Zn in organomineral fertilizers (OMFs) is present in complexed forms[2,7]. When complexed by organic compounds, Zn is less prone to being adsorbed into soil mineral colloids and is a suitable strategy to avoid Zn precipitation with different anions, such as phosphate in tropical soils fertilized with P[2,6]. When Zn-P precipitation is reduced, soil P availability increases; thus, the use of OMFs as a Zn source may indirectly improve the P uptake by plants. Thus, the supply of Zn in organic complexes is a suitable way to improve the agronomic performance of Zn sources in tropical soils[2,6,15].

The agronomic performance of Zn fertilization is highly related to fertilizer properties, soil type and plant species[2,3,5–7,15]. Maize is highly susceptible to Zn deficiency in the soil, while *Brachiaria brizantha* is supposed to grow well in soils with low levels of Zn[3]. Soils with high OM levels should have more Zn complexed to organic molecules derived from native OM; thus, the formation of OMCs in some OMFs may be less effective in soils with high rather than low levels of OM[2,6,15]. Regarding fertilizer properties, the kinetics of nutrient release from fertilizer indicates the fertilizer efficiency in supplies Zn to plants at different stages[7,16]. The release pattern from fertilizer depends on the crop; however, a rapid release is highly desirable to attend initial plant nutritional requirements, followed by a slower nutrient release throughout other plant growth stages[7].

Additionally, the synthesis of fertilizers that gradually releases Zn is useful for determining fertilizer longevity and rate and the amount and time of splitting fertilization during different plant growth stages. A more gradual Zn release can result in a more significant residual effect of Zn fertilization in the soil on plants grown in succession to the fertilized main crop. When HA is combined with $ZnSO_4$, Zn organic metallic complexes can promote a higher Zn residual effect in Oxisol to brachiaria grown in pots[6]. Thus, it is necessary to determine the potential residual effects of Zn-HA fertilizers on grasses successively cultivated in sequence to maize grown in tropical soils.

The use of OMFs is increasing in Brazilian crop fields. However, little is known about their residual effect and agronomic performance of Zn organomineral sources for crops successively cultivated in highly weathered soils. Besides, there are no HA-based Zn-OMF with a more gradual Zn release from the fertilizer compatible with the demand of different crops in Oxisols. Thus, this study aimed to synthesize new Zn-fertilizers based on HA enhancing agronomic performance through Zn fertilizers containing Zn complexed with a more gradual Zn release over conventional Zn source, besides improving P crop nutrition to grasses grown in contrasting Oxisols. The specific objectives of the study were: (1) to synthesize and characterize new Zn-OMFs and evaluate the potential formation of organic Zn complexes in OMFs; (2) to use infrared spectroscopy to indicate the main organic groups capable of complexing Zn in OMFs; (3) to measure the kinetics of Zn release in water from fertilizers and diffusion in Oxisols treated with OMFs over $ZnSO_4$; (4) to evaluate the main effects of OMFs on Zn availability in whole soil and its solution and soil Zn residual Zn to brachiaria plants grown successively to maize; (5) to test the capacity of at least one new synthesized OMFs in supplying Zn in an efficient way to maize-brachiaria succession over the exclusive use of $ZnSO_4$; and (6) to verify the role played by Zn-OMFs in improving the supply of P to maize and brachiaria.

2 Material and Methods

2.1 Synthesis and chemical analysis of organomineral fertilizers

OMFs were formulated through different routes, using the insertion of Zn sources in different phases of humic acid extraction, which were protected by the BR1020210079568 deposited patent at INPI[17]. Details of OMFs synthesis were described in **Supplementary material 1**. Four OMFs produced from routes described in the patent aforementioned were characterized along with the $ZnSO_4$. In all studies, zinc sulfate was used in a heptahydrate form ($ZnSO_4.7H_2O$). All OMFs were produced with three repetitions.

OMFs and Zn sulfate were characterized for pH in a $CaCl_2$ 0.01 mol L^{-1} solution at the ratio of 1:10 (m:v). The total carbon content of fertilizers was determined in a dry combustion carbon analyzer (Elementar, model Vario TOC Cube, Germany). The total Zn content was determined by digesting the fertilizers samples in a mixture of nitric and perchloric acids at a 4:1 ratio[18]. The Zinc availability in citric acid was determined by boiling fertilizer sample (1 g) in 100 ml of a 2% citric acid solution[18]. The Zn soluble in water from fertilizers was extracted by successive washings with deionized water of 2.5 g fertilizer until reaching a final volume of 250 mL[19]. Total Zn content, Zn soluble in CA and water extracted from the methods mentioned were determined in an inductively coupled plasma optical emission spectrometer (ICP-OES).

The solubility of various nutrient sources with different total nutrient contents must be compared by indices that relate their solubility levels to the total nutrient concentration in fertilizers, eliminating the effect of increased or decreased concentrated sources[20]. Thus, based on the solubility of Zn in CA or water according to the total Zn content in each fertilizer, the Zn index was calculated by the following equation (Eq. 1):

$$\text{Zn fertilizer index (\%)} = \left(\frac{\text{Zn content soluble in water or in citric acid(g kg}^{-1})}{\text{Total Zn content (g kg}^{-1})}\right) * 100 \qquad \text{(Eq. 1)}$$

2.2 Infrared spectroscopy

Using infrared spectroscopy, OMFs synthesized were scanned in the medium infrared region and spectra were compared to pure HA used to synthesize OMFs. Thus, Zn sources spectroscopic signature and features were assessed regarding the main peak, bonds, free functional groups, and organic groups capable of complexing Zn. The FTIR spectrum of $ZnSO_4$ was also recorded to identify the main peak features of the mineral Zn source. Spectra were obtained using the Fourier transform infrared with attenuated total reflectance (ATR-FTIR) spectroscopy and recorded in an Agilent® Cary 630 spectrometer. Peaks and bonds in spectra were recorded at 4000 to 650 cm^{-1} wavenumber range with a resolution of 4 cm^{-1}. For each ATR-FTIR spectrum, pre-processing of the dataset was performed using the normalization procedures[21]. The main peaks were identified, interpreted and assigned based on infrared libraries spectra features, bands and peaks assignments available elsewhere[6,10,22–28].

2.3 Kinetics of Zn release

The four OMFs synthesized and $ZnSO_4$ had their kinetics of Zn release in water evaluated through periodic leaching of mini-lysimeters filled with fertilizer-sand mixtures (**Supplementary material 2**), using three repetitions. The kinetics of Zn release was performed in an incubation room with constant and controlled temperature and luminosity. From the bottom to the upper chamber of mini-lysimeters, it was inserted a 0.45 μm pore filter; in sequence, a 2 cm of glass wool, 20 g sand; 35 mg of total Zn in the fertilizer; 20 g of sand; and finally a 2 cm of glass wool, aiming to eliminate the direct contact of water with fertilizers samples, as well as, to promote a regular flow of leachates in the sand-fertilizer mixtures, thus, minimizing preferential water percolation in lysimeters. Sand and glass wool were pre-washed with hydrochloric acid, followed by three samples washed with distilled water.

To perform the kinetics of Zn release study, 50 ml of distilled water were initially added to each sand-fertilizer mixture, characterizing the initial leaching time (0 h). Then, the water leachates were collected to determine the nutrients released by each experimental unit over the following times: 0, 4, 8, 12, 24, 48, 72, 120, 168 and 240 hours in cumulative water flow equivalent to 7 mL h^{-1}. In leachates, Zn concentration was determined in an ICP-OES machine. Zinc leached from sand-fertilizer mixtures was calculated by multiplying Zn concentration by the leachate volume; then, the Zn amount was presented as Zn accumulated over time and normalized according to total Zn contents in OMFs and $ZnSO_4$.

2.4 Diffusion of Zn from fertilizers

The Zn diffusion study was based on the methodology described in Degryse et al.[16]. Four OMFs synthetized and $ZnSO_4$ were evaluated regarding Zn diffusion with three repetitions in two Oxisols, Red Oxisol (RO) and Yellow Oxisol (YO), with contrasting texture and soil organic matter content (**Table 1**). In the RO, liming was performed to raise soil pH in water to 6.4, using $CaCO_3$ and $MgCO_3$ (Synth, reagent grade) at a 4:1 ratio. In the YO, liming was not performed, considering optimum Ca exchangeable and base saturation levels in the soil for plentiful plant growth. Petri dishes (5.5 cm diameter, 1 cm height) were filled with Oxisol samples, and soil moisture was kept at ~70% of soil maximum water-holding capacity of the soil (MWHC). Fertilizer samples were applied in a 5 mg of Zn based on fertilizer total Zn content in powder form in the center of the petri dish, gently pushing it just below the soil surface. The petri dishes were sealed to reduce water losses while keeping plentiful aeration. Zn diffusion was measured after incubating soil-Zn sources at 25 ^{o}C for 48 hours.

Table 1. Main chemical and physicochemical properties of Oxisols used in this study.

Oxisol	pH	C	Clay	Silt	Sand	P-resin	Zn-DTPA
		——————g kg^{-1}——————				——mg kg^{-1}——	
Red (RO)	4.9	19.8	770	100	130	8.3	0.9
Yellow (YO)	6.2	4.49	460	85	455	6.1	0.6

pH was determined in water; C: C determined (dry combustion) in an automatic TOC analyzer; clay, silt and sand were determined following the Boyoucos method; P-resin: P available determined by resin soil test; Zn-DTPA: Zn available by the DTPA soil test. The results reported in this Table were adapted from Morais et al.[6].

After incubation, the Zn diffusion was assessed using the method described in Degryse et al.[29]. Initially, the filter papers (Whatman N°1, 55 mm diameter) were impregnated with $CaCO_3$, which acts as a sink for Zn. In sequence, the paper was placed on the soil surface of the petri dish. After 1 hour of exposure, the Zn was captured in the paper; the filter was washed with distilled water to remove adhered soil particles, and, then, the coloration process was performed using the dithizone (Diphenylthiocarbazone)(Merck, reagent grade). In a further step, filter papers were scanned, and images were processed using the GIMP (v. 2.10.24) software to quantify the pink area corresponding to the high Zn diffusion zone. Finally, the Zn diffusion radius (DR) of each fertilizer was calculated by the following equation (Eq. 2):

$$\text{Diffusion radius (mm)} = \sqrt{\frac{\text{area of the high Zn zone (mm)}}{\pi}} \qquad \text{(Eq. 2)}$$

2.5 Maize and brachiaria growth conditions

Six treatments with three repetitions related to Zn fertilizers were tested on maize and, in sequence, brachiaria in succession and grown in two Oxisols with contrasting texture and soil organic matter content (**Table 1**) under greenhouse conditions. As aforementioned, in RO, liming was performed to increase pH and base saturation to levels capable of optimizing maize growth. The treatments tested were: four OMFs, $ZnSO_4$ and control (no Zn added to the soil)

and the fertilizers were applied in powdered form. Plants were grown in pots filled with 1.8 kg of each Oxisol sample. During pot filling, the *Suolo Acqua*® soil solution sampler was inserted in the middle of the pot[30]. Zinc fertilization for maize plants was based on citric acid at 2% available Zn and added to soil at 20 mg kg^{-1} of Zn, mixed and added to whole soil at the beginning of maize cultivation. Zinc concentration added to soil was based on a previous study done by Alvarez[31], where the Zn accumulation by maize was higher to Zn application of 20 over 10 mg kg^{-1} in pots experiments filled with weakly acidic soil and according to Zn recommendation for same Oxisols during a study involving the Zn fertilization combined with humic acid[6].

In the maize growing experiment, in the sowing fertilization phase, it was applied 135, 300, 100, 40, 0.81, 1.33, 3.66, 0.15, and 1.55 mg kg^{-1}, respectively, of N, P, K, S, B, Cu, Mn, Mo, and Fe, using, respectively, the following nutrient sources: $NH_4H_2PO_4$, K_2SO_4, H_3BO_3, $CuSO_4.5H_2O$, $MnCl_2.4H_2O$, $(NH_4)6Mo7O_{24}.4H_2O$, and $FeCl_3.6H_2O$ (Synth, reagent grade). In RO, Ca and Mg were supplied by calcium and magnesium carbonates. In YO, Mg was provided at 15 mg kg^{-1} using $MgSO_4.7H_2O$ (Synth, reagent grade). These nutrients were provided to ensure an adequate supply for plentiful plant growth[32] based on the nutrient recommendation for pot experiments using soil[33].

In sequence, soil moisture was kept at 70% MWH, and then ten maize seeds were sowed per pot. Ten days after planting, thinning was done, and two maize plants were grown in each pot. The topdressing fertilization was carried out at 15 and 20 days after maize planting, and 100 mg kg^{-1} N provided as NH_4NO_3 (Synth, reagent grade) was added to the soil. Maize was grown for 30 days. To evaluate the Zn fertilization residual effect (Zn residual), ten seeds of *Brachiaria brizantha* cv. Paiaguás, after maize cultivation, were sowed in the same pot used to grow maize plants. Ten days after planting, thinning was performed, remaining two brachiaria plants in each pot. In the planting fertilization of brachiaria was used 100 mg kg^{-1} N

and of K, respectively, supplied as NH_4NO_3 and KCl (Synth, reagent grade). The topdressing fertilization of brachiaria was carried out at 15, 25, and 35 days after planting, using 100 mg kg^{-1} N provided by NH_4NO_3 (Synth, reagent grade). Brachiaria plants were grown for 45 days, and no Zn was supplied to the grass; thus, residual Zn supplied to the main crop (maize) plus natural soil Zn were available in soils for brachiaria growth.

At the beginning of each crop cultivation, after 12 hours of sowing, an aliquot of 20 ml of the soil solution was collected using the *Suolo Acqua*® sampler[30] and filtered (<0.45 µm). Soil solution was characterized for pH (solution pH) determined through a digital bench pH meter in an aliquot of 10 ml of the soil solution. In another part of the soil solution (aliquot of 10 ml of soil solution), Zn (solution Zn) and P (solution P) contents were determined in an ICP-OES machine. After 18 hours of sowing, 30 g of whole soil was collected in each experimental unit, then soil samples were dried and sieved (2-mm). In the dried soil samples, pH was determined in water (soil pH), soil available Zn (soil Zn-DTPA) was assessed by the DTPA soil test, and available P by the resin soil test (soil P-resin)[34].

After cultivation, maize and brachiaria plants were harvested and separated into shoot and root. Plant tissues were dried in an oven with air circulation at 60°C until constant weight. The dried biomass was weighed, and shoot and root dry matter production were determined. Total dry matter was obtained by adding the shoot to the root. Shoot dried biomass was ground in a Wiley mill (1 mm-sieve), and between each sample, the mill was cleaned to avoid contamination. The shoot samples were digested in a mixture of nitric and perchloric acids at a 4:1 ratio[35], and Zn and P contents in the plant shoot were determined in an ICP-OES machine.

Since concentration/dilution effects of nutrient concentration are commonly verified in pots experiments due to effects on higher or lower biomass production and for the correct comparison of Zn and P nutrition between fertilizers, the accumulation of Zn and P in the shoot was calculated[7,32,36]. In pots experiments realized by Leite et al.[37,] the concentration of Zn in the

maize leaf for this element to be toxic to grasses growth can be higher than 175.2 mg kg^{-1} with a critical deficiency limit of 34.07 mg kg^{-1}. The optimal range for grasses in Leite et al.[37] study varied from 34.07 to 175.16 mg kg^{-1}, a range within the finding in our dataset contained in **Supplementary material 3.** Thus, nutrient accumulation of Zn or P (NuAc) in the shoot was calculated by the following equation (Eq. 3):

NuAc (mg pot^{-1}) = shoot dry matter (g pot^{-1})*nutrient concentration in shoot (mg g^{-1})(Eq. 3)

2.6 Quality of zinc and phosphorus analysis

In the Zn and P analysis performed in an ICP-OES machine, curves ranging from 0.03 to 1.2 mg L^{-1} for Zn, and 2 to 80 mg L^{-1} for P, with an ICP detection limit of quantification of 0,001 mg L^{-1} for Zn and 0.019 mg L^{-1} for P. The quality control of the Zn analysis was ensured using reference material (zinc sulfate heptahydrate (CAS 7446-20-0, purity 99.67%), tomato leaves SRM 1573a and NIST Montana Soil SRM 2710a) during laboratory analysis. In addition, to ensure that the extracts mentioned were in the concentration ranges of the curves, dilutions with distilled water were made. In distilled water used for dilution of extracts, the contain Zn and P also were determined to verify the quality of distilled water used.

In addition, to verify the contamination during the analysis of each method, thus subtracting this value in each methodology, two blank samples were carried out as follows: I) In the case of solubility in water and CA, the methodology was carried out without the addition of fertilizer; II) In the kinetics of Zn release study, the mini-lysimeter was filled with sand in the scheme of **Supplementary material 2** without the addition of fertilizer and the kinetics of Zn release was performed at times aforementioned; III) In soil solution samples, the same equipment (soil solution sampler) was used, collecting in a beaker the same water used during plant irrigation (distilled water); IV) In the analysis of Zn-DTPA and P-resin methods, the

methodology was performed without adding samples soil; In the nitro-perchloric digestion samples, digestion was performed without the addition of plant material.

2.7 Statistical analysis

All statistical analysis were carried out using the R software[38] through the stats, agricolae, corrplot, factoextra and FactoMineR, nlstools and Metrics R packages[38–43]. Treatment means of Zn index, Zn diffusion radius, and means of plant and soil attributes were compared by the Duncan test ($p<0.05$) after basic assumptions of analysis variance (normality, homoscedasticity, additivity, and independence of residuals) were attained, and the significance of the F-test was reached ($p<0.05$). Principal component analysis (PCA) was performed to evaluate the relationship of properties of the synthesized OMFs and $ZnSO_4$, contents and release constant parameters related to the kinetics of Zn release, and the diffusion radius of Zn in RO and YO soils. In the kinetics of Zn release study, different nonlinear models were adjusted to the dataset to verify the effect of leaching time on Zn release for each fertilizer[44–46]. The mathematical models tested were Elovich model (Eq. 4), simple exponential model (Eq. 5), power function (Eq. 6), and hyperbolic model (Eq. 7) as follows:

$$Znt = a + b \ln t \quad \text{(Eq. 4)}$$

$$Znt = N0\left(1 - e^{-kt}\right) \quad \text{(Eq. 5)}$$

$$Znt = a * t^{b} \quad \text{(Eq. 6)}$$

$$Znt = \frac{N0 * t}{(N0 * b + t)} \quad \text{(Eq. 7)}$$

Where: Znt: fraction of Zn released from fertilizer in time evaluated; a, initial Zn content released from fertilizer; b, Zn release rate constants from fertilizer, t, time of release (hour); N0, the maximum amount of Zn released from fertilizer during the whole kinetics study.

The chosen mathematical model that best fitted the kinetics of Zn release from the fertilizer dataset was based on the highest value of the coefficient of determination (R^2), the lowest value of root-mean-square error (RMSE), and the Akaike information criterion (AIC)[47]. Mathematical models adjusted to Zn kinetics to each Zn source were compared by adopting a confidence interval generated through a 95% bootstrap confidence interval using 1000 bootstrap interactions. Based on the model that best fitted as a whole to OMFs and $ZnSO_4$ dataset, Zn release constant parameters (b) were compared by the confidence interval generated previously through the bootstrap interactions.

3 Results

3.1 Fertilizers properties

The chemical properties of OMFs and $ZnSO_4$ fertilizers investigated in this study were shown in **Table 2**. Zn index was calculated to normalize different Zn concentrations in fertilizers, allowing comparison of different sources regarding availability for plants of fertilizer Zn solubility in CA or water. OMF3 had a lower Zn soluble index in CA than OMFs 1, 2, and 4, and $ZnSO_4$. The index based on Zn soluble in water showed that all OMFs synthesized had a lower Zn index than $ZnSO_4$. Within the OMFs, OMF1 and OMF3 had Zn water indices lower than the other OMFs.

Table 2. pH, total C and total and soluble Zn in water and citric acid of organomineral fertilizers (OMF) and zinc sulfate ($ZnSO_4$).

Fertilizer	pH	C	Zn			Zn index	
			Total	CA	Water	CA	Water
			g kg^{-1}			%	
OMF1	5.9 ±0.01	246.4 ±2.7	146.1 ±1.6	145.6 ±1.5	29.1 ±3.0	99.7 A	15.9 C
OMF2	5.2 ±0.01	140.5 ±5.1	133.2 ±2.1	133.1 ±2.1	73.9 ±9.4	99.9 A	55.6 B
OMF3	4.0 ±0.01	290.9 ±0.7	146.7 ±1.0	114.4 ±1.2	45.4 ±1.5	77.9 B	30.9 C
OMF4	3.5 ±0.01	175.8 ±1.8	156.8 ±2.8	156.0 ±3.1	76.5 ±1.9	99.5 A	48.8 B
$ZnSO_4$	5.3 ±0.03	-	235.4 ±0.1	235.3 ±0.1	235.1 ±0.1	99.9 A	99.9 A

C: total content of C in fertilizer; CA: Zn soluble in citric acid at 2%, water: Zn soluble in water. The means with the same letter in each column did not differ regarding fertilizer-Zn solubility index based on the Duncan test ($p<0.05$).

3.2 Infrared spectroscopy

Compared to pure HA, OMFs, whose synthesis was based on HA with mineral Zn sources, had specific infrared spectra, new peaks, and changes in spectral signature (**Figure 1 and Supplementary material 4**). The OH stretching related to H-bonded OH, free OH, intermolecular bonded OH were found for all HAs and OMFs, and in $ZnSO_4$ as well, with peaks recorded at 3370 cm^{-1} (OMF3), 3290 cm^{-1} (OMF1, HA3, and OMF4), 3170 cm^{-1} (OMF2, OMF4, and $ZnSO_4$) and 3100 cm^{-1} (HA1). Aliphatic CH groups were present in FTIR spectra at 2915 cm^{-1} (HA1, OMF1, HA3, OMF3, and OMF4), 2900 cm^{-1} (HA2) and 2845 cm^{-1} (HA3, OMF3 and OMF4). Carboxylic radical (COOH) in the alkyl group was found only in HA2 at 2400 cm^{-1} spectra region. The carboxylic acid C=O stretch was found in HA1 at 1700 cm^{-1} and in HA2 at 1720 cm^{-1}. The peak related to water at 1640 cm^{-1} was found for HA3, HA4 and $ZnSO_4$. The C=C aromatic stretching was found at 1620 cm^{-1} (HA, OMF1 and HA2), 1590 cm^{-1} (OMF2), 1560 cm^{-1} (HA3 and OMF4) and 1495 cm^{-1} (HA1 and OMF1). OH phenolic

stretching was assigned for peaks at 1400 cm^{-1} (HA1 and OMF2) and 1380 cm^{-1} (OMF1 and HA2).

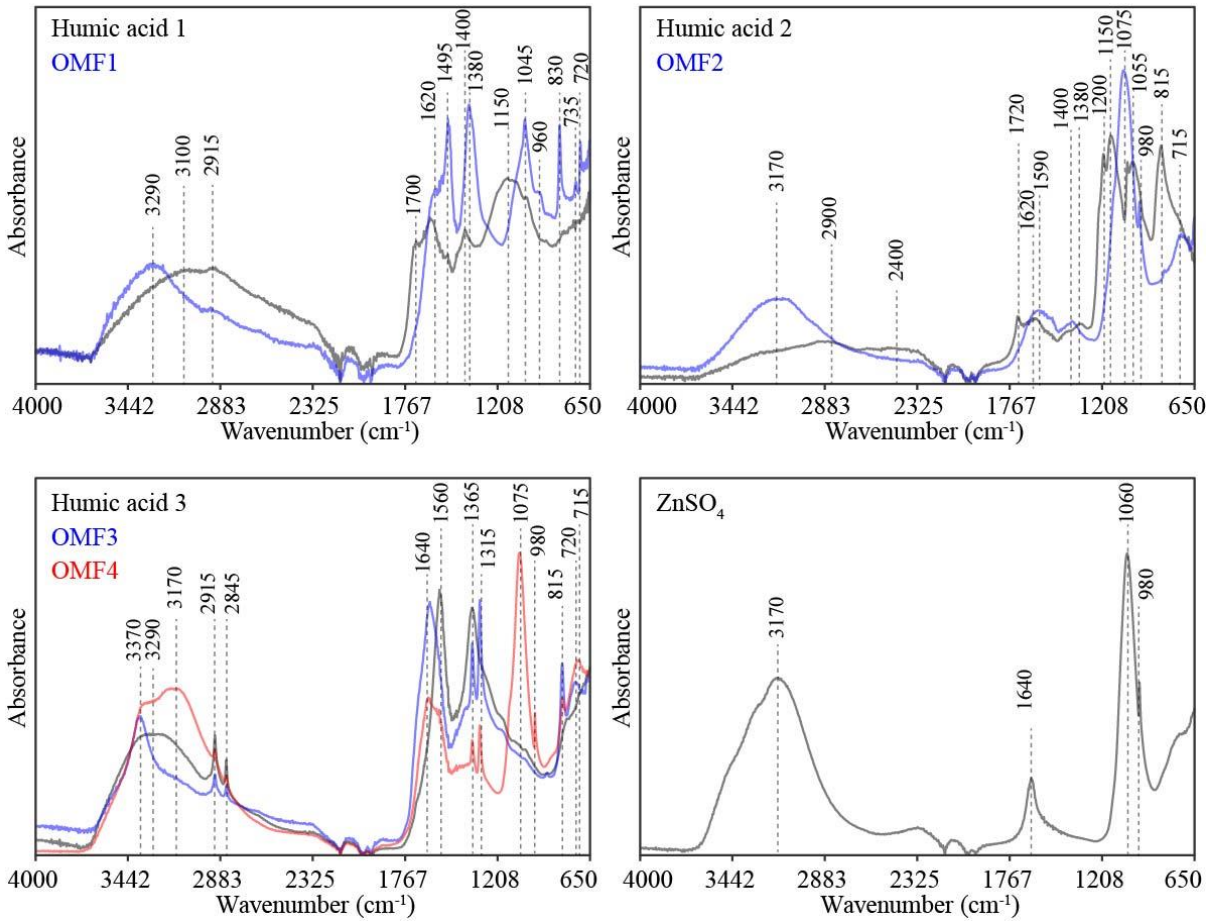

Figure 1. Attenuated total reflection Fourier-transform infrared (ATR-FTIR) spectroscopy and the main peaks and features of chemical groups in humic acid Zn-HA-based organomineral fertilizer (OMF) and its respective precursor HA, as well as zinc sulfate ($ZnSO_4$).

C-CH3 groups bending were found in HA3 and their derived OMFs (OMF3 and OMF4) with peaks at 1365 cm^{-1}. The SO_2 stretches (sulfone) were found at 1315 cm^{-1} (OMF3 and OMF4) and 815 cm^{-1} (HA2, OMF3, and OMF4). The C=S thiocarbonyl was only found in HA2 at 1200 and 1055 cm^{-1}. The polysaccharide C-O stretching was assigned for peaks at 1150 cm^{-1} (HA1 and HA2) and 1045 cm^{-1} (HA1 and OMF1). SO_2 stretching (alkyl sulfate)-$RSO_4^-M^+$ at 1075 cm^{-1} was found for OMF2 and OMF4. S as SO_4^{2-} stretching (free sulfate groups) was

assigned for peaks at 1060 cm^{-1} ($ZnSO_4$) and 980 cm^{-1} (OMF2, OMF3, OMF4, and $ZnSO_4$). Aromatic C-H out-of-plane bend was verified only in OMF1 at 960 cm^{-1}. The C-Cl stretching modes were found in OMF1 at 830, 735, and 720 cm^{-1} and in OMF3 at 720 cm^{-1}. The C-S stretching (Methyl sulfone - CH_3-SO_2) was found at 715 cm^{-1} in OMF2 and OMF4.

Compared to the HA1 chemical nature, changes in OMF1 spectral signature involved the disappearance of peaks related to carboxylic acid C=O stretching (1700 cm^{-1}), polysaccharide C-O stretching (1150 cm^{-1}), and the formation of new peaks related to aromatic C-H out-of-plane bending (960 cm^{-1}) and the C-Cl stretching mode (830, 735, and 720 cm^{-1}) (**Figure 1**). Additionally, changes in peaks from 3100 to 3290 cm^{-1} were related to OH stretching; for example, the change from 1400 to 1380 cm^{-1} was related to OH phenolic stretching, and the increase in absorbance intensities was related to C=C aromatic stretching (1620 and 1495 cm^{-1}) and polysaccharide C-O stretching (1045 cm^{-1}), and the decrease in absorbance intensity was related to aliphatic C-H groups (2915 cm^{-1}).

Compared to its precursor HA (HA2), the spectral signature of OMF2 was characterized by the disappearance of peaks related to aliphatic CH groups (2900 cm^{-1}), COOH in alkyl groups (2400 cm^{-1}), carboxylic acid C=O stretch (1720 cm^{-1}), C=S thiocarbonyl (1200 and 1055 cm^{-1}), polysaccharide C-O stretching (1150 cm^{-1}), and SO_2 stretching (sulfone) (815 cm^{-1}), and the formation of new peaks occurred from OH stretching (3170 cm^{-1}), SO_2 stretching (alkyl sulfate)-$RSO_4^-M^+$ (1075 cm^{-1}), SO_4^2 stretching (free sulfate groups) (980 cm^{-1}) and C-S stretching (methyl sulfone-CH_3-SO_2) (715 cm^{-1}) (**Figure 1**). In the same direction, the peaks from 1620 to 1590 cm^{-1} related to C=C aromatic stretching and from 1380 to 1400 cm^{-1} related to OH phenolic stretching also were modified.

Compared to the HA precursor (HA3), OMF3 resulted in peaks that changed from 3290 to 3370 cm^{-1} related to OH stretching, the peaks related to C=C aromatic stretching (1560 cm^{-1}) disappeared, and new peaks related to water (1640 cm^{-1}), SO_2 stretching (sulfone) (1315 and

815 cm^{-1}) and the C-Cl stretching mode (720 cm^{-1}) formed (**Figure 1**). In addition, the absorbance intensities to aliphatic groups (2915 and 2845 cm^{-1}) and C-CH_3 groups bending (1365 cm^{-1}) were reduced compared to HA precursor. HA3 was also the precursor of OMF4, and compared to HA3, in OMF4, new peaks were formed related to OH stretching (3170 cm^{-1}), water (1640 cm^{-1}), SO_2 stretching (sulfone) (1315 and 815 cm^{-1}), SO_2 stretching (alkyl sulfate)-$RSO_4^-M^+$ (1075 cm^{-1}), SO_4^{2-} stretching (free sulfate groups) (980 cm^{-1}) and C-S stretching (methyl sulfone - CH_3-SO_2) (715 cm^{-1}). In comparison to HA3, OMF4 had absorbance intensities related to OH stretching (3290 cm^{-1}) increased; however, aliphatic CH groups (2915 and 2845 cm^{-1}), C=C aromatic stretching (1560 cm^{-1}), and C-CH_3 group bending (1365 cm^{-1}) decreased.

3.3 The kinetics of Zn release

In relation to OMFs, $ZnSO_4$ had a higher initial (0 hour) and final (240 hours) Zn release (**Figure 2**). After 4 hours, 95.8% of Zn from $ZnSO_4$ was released in the water. The OMF1 and OMF3 had Zn release similar to each other at time 0 hour (~1.3% of Zn), though they released less Zn than other OMFs and $ZnSO_4$. In the final time analyzed (240 hours), OMF1 and OMF3 had a lower Zn released with the lowest Zn leached from OMF1. The OMF2 and OMF4 had an intermediate Zn released; initially, OMF4 had a lower Zn released (10 % of Zn) over OMF2 (17.4% of Zn). After 72 hours, the amounts of Zn released from OMF2 and OMF4 were similar and constant at 240 hours (~ 70% of applied Zn).

The best models to explain the kinetics of Zn release by OMFs were the power model for OMF1 and OMF3, the hyperbolic model for OMF2 and OMF4, and the Elovich model for Zn leached from $ZnSO_4$ (**Supplementary material 5**). Only the Power model was analyzed to compare the Zn release rate constant parameter (b) among fertilizers (**Supplementary material**

5). Thus, it verified that $ZnSO_4$ had a faster Zn release rate constant, followed by OMF2. OMF1, OMF3, and OMF4 had similar and lower release rate constants than OMF2 and $ZnSO_4$.

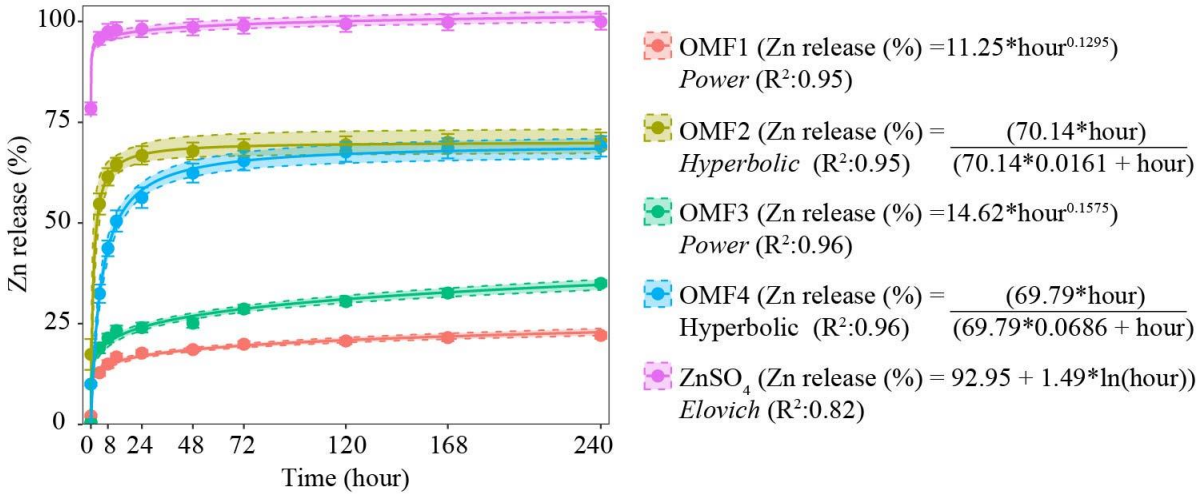

Figure 2. The kinetics of Zn release in water from organomineral fertilizers (OMFs) and zinc sulfate ($ZnSO_4$).

3.4 Soil zinc diffusion

The Zn diffusion was higher in YO over RO (**Figure 3**). In RO, the highest Zn diffusion was verified for $ZnSO_4$. The OMFs reduced the Zn diffusion, and OMF1 and OMF2 had a lower Zn diffusion than other OMFs (**Figure 3**). In YO, only OMF1 and OMF4 had a lower Zn diffusion than $ZnSO_4$, while OMF2 and OMF4 diffused Zn in an equivalent radius of $ZnSO_4$ diffusion in soils.

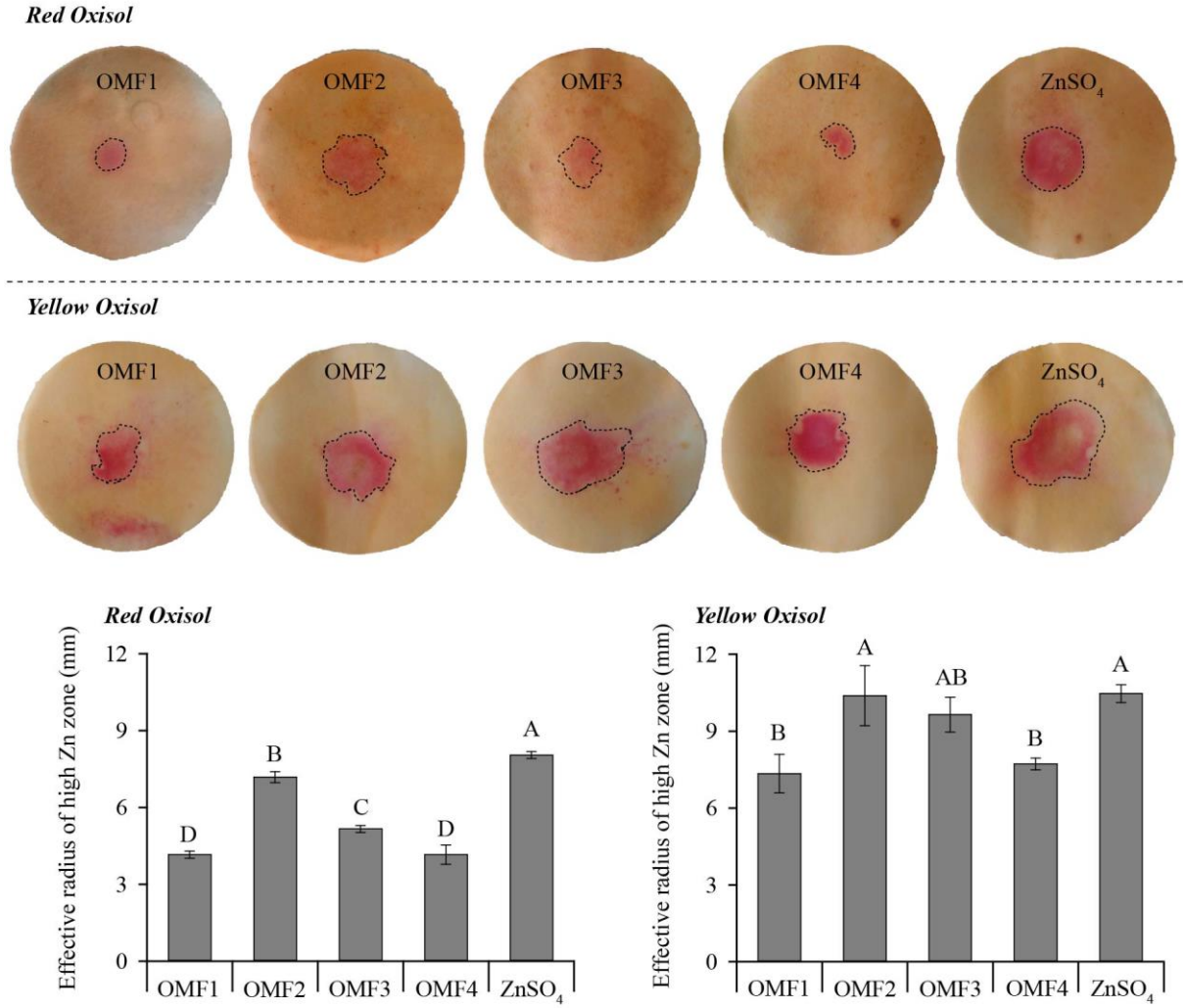

Figure 3. The effective radius of high Zn zone diffusion for the organomineral (OMF) and zinc sulfate ($ZnSO_4$) fertilizers in the Red and Yellow Oxisols. Bars with standard error followed by the same letter did not differ by the Duncan test ($p<0.05$).

3.5 Zn sources on maize growth and nutrition

Soil and solution pH was not affected by the fertilizers studied. Soil pH mean values of 6.32 and 6.51 were verified, respectively, for RO and YO cultivated with maize (**Supplementary material 7).** Solution pH means value for maize cultivated in RO and YO were, respectively, 6.40 and 6.50. The slight differences in pH values from whole soil and soil solution were related to differences in the determination process, mainly related to the relationship between soil mass and water volume. When Zn was not added to both Oxisols, the solution Zn and soil Zn-DTPA were lower than in Zn-treated soils (**Table 3**). Compared to

$ZnSO_4$, solution Zn in RO was similar for OMF2, OMF3, and OMF4, and lower for OMF1-treated samples. In YO, solution Zn was similar for all OMFs and $ZnSO_4$. Among the OMFs, OMF2 and OMF4 reduced the solution Zn over OMF3. Compared to $ZnSO_4$, OMF3 increased, and OMF1, OMF2, and OMF4 decreased Zn-DTPA in RO. In YO, all OMFs reduced soil Zn-DTPA over $ZnSO_4$. Among all fertilizers, in RO, OMF1, OMF2 and OMF3 increased the solution P over $ZnSO_4$. Solution P in YO increased in response to OMF2 and OMF3 though they were lower than other fertilizers studied, though a higher level of P in whole soil was verified for OMF3. Compared to $ZnSO_4$, soil P-resin was not affected by Zn sources added to RO, while OMF2 and OMF4 increased soil P-resin in YO.

Table 3. Contents of Zn and P in soil solution, Zn and P available in the whole soil as a function of OMFs, zinc sulfate ($ZnSO_4$), and Oxisol type used for maize cultivation.

Soil solution				
	Red Oxisol		Yellow Oxisol	
Treatment	Zn ($mg\ L^{-1}$)	P ($mg\ L^{-1}$)	Zn ($mg\ L^{-1}$)	P ($mg\ L^{-1}$)
-Zn	0.071 ±0.006 C	6.11 ±0.36 A	0.006 ± 0.002 C	0.21 ±0.01 C
OMF1	0.132 ±0.008 B	2.03 ±0.07 C	0.035 ± 0.003 AB	0.25 ±0.07 C
OMF2	0.169 ±0.009 A	2.85 ±0.10 B	0.033 ± 0.003 B	1.10 ±0.22 B
OMF3	0.178 ±0.008 A	2.23 ±0.08 C	0.043 ± 0.003 A	4.23 ±0.28 A
OMF4	0.182 ±0.009 A	1.85 ±0.15 CD	0.028 ± 0.003 B	0.53 ±0.11 C
$ZnSO_4$	0.163 ±0.010 A	1.40 ±0.09 D	0.035 ± 0.003 AB	0.36 ±0.10 C
Whole Soil				
	Red Oxisol		Yellow Oxisol	
Treatment	Zn-DTPA ($mg\ kg^{-1}$)	P-resin ($mg\ kg^{-1}$)^{NS}	Zn-DTPA ($mg\ kg^{-1}$)	P-resin ($mg\ kg^{-1}$)
-Zn	0.08 ±0.01 F	91.6 ±2.6	0.05 ±0.01 E	173.4 ±2.3 C
OMF1	4.90 ±0.15 E	84.6 ±3.3	4.85 ±0.07 D	172.0 ±0.7 C
OMF2	5.42 ±0.07 D	92.5 ±3.9	5.47 ±0.13 C	200.1 ±2.0 A
OMF3	7.26 ±0.09 A	81.3 ±4.4	6.50 ±0.12 B	193.1 ±2.8 AB
OMF4	5.68 ±0.04 C	83.8 ±2.7	5.73 ±0.09 C	196.6 ±8.3 A
$ZnSO_4$	6.52 ±0.05 B	95.8 ±4.0	7.26 ±0.07 A	180.6 ±4.7 BC

Means with standard error followed by the same letter in each column were not differ by the Duncan test ($p<0.05$). ^{NS}: difference not significant ($p<0.05$). -Zn: no-Zn added to the soil.

The absence of Zn in fertilization sharply reduced shoot, root, and total dry matter, Zn and P accumulated in maize shoot, in both Oxisols (**Figure 4**). In RO, shoot biomass was higher when plants were fertilized with OMF1 and OMF4 over $ZnSO_4$, while root biomass was higher for all OMFs over $ZnSO_4$. In RO, total biomass production was higher for OMF1, OMF2, and OMF4 over $ZnSO_4$. The Zn accumulated in maize shoot cultivated in RO was higher for OMF3

and OMF4 over $ZnSO_4$, while OMF2 reduced Zn accumulated in maize over $ZnSO_4$ fertilized plants. In RO, P accumulated in maize shoot was improved only by OMF4 compared to $ZnSO_4$. In YO, over Zn sulfate, shoot biomass increased in response to OMF2 and OMF3, root biomass increased due to OMF1 and OMF3, and total biomass production only increased in OMF3-treated soils. In YO, Zn and P accumulated in maize shoot increased by OMF2, OMF3, and OMF4 as Zn sources over $ZnSO_4$, and the highest Zn accumulated in maize shoot was verified for OMF3-treated plants.

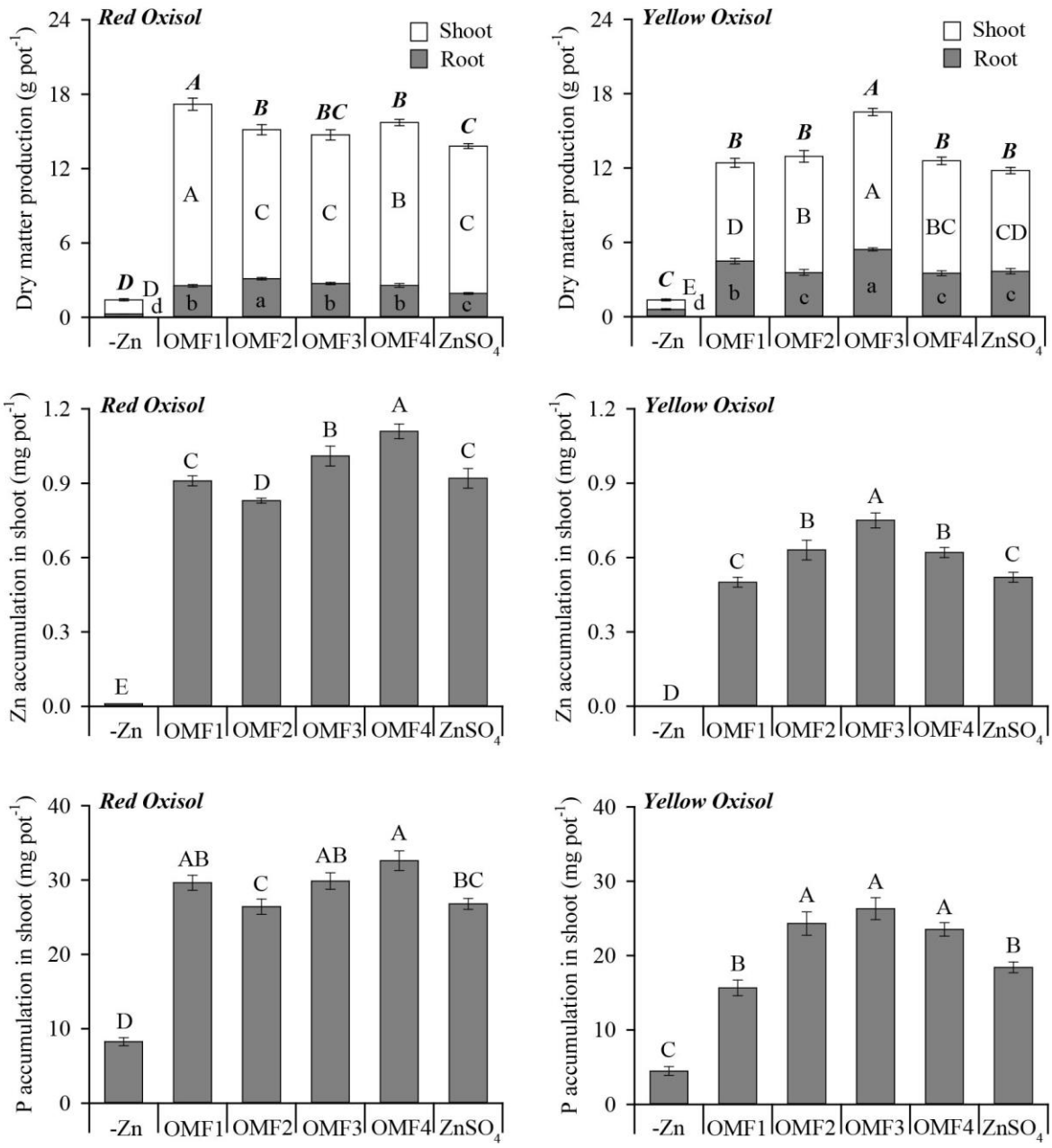

Figure 4. Total (full bar), shoot (Shoot) and root (Root) maize biomass production, and Zn and P accumulated in shoot according to organomineral (OMF) and zinc sulfate ($ZnSO_4$) fertilizers in Red and Yellow Oxisols. Bars with standard error followed by the same letter were not differ by the Duncan test ($p<0.05$). Uppercase-italic, uppercase, and lowercase letters compared respectively total, shoot, and root dry matter production respectively. - Zn: no-Zn added to the soil.

3.6 Zn residual: brachiaria growth and nutrition

After maize cultivation, soil pH was not affected by the fertilizers studied (**Supplementary material 7**). Soil pH means were 5.99 and 6.53, respectively, for RO and YO. Solution pH mean in RO and YO were, respectively, 6.69 and 7.09. The Solution Zn and soil Zn-DTPA were lower in control (no Zn addition) over Zn-treated Oxisols (**Table 4**). In RO, solution Zn increased in OMF3 and OMF4-treated soils over $ZnSO_4$. OMF1 and OMF2 had similar contents of Zn in RO solution over $ZnSO_4$. In YO, all OMFs increased the solution Zn over $ZnSO_4$, and greater solution Zn was verified for OMF3-treated soils. Regarding Zn-DTPA in the whole RO samples, compared to $ZnSO_4$, OMF1 and OMF4 reduced soil Zn-DTPA, while availability (DTPA) of Zn in the whole soil was higher for OMF3. In YO, OMF3 had similar values of soil Zn-DTPA compared to $ZnSO_4$, and OMF1, OMF2, and OMF4 reduced levels of Zn-DTPA over $ZnSO_4$.

Table 4. Contents of Zn and P in soil solution, Zn and P available in the whole soil in the successive cultivation of brachiaria as related to soil type and OMFs and zinc sulfate ($ZnSO_4$) used in the fertilization of maize.

Soil solution				
	Red Oxisol		Yellow Oxisol	
Treatment	Zn ($mg\ L^{-1}$)	P ($mg\ L^{-1}$)	Zn ($mg\ L^{-1}$)	P ($mg\ L^{-1}$)
-Zn	0.038 ±0.005 C	0.296 ±0.011 A	0.010 ±0.001 D	$^{<LD}$
OMF1	0.061 ±0.006 B	0.202 ±0.013 B	0.021 ±0.002 B	$^{<LD}$
OMF2	0.059 ±0.005 B	0.023 ±0.002 D	0.023 ±0.001 B	$^{<LD}$
OMF3	0.089 ±0.002 A	0.097 ±0.011 C	0.032 ±0.001 A	0.095 ±0.006
OMF4	0.095 ±0.005 A	0.085 ±0.012 C	0.024 ±0.002 B	$^{<LD}$
$ZnSO_4$	0.064 ±0.004 B	0.041 ±0.007 D	0.014 ±0.001 C	$^{<LD}$
Whole soil				
	Red Oxisol		Yellow Oxisol	
Treatment	Zn-DTPA ($mg\ kg^{-1}$)	P-resin ($mg\ kg^{-1}$)	Zn-DTPA ($mg\ kg^{-1}$)	P-resin ($mg\ kg^{-1}$)
-Zn	0.13 ±0.02 D	120 ±1.9 A	0.08 ±0.02 D	180 ±5.0 A
OMF1	5.85 ±0.09 C	121 ±5.0 A	4.94 ±0.14 C	168 ±7.3 AB
OMF2	6.07 ±0.03 BC	90 ±3.2 B	4.91 ±0.12 C	164 ±5.1 AB
OMF3	7.32 ±0.14 A	65 ±1.9 D	6.24 ±0.03 A	153 ±5.0 B
OMF4	5.88 ±0.12 C	77 ±3.3 C	5.28 ±0.16 B	154 ±3.4 B
$ZnSO_4$	6.41 ±0.02 B	6 ±1.9 D	6.35 ±0.02 A	156 ±4.9 B

Means with standard error followed by the same letter in each column were not differ by the Duncan test ($p<0.05$). $^{<LD}$: Values below the nutrient detection limit of ICP-OES machine. -Zn: no-Zn added to the soil.

The absence of Zn in maize fertilization increased the contents of P in RO solution at the beginning of brachiaria cultivation (**Table 4**). Among Zn fertilizers applied to RO, over Zn sulfate, OMF1 OMF3 and OMF4 increased solution P contents. In YO, increasing levels of solution P were only found for maize-OMF3 fertilized pots. In RO, a greater P-resin was only

found for control (no Zn) and OMF1 pots over other Zn sources. OMF1, OMF2, and OMF4 increased soil P-resin over $ZnSO_4$ in RO. In YO, the OMFs studied did not differ statistically regarding soil P-resin content compared to $ZnSO_4$.

In RO, in control pots (no-Zn added to the soil), Zn deficiency was a factor ruling plant growth as it was in YO; the absence of Zn in the maize fertilization in RO caused a lower shoot, root, and total biomass production, and Zn and P accumulated in the shoot in relation to the use of other Zn sources (**Figure 5**). Thereby, OMF2 and OMF3 increased shoot, root, and total biomass production, and Zn and P accumulated in the brachiaria shoot compared to plants fertilized with $ZnSO_4$ and cultivated in RO. However, OMF1 and OMF4 reduced the shoot biomass, and Zn accumulated in the brachiaria shoot over $ZnSO_4$. The OMF1 increased root biomass compared to $ZnSO_4$, and total biomass production was reduced by OMF4 over $ZnSO_4$.

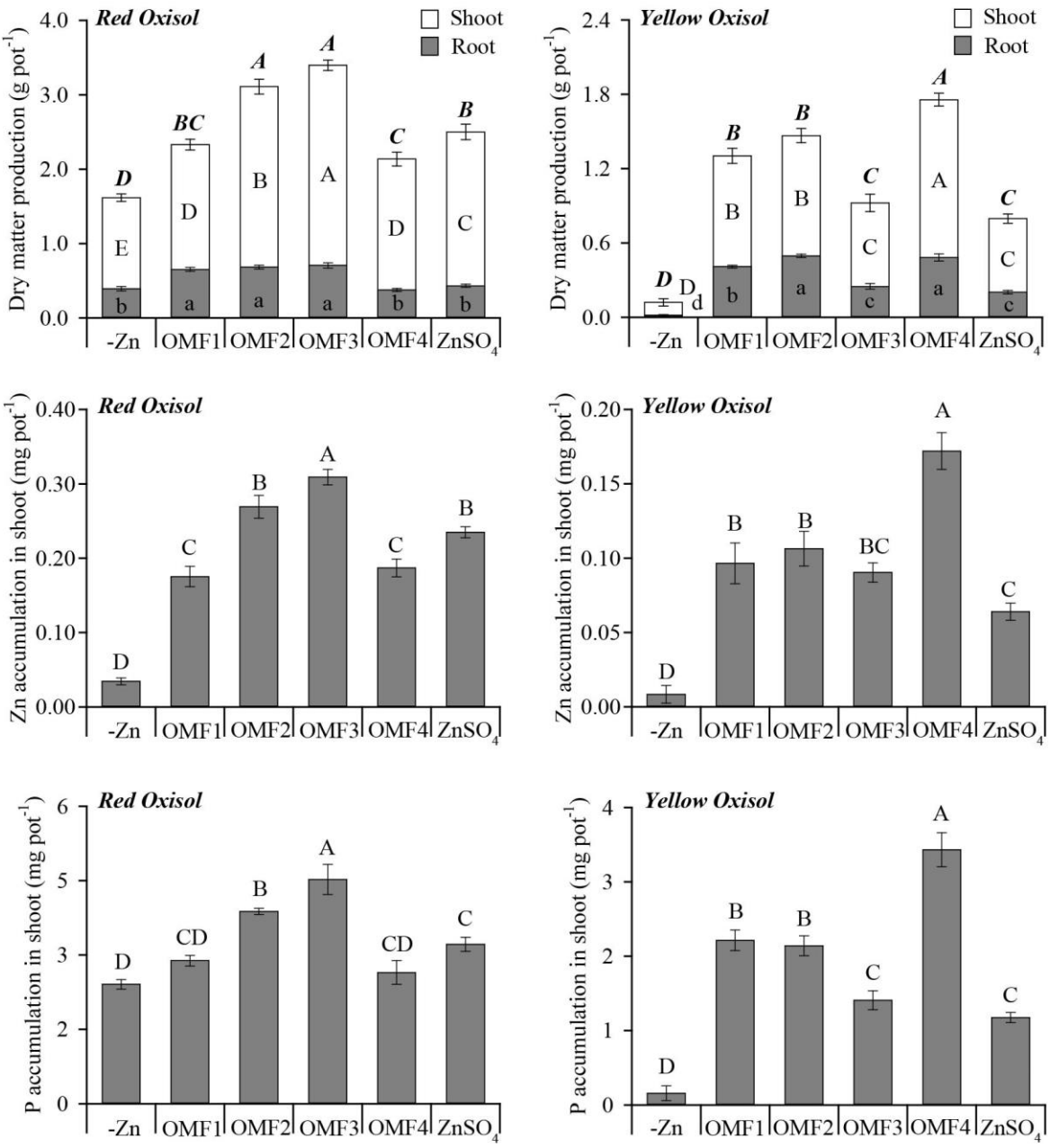

Figure 5. Total (full bar), shoot (Shoot) and root (Root) maize brachiaria production, and Zn and P accumulated in shoot according to organomineral (OMF) and zinc sulfate ($ZnSO_4$) fertilizers in Red and Yellow Oxisols. Bars with standard error followed by the same letter were not differ by the Duncan test ($p<0.05$). Uppercase-italic, uppercase, and lowercase letters compared respectively total, shoot, and root dry matter production respectively. - Zn: no-Zn added to the soil.

When Zn was not supplied to maize, brachiaria growth was sharply limited in YO, with a reduction of shoot, root, and total biomass production, and Zn and P accumulated in the

brachiaria shoot as well (**Figure 5**). The OMF1, OMF2 and OMF4 increased the shoot, root and total biomass production, Zn and P accumulated in brachiaria shoot over $ZnSO_4$-fertilized plants cultivated. In the sandy Oxisol (YO), the greatest brachiaria biomass productions (shoot, root, and total) were verified for OMF4-fertilized plants; and OMF3 and $ZnSO_4$ had a similar shoot, root, and total biomass production, and Zn and P accumulated in brachiaria shoot as well.

3.7 Multivariate analysis approach

Using the multivariate approach, PCA outputs showed that total C content in fertilizers and Zn release rate constants (b parameter in the fitted mathematical power model) were positively related. The C content in fertilizers was negatively related to water-soluble Zn index, initial and final content in the kinetics of Zn release from fertilizer, and diffusion radius of Zn in RO and YO (**Figure 6**). The pH and Zn-CA index were positively related and little influenced by other variables depicted in the PCA diagram.

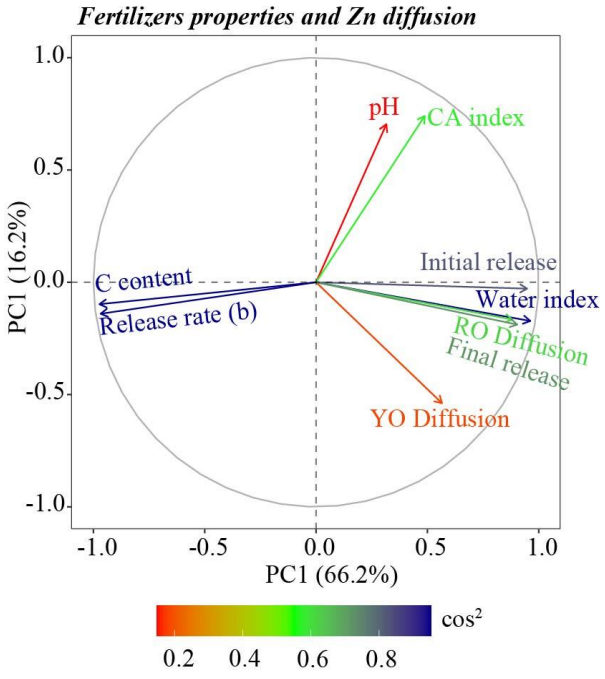

Figure 6. Principal component analysis (PCA) between fertilizers properties, the kinetics of Zn release, and the Zn diffusion in Red and Yellow Oxisols. C content: total C content of fertilizers.

CA and water index: soluble Zn in fertilizers in relation to the Zn total content evaluated by citric acid at 2% solution and water, respectively. Initial and final release: The content of Zn release in water respectively to initial (0 hour) and final (240 hours) time in relation to the Zn total content evaluated to the kinetics of Zn release. Release rate (b): Zn release rate constant in kinetics of Zn release adopting the power model in all fertilizers. RO and YO Diffusion: Zn diffusion radius in Red (RO) and yellow (YO) Oxisols respectively. COS^2: represents the quality of representation for variables on the factor map.

4 Discussion

4.1 Chemical properties, pools and kinetics of Zn release from OMFs

Compared to readily available Zn sulfate, Zn-OMFs may have higher agronomic performance for crops increasing the biomass production and Zn uptake for plants, an effect dependent on OMF properties such as pH of fertilizer, Zn-organic matrix interaction, complexation and adsorption of Zn in the organic matrix, Zn solubility in different extractors and Zn release rate evaluate by kinetics studies[3,5,7,10,19,48].

Among the properties of fertilizers, the pH of OMFs synthetized varied between 3.5-5.9, conditioned by the synthesis route (**Table 2**). The pH of fertilizer affects the nutrient dynamics in the soil-plant system, controlling the dissolution and reactions of nutrients in the soil-fertilizer interface[49]. Besides, the increase in pH of fertilizer increases the formation of insoluble mineral precipitate forms of Zn; thus, overall, a negative relationship between pH and % water-soluble Zn content is commonly reported for fertilizers[2]. However, in our dataset, the relationship between the increase of pH of fertilizer and the reduction of Zn solubility in water was not observed (**Figure 6**) due to the presence of the humic matrix in Zn-OMFs. When the pH of this humic matrix is increased, the HA supramolecular structure reduces its condensation degree, and the formation of more soluble OMCs is magnified[10,50], possibly contributing to the increase of Zn availability for plants. Thus, in Zn-OMFs synthesized, there is a double effect of

pH of fertilizer on the availability of Zn in water, either on controlling the formation or dissolution of mineral precipitates or on changes in the conformation of the humic matrix.

As shown in the PCA plot (**Figure 6**), the pH of fertilizer only positively influenced Zn solubility in CA. The influence of this pH on the CA-Zn index is partly explained due to the use of humic acid in the OMFs synthesis. Since in humic matrices, the increase in pH reduces the condensation degree of HA supramolecular structure, citric acid is a low molecular weight organic acid that interacts more efficiently with the humic supramolecular structure; thus, consequently destabilizing and fragmenting them into more bioactive smaller humic fragments capable of interacting with and consequently increasing Zn solubility[50] as observed by the relation between pH and Zn availability accessed by CA extractor.

In addition to this feat of CA in destabilizing the HA supramolecular structure, the solubility of fertilizer Zn in CA is commonly used because the CA solution simulates the capacity of roots to acquire and uptake Zn from fertilizers[19,51] and is the official method adopted by the Brazilian Ministry of Agriculture - MAPA[18]. Besides, the solubility of Zn in different extractors allows the differentiation of Zn sources concerning the availability of Zn for plants and in the behavior of Zn release, since the Zn soluble in water indicates the readily soluble Zn and Zn available in CA indicates the Zn available in the short and long term for plants[19,51]. A faster release of Zn-fertilizer enables rapid plant growth, although this rapid release can be not a suitable strategy to manage fertilizer in Oxisols due to the high affinity of Zn to adsorption sites prevalent in weathered mineral colloids found in Brazilian soils[2,5]. Thus, new fertilizers routes of production should be proposed to increase the efficiency of Zn fertilization in Oxisols.

According to these Zn solubility assumptions aforementioned, we developed routes of synthesis of new OMFs promoted fertilizers with different solubility in CA and water, allowing the development and selection of Zn fertilization management strategies. Zinc sulfate used as a standard Zn source has almost all soluble Zn in water and CA (Zn water and CA index: 99.9%)

(**Table 2**). In our synthesized OMFs, high Zn solubility was found in CA (77.9-99.9% Zn CA index), with OMF1, 2 and 4 having values similar to $ZnSO_4$. However, the Zn soluble in water of all OMFs (15.9-55.6% Zn water index) was lower than that of $ZnSO_4$. The reduction of Zn soluble in water (Zn water index) from the OMFs is related to the presence of functional carbon from HA in the OMF matrix, as demonstrated by the close relationship between the total C content and water-soluble Zn index (**Figure 6**). The interaction of Zn and functional organic matrix caused causes both fertilizers with a lower proportion of water-soluble Zn and fertilizers with a slow Zn release to favor Zn uptake by plants[7,48].

The kinetics of nutrient release in water is the fertilizer property to release a specific nutrient as a function of the time, allowing to differentiate speed patterns of dissolution and release of nutrients from different fertilizers[7,48]. Similar to results found in Carneiro et al.[48], in our dataset, the presence of carbon in OMFs reduced the proportion of Zn release in the kinetics of Zn study and the velocity of the release of Zn (**Figure 6 and Supplementary material 6**). Once higher total C content in the fertilizers decreased the initial and final releases of Zn in the kinetics of Zn release in water from fertilizers and increased b parameter in the power model used in the Zn release kinetics study showed the more gradual Zn release according to the time evaluated.

In our study, the final release amount of Zn decreased as follows: $ZnSO_4$ > OMF2 = OMF4 > OMF3 > OMF1, while the velocity of Zn release was as follows: $ZnSO_4$ > OMF2 > OMF1 = OMF3 = OMF4, highlighting that at 4 hours, 95.8% of Zn from $ZnSO_4$ was released, while in OMFs, the amount of Zn released enhanced the limit value of OMF2 and OMF4 at 240 hours, and in OMF1 and OMF3, the limit was not reached. However, after 240 hours, the amount of Zn released was low for all OMFs over $ZnSO_4$ (**Figure 2**). In line with the results of Kabiri et al.[7] that compared $ZnSO_4$ with Zn-graphene fertilizer (Zn-OMF), and Carneiro et al.[48] that compared $ZnSO_4$ with biochar-graphene oxide composite (Zn-OMF), the Zn-OMFs

promoted a more gradual release of Zn when compared to soluble mineral sources. When Zn is bound to organic compounds, either by complexation or adsorption in OMFs, there is a nutrient protection reaction offered by organic radicals that contribute to a more gradual nutrient release[2,7,15,48] as observed in our study, considering that in comparison to $ZnSO_4$, the OMFs had a smaller amount of Zn and gradual release the nutrient over time (**Figure 2**).

4.2 Zn diffusion from OMFs in Oxisols

The Zn diffusion is controlled by soil pH, clay and OM contents, clay mineralogy and fertilizer properties[7,16,29]. The increase in pH, OM, clay and Fe oxide contents in soils was followed by a decrease in Zn diffusion, possibly due to more Zn adsorbed in soil colloids[2]. For these reasons, Zn diffusion was lower in RO with higher clay and OM contents than in YO. In the same soil type, the Zn diffusion radius compared to the velocity of Zn diffusion[16,29] and, as verified in our study (**Figure 3**) and reported by Kabiri et al.[7], compared to $ZnSO_4$, slow-release fertilizers promoted a lower Zn diffusion.

According to readily soluble Zn in fertilizers was reduced (Zn soluble in water) by OMFs; consequently, Zn diffusion radius decreases in both Oxisols (**Figure 6**). Zn diffusion in Petri dishes with colored papers is strongly correlated with the water-soluble Zn in fertilizers[16]. The higher the water-soluble Zn content favored, the faster the Zn dissolution; consequently, the Zn diffusion is greater in the soil[7,16]. Fertilizers with the slower Zn dissolution contribute initially to reducing the Zn diffusion radius[52], being a strategy to increase biomass production and the accumulation of Zn by plants[7]. In our OMFs synthesized compared to ZnSO4, a lower diffusion radius was verified for OMF1 and OMF4 in both Oxisols (**Figure 3**). Compared to $ZnSO_4$, a reduction in Zn diffusion for only OMF2 and OMF3 was verified in RO; thus, our OMFs were promised to increase the fertilization efficiency with Zn from the study of Zn diffusion in Oxisols.

4.3 Infrared as an indicator of Zn complexation in OMFs

When Zn is applied together with organic sources as in OMFs, there is greater efficiency in using Zn by plants[7,48]. The beneficial effects of organic sources and Zn are closely related to the complexation of Zn by organic molecules[2,5,7] as happened in Zn-HA interaction[6,10] and verified through changes in the infrared spectrum. The water solubility of Zn-HA complexes depends on the chemical stability and reactivity of the formed humic-metal complexes, which are regulated by the stoichiometry of the Zn-HA mixture, pH, and humic acid properties[10,53]. Compared to slow Zn fertilizers com Zn complexed, the rapid Zn dissolution with free forms of Zn^{2+} in mineral fertilizers favored reactions with phosphate fertilizers, with subsequent precipitation of Zn with phosphates and other anions present in soils[2,5,7].

The main information extracted from the infrared analysis is which organic functional groups are related to Zn complexation; once when Zn is mixed with humic matrix, there are changes in peaks and absorbance intensity that indicate the Zn-HA complexation[10]. The complexation of Zn mixed HA indicated by the infrared spectrum analysis of OMFs showed that Zn interacts with the HA through bonds between Zn and C or S from HA, reducing the formation of Zn^{2+} ions and the prevalence of free forms of Zn found in $ZnSO_4$ **(Figure 1)**.

The formation of a new peak at 3290 cm^{-1} related to OH stretching verified in OMF1 and OMF4 compared to HA precursor used in the synthesis is an indicator of the hydration and production of Zn aqueous complexes in HA structure[6,10]. When HA3 was used in the synthesis of OMF3, the OH stretching peak at 3290 cm^{-1} moved to 3370 cm^{-1}, indicating the interaction of the Zn mineral source and HA during OMF3 synthesis forming Zn-HA complexes as demonstrated by Boguta and Sokołowska[10], where increasing the proportion of $ZnCl_2$ over HA promotes changes in the peaks in the ranges mentioned above.

The interaction of Zn-HA also involves aliphatic C-H groups through the reduction of the absorbance intensities of the Zn-HA samples compared to those of the HA precursor[10] as observed in this study for those of the OMFs (OMF1, 3 and 4) compared to those for the HA precursors (**Figure 1).** The changes in C=C aromatic, polysaccharide C-O, carboxylic acid C=O and OH phenolic stretching, C-CH_3 group bending and COOH in alkyl groups are also fingerprints of the formation of Zn-HA complexes[6,10,22]. In all OMFs compared to HA precursor used in the OMFs synthesis, this interaction of Zn-HA was indicative of C=C aromatic stretching (**Figure 1**); however, polysaccharide C-O stretching, carboxylic acid C=O stretching and OH phenolic stretching were important indicators of Zn complexation to OMF1 and OMF2, COOH in alkyl groups occurred and characteristic to OMF2, while C-CH3 group bending was recorded for OMF3 and OMF4.

The sulfur groups found in OMF2 and OMF4 are related to SO_2 stretching (alkyl sulfate)-$RSO_4^-M^+$ (1075 cm^{-1}) and C-S stretching (methyl sulfone-CH_3-SO_2) and indicated Zn-HA complexation because in OMF2 compared to in the HA precursor, the peaks related to C=S thiocarbonyl and SO_2 stretching (sulfone) disappeared, indicating the reactions between S organic groups with Zn from mineral sources (**Figure 1**). In the OMF4-HA precursor, S-groups were not found; however, the Zn mineral source used in the synthesis contained sulfur in free forms, and the formation of C-S bonds indicated reactions between HA and Zn sulfate[6]. In OMF2, the mineral source of Zn did not contain sulfur, although peaks of SO_4^{2-}(free sulfate groups) appeared; thus, it is possible that the Zn source with the humic matrix also formed complex forms of HA-Zn, as well as free sulfate forms that were bonded to Zn.

SO_2 stretching (sulfone) occurred in OMF3 synthesis rather than in the HA used in its synthesis, indicating the interaction of the Zn mineral source and HA during the synthesis process. The sulfur groups present in Zn-HA complexes are reported elsewhere for single mixtures of HA and Zn without the aim of producing fertilizers[6]. Complexation of Zn by HA

through sulfur groups promotes composted-based fertilizers with low stability and high water solubility as verified for OMF2 and OMF4. In comparison, the C-Cl stretching mode may be related to lower water solubility, as the OMFs had lower water solubility, and C-Cl groups were found only in OMF2, OMF4, and OMF3. Thus, OMF synthesis involving the HA type, stoichiometry, and Zn sources and process control during the OMF manufacturing process promote fertilizers with Zn complexed in different organic functional groups that promote differences in fertilizers when their properties.

4.4 Agronomic performance of OMFs for maize and brachiaria

Evaluating the agronomic performance of the OMFs over $ZnSO_4$, it showed differences of the OMFs in the availability of Zn and P in the soil solution and the solid phase, and the production of biomass and accumulation of Zn and P in the shoot of maize and brachiaria in a soil-dependent effect (**Tables 3 and 4, Figures 4 and 5**). Besides, it was observed that no Zn fertilization limited the maize and brachiaria grown in both Oxisols studied (**Figures 4 and 5**).

At least one of the OMFs overcame the biomass production and Zn accumulation by maize and brachiaria in both Oxisols (**Figures 4 and 5**). The effect happens because, in tropical soils, soluble Zn mineral sources are less efficient in delivering Zn to crops, considering that readily available Zn compounds are prone to react with soil components through sorption and precipitation processes[2,6,7,54]. Thus, supplying Zn via OMCs is a feasible and smart solution for minimizing the substantial loss of Zn in highly weathered soils, as organic ligands in Zn complexes prevent the adsorption on the clay surface and the formation of Zn precipitates; thus positively regulating Zn availability in whole soil and its solution[2,6,7,54].

Using the buffer solution to simulate the ability of Zn-OMFs to release Zn complexed by humic acid to the soil solution, it was observed that Zn-OMFs have the ability to release Zn to the soil solution gradually[55]. However, little is known about the effect of Zn complexed in

OMFs on the soil solution evaluated under plant growing conditions. Positive effects of Zn-complexed forms on Zn-free forms have been observed mainly in soil solution in response to humic substances added to the soil with Zn complexed in a HA structure[6].

Soil solution is the pool where plants acquire readily available nutrients[1,2,30]. Overall, Zn contents in the soil solution are low, in the range of 0.000026 to 0.26 mg L^{-1} Zn, which is in line with the Zn soluble contents determined in this study and close to the Zn threshold level (0.131 mg L^{-1}) recommended for plant plentiful growth in nutritive solution for plant growth[2,32]. It is important to highlight that only for Zn-fertilized maize plants Zn contents RO solution were above the aforementioned critical level for nutritive solutions (**Tables 3 and 4**). However, due to the balance between the solid phase and the liquid phase, the critical value of a nutrient in solution may not be an adequate fertility index for crops; the reason why new nutrient indices in solution should be investigated across soil types and plant species. According to the assumption mentioned, Zn in the soil solution was correlated with total biomass production to determine the critical levels of Zn in soil solution for maize grown in both Oxisols and brachiaria cultivated in YO. At the beginning of each cultivation cycle, the critical levels for solution Zn were 0.164, 0.045 and 0.025 mg L^{-1} Zn for maize cultivated in RO and YO and brachiaria cultivated in YO, respectively (**Supplementary material 9**).

In soil solution, the main forms of Zn are free hydrated $Zn(6H_2O)^{2+}$ and soluble organic complexes, although the abundance of Zn mainly depends on the Zn source and soil type properties, with mineral sources favoring Zn free forms, while OM favors the formation of Zn in organic complexes[1,2]. A higher Zn availability was verified when organic molecules complex Zn instead of being precipitated by other anions and, or adsorbed into soil colloids[2], consequently improving Zn content in soil solution[6]. In the maize experiment, in comparison to $ZnSO_4$, OMFs produced with different HA sources did not increase Zn in the soil solution (**Table 3**). In addition, RO fertilized with OMF1 decreased Zn in solution, mirrored by the

kinetics of Zn release study (**Figure 2**). The main effect of OMFs was verified in soil solution when brachiaria was cultivated in sequence to maize. In addition, in comparison to $ZnSO_4$, all OMFs increased the Zn in solution in YO. In RO, OMF3 and OMF4 improved Zn availability in the soil liquid phase when brachiaria was cultivated in sequence to maize (**Table 4**).

Despite the null effect of OMFs on solution Zn contents, when maize was cultivated, compared to $ZnSO_4$, OMF1, OMF2 and OMF3 increased the solution P in RO, and OMF2 and OMF3 increased the solution P in YO, indicating the secondary effect of OMFs on P chemistry and available forms in soil solution (**Table 3**). The positive residual effect of OMFs on solution P was demonstrated through the brachiaria experiment, considering that OMF1, OMF3 and OMF4 (the Zn source with the lowest Zn rate constant release) over $ZnSO_4$ increased solution P contents. In YO, an increase in solution P content was only verified in OMF3-treated samples (**Table 4**).

The main sources of P in agriculture are fully acidified phosphate fertilizers, which can rapidly increase the P content of soil solution[56,57]. The readily available P from soluble phosphate sources is prone to react with Zn in soil solution[2,3], with a subsequent synthesis of insoluble precipitates such as $Zn_3(PO_4)_2$. Precipitation of Zn in soil solution reduces the availability of Zn and P for plants, and such a negative interaction is usually termed "P-induced Zn deficiency" [5]. When bonded to organic compounds, Zn experiences some protection, which translates into fewer amounts of Zn adsorbed into mineral colloids and or precipitated in soil [2,5]; consequently, soil Zn and P availability increases. In addition, when humic fractions are present in soil and combined with P soluble sources, the formation of metal-P-HA complexes inhibits P fixation and improves the agronomic performance of P sources in different cropping systems[58]. This effect of OMFs increasing the availability of P in the soil was observed for soil P-resin levels; it was observed for OMF1, OMF2 and OMF4-fertilized plants, including

brachiaria plants grown in RO, and OMF2 and OMF4-treated maize plants grown in YO (**Tables 3 and 4**).

Concerning Zn availability in whole soil, soil Zn-DTPA contents were reduced due to the use of Zn slow-release fertilizers (OMFs) rather than the use of $ZnSO_4$, excepted for OMF3 in RO, the Zn source with the highest amount of total Zn added to the soil (**Tables 3 and 4**). Results contrary to ours were found by Carneiro et al.[48] where the application of Zn-OMFs based on biochar-graphene oxide composite increased the availability of Zn in the soil. The main effect of OMFs increasing the soil Zn-DTPA is related to Zn recommendations based on the CA-Zn index, and the Zn-CA index in OMF3 was the lower (77.9%) between OMFs, which promoted greater amounts of total Zn applied. The close relationship between the total Zn added by the OMFs, and increased contents of soil Zn-DTPA in RO was probably due to the relatively high OM content and consequently higher levels of lower molecular weight organic acids[59]. Because some organic acids can ptomote HA supramolecular structure fragmentation into small bioactive humic units that can increase Zn availability[50], thus accessing destabilized and release Zn in organic forms not accessed in Zn availability chemical extractor for Zn recommendation for plants.

It is expected that OMFs with Zn in complex forms will gradually release Zn, affecting the Zn availability in the soil and may have a higher agronomic performance than mineral fertilizers. In fact, OMFs positively affected the maize and brachiaria successively cultivated in a soil type-dependent way (**Table 5**). The maize and brachiaria successively cultivation was adopted to study plants with high sensitivity (maize) and less affected (brachiaria) to soil Zn deficiency[3]. The Oxisols investigated are contrasting regarding clay and OM contents, with a greater potential of Zn deficiency in RO, considering that a higher clay and OM increased Zn adsorption, inducing Zn deficiency in soils[2,3,5].

Table 5. Summary of main effects of OMFs over $ZnSO_4$.

Red Oxisol								
Variable	OMF1		OMF2		OMF3		OMF4	
	Mai.	Brac.	Mai.	Brac.	Mai.	Brac.	Mai.	Brac.
Solution Zn	↓	-	-	-	-	↑	-	↑
Solution P	↑	↑	↑	-	↑	↑	-	↑
Soil Zn-DTPA	↓	↓	↓	-	↑	↑	↓	↓
Soil P-resin	-	↑	-	↑	-	-	-	↑
TDM	↑	-	↑	↑	-	↑	↑	↓
SDM	↑	↓	-	↑	-	↑	↑	↓
RDM	↑	↑	↑	↑	↑	↑	↑	-
Zn in shoot	-	↓	↓	-	↑	↑	↑	↓
P in shoot	-	-	-	↑	-	↑	↑	-
Yellow Oxisol								
Variable	OMF1		OMF2		OMF3		OMF4	
	Mai.	Brac.	Mai.	Brac.	Mai.	Brac.	Mai.	Brac.
Solution Zn	-	↑	-	↑	-	↑	-	↑
Solution P	-	-	↑	-	↑	↑	-	-
Soil Zn-DTPA	↓	↓	↓	↓	↓	-	↓	↓
Soil P-resin	-	-	↑	-	-	-	↑	-
TDM	-	↑	-	↑	↑	-	-	↑
SDM	-	↑	↑	↑	↑	-	-	↑
RDM	↑	↑	-	↑	↑	-	-	↑
Zn accumulation	-	↑	↑	↑	↑	-	↑	↑
P accumulation	-	↑	↑	↑	↑	-	↑	↑

↑: improving, ↓: reducing; -: similar effect. Solution Zn and P: Zn and P soluble in soil solution, respectively; Soil Zn-DTPA: Zn available in soil by the DTPA method; Soil P-Resin: P available in soil by the resin method; SDM, RDM and TDM: shoot, root and total dry matter production respectively; Zn and P accumulation: Zn and P accumulation in the shoot respectively. Mai: maize cultivation; Brac.: Brachiaria cultivation.

Similar to our results, Zn-OMFs can affect the availability of nutrients in the soil and increase the production and accumulation of Zn compared to $ZnSO_4$[48]. In RO, OMF1 improved shoot and total biomass production for maize plants (**Figure 4**). OMF2 improved total maize and root biomass production for the maize-brachiaria succession in RO (**Figures 4 and 5**), although Zn in the maize shoot decreased for the main crop, while for brachiaria plants, shoot biomass and P in the shoot were increased in response to OMFs as Zn sources. In RO, OMF was used to nourish brachiaria, considering that root biomass and Zn in shoot increased compared to $ZnSO_4$-fertilized plants. In addition to improving brachiaria, in comparison to Zn sulfate-nourished plants, those that received OMFs were characterized by a high residual Zn effect in soils, ensuring greater total, shoot and root brachiaria biomasses, as well as a greater Zn and P in brachiaria shoot. When applied to RO, OMFs had a high potential to improve maize biomass production and Zn and P in their shoot.

In YO cultivated with maize, in comparison to $ZnSO_4$, OMF1 promoted greater root biomass production, while OMF2 and OMF3 increased maize shoot biomass, and OMF2 and OMF4 increased Zn and P in the shoot. In RO, compared to $ZnSO_4$, the OMF3 had a higher residual effect (brachiaria experiment). An increase in Zn in soil solution in response to OMF1, OMF2 and OMF4 in RO cultivated with brachiaria improved the total, shoot and root biomass, and the Zn and P in the grass shoot. Thus, OMF1, OMF2 and OMF4 slightly improved maize growth, but these Zn sources were capable of supplying Zn to brachiaria plants. On the contrary, OMF3 effectively improved maize growth while its effect on brachiaria growth is limited, as well as the Zn residual for the grass grown in succession to maize.

As observed in our study, the zinc fertilization and OMF effects on soil and crops are soil type-dependent, and soil OM is one of the main factors controlling the effect of mineral and organic fertilizers on plants[2,3,5,60]. Zinc strongly interacts with tropical soil components, including OM compounds, as the functionalized organic fragments increase in response to OM

increased storage in soils, promoting the complexation of Zn with subsequent formation of organometallic complexes whose stability and solubility are regulated by the strength of bonds formed[10,12]. In addition, some OM fractions and functional groups act to block adsorption sites in clay minerals and Fe and Al (hydro) oxides, with subsequent improvements of Zn and P availability in soil[15,61]. Results reported in this study corroborate the role played by soil OM on Zn and P chemistry, considering that Zn and P availability for maize and brachiaria were improved in the Oxisol enriched in OM (RO) (**Tables 3, 4 and 5**).

Zinc sulfate is commonly used to nourish plants, including maize, an annual crop, at least in the short term, considering that Zn residual of sulfate was not yet appropriately studied according to different crop successes[2,62]. However, over a long period (36 years), the simultaneous application of zinc sulfate plus NPK fertilizer provides a residual effect of Zn, increasing the proportion of Zn bound to organic components of the soil, which contributes to improving the production and nutrition of Zn[63]. However, in this study, only one source of Zn was tested. The synthesis of slow-release Zn fertilizers could be a new approach for improving plant growth and Zn uptake in crops successively cultivated. According to Kabiri et al.[7], Zn complexed to graphene reduced Zn water solubility due to Zn incorporation into the graphene structure, hampering Zn uptake and growth of durum wheat, although the residual effect of Zn was not evaluated.

The residual effect of Zn fertilization relies on the fertilizer rate, soil type, and crop[2]. The residual effect of Zn evaluated in successive crop cultivation requires the correct evaluation of fertilizer agronomic value. In such studies, different plants should be tested and successively studied. The results reported by Mattiello et al.[62] attested that $ZnSO_4$ rather than ZnO resulted in higher biomass production of a wheat-ryegrass-maize sequentially cultivated. The longer Zn stays in contact with soil, the lower the agronomic performance of fertilizers, as Zn tends to be slowly released to plants due to previous strong sorption reactions with soil components.

Improving the knowledge of the residual value of Zn fertilizer is necessary for determining the rate and frequency of fertilizer application to different crops or plant rotation schemes[2].

In the same Oxisols used in our study, evaluating the residual effect of HA application combined with $ZnSO_4$, the HA effect on Zn complexation and maize-brachiaria rotation was also soil-dependent, with a higher growth of brachiaria grown in YO in a sequence of Zn-fertilized maize cultivation[6]. Mirroring the results reported, in YO, OMF1, OMF2 and OMF4 rather than Zn sulfate showed a higher residual Zn effect, increasing brachiaria biomass production. The new Zn-OMFs improve agronomic management of the first crop and the Zn residual effect on brachiaria, a successively grown sequence to the main crop, maize. We demonstrated that OMFs improve maize and brachiaria growth and Zn nutrition with secondary and positive effects on crop P uptake.

In addition, there were effects due to the application of organic sources on the availability of Zn, and its absorption by the culture can happen as the increase of the C-input stimulates the microbial activity that can solubilize the Zn[64]. However, these effects do not usually happen in the short term, such as at the experiment time. However, this increased C-Input showed correlated with an increase in biomass production and the accumulation of Zn in maize in soil with the lower OM content **(Supplementary Material 8**), without affecting the Zn availability in the soil and its solution. In addition, OMFs contain organic molecules in humic substances that may have biostimulant effects[8,9].

4.5 Study limitations and future perspectives

The importance of pot studies is to indicate promising materials to be tested at stages after the field level, being an initial and crucial stage in validating technologies, reducing the cost of experimentation, and field validation steps should be performed after the first. In experiments, contrary to what happens at the field level, leaf nutrient contents are not the best

index for evaluating adequate Zn nutrition, and concentration in leaf tissues can be much higher than found in the field as in our experiment (Supplementary Material 3). However, once the potential of our synthesized Zn-OMFs to more adequately supply maize and brachiaria successively cultivated, as well as other Zn-OMFs in studies already performed, there is a need to validate these fields to the field level evaluating its potential in different agricultural scenarios defining more efficient management of fertilization with Zn improving the crops production and concentration of Zn in leaves.

In addition, very little explored the OMF effect is related to the C-Input on microbial activity and the possible biostimulant effects related to this C. For example, humic substances have a biostimulant role on plants which can increase nutrient acquisition by the stimulus on H+-ATPase of the plasmatic membrane, carries and transports of nutrients in plants, and increase the root growth[8,9]. Thus, fertilizers based on the organic matrix can also have biostimulant effects on plants, stimulant effects on microbial activity and chemical effects. These effects need to be better elucidated for OMFs in future papers indicating the chemical and biological mechanisms responses due to OMFs application.

5 Conclusions

Synthesis of humic acid-based Zn organomineral fertilizers (OMFs) reduced the water solubility of Zn due to the formation of organic Zn complexes, as indicated by infrared analysis. This gave the OMFs slow-release property of Zn and reduced diffusion of this micronutrient in Oxisols tested. These new properties provided OMF2 with greater agronomic performance over zinc sulfate in nourishing maize and brachiaria in successively grown. Zinc source effects on plants are highly dependent on the interaction of OMF-soil properties, especially organic matter content and size particle distribution, and on the crop studied. Zn diffusion was largely controlled by attributes of the OMFs, mainly water solubility and the Oxisols properties.

Regardless of the soil investigated, Zn diffusion is greater for zinc sulfate than for OMFs, except in Yellow Oxisol, where OMF2 has diffusion similar to this soluble source. The OMFs increased the available contents of Zn and P in soil and solution and can be suitable slow release Zn sources to nourish maize and brachiaria (Zn residual) in highly weathered Oxisols.

6 Acknowledgments

Many thanks to the Coordination for the Improvement of Higher Education Personnel (CAPES) (CAPES-PROEX/AUXPE 593/2018), the National Council for Scientific and Technological Development (CNPq) (303899/2015-8 and 307447/2019-7 grants), and the Foundation for Research of the State of Minas Gerais (FAPEMIG) for the financial support and scholarships provided. UFLA is an equal opportunity provider and employer.

7 References

(1) Broadley, M.; Brown, P.; Cakmak, I.; Rengel, Z.; Zhao, F. Function of Nutrients: Micronutrients. In *Marschner's mineral nutrition of higher plants*; Elsevier, 2012; pp 191–248.

(2) Montalvo, D.; Degryse, F.; da Silva, R. C.; Baird, R.; McLaughlin, M. J. *Agronomic Effectiveness of Zinc Sources as Micronutrient Fertilizer*; Elsevier Inc., 2016; Vol. 139. https://doi.org/10.1016/bs.agron.2016.05.004.

(3) Alloway, B. J. Soil Factors Associated with Zinc Deficiency in Crops and Humans. *Environ. Geochem. Health* **2009**, *31* (5), 537–548. https://doi.org/10.1007/s10653-009-9255-4.

(4) Lopes, A. S.; Guilherme, L. R. G. *A Career Perspective on Soil Management in the Cerrado Region of Brazil*; Elsevier Inc., 2016; Vol. 137. https://doi.org/10.1016/bs.agron.2015.12.004.

(5) Suganya, A.; Saravanan, A.; Manivannan, N. Role of Zinc Nutrition for Increasing Zinc Availability, Uptake, Yield, and Quality of Maize (Zea Mays L.) Grains: An Overview. *Commun. Soil Sci. Plant Anal.* **2020**, *51* (15), 2001–2021. https://doi.org/10.1080/00103624.2020.1820030.

(6) Morais, E. G. de; Silva, C. A.; Jindo, K. Humic Acid Improves Zn Fertilization in Oxisols Successively Cultivated with Maize–Brachiaria. *Molecules* **2021**, *26* (15), 4588. https://doi.org/10.3390/molecules26154588.

(7) Kabiri, S.; Degryse, F.; Tran, D. N. H.; da Silva, R. C.; McLaughlin, M. J.; Losic, D. Graphene Oxide: A New Carrier for Slow Release of Plant Micronutrients. *ACS Appl. Mater. Interfaces* **2017**, *9* (49), 43325–43335. https://doi.org/10.1021/acsami.7b07890.

(8) Nardi, S.; Schiavon, M.; Francioso, O. Chemical Structure and Biological Activity of Humic Substances Define Their Role as Plant Growth Promoters. *Molecules* **2021**, *26* (8). https://doi.org/10.3390/molecules26082256.

(9) Zanin, L.; Tomasi, N.; Cesco, S.; Varanini, Z.; Pinton, R. Humic Substances Contribute to Plant Iron Nutrition Acting as Chelators and Biostimulants. *Front. Plant Sci.* **2019**, *10* (May), 1–10. https://doi.org/10.3389/fpls.2019.00675.

(10) Boguta, P.; Sokołowska, Z. Interactions of Zn(II) Ions with Humic Acids Isolated from Various Type of Soils. Effect of PH, Zn Concentrations and Humic Acids Chemical Properties. *PLoS One* **2016**, *11* (4), 1–20. https://doi.org/10.1371/journal.pone.0153626.

(11) Oste, L. A.; Temminghoff, E. J. M.; Lexmond, T. M.; Van Riemsdijk, W. H. Measuring and Modeling Zinc and Cadmium Binding by Humic Acid. *Anal. Chem.* **2002**, *74* (4), 856–862. https://doi.org/10.1021/ac0105080.

(12) Justi, M.; de Freitas, M. P.; Silla, J. M.; Nunes, C. A.; Silva, C. A. Molecular Structure Features and Fast Identification of Chemical Properties of Metal Carboxylate Complexes by FTIR and Partial Least Square Regression. *J. Mol. Struct.* **2021**, *1237*, 130405. https://doi.org/10.1016/j.molstruc.2021.130405.

(13) Legros, S.; Doelsch, E.; Mason, A.; Rose, J.; Borschneck, D.; Proux, O.; Hazemann, J.-L.; Saint-Macary, H.; Bottero, J.-Y. Combining Size Fractionation, Scanning Electron Microscopy, and X-Ray Absorption Spectroscopy to Probe Zinc Speciation in Pig Slurry. *J. Environ. Qual.* **2010**, *39* (2), 531–540. https://doi.org/10.2134/jeq2009.0096.

(14) Rouff, A. A.; Juarez, K. M. Zinc Interaction with Struvite During and After Mineral Formation. *Environ. Sci. Technol.* **2014**, *48* (11), 6342–6349. https://doi.org/10.1021/es500188t.

(15) Dhaliwal, S. S.; Naresh, R. K.; Mandal, A.; Singh, R.; Dhaliwal, M. K. Dynamics and Transformations of Micronutrients in Agricultural Soils as Influenced by Organic Matter Build-up: A Review. *Environ. Sustain. Indic.* **2019**, *1–2* (September), 100007. https://doi.org/10.1016/j.indic.2019.100007.

(16) Degryse, F.; da Silva, R. C.; Baird, R.; Cakmak, I.; Yazici, M. A.; McLaughlin, M. J. Comparison and Modelling of Extraction Methods to Assess Agronomic Effectiveness of Fertilizer Zinc. *J. Plant Nutr. Soil Sci.* **2020**, *183* (2), 248–259. https://doi.org/10.1002/jpln.201900340.

(17) Silva, C. A.; Morais, E. G. de; Maluf, H. J. G. M. Novo Fertilizante de Liberação Controlada de Zinco Complexado a Ácido Húmico. BR1020210079568, 2021.

(18) Brazil. *Manual de Métodos Analíticos Oficiais Para Fertilizantes e Corretivos*; Brasil, Ed.; MAPA: Brasília, 2017.

(19) Vale, F.; Alcarde, J. C. Solubilidade e Disponibilidade Dos Micronutrientes Em Fertilizantes. *Rev. Bras. ciência do solo* **1999**, *23* (2), 441–451.

(20) Chien, S. H.; Prochnow, L. I.; Tu, S.; Snyder, C. S. Agronomic and Environmental Aspects of Phosphate Fertilizers Varying in Source and Solubility: An Update Review. *Nutr. Cycl. Agroecosystems* **2011**, *89* (2), 229–255. https://doi.org/10.1007/s10705-010-9390-4.

(21) Gautam, R.; Vanga, S.; Ariese, F.; Umapathy, S. Review of Multidimensional Data Processing Approaches for Raman and Infrared Spectroscopy. *EPJ Tech. Instrum.* **2015**, *2* (1), 1–8. https://doi.org/10.1140/epjti/s40485-015-0018-6.

(22) Parikh, S. J.; Goyne, K. W.; Margenot, A. J.; Mukome, F. N. D.; Calderón, F. J. Soil Chemical Insights Provided through Vibrational Spectroscopy; 2014; pp 1–148. https://doi.org/10.1016/B978-0-12-800132-5.00001-8.

(23) Canellas, L. P.; Espindola, J. A. A.; Rezende, C. E.; Camargo, P. B. de; Zandonadi, D. B.; Rumjanek, V. M.; Guerra, J. G. M.; Teixeira, M. G.; Braz-Filho, R. Organic Matter Quality in a Soil Cultivated with Perennial Herbaceous Legumes. *Sci. Agric.* **2004**, *61* (1), 53–61. https://doi.org/10.1590/s0103-90162004000100010.

(24) Sadeek, S. A. Preparation, Infrared Spectrum and Thermal Studies of [Zn2(H2O)4(SO4)2] Complex Formed by the Reaction of Urea with Zinc (II) Sulphate. *J. Phys. Chem. Solids* **1993**, *54* (8), 919–922. https://doi.org/10.1016/0022-3697(93)90219-H.

(25) Chen, W.; Ouyang, Z. Y.; Qian, C.; Yu, H. Q. Induced Structural Changes of Humic Acid by Exposure of Polystyrene Microplastics: A Spectroscopic Insight. *Environ. Pollut.* **2018**, *233*, 1–7. https://doi.org/10.1016/j.envpol.2017.10.027.

(26) Socrates, G. *Infrared and Raman Characteristic Group Frequencies: Tables and Charts*; John Wiley \& Sons, 2004.

(27) Rufford, T. E.; Zhu, J.; Hulicova-Jurcakova, D. *Green Carbon Materials: Advances and Applications*; Pan Stanford, 2019.

(28) Lin-Vien, D.; Colthup, N. B.; Fateley, W. G.; Grasselli, J. G. *The Handbook of Infrared and Raman Characteristic Frequencies of Organic Molecules*; Elsevier, 1991.

(29) Degryse, F.; Baird, R.; McLaughlin, M. J. Diffusion and Solubility Control of Fertilizer-Applied Zinc: Chemical Assessment and Visualization. *Plant Soil* **2014**, *386* (1–2), 195–204. https://doi.org/10.1007/s11104-014-2266-7.

(30) Carmo, D. L. do; Silva, C. A.; Lima, J. M. de; Pinheiro, G. L. Electrical Conductivity and Chemical Composition of Soil Solution: Comparison of Solution Samplers in Tropical Soils. *Rev. Bras. Ciência do Solo* **2016**, *40*. https://doi.org/10.1590/18069657rbcs20140795.

(31) Alvarez, J. M. Influence of Soil Type on the Mobility and Bioavailability of Chelated Zinc. *J. Agric. Food Chem.* **2007**, *55* (9), 3568–3576. https://doi.org/10.1021/jf063236g.

(32) Marschner, P. *Marschner's Mineral Nutrition of Higher Plants*; Elsevier: Oxford, 2012. https://doi.org/10.1016/C2009-0-63043-9.

(33) Novais, R. F. .; Neves, J. C. L. .; Barros, N. F. Ensaio Em Ambiente Controlado. In

Métodos de pesquisa em fertilidade do solo; Oliveira, A. J. ., Garrido, W. E. ., Araújo, J. D. ., Lourenço, S., Eds.; Embrapa-SEA: Brasília, 1991; p 189−253.

(34) *Manual de Métodos de Análise de Solo*, 3rd ed.; Teixeira, P. C., Donagemma, G. K., Fontana, A., Teixeira, W. G., Eds.; Embrapa: Brasília, 2017.

(35) Kalra, Y. *Handbook of Reference Methods for Plant Analysis*; CRC press, 1997.

(36) Jarrell, W. M.; Beverly, R. B. The Dilution Effect in Plant Nutrition Studies; 1981; pp 197–224. https://doi.org/10.1016/S0065-2113(08)60887-1.

(37) Leite, U. T.; Aquino, B. F.; Rocha, R. N. C.; Silva, J. Níveis Críticos Foliares de Boro, Cobre, Manganês e Zinco Em Milho. *Biosci. J.* **2006**, *19* (2), 115–125.

(38) R Core Team. R: A Language and Environment for Statistical Computing. R Foundation for Statistical Computing: Vienna, Austria 2020.

(39) Mendiburu, F. Agricolae: Statistical Procedures for Agricultural Research. 2020.

(40) Wei, T.; Simko, V. R Package "Corrplot": Visualization of a Correlation Matrix. 2017.

(41) Kassambara, A.; Mundt, F. Factoextra: Extract and Visualize the Results of Multivariate Data Analyses. 2020.

(42) Baty, F.; Ritz, C.; Charles, S.; Brutsche, M.; Flandrois, J.-P.; Delignette-Muller, M.-L. A Toolbox for Nonlinear Regression in R : The Package Nlstools. *J. Stat. Softw.* **2015**, *66* (5). https://doi.org/10.18637/jss.v066.i05.

(43) Hamner, B.; Frasco, M. Metrics: Evaluation Metrics for Machine Learning. 2018.

(44) Dou, Z.; Toth, J. D.; Jabro, J. D.; Fox, R. H.; Fritton, D. D. Soil Nitrogen Mineralization during Laboratory Incubation: Dynamics and Model Fitting. *Soil Biol. Biochem.* **1996**, *28* (4–5), 625–632. https://doi.org/10.1016/0038-0717(95)00184-0.

(45) Liu, C.; Liu, X.-W.; Wu, W.-C.; Cai, X.-D.; Liang, X.; Li, Y.-B.; Nan, Z.-R. Effect of Biochar and Biochar Based Fertilizer on Growth of Lactuca Sativa L. and Absorption of Heavy Metals. *Zhongguo Huanjing Kexue/China Environ. Sci.* **2016**, *36* (10), 3064–3070.

(46) Lustosa Filho, J. F.; Penido, E. S.; Castro, P. P.; Silva, C. A.; Melo, L. C. A. Co-Pyrolysis of Poultry Litter and Phosphate and Magnesium Generates Alternative Slow-Release Fertilizer Suitable for Tropical Soils. *ACS Sustain. Chem. Eng.* **2017**, *5* (10), 9043–9052. https://doi.org/10.1021/acssuschemeng.7b01935.

(47) Akaike, H. A Bayesian Extension of the Minimum AIC Procedure of Autoregressive Model Fitting. *Biometrika* **1979**, *66* (2), 237. https://doi.org/10.2307/2335654.

(48) Carneiro, J. S. da S.; Leite, D. A. da C.; Castro, G. M. de; Franca, J. R.; Botelho, L.; Soares, J. R.; Oliveira, J. E. de; Melo, L. C. A. Biochar-Graphene Oxide Composite Is Efficient to Adsorb and Deliver Copper and Zinc in Tropical Soil. *J. Clean. Prod.* **2022**, *360* (May), 132170. https://doi.org/10.1016/j.jclepro.2022.132170.

(49) Lombi, E.; McLaughlin, M. J.; Johnston, C.; Armstrong, R. D.; Holloway, R. E. Mobility, Solubility and Lability of Fluid and Granular Forms of P Fertiliser in Calcareous and Non-Calcareous Soils under Laboratory Conditions. *Plant Soil* **2005**, *269* (1–2), 25–34. https://doi.org/10.1007/s11104-004-0558-z.

(50) Morais, E.; Silva, C. A.; Maluf, H. J. G. M. UV-Visible Spectroscopy as a New Tool to Predict the Bioactivity of Humic Fragments Induced by Citric/ Oxalic Acids on Eucalyptus Nutrition and Growth. *Commun. Soil Sci. Plant Anal.* **2020**, *51* (22), 2830–2845. https://doi.org/10.1080/00103624.2020.1849266.

(51) López-Rayo, S.; Imran, A.; Bruun Hansen, H. C.; Schjoerring, J. K.; Magid, J. Layered Double Hydroxides: Potential Release-on-Demand Fertilizers for Plant Zinc Nutrition. *J. Agric. Food Chem.* **2017**, *65* (40), 8779–8789. https://doi.org/10.1021/acs.jafc.7b02604.

(52) Mattiello, E. M.; Da Silva, R. C.; Degryse, F.; Baird, R.; Gupta, V. V. S. R.; McLaughlin, M. J. Sulfur and Zinc Availability from Co-Granulated Zn-Enriched Elemental Sulfur Fertilizers. *J. Agric. Food Chem.* **2017**, *65* (6), 1108–1115. https://doi.org/10.1021/acs.jafc.6b04586.

(53) Rose, M. T.; Patti, A. F.; Little, K. R.; Brown, A. L.; Jackson, W. R.; Cavagnaro, T. R. A Meta-Analysis and Review of Plant-Growth Response to Humic Substances. In *Plant and Soil*; 2014; pp 37–89. https://doi.org/10.1016/B978-0-12-800138-7.00002-4.

(54) Olaetxea, M.; De Hita, D.; Garcia, C. A.; Fuentes, M.; Baigorri, R.; Mora, V.; Garnica, M.; Urrutia, O.; Erro, J.; Zamarreño, A. M.; Berbara, R. L.; Garcia-Mina, J. M. Hypothetical Framework Integrating the Main Mechanisms Involved in the Promoting Action of Rhizospheric Humic Substances on Plant Root- and Shoot- Growth. *Appl. Soil Ecol.* **2018**, *123* (June 2017), 521–537. https://doi.org/10.1016/j.apsoil.2017.06.007.

(55) Santos, A. M. P.; Bertoli, A. C.; Borges, A. C. C. P.; Gomes, R. A. B.; Garcia, J. S.; Trevisan, M. G. New Organomineral Complex from Humic Substances Extracted from Poultry Wastes: Synthesis, Characterization and Controlled Release Study. *J. Braz. Chem. Soc.* **2018**, *29* (1), 140–150. https://doi.org/10.21577/0103-5053.20170122.

(56) Hart, M. R.; Quin, B. F.; Nguyen, M. L. Phosphorus Runoff from Agricultural Land and Direct Fertilizer Effects: A Review. *J. Environ. Qual.* **2004**, *33* (6), 1954–1972. https://doi.org/10.2134/jeq2004.1954.

(57) Kahiluoto, H.; Kuisma, M.; Ketoja, E.; Salo, T.; Heikkinen, J. Phosphorus in Manure and Sewage Sludge More Recyclable than in Soluble Inorganic Fertilizer. **2015**. https://doi.org/10.1021/es503387y.

(58) Erro, J.; Urrutia, O.; Baigorri, R.; Aparicio-Tejo, P.; Irigoyen, I.; Torino, F.; Mandado, M.; Yvin, J. C.; Garcia-Mina, J. M. Organic Complexed Superphosphates (CSP): Physicochemical Characterization and Agronomical Properties. *J. Agric. Food Chem.* **2012**, *60* (8), 2008–2017. https://doi.org/10.1021/jf204821j.

(59) Adeleke, R.; Nwangburuka, C.; Oboirien, B. Origins, Roles and Fate of Organic Acids in Soils: A Review. *South African J. Bot.* **2017**, *108*, 393–406. https://doi.org/10.1016/j.sajb.2016.09.002.

(60) Antille, D. L.; Sakrabani, R.; Godwin, R. J. Phosphorus Release Characteristics from Biosolids-Derived Organomineral Fertilizers. *Commun. Soil Sci. Plant Anal.* **2014**, *45* (19), 2565–2576. https://doi.org/10.1080/00103624.2014.912300.

(61) Wang, K.; Xing, B. Structural and Sorption Characteristics of Adsorbed Humic Acid on Clay Minerals. *J. Environ. Qual.* **2005**, *34* (1), 342–349. https://doi.org/10.2134/jeq2005.0342.

(62) Mattiello, E. M.; CANCELLIER, E. L.; Silva, R. C.; Degryse, F.; Baird, R.; McLaughlin, M. J. Efficiency of Soil-Applied 67Zn-Enriched Fertiliser across Three Consecutive Crops. *Pedosphere* **2021**, *31* (4), 531–537. https://doi.org/10.1016/S1002-0160(20)60044-3.

(63) Shambhavi, S.; Kumar, R.; Padbhushan, R.; Verma, G.; Sharma, S. P.; Sharma, S. K.; Sharma, R. P. Dynamics of Zinc under Long-term Application of Chemical Fertilizers and Amendments by Maize–Wheat Cropping Sequence in Typic Hapludalfs. *Soil Use Manag.* **2020**, *36* (3), 507–523. https://doi.org/10.1111/sum.12566.

(64) Yan, B.-F.; Dürr-Auster, T.; Frossard, E.; Wiggenhauser, M. The Use of Stable Zinc Isotope Soil Labeling to Assess the Contribution of Complex Organic Fertilizers to the Zinc Nutrition of Ryegrass. *Front. Plant Sci.* **2021**, *12*. https://doi.org/10.3389/fpls.2021.730679.

Synopsis

We synthesized new Zn fertilization based on humic acid, capable of adequately nourishing plants and reducing the loss of this nutrient in Oxisols.

SUPPLEMENTARY DOCUMENT

Supplementary material 1. Production routes developed to formulate Zn-organomineral fertilizers, which are protected by BR1020210079568 deposit patent of OMF1 (10), OMF2 (11), OMF3 (18) and OMF 4(19) [17]. The new fertilizers were formulated by two different routes (A and B). Process for obtaining the new slow-release Zn-humic based-fertilizers (10 and 11) through A route; organic material (1); addition of a solution of KOH 0.5 mol L-1 (2); extraction of humic substances (3); addition of monoprotic acid (4) or diprotic acid (6) until the reduction of the pH of the solution to 1 (4); Humic acid fraction separation (5 e 7); Addition of alkaline sources of Zn (8); drying in the stove at 70 ºC (9). B: Process for obtaining the new slow-release Zn-humic based-fertilizers (18 and 19) through the B route; Commercial humic acid with a pH in the alkaline range (12); humic acid solubilization in distilled water (13); reduction of pH to 5-6 by the use of organic and or inorganic acids (14); addition of monovalent Zn salts (15) or divalent acids (16); the reaction of the aqueous mixture and drying in an oven at 70 ºC (17).

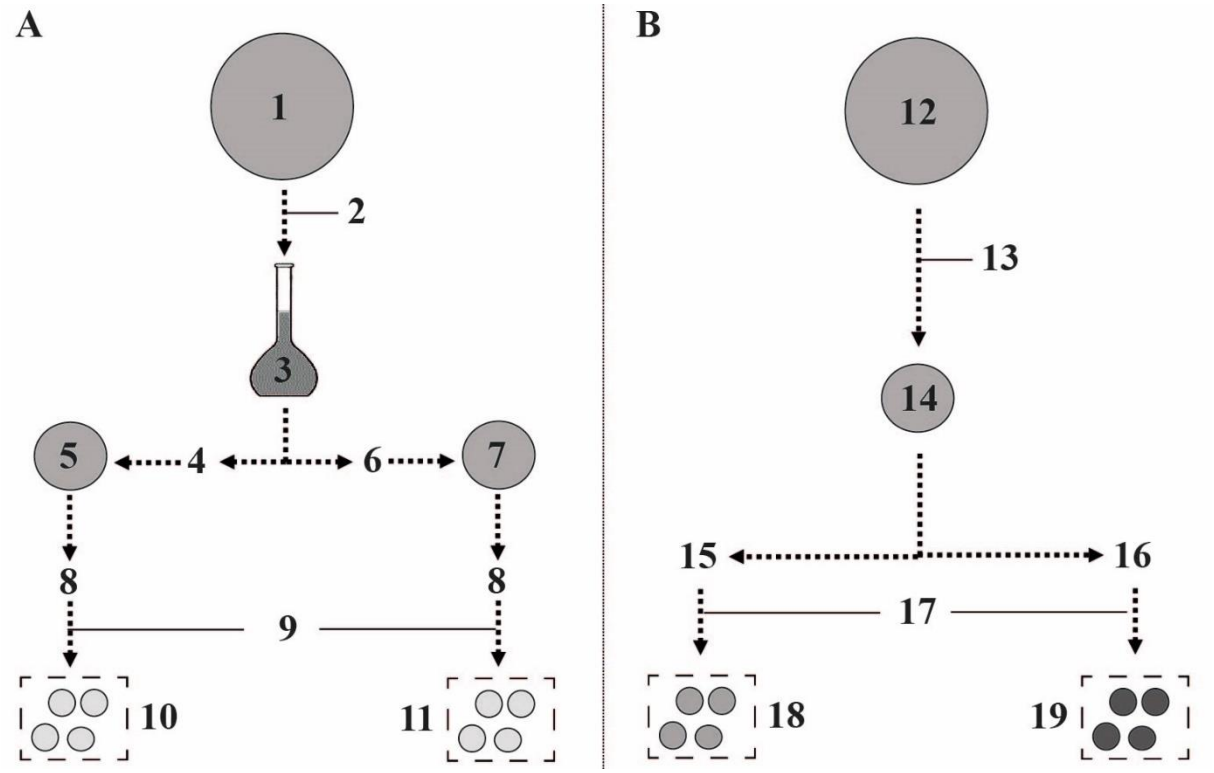

Supplementary material 2. Scheme of the kinetics of Zn release adopted.

Supplementary material 3. The concentration of Zn and P in shoot tissue of maize and brachiaria according to soil type and OMFs and zinc sulfate ($ZnSO_4$) used in the fertilization.

Maize				
Treatment	Red Oxisol		Yellow Oxisol	
	Zn (mg kg^{-1})	P (g kg^{-1})	Zn (mg kg^{-1})	P (g kg^{-1})
-Zn	12.9 ±1.1 D	7.2 ±0.2 A	1.1 ±0.2 B	5.9 ±0.2 A
OMF1	62.5 ±3.4 C	2.0 ±0.1 C	64.0 ±4.1 A	2.0 ±0.1 C
OMF2	68.7 ±2.0 BC	2.2 ±0.1 BC	67.1 ±1.5 A	2.6 ±0.2 B
OMF3	84.0 ±3.3 A	2.5 ±0.1 B	67.8 ±3.9 A	2.4 ±0.2 BC
OMF4	84.6 ±2.1 A	2.5 ±0.1 B	68.0 ±0.6 A	2.6 ±0.1 B
$ZnSO_4$	77.3 ±4.1 AB	2.3 ±0.1 BC	63.7 ±3.5 A	2.3 ±0.1 BC
Brachiaria				
Treatment	Red Oxisol		Yellow Oxisol	
	Zn (mg kg^{-1})	P (g kg^{-1})	Zn (mg kg^{-1})	P (g kg^{-1})
-Zn	28.0 ±3.5 B	2.0 ±0.1 A	62.8 ±32.7 B	1.2 ±0.5 B
OMF1	104.2 ±3.9 A	1.7 ±0.1 B	107.2 ±8.6 AB	2.5 ±0.2 A
OMF2	110.9 ±3.4 A	1.6 ±0.1 B	108.9 ±5.5 AB	2.2 ±0.1 A
OMF3	115.2 ±6.0 A	1.7 ±0.1 B	135.0 ±5.7 A	2.1 ±0.1 A
OMF4	106.1 ±2.2 A	1.5 ±0.1 B	134.7 ±4.5 A	2.7 ±0.1 A
$ZnSO_4$	114.2 ±7.2 A	1.6 ±0.1 B	108.3 ±9.5 AB	2.0 ±0.1 A

Means with standard error followed by the same letter in each column did not differ by the Duncan test ($p<0.05$). -Zn: no-Zn added to the soil.

Supplementary material 4. Main peaks identified in humic acid (HA) matrix, Zn organomineral (OMF) and sulfate ($ZnSO_4$) fertilizers.

Bond related	Peaks (cm^1)	HA1	OMF1	HA2	OMF2	HA3	OMF3	OMF4	ZnSO4
OH stretching: H-bonded OH, free OH, intermolecular bonded OH	3370	-	-	-	-	-	Yes	-	-
	3290	-	Yes	-	-	Yes	-	Yes	-
	3170	-	-	-	Yes	-	-	Yes	Yes
	3100	Yes	-	-	-	-	-	-	-
Aliphatic CH groups	2915	Yes	Yes	-	-	Yes	Yes	Yes	-
	2900	-	-	Yes	-	-	-	-	-
	2845	-	-	-	-	Yes	Yes	Yes	_
COOH groups in alkyl groups	2400	-	-	Yes	-	-	-	-	-
Carboxylic acid C=O stretch	1720	-	-	Yes	-	-	-	-	-
	1700	Yes	-	-	-	-	-	-	-
Water	1640	-	-	-	-	-	Yes	Yes	Yes
C=C aromatic stretching	1620	Yes	Yes	Yes	-	-	-	-	-
	1590			-	Yes	-	-	-	-
	1560	-	-	-	-	Yes	-	Yes	-
	1495	Yes	Yes	-	-	-	-	-	-
OH phenolic stretching	1400	Yes	-	-	Yes	-	-	-	-
	1380	-	Yes	Yes	-	-	-	-	-
$C-CH_3$ groups bending	1365	-	-	-	-	Yes	Yes	Yes	-
SO_2 stretching (sulfone)	1315	-	-	-	-	-	Yes	Yes	-

C=S thiocarbonyl	1200	-	-	Yes	-	-	-	-	-
polysaccharide C-O stretching	1150	Yes	-	Yes	-	-	-	-	-
SO_2 stretching (alkyl sulfate)-$RSO_4^-M^+$	1075	-	-	-	Yes	-	-	Yes	-
SO_4^- stretching (free sulfate groups)	1060	-	-	-	-	-	-	-	Yes
C=S thiocarbonyl	1055	-	-	Yes	-	-	-	-	-
polysaccharide C-O stretching	1045	Yes	Yes	-	-	-	-	-	-
SO_4^- stretching (free sulfate groups)	980	-	-	-	Yes	-	-	Yes	Yes
Aromatic C-H out-of-plane bend	960	-	Yes	-	-	-	-	-	-
C-Cl stretching mode	830	-	Yes	-	-	-	-	-	-
SO_2 stretching (sulfone)	815	-	-	Yes	-	-	Yes	Yes	-
C-Cl stretching mode	735	-	Yes	-	-	-	-	-	-
	720	-	Yes		-	-	Yes	-	-
C-S stretching (Methyl sulfone - CH_3-SO_2)	715	-	-	-	Yes	-	-	Yes	-

Supplementary material 5. Parameters of models adjusted to the kinetics of Zn release from Zn organomineral (OMF) and sulfate ($ZnSO_4$) fertilizers.

Kinetics of Zn release as related to Zn total content (%)												
Treat.	Elovich			Exponential			Power			Hyperbolic		
	R^2	RMSE	AIC	R^2	RMSE	AIC	R^2	RMSE	AIC	R^2	RMSE	AIC
OMF1	0.92	1.61	120	0.72	3.00	157	0.95	1.34	109	0.94	1.52	116
OMF2	0.94	4.82	172	0.87	5.66	195	0.90	4.97	187	0.95	4.43	203
OMF3	0.92	2.68	150	0.71	5.02	188	0.96	1.95	131	0.91	2.78	152
OMF4	0.84	7.45	212	0.59	11.91	240	0.93	5.01	188	0.96	4.60	183
$ZnSO_4$	0.82	2.84	154	0.81	2.95	156	0.81	2.90	155	0.81	2.95	156

R^2: coefficient of determination; RMSE: root-mean-square error (%); AIC: The Akaike information criterion. Treat.: Treatments studied.

Supplementary material 6. The kinetics of Zn release in water by the organomineral fertilizers (OMFs) and zinc sulfate ($ZnSO_4$) adopting the same model regardless of the fertilizer studied.

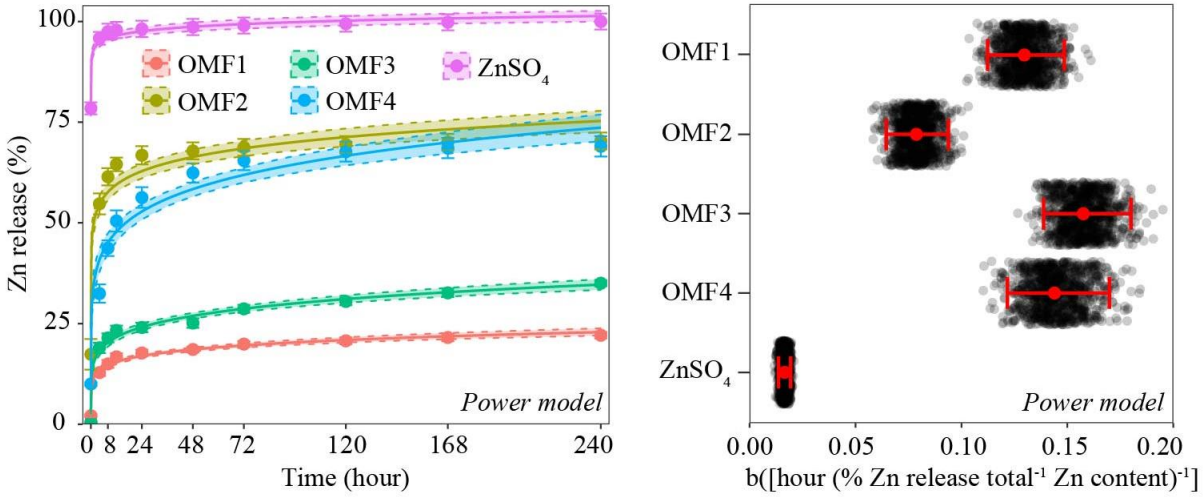

Supplementary material 7. Soil pH and soil solution pH according to Zn organomineral (OMF) and sulfate ($ZnSO_4$) fertilizers in each Oxisol type.

Maize cultive				
Treatments	Solution pH		Soil pH	
	Red Oxisol	Yellow Oxisol	Red Oxisol	Yellow Oxisol
-Zn	6.49 ±0.04	6.56 ±0.15	6.40 ±0.06	6.47 ±0.12
OMF1	6.35 ±0.01	6.62 ±0.05	6.23 ±0.03	6.50 ±0.01
OMF2	6.40 ±0.06	6.45 ±0.11	6.20 ±0.06	6.50 ±0.06
OMF3	6.47 ±0.05	6.29 ±0.03	6.23 ±0.12	6.53 ±0.09
OMF4	6.38 ±0.05	6.46 ±0.13	6.40 ±0.10	6.57 ±0.03
$ZnSO_4$	6.30 ±0.07	6.62 ±0.12	6.33 ±0.07	6.57 ±0.03
Mean	6.40 ±0.05	6.50 ±0.10	6.32 ±0.07	6.51 ±0.06

Brachiaria cultive				
Treatments	Solution		Soil	
	Red Oxisol	Yellow Oxisol	Red Oxisol	Yellow Oxisol
-Zn	5.98 ±0.08	6.90 ±0.04	6.10 ±0.09	6.63 ±0.12
OMF1	6.73 ±0.10	7.04 ±0.04	6.00 ±0.06	6.27 ±0.15
OMF2	6.87 ±0.07	7.28 ±0.10	5.93 ±0.10	6.30 ±0.15
OMF3	6.98 ±0.08	7.05 ±0.08	5.93 ±0.09	6.70 ±0.10
OMF4	6.84 ±0.11	7.02 ±0.05	5.83 ±0.15	6.57 ±0.03
$ZnSO_4$	6.71 ±0.08	7.17 ±0.04	5.87 ±0.12	6.73 ±0.07
Mean	6.69 ±0.09	7.09 ±0.06	5.99 ±0.10	6.53 ±0.10

-Zn: no Zn added to soil.

Supplementary material 8. Correlation between amount of C applied and whole soil and solution properties and biomass production, Zn and P concentration and accumulation by maize and brachiaria according to Oxisol. The means of treatment related to no Zn added in soil was removed from the dataset to perform correlation analysis.

	Maize		Brachiaria	
	RO	YO	RO	YO
Soil solution Zn	0.03	0.43	0.42	0.86*
Soil solution P	0.39	0.73*	0.52*	-
Soil Zn-DTPA	0.20	-0.35	0.45	-0.06
Soil P-resin	-0.66*	0.09	0.15	-0.02
Shoot biomass	0.22	0.62*	0.31	0.05
Root biomass	0.48	0.78*	0.60*	0.05
Total biomass	0.37	0.77*	0.43	0.05
Zn concentration in shoot	0.11	0.19	-0.03	0.45
Zn accumulation in shoot	0.28	0.61*	0.28	0.15
P concentration in shoot	0.24	-0.09	0.36	0.17
P accumulation in shoot	0.42	0.37	0.44	0.07

*Pearson correlation significant ($p<0.05$).

Supplementary material 9. Relation between Zn content in soil solution and total dry matter production.

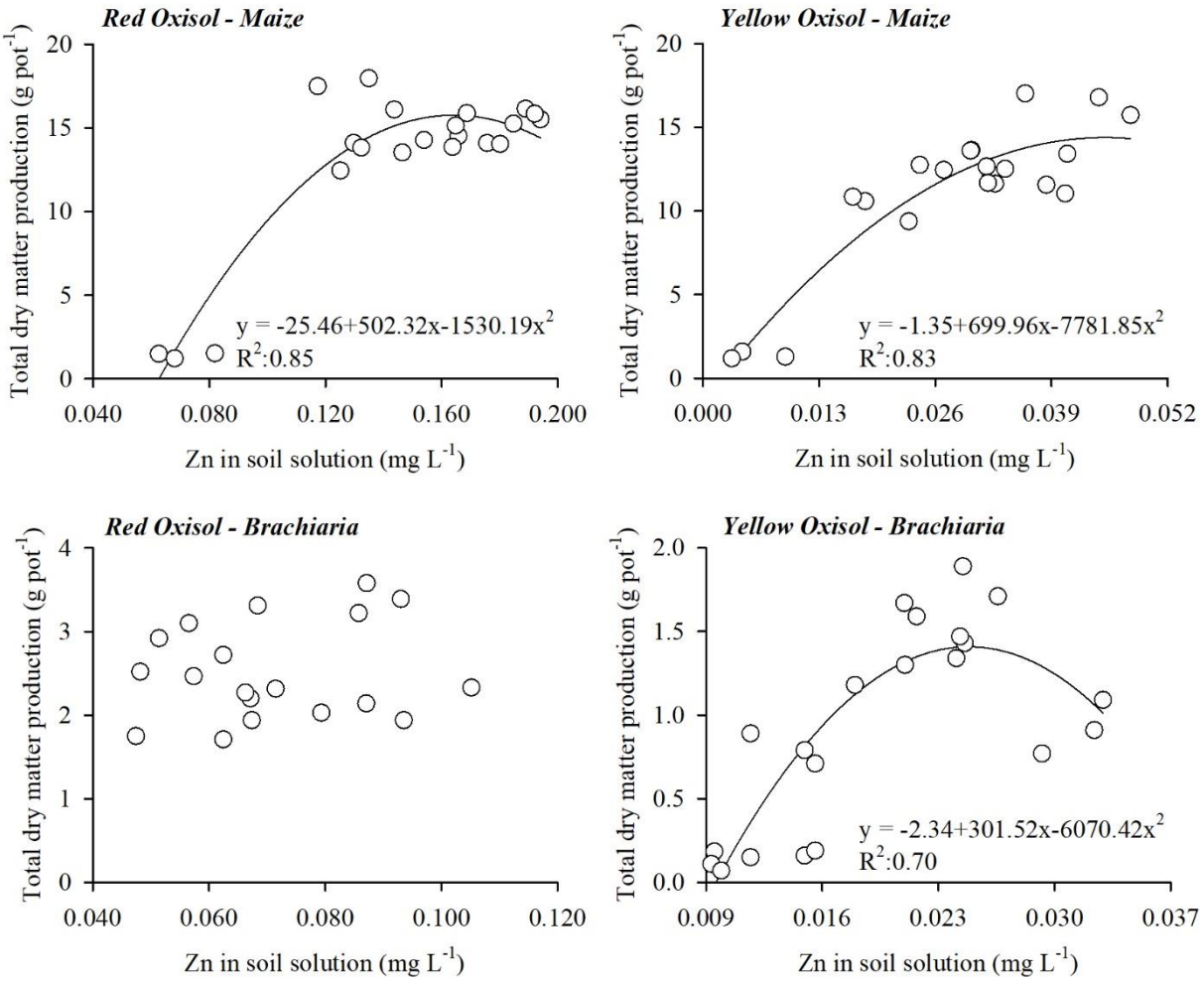

Preliminary version of manuscript edited following the rules of Communications in Soil Science and Plant Analysis Journal

PLS regression based on ATR-FTIR to predict organomineral fertilizers properties and nutrient pools

Everton Geraldo de Morais[1*], Henrique José Guimarães Moreira Maluf[1], Carlos Alberto Silva[1], Leonardo Henrique Duarte de Paula[2]

[1]Departament of Soil Science, Federal University of Lavras, Av. Doutor Sylvio Menicucci 1001, zip code: 37200-000, Lavras-Minas Gerais, Brazil.
[2]Departament of Agrarian Science, Federal Institute of Minas Gerais, Bambuí/Medeiros road, Km 05, zip code: 38900-000, Bambuí-Minas Gerais, Brazil.

Abstract

Enrichment of organic residues with mineral fertilizers is a sustainable route to produce high agronomic value organomineral fertilizers (OMFs). Partial least squares regression (PLS) based on infrared analysis is a fast and alternative technique to assess the properties of OMFs, while replacing laborious, non-environmentally friendly, time-consuming, and high-cost conventional lab analytical procedures. OMFs were produced by composting of mixtures of low-grade and soluble P sources with chicken manure and coffee husk. In lab conditions, OMFs were analyzed for: pH in $CaCl_2$, electrical conductivity, total contents of C, P, N, and K, and C soluble in water, as well as for fertilizer-P soluble in water, citric acid, and neutral ammonium citrate. The compost MAP-based OMFs had a higher agronomic value than low-grade rock P-based OMFs. PLS regression models based on the ATR-FTIR spectral signature were a suitable tool to predict all OMFs chemical properties and nutrient pools evaluated through lab

conventional analytical procedures. The good performance, robustness, and non-random correlation of PLS regression models were attested by their high coefficient of determination (R^2) to calibration (0.92-0.99), cross-validation (0.87-0.99), and prediction capacity (0.89-0.99) combined with the lowest values of the root-mean-square error (RMSE) and reduced values of R^2 (0.19-0.44), as well as to high values of RMSE to y-randomization. PLS based on ATR-FTIR is a rapid and alternative chemometric approach to assess the properties and nutrients pools of OMFs and may replace laborious, time-consuming, and high-cost lab chemical routine and laborious analytical protocols used for the same purpose.

Keywords: Multivariate calibration; ATR-FTIR; chemometrics; compost-based fertilizers; composting.

1 Introduction

Composted in the right way, mixing wastes, manures, and crop residues with low-grade phosphorus (P) rocks and soluble mineral P fertilizers is a suitable route to recycle nutrients and produce high agronomic value organomineral fertilizers (OMFs) (Maluf et al. 2018; Frazão et al. 2019). The correct definition of rate fertilizer and the balanced nutrients supply are key factors controlling plant growth, yield, fiber, and biomass production. Nitrogen (N), P, and potassium (K) are supplied to plants through different sources, including mineral, organic, and organomineral fertilizers, but mineral fertilizers are the main sources world widely used to nourish plants (FAO 2017; Mumbach et al. 2020). Overall, nutrients supplied by mineral fertilizers are readily available to attend plant nutritional requirements, while nutrient pools contained in them are prone to negative reactions with soil components becoming unavailable to plants (McLaughlin et al. 2011). Compared to soluble mineral sources, organic fertilizers are characterized by their low or unbalanced contents of nutrients, such as those contained in manures, composts, sewage sludge, and crop residues; thus, some organic fertilizers are not

capable of attending in a balanced way most crop nutrient demands (Mumbach et al. 2020). Additionally, high rates of organic fertilizers are needed to attend to plant nutritional requirements; the reason why organic fertilizers can only be transported to short distances from their local of production, which decrease the scale and profitability of organic fertilization (Mumbach et al. 2020).

Synthesis of OMFs is a strategy to add value to organic fertilizers by increasing their nutrient concentration, besides enhancing agronomic efficiency through a gradual release of nutrients while decreasing negative reactions of nutrients in fertilizers with soil components (McLaughlin et al. 2011; Erro et al. 2012; Kominko et al. 2017; Lustosa Filho et al. 2017). OMFs can be produced by mixing crop residues, manures, sewage sludge, compost, food wastes, wood wastes, humic substances, biodigester slurry, etc., and processes, such as composting, pyrolysis, and fermentation; the reason why this category of fertilizers have contrasting properties, and nutrient pools with variable kinetics of nutrient release (Erro et al. 2012; Maluf et al. 2018; Lustosa Filho et al. 2019). The agronomic value of OMFs is determined by properties routinely assessed by classical laboratory analyses, including pH, electrical conductivity (EC), contents of C as well as P soluble in water, in citric acid (CA) at 2% and in neutral ammonium citrate plus water (NAC+H_2O), and total contents of C, P, N, and K as well (Erro et al. 2012; Maluf et al. 2018; Lustosa Filho et al. 2019; Ruangratanakorn et al. 2020). Classical methods commonly used in lab analysis of OMFs are destructive, time-consuming, require lab maintenance, have a high cost, enclose multiple-step during analyses, and generate several non-ecofriendly chemical wastes (Yao et al. 2010; Ruangratanakorn et al. 2020).

Infrared spectroscopy analysis is a tool already used to predict the agronomic value and properties of fertilizers (Wang et al. 2019; Ruangratanakorn et al. 2020). With the infrared spectroscopy analysis is possible to generate a big dataset that mirrors the OMF organic and inorganic nutrient pools. Multivariate analysis can extract additional information from the

whole infrared spectra to predict fertilizer properties and capacity to supply nutrients to crops while reducing the time required to perform lab conventional analysis methods (Higashikawa et al. 2014; Wang et al. 2019). The partial least squares regression (PLS) based on infrared spectroscopy is a potential tool to replace conventional fertilizer invasive analysis chemical methods (Van Vuuren & Groenewald 2013; Lin et al. 2018; Lu et al. 2020). The use of infrared spectroscopy conjugated with PLS regression mainly using the Attenuated Total Reflectance with Fourier Transform Infrared Spectroscopy (ATR-FTIR) has many advantages over traditional chemical lab analyses, including ease of sample preparation, fast and non-invasive spectrum acquisition, non-destructive nature of the analysis, portability of the infrared machine, and low generation of wastes; thus, this approach is an environmentally friendly low-cost technique (Chen et al. 2013; Higashikawa et al. 2014; Wang et al. 2014; Lin et al. 2018; Lu et al. 2019; Ruangratanakorn et al. 2020). If the prediction analysis involving PLS and infrared spectroscopy is robust and has good prediction performance, the classical lab methods used for the same purpose could be replaced. PLS regression based on infrared analysis was already used to predict fertilizer properties, nutrient pools, and indices of fertilizer agronomic efficiency (Chen et al. 2013; Wang et al. 2014; Lin et al. 2018; Ruangratanakorn et al. 2020).

PLS regression based on infrared spectroscopy was also effective to predict the contents of N, P, and K in mineral fertilizers (Van Vuuren & Groenewald 2013; Lin et al. 2018; Lu et al. 2019). In a broad review, the potential of PLS models based on infrared spectroscopy was reported in predicting the total contents of C, N, P, and K in manure (Chen et al. 2013). Current literature also reported the high accuracy of PLS regression based on the infrared spectra dataset to predict the pH, EC, contents of C soluble, and total contents of C and N of organic fertilizers (Wang et al. 2014). However, few studies aimed to predict the main properties of OMFs through PLS based on the infrared analysis, although the potential of this

technique to predict pH, C and N organic contents, and available P in OMFs was reported (Ruangratanakorn et al. 2020).

Accurate analysis of OMFs properties and nutrient contents and pools is the first step to enhancing crop response to fertilization, while the fast, reliable, and low-cost analysis of fertilizers properties remain an important issue in different countries (Lin et al. 2018). The prediction of OMFs properties through PLS models based on infrared spectra need to be better elucidated, especially regarding evaluation of the agronomic value of contrasting composted-based OMFs. We hypothesized that the mixture of organic residues and soluble and low-grade mineral P sources can generate OMFs with contrasting properties and variable agronomic efficiency. It is possible to anticipate that the PLS regression based on infrared analysis is a suitable approach to predict the main properties and nutrient pools contained in the synthesized low and high agronomic value OMFs. The aims of this study were: 1) to show the agronomic value of OMFs produced after composting of different proportions of chicken manure (CM), coffee husk (CH), and soluble and low-grade and high soluble phosphates; II) to generate PLS regression models based on the ATR-FTIR spectra to predict the pH, EC, contents of C as well as the pools of P soluble in water, CA and NAC+H_2O, and the total contents of C, P, N and K in the compost-based OMFs.

2 Material and Methods

2.1 Organomineral fertilizers synthesis

The OMFs were produced by composting during 150 days of mixtures of three sources of phosphorus (Araxá, Bayóvar (low-grade phosphates), and monoammonium phosphate (MAP)) with two organic residues (CM and CH) in six different proportions, thus totaling 54 OMFs samples. Moisture during composting was kept close to 70 % of the maximum water retention capacity for each mixture. Each OMF was produced with three repetitions, and

composting conditions and management of compost piles are described in detail in (Maluf et al. 2018). After composting, the OMFs were dried in an air circulation stove at 60 ºC until constant weight. In sequence, OMFs samples were ground to passing a sieve size of <1 mm. The mixture and proportions of the composted P sources -organic residues in each composting pile and their respective derived-OMFs were shown in Table 1.

Table 1. Description of mixture and proportions of phosphate sources and organic residues (CM and CH) used to synthesize compost-based organomineral fertilizers (OMFs).

Identification	Phosphate source	P source	Chicken manure	Coffee husk
		Proportion*(%)		
$AP^{25}CM^{37.5}CH^{37.5}$	Araxá phosphate rock	25	37.5	37.5
$AP^{40}CM^{20}CH^{40}$		40	20	40
$AP^{40}CM^{40}CH^{20}$		40	40	20
$AP^{50}CM^{25}CH^{25}$		50	25	25
$AP^{60}CM^{20}CH^{20}$		60	20	20
$AP^{75}CM^{12.5}CH^{12.5}$		75	12.5	12.5
$BP^{25}CM^{37.5}CH^{37.5}$	Bayóvar phosphate rock	25	37.5	37.5
$BP^{40}CM^{20}CH^{40}$		40	20	40
$BP^{40}CM^{40}CH^{20}$		40	40	20
$BP^{50}CM^{25}CH^{25}$		50	25	25
$BP^{60}CM^{20}CH^{20}$		60	20	20
$BP^{75}CM^{12.5}CH^{12.5}$		75	12.5	12.5
$MAP^{25}CM^{37.5}CH^{37.5}$	Monoammonium Phosphate	25	37.5	37.5
$MAP^{40}CM^{20}CH^{40}$		40	20	40
$MAP^{40}CM^{40}CH^{20}$		40	40	20
$MAP^{50}CM^{25}CH^{25}$		50	25	25
$MAP^{60}CM^{20}CH^{20}$		60	20	20
$MAP^{75}CM^{12.5}CH^{12.5}$		75	12.5	12.5

* Proportion based on dry mass.

2.2 Infrared spectroscopy analysis

The OMFs samples (54 samples) were ground and homogenized and sieved to have particles less than 0.149 mm diameter and dried. Identification of the main infrared band assignments of OMFs was performed using the attenuated total reflectance with Fourier Transform Infrared Spectroscopy (ATR-FTIR) in a Bruker Vertex 70v series spectrophotometer with a ZnSe crystal. Infrared spectra were recorded at the Mid-infrared region (4000 to 400 cm^{-1} wavelength) by collecting 32 scans with a resolution of 2 cm^{-1}. All ATR-FTIR spectra samples were submitted to minimum normalization (Gautam et al. 2015). ATR-FTIR spectra of each OMF and the main absorption bands were identified through libraries and assignments for organic and inorganic functional groups and compound bonds (Stevenson 1994; Silverstein et al. 2005; Berzina-Cimdina & Borodajenko 2012; Maluf et al. 2018).

2.3 OMFs lab chemical characterization

The pH of OMFs was determined in a 0.01 mol L^{-1} $CaCl_2$ solution at the ratio of 10 g of OMF to 50 ml of $CaCl_2$ solution and determined in a bench digital pH meter. EC was determined in water at the ratio of 10 g of OMF to 50 ml of water and measured through a bench digital electrical conductivity meter. One g of the fertilizer was stored in a funnel with a quantitative filter paper (grade 40), then washed successively with distilled water up to a final volume of 250 ml. In sequence, the filtered extract was used to determine the contents of C and P soluble in water. Dissolved C contents in OMFs were determined in the liquid mode of a dry combustion analyzer (Elementar, Vario Cube model, Germany). Phosphorus was determined in an inductively coupled plasma optical emission spectrometer (ICP-OES, Spectro Blue, Spectro Analytical Instruments, Germany). Total C content in OMFs was quantified in the solid mode of that already mentioned TOC combustion analyzer.

Content of P soluble in a CA solution was extracted by stirring for 30 min 1 g OMFs mixed with 50 ml of a 2% CA solution. The P soluble in NAC+H_2O was extracted by boiling 0.5 g of OMF with 25 ml neutral ammonium citrate solution (pH 7). The P extracts in CA or NAC+H_2O had their volume completed to 250 ml with distilled water; in sequence, the OMFs derived samples were filtered using quantitative filter paper (grade 40), and P was quantified in an ICP-OES machine. OMF samples were also digested in a nitric-perchloric solution at a 4:1 ratio (nitric acid: perchloric acid); in sequence, the extract was diluted in water, and the total contents of P and K were determined in an ICP-OES machine. Total N contents in OMFs were determined by digesting 0.1 g of OMF sample in glass flasks containing 3 ml of sulfuric acid combined with a catalytic mixture (K_2SO_4+$CuSO_4.5H_2O$). After digestion, N was determined by the *Kjeldahl* distillation method. Analytical methods used in the OMFs characterization were based on the official analytical protocols and methods described and required by the Brazilian Ministry of Agriculture (Brazil 2017).

2.4 Statistical analysis

All statistical analyses were carried out using the R software (R Core Team 2020). The classical lab OMF chemical properties dataset was staggered using the stats package (R Core Team 2020); then, the heatmap analysis was performed through the gplots package (Warnes et al. 2020) to cluster OMFs regarding their evaluated chemical properties.

ATR-FTIR spectral signature of the 54 OMFs samples (three repetitions x 18 OMFs) was used to generate and validate the PLS regression models (part of the dataset used for calibration and cross-validation phase (80%) and the other part for independent external validation (20%). The ATR-FTIR spectra signatures recorded in the 4000 to 400 cm^{-1} range were calibrated against the respective properties of each OMF chemical indices (previously determined by classical lab routines) using the PLS regression. Among the 54 observations,

20% of samples (11 independent random samples) were not included in the calibration, defined as “blind samples”; thus, they did use in the modeling PLS procedures and steps. The blind samples were randomly chosen as an external group to test the robustness of PLS models. PLS models were developed to predict with accuracy the OMFs properties routinely determined in wet classical lab methods. PLS regression was performed using the stats, base, and pls packages (R Core Team 2020; Liland et al. 2021).

The PLS models developed were characterized for the following statistics indices: root mean square error (RMSE) of calibration ($RMSE_{cal}$) and the squared correlation coefficient (R^2) of calibration (R^2_{cal}). The models were validated by the leave-one-out cross-validation, using the RMSE of cross-validation ($RMSE_{cv}$) and R^2 of cross-validation (R^2_{cv}). The validation of PLS regression models was also performed by the y-randomization test, with the calculation of RMSE of y-randomization ($RMSE_{y\text{-}rand}$) and R^2 of y-randomization ($R^2_{y\text{-}rand}$). The RMSE of prediction ($RMSE_{pred}$) and R^2 of prediction (R^2_{pred}) were used as statistical parameters to evaluate the performance of the regression model prediction (Kiralj & Ferreira 2009). The RMSE and R^2 were calculated as follows:

$$\mathrm{RMSE} = \sqrt{\frac{\sum_{i=1}^{n}(yi-\hat{y}i)^2}{n}} \quad (1)$$

$$R^2 = 1 - \frac{\sum_{i=1}^{n}(yi-\hat{y}i)^2}{\sum_{i=1}^{n}(yi-\bar{y})^2} \quad (2)$$

Where, yi is the reference value of the dependent variable, $\hat{y}i$ is the predicted value, $\bar{y}$ is the mean value, and n is the number of samples.

To validate the PLS models, it was calculated the squared correlation between the experimental and predicted values for the tested dataset (r^2_m), and the R^2 of y-randomization prediction (r^2_p) as described in Equations 3 and 4 (Roy et al. 2009).

$$r^2_m = R^2\left[1 - (R^2 - R^2_0)^{1/2}\right] \quad (3)$$

$$r^2_p = R^2_{cal}\left(R^2_{cal} - R^2_{y-rand}\right)^{1/2} \quad (4)$$

Where R^2 and R^2_0 were the R^2 values between the observed *versus* predicted values for the tested dataset with and without the use of intercept, respectively.

3 Results and discussion

3.1 Infrared spectroscopy

In ATR-FTIR spectra of OMFs, the main bands were assigned for O-H bonds at 3300 and 1640 cm^{-1}, C-H aliphatic at 2918 cm^{-1}, N-H bonds at 3220, 3050, 2850, and 1420 cm^{-1}, CO_3^{2-} groups at 1460 and 870 cm^{-1}, P-O bonds at 1100, 1010, 1000, 968 600, 560, and 470 cm^{-1}, P=O bond at 1270 cm^{-1}, P-OH bond at 890 cm^{-1} (Figure 1). These organic and mineral chemical groups were identified based on the mid-infrared spectral peaks and bands assignments, and libraries mentioned in the section of material and methods (Stevenson 1994; Silverstein et al. 2005; Berzina-Cimdina & Borodajenko 2012; Maluf et al. 2018). The main features and ATR-FTIR spectral bands and spectral signature of the raw phosphate rocks, MAP, CM, and CH used in the synthesis of OMFs are discussed in detail in Maluf et al. (2018).

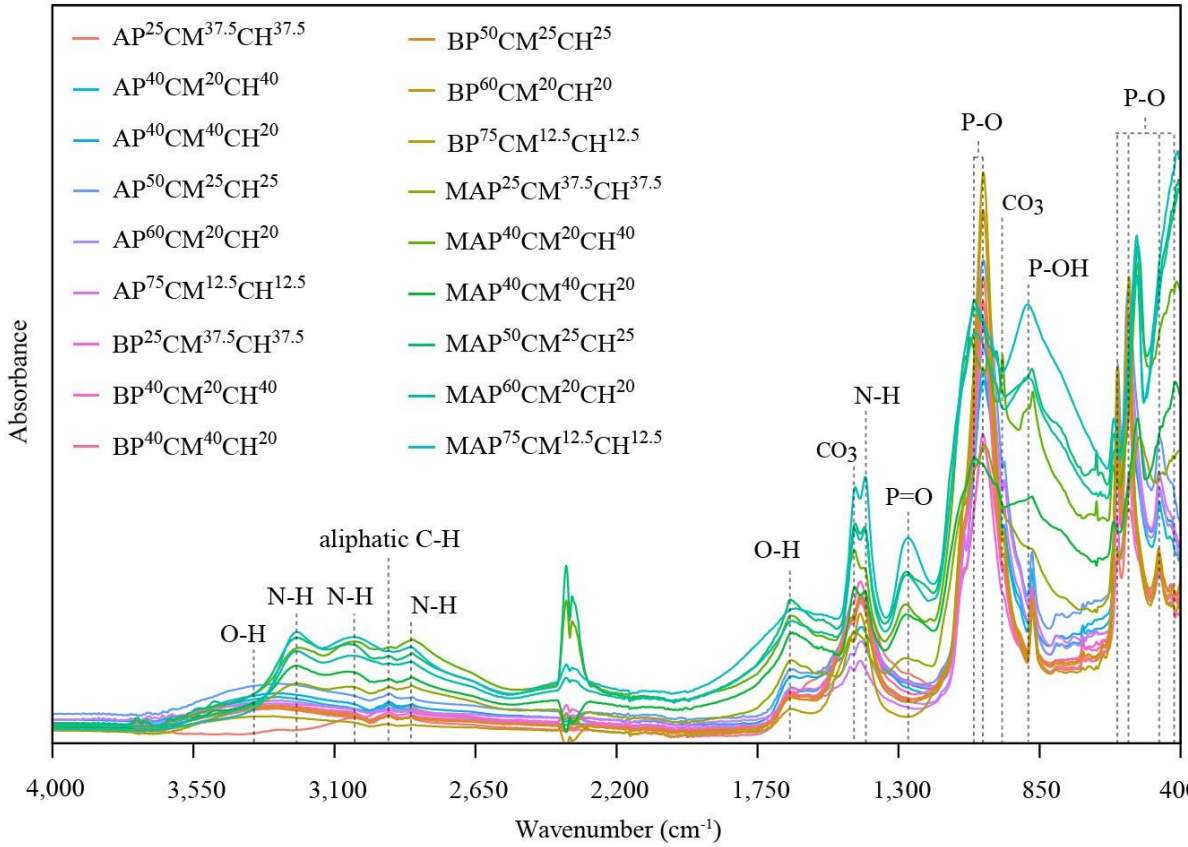

Figure 1. Mid-infrared spectral signatures and the main band signals assigned for the organomineral fertilizers formulated after composting variable mixtures and proportions of P sources (soluble and low-grade phosphates) with chicken manure and coffee husk. AP: Araxá phosphate; BP: Bayóvar phosphate; MAP: monoammonium phosphate; CM: chicken manure; CH: coffee husk; superscripted numbers after abbreviations refer to the proportion (%) of each material (P source or organic residue) used in the mixtures composted to produce OMFs.

OH bands were identified in all OMFs spectra, while MAP-based OMFs were richer in this spectral peak than low-grade phosphate-based OMFs (Figure 1 and supplementary material 1). C-H aliphatic bands were also recorded for all OMFs, with stronger peaks observed for low-grade phosphate-based OMFs. A greater presence of N-H groups was found in the spectra of MAP-based OMFs. As the proportion of MAP over organic residues increased in the composting piles, the greater the N-H groups present in OMFs. The CO_3^{2-} bands were only verified in low-grade phosphate-based OMFs. A greater presence of organic residues in the composting piles favored the presence of CO_3^{2-} in the OMF-ATR-FTIR spectra. P-O bonds

were verified in all OMFs with a higher intensity in low-grade phosphate-based OMFs. P=O and P-OH bonds were founded only in MAP-based OMFs. A higher proportion of organic residues in compost-based OMFs increased the presence and intensity of P=O bands and reduced the P-OH peaks. Thus, it was generated an ample ATR-FTIR dataset covering a large amplitude of spectral signatures of the contrasting OMFs synthesized with high or poor soluble P sources and different proportions of CM and CH, which is suitable for creating a large dataset of ATR-FTIR bands and OMF spectral signatures, which mirror the contrasting properties, and nutrient contents and pools of fertilizers investigated in this study.

3.2 Chemical properties and agronomic value

The chemical and physicochemical properties of OMFs determined by classical methods were shown in Table 2. The OMFs pH ranged from 4.9 to 9.7, EC was in the range of 1.9-62.3 dS m^{-1}, C soluble in water ranged from 6.2-22.0 g kg^{-1}, and total C encloses contents from 34.9 to 218.3 g kg^{-1}. Contents of P soluble in water were in the range of 0.2 to 159.2 g kg^{-1}. The following ranges of values were determined and accounted for P soluble in citric acid (14.4-179.2 g kg^{-1}), P soluble in NAC+H_2O (5.3-187.3 g kg^{-1}), total P in OMFs (68.2-219 g kg-1), total N (4.4-97.3 g kg^{-1}) and total K (7.4-33.9 g kg^{-1}). The wide amplitude of OMFs properties allowed to build a robust and reliable relation between the infrared spectral signatures and OMFs properties (Wang et al. 2014). Thus, from the OMFs characterized in this study, a wide range of chemical properties, nutrient contents, and pools were identified and representing most of the OMFs marketed in Brazil.

Table 2. Chemical properties of the composted-based organomineral fertilizers.

Fertilizer	pH	EC	C^{Water}	C^{T}	P^{Water}	P^{CA}	P^{NAC}	P^{T}	N^{T}	K^{T}
		dS m^{-1}	g kg^{-1}							
$AP^{25}CM^{37.5}CH^{37.5*}$	9.7 ± 0.1	7.3 ± 0.3	20.3 ± 0.1	167.7 ± 1.5	1.7 ± 0.1	16.0 ± 0.2	9.9 ± 0.6	69.0 ± 0.4	16.3 ± 0.7	26.7 ± 0.6
$AP^{40}CM^{20}CH^{40}$	9.5 ± 0.1	5.9 ± 0.1	21.6 ± 0.2	130.8 ± 1.3	1.2 ± 0.1	15.2 ± 0.4	7.2 ± 0.1	86.2 ± 0.5	12.4 ± 0.1	24.0 ± 0.9
$AP^{40}CM^{40}CH^{20*}$	9.6 ± 0.1	6.1 ± 0.2	18.9 ± 0.2	109.3 ± 1.6	1.3 ± 0.1	17.2 ± 0.2	10.5 ± 0.2	89.8 ± 1.2	12.1 ± 0.2	22.9 ± 0.9
$AP^{50}CM^{25}CH^{25*}$	9.4 ± 0.1	4.8 ± 0.1	15.6 ± 0.4	104.0 ± 0.7	0.9 ± 0.1	16.2 ± 0.4	7.7 ± 0.3	105.2 ± 0.3	10.1 ± 0.3	19.0 ± 1.3
$AP^{60}CM^{20}CH^{20}$	9.3 ± 0.1	3.3 ± 0.1	12.9 ± 0.5	58.3 ± 0.3	0.9 ± 0.1	17.2 ± 0.2	7.0 ± 0.2	120.4 ± 0.8	7.5 ± 0.4	16.7 ± 0.2
$AP^{75}CM^{12.5}CH^{12.5*}$	8.9 ± 0.1	1.9 ± 0.1	7.1 ± 0.6	36.9 ± 1.2	0.5 ± 0.1	17.6 ± 0.1	5.6 ± 0.2	134.2 ± 1.7	4.7 ± 0.3	10.0 ± 0.3
$BP^{25}CM^{37.5}CH^{37.5*}$	9.5 ± 0.1	7.4 ± 0.1	20.1 ± 0.1	169.1 ± 4.3	1.5 ± 0.1	20.3 ± 1.0	8.9 ± 0.2	75.3 ± 0.4	16.2 ± 0.5	29.3 ± 0.6
$BP^{40}CM^{20}CH^{40}$	9.3 ± 0.1	5.3 ± 0.1	17.7 ± 0.5	134.6 ± 1.0	0.8 ± 0.1	21.5 ± 1.4	7.4 ± 0.5	102.9 ± 3.4	11.9 ± 0.7	23.8 ± 1.1
$BP^{40}CM^{40}CH^{20*}$	9.3 ± 0.1	5.8 ± 0.1	17.9 ± 0.1	122.4 ± 3.3	1.2 ± 0.1	21.2 ± 0.3	9.0 ± 0.2	104.9 ± 2.6	11.2 ± 0.5	26.1 ± 0.8
$BP^{50}CM^{25}CH^{25*}$	9.2 ± 0.1	4.3 ± 0.2	13.2 ± 0.2	112.3 ± 1.3	0.6 ± 0.1	23.5 ± 0.8	8.4 ± 0.4	115.7 ± 2.8	9.1 ± 0.3	21.6 ± 0.4
$BP^{60}CM^{20}CH^{20}$	8.7 ± 0.1	3.6 ± 0.1	9.3 ± 0.4	75.0 ± 2.0	0.3 ± 0.1	24.4 ± 0.8	7.0 ± 0.2	132.0 ± 2.1	6.9 ± 0.2	16.9 ± 0.2
$BP^{75}CM^{12.5}CH^{12.5}$	7.9 ± 0.1	3.0 ± 0.1	6.4 ± 0.1	51.9 ± 1.1	0.4 ± 0.1	37.9 ± 0.6	8.5 ± 0.4	147.7 ± 1.6	5.2 ± 0.2	11.0 ± 0.2
$MAP^{25}CM^{37.5}CH^{37.5*}$	6.5 ± 0.1	25.0 ± 0.6	19.6 ± 0.3	214.7 ± 2.0	45.2 ± 3.2	84.2 ± 1.3	73.6 ± 1.6	97.0 ± 0.5	49.9 ± 1.4	32.1 ± 1.6
$MAP^{40}CM^{20}CH^{40}$	5.5 ± 0.1	39.4 ± 0.4	21.3 ± 0.1	184.3 ± 4.7	86.7 ± 1.0	105.3 ± 4.0	98.7 ± 1.1	147 ± 2.6	67.2 ± 0.9	23.9 ± 0.3
$MAP^{40}CM^{40}CH^{20*}$	6.1 ± 0.1	41.6 ± 0.5	19.6 ± 0.3	139.0 ± 2.8	80.5 ± 0.4	117.9 ± 2.3	112.4 ± 0.9	173.3 ± 0.8	63.9 ± 1.6	23.4 ± 0.2
$MAP^{50}CM^{25}CH^{25*}$	5.5 ± 0.1	45.8 ± 0.9	16.6 ± 0.3	122.8 ± 2.3	95.5 ± 2.3	116.1 ± 4.0	122.4 ± 1.2	177.9 ± 1.8	72.9 ± 1.3	20.1 ± 0.8
$MAP^{60}CM^{20}CH^{20}$	5.3 ± 0.1	52.7 ± 0.3	13.2 ± 0.3	115.1 ± 1.7	114.4 ± 2.4	140.6 ± 1.8	141.9 ± 2.6	215.1 ± 2.4	76.7 ± 2.1	13.4 ± 0.6
$MAP^{75}CM^{12.5}CH^{12.5*}$	4.9 ± 0.1	61.9 ± 0.5	7.3 ± 0.2	50.8 ± 0.4	158.0 ± 0.7	178.4 ± 0.4	184.1 ± 1.6	186.5 ± 0.4	94.3 ± 1.7	7.7 ± 0.1
Mean	8.0	18.1	15.5	116.6	32.9	55.0	46.1	126.7	30.5	20.5
SD	1.8	20.4	5.1	49.1	50.7	53.2	59.1	41.0	30.6	6.8

Means of three replicates with standard error. *:Source: adapted from Maluf et al. (2018). EC: electrical conductivity; C^{Water} and C^{T}: content of carbon soluble in water and total, respectively; P^{Water}, P^{CA} and P^{NAC}: content of phosphorus soluble in water, citric acid at 2% and neutral ammonium citrate plus water, respectively; P^{T}, N^{T} and K^{T}: total content of phosphorus, nitrogen and potassium, respectively; SD: standard deviation. AP: proportion of Araxá phosphate; BP: proportion of Bayóvar phosphate; MAP: proportion of monoammonium phosphate; CM: proportion of chicken manure; CH: proportion of coffee husk; overscribed numbers refer to the proportion (%) of each material used in OMFs mixture synthesis.

The heatmap analysis showed that classical lab methods are clustered mainly in four groups regarding the OMFs properties (Figure 2), as follows: increase of pH (group I) was favored by the use of MAP during OMFs synthesis; total content of K and C, and C soluble in water (group II) prevail over those of OMFs with proportions of organic residues higher than 50% in the composted OMFs; N total content, EC and P soluble in water or citric acid or NAC+H_2O (group III) favored by the use of MAP in the OMFs synthesis; and P total content (IV) favored by proportions of MAP higher than 25% and proportion of low-grade phosphates of 75% in the OMFs synthesis.

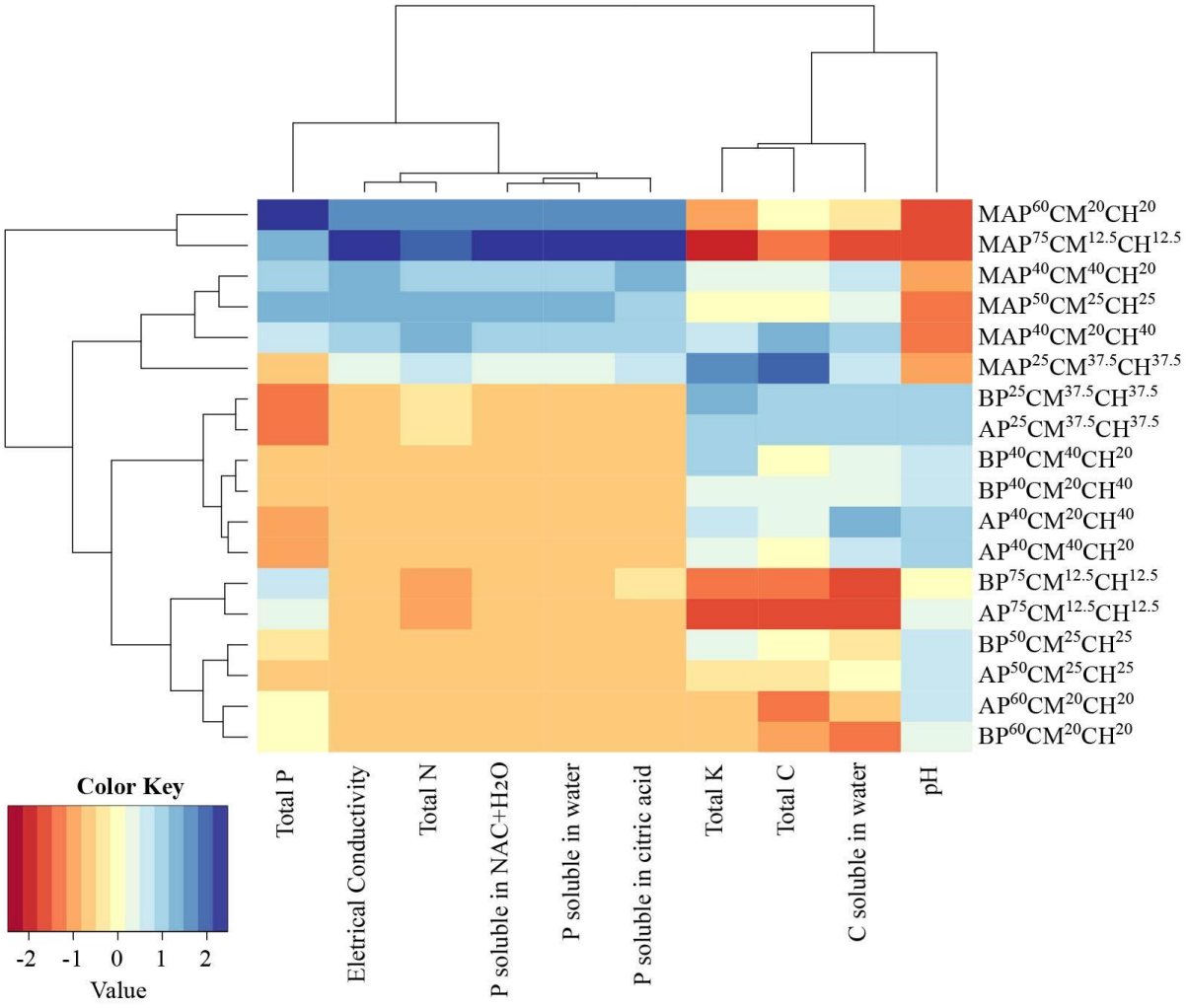

Figure 2. The heatmap of different organomineral fertilizers based on their chemical and physicochemical properties evaluate through wet fertilizer chemical analysis methods. AP: proportion of Araxá phosphate in composting piles; BP: proportion of Bayóvar phosphate in composting piles; MAP: proportion of monoammonium phosphate in mixtures composted; CM: proportion of chicken manure in mixtures composted; CH: proportion of coffee husk in the mixtures composted; overscribed numbers refer to the proportion (%) of each material used in OMFs mixture synthesis. Each variable from the dataset has been scaled to have the same weight during the statistical step used to generate the Heatmap.

The pH of fertilizer affects the nutrient dynamics in the soil-plant system, controlling the fertilizer dissolution and reactions in the soil-fertilizer interface (Lombi et al. 2005). In OMFs, total and soluble contents of C affect the dynamics of nutrients in the soil due to the role of humified compounds in complexing metals, blocking P adsorption, and bioactivity of some

organic compounds and functional groups on roots and plant growth (McLaughlin et al. 2011; Erro et al. 2012; Rose et al. 2014; Abd El-Mageed & Semida 2015; Fink et al. 2016). High total C and K contents and C soluble in water were favored by the enrichment of compost piles with organic residues (CM and CH) over proportions of P sources (MAP and low-grade phosphates). Potassium contents are positively correlated with the proportions of CH in the compost-based OMFs. Coffee husk is an alternative and fast-release source of K for plants (Zoca et al. 2014); therefore, K total content is a suitable index of K availability for plants in CH-based OMFs. EC is an index used to estimate the agronomic efficiency of fertilizers as it can infer fertilizer nutrient availability, and predict fertilizer nutrient release over time (Cancellier et al. 2018; Maluf et al. 2018). Nitrogen total and soluble contents were favored in MAP-based OMFs due to the higher presence of readily available forms of N as ammonium in MAP.

Extractant solutions used to measure fertilizer-available P pools simulate the capacity of roots to acquire different forms of phosphate (Binh & Zapata 2002). According to the Brazilian Legislation, the NAC+H_2O solution is recommended fertilizer test to measure P forms soluble in ammonium phosphates, while the 2% citric acid solution is the recommended to evaluate low-grade rock available P forms to crops (Brazil 2017). P soluble in water is an additional index to determine the readily available phosphate pools to crops (Brazil 2017). Overall, the increased agronomic efficiency of P fertilizers added to soils is related to the high levels of P soluble in NAC+H_2O or CA at 2%, and levels of P soluble in water (Urrutia et al. 2014; Maluf et al. 2018; Lustosa Filho et al. 2019). For fertilizers, the high solubility of P in water promotes a high amount of readily available phosphate in soil solution, favoring P specific adsorption in tropical soils, which hamper the acquisition of phosphate by crops (Fink et al. 2016). In this sense, the fertilizer agronomic value is higher when the OMFs formulated have pH fertilizer values optimum range (5-6.5), high values of EC, and total contents of C, N, P, K, and soluble C, as well as high levels of P soluble in NAC+H_2O and CA, and intermediate

levels of P soluble in water. Thus, considering all properties of the OMFs formulated, it is possible to anticipate the agronomic efficiency of the compost-based fertilizers as sources of nutrients to crops in different soils.

OMFs were mainly subdivided into categories based on the high or poor soluble P sources used in the OMFs synthesis. A trend was observed in grouping the OMFs from MAP with higher P solubility, subdivided into groups with MAP proportions lower than 40%, between 40 and 50%, and higher than 50%. These groups related to MAP-based OMFs had higher P and N total contents, EC and P soluble in water or CA or NAC+H_2O over other low-grade phosphate-based OMFs. The OMFs derived from the low-grade phosphate rocks had their pH increased during composting; the reason why this class of OMFs was clustered around pH value ranges, as follows: OMFs were subdivided into two groups, one formed for proportions of Araxá and Bayóvar phosphates with higher than 40% in composting piles; on the contrary, proportion lower than 40% of low-grade phosphate-based OMFs resulted in higher values of K and C total, and C soluble in water, compared to P-phosphate proportions below 40%. The prevalence of organic residues over the mineral P sources increased C and K contents and decreased P contents in OMFs.

In a multifaceted analysis, the MAP-based OMFs have a greater agronomic potential to nourish plants than low-grade phosphates-based OMFs, considering that MAP-based OMFs showed pH values in the optimum range for plentiful plant growth, besides a greater total and soluble P contents (Figure 2 and Table 2). Within MAP-based OMFs, MAP proportion in composting piles lower than 60% generate OMFs with high agronomic value, characterized by the higher P contents. Carbon and K contents in OMFs were increased as the proportions of organic residues in OMFs were increased. The OMFs are effective multi-functional fertilizers capable of supplying P, K, and most of the N required by plants, besides acting as a soil conditioner, depending on the rate applied.

3.3 Prediction capacity of PLS models

Based on the ATR-FTIR -spectra of OMFs, a multivariate calibration using the PLS regression was performed to obtain models capable of predicting different properties of OMFs evaluated by classical lab methods. The parameters of PLS regression modeled for each OMF property were shown in Table 3. The number of latent variables (LV) in each PLS model was determined by a lower value of RMSE obtained during the cross-validation phase. The regression coefficients of PLS regression to each variable measurement were contained in supplementary material B.

Table 3. Parameters of PLS regression models generated and used to predict the chemical properties of organomineral fertilizers.

	pH	EC	C^{Water}	C^{T}	P^{Water}	P^{CA}	P^{NAC}	P^{T}	N^{T}	K^{T}
		dS m^{-1}	g kg^{-1}							
LV	14	4	12	4	6	5	6	13	4	6
$RMSE_{cal}$	0.1	1.1	0.4	12.2	2.2	3.4	1.9	2.6	1.8	1.3
R^2_{cal}	0.99	0.99	0.99	0.92	0.99	0.99	0.99	0.99	0.99	0.95
$RMSE_{cv}$	0.1	1.5	0.8	15.0	3.1	4.8	2.8	11.3	2.4	1.8
R^2_{cv}	0.99	0.99	0.97	0.87	0.99	0.99	0.99	0.93	0.99	0.91
$RMSE_{y\text{-}rand}$	1.4	18.5	3.5	37.6	46.1	46.9	49.6	33.7	27.6	5.4
$R^2_{y\text{-}rand}$	0.39	0.20	0.44	0.20	0.21	0.25	0.32	0.35	0.19	0.24
r^2_p	0.78	0.89	0.74	0.81	0.88	0.86	0.82	0.80	0.89	0.83
$RMSE_{pred}$	0.1	1.2	1.0	18.6	3.4	5.6	4.0	4.2	2.7	3.1
R^2_{pred}	0.99	0.99	0.97	0.93	0.99	0.99	0.99	0.98	0.99	0.89
r^2_m	0.98	0.95	0.97	0.85	0.96	0.92	0.96	0.97	0.96	0.68

EC: electrical conductivity; C^{Water} and C^{T}: content of carbon soluble in water and total, respectively; P^{Water}, P^{CA} and P^{NAC}: content of phosphorus soluble in water, citric acid at 2% and neutral ammonium citrate plus water, respectively; P^{T}, N^{T} and K^{T}: total content of phosphorus, nitrogen and potassium, respectively; LV: latent variable; RMSE: root mean square error; R^2 or r^2: squared correlation coefficient; $RMSE_{cal}$: RMSE of calibration; R^2_{cal}: R^2 of calibration; $RMSE_{cv}$: RMSE of cross-validation; R^2_{cv}: R^2 of cross-validation; $RMSE_{y\text{-}rand}$: RMSE of y-randomization; $R^2_{y\text{-}rand}$: R^2 of y-randomization; r^2_p: r^2 of y-randomization prediction; $RMSE_{pred}$: RMSE of prediction; R^2_{pred}: R^2 of prediction; r^2_m: r^2 between the experimental and predicted values for the test set.

All PLS regression models had low values of $RMSE_{cal}$ over the predicted value range for each property of OMFs (Table 3). PLS models were also characterized by the high correlation coefficient with R^2_{cal}, values above 0.92 (Table 3). R^2 values are considered good for PLS models during the calibration and cross-validation process when R^2 is higher than 0.81 (Wang et al. 2014). During the cross-validation phase, R^2 values above 0.60 are acceptable (Kiralj & Ferreira 2009). In this study, R^2_{cv} reported for the models developed had R^2_{cv}, values above 0.90, except for the total C content whose PLS model had R^2_{cv} of 0.87, classified both as good. In the cross-validation phase, the $RMSE_{cv}$ prevails in low values. The difference between R^2_{cal} and R^2_{cv} for each PLS regression was lower than 0.2, a limit that indicates that the models are not characterized by overfitting, being an index to validate PLS models (Kiralj & Ferreira 2009).

The variable y was randomized and used in the calibration and to measure the robustness of each PLS model. Low $R^2_{y\text{-}rand}$ values and high $RMSE_{y\text{-}rand}$ values suggest that the correlation obtained for each model was non-randomized. The r^2_p parameter was proposed to ensure that the models developed are not obtained by chance, penalizing the R^2 of models for the difference between the R^2 of randomized and non-randomized models (Roy et al. 2009). The value of r^2_p should be greater than 0.5 for a model to be an acceptable model (Roy et al. 2009). All models in this study presented values above 0.5, considering that r^2_p values obtained in this study ranged from 0.71 to 0.89.

The RMSE and R^2 of prediction obtained by validation external from the test dataset showed the good predictive ability of PLS since R^2_{pred} values ranged from 0.89-0.99. However, the R^2_{pred} may not be sufficient to indicate external predictability; even maintaining an overall good inter-correlationship, the PLS models may have a considerable numerical difference between the values predicted and observed. Thus, the r^2_m was calculated to eliminate this effect aforementioned, and all PLS models confirmed had a good correlation between measured and

predicted values from the external validation; once the values of r^2_m values ranged from 0.68-0.98, being the 0.5, the value limit to attest a good correlation (Roy et al. 2009).

Measured *versus* predicted values of classical methods used to determine OMFs properties of calibration, cross-validation, and test dataset validation were shown in Figure 3, mirroring the good correlation coefficient of PLS models obtained. The classical methods used to determine the properties of the mineral, organic, and organomineral fertilizers are an essential step in inferring the use efficiency of fertilizers by crops. Additionally, they are factors ruling fertilizer rate and o anticipating crop nutrient use efficiency (Chien et al. 2011; Václavková et al. 2018; Frazão et al. 2019). For example, the determination in OMFs of P soluble difference in NAC+H_2O or H_2O has a relationship with its use by crops (Maluf et al. 2018; Lustosa Filho et al. 2019).

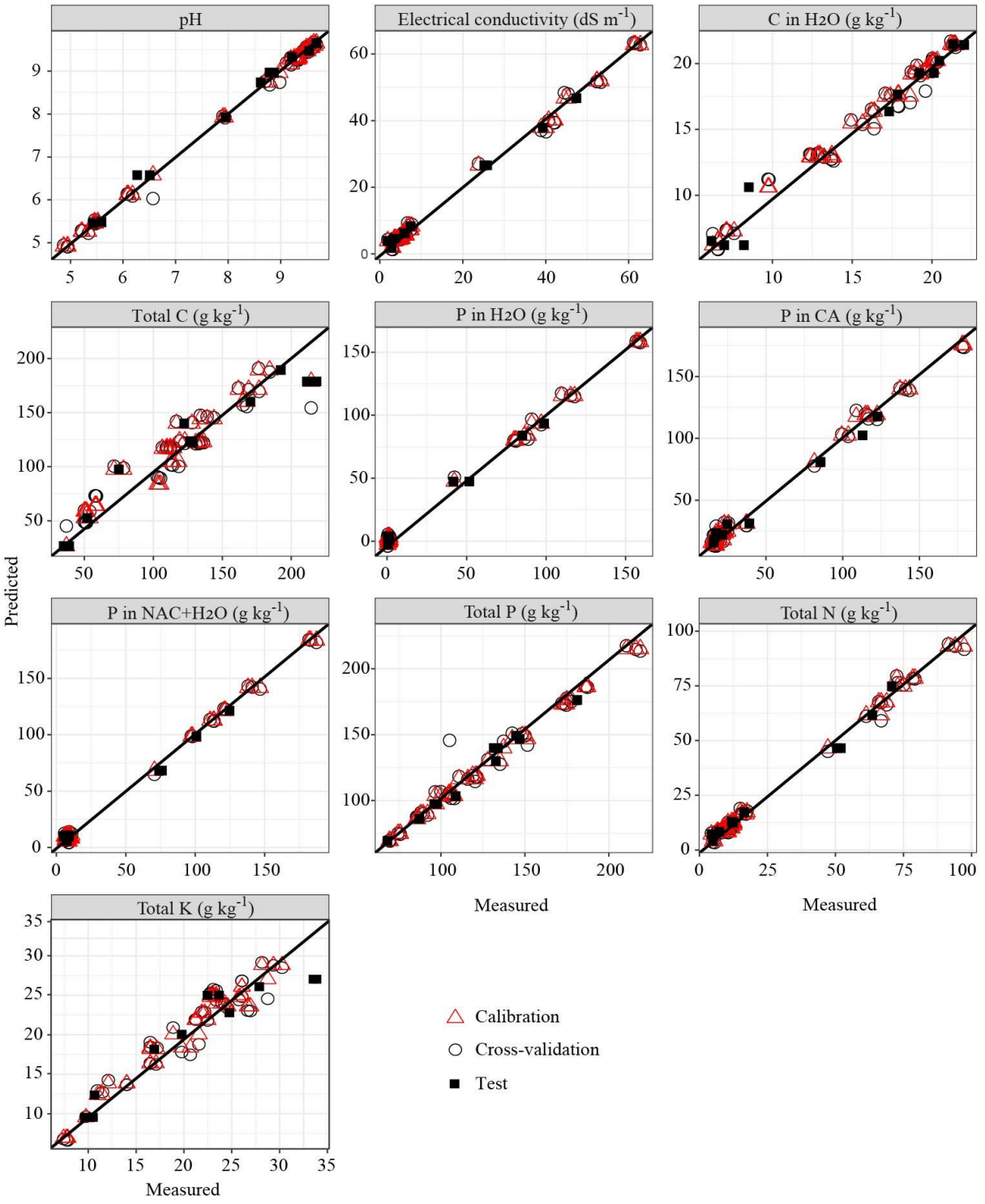

Figure 3. Relationships between the measured and predicted values of pH, electrical conductivity (EC), content of water-soluble C (C in H_2O), total carbon content (Total carbon), content of phosphorus soluble in water (P in H_2O), citric acid at 2% (P in CA) and neutral ammonium citrate plus water (P in NAC+H_2O), total content of phosphorus (Total P), nitrogen (Total N) and potassium (Total K) in OMFs. ○: calibration; Δ: cross-validation; ■: test.

Use of PLS regression models based on infrared spectroscopy to predict with accuracy the pH of mineral, organomineral and organic fertilizers were reported by Ruangratanakorn et al. (2020) and Wang et al. (2014) with values of R^2_{cal} (0.73), R^2_{cv} (0.71-0.73), R^2_{pred} (0.88), the $RMSE_{cal}$ (0.11), $RMSE_{cv}$ (0.11-0.96) and $RMSE_{pred}$ (0.27). In this study, we reported that the PLS models had greater accuracy due to similar values of $RMSE_{cal}$, $RMSE_{cv}$, and $RMSE_{pred}$, and higher values for R^2_{cal}, R^2_{cv}, and R^2_{pred} (Table 3) over those studies already mentioned. Regarding the OMFs EC prediction reported by Wang et al. (2014), R^2_{cal} verified it was similar (0.99), while the R^2_{pred} observed in this study (R^2_{pred}:0.99) was higher than the values reported in the literature as mentioned earlier (R^2_{pred}:0.74).

Prediction of soluble C in OMFs showed good accuracy, as shown in Table 3 and Figure 3. The prediction of soluble C contents in plant substrate using PLS regression and infrared was also reported by Higashikawa et al. (2014) for growth media with different maturity indices. PLS regression models proved to effectively predict the soluble C contents in organic commercial fertilizers (Wang et al. 2014). Compared to the results reported in this study, the studies already mentioned reported lower values of R^2_{cal} (0.75), R^2_{cv} (0.64-0.88), and R^2_{pred} (0.76-0.76), and higher values of $RMSE_{cv}$, $RMSE_{pred}$ were reported by Wang et al. (2014) and similar values to $RMSE_{cal}$, $RMSE_{cv}$, and $RMSE_{pred}$ were reported by Higashikawa et al. (2014). Also evaluated others parameters to determine the accuracy of models, Higashikawa et al. (2014) showed values of $RMSE_{y\text{-}rand}$ (1.8 g kg^{-1}), $R^2_{y\text{-}rand}$ (0.11) similar C soluble prediction in this study. Compared to Higashikawa's PLS models (Higashikawa et al. 2014), the regression models used to predict soluble C in this study had higher values of r^2_p and r^2_m.

Among all classical analysis to evaluate the properties of OMFs through PLS, the total C content prediction models showed a lower R^2; however, the PLS models had a good performance in predicting C (Table 3). R^2_{cv}, R^2_{pred}, $RMSE_{cv}$ and $RMSE_{pred}$ values for the prediction models of total C content (Table 3) were similar to that reported by Wang et al., 2014

for commercial organic fertilizers (R^2_{cv}:0.93; R^2_{pred}:0.78; $RMSE_{cv}$: 22.92 g kg^{-1} and $RMSE_{pred}$:19.38 g kg^{-1}). Upon the parameters for the models used to predict organic C in OMFs reported by Ruangratanakorn et al. (2020), we verified higher values of R^2_{cal}, R^2_{cv}, $RMSE_{cal}$ and $RMSE_{cv}$ (Table 3), the values presented by these authors were R^2_{cal}: 0.82, R^2_{cv}: 0.67, $RMSE_{cal}$: 7.1 g kg^{-1} and $RMSE_{cv}$: 9.7 g kg^{-1}.

PLS based on infrared spectroscopy effectively predicted the P availability for plants inferred by different soil tests (Ma et al. 2019; Pätzold et al. 2020). In OMFs, the P available evaluated through the AOAC 957.02 method was predicted by PLS based on infrared spectra with the following parameters of the regression models: R^2_{cal}, R^2_{cv}, $RMSE_{cal}$, $RMSE_{cv}$, of 0.82, 0.80, 2.21 and 2.31, respectively (Ruangratanakorn et al. 2020). However, following the assumptions described in Ruangratanakorn et al. (2020), the methodology used to evaluate P may not represent the accurate contents of P available to plants, considering that strong acids, such as nitric acid, were used as P extractants (Horwitz 2000). In the three approaches used to determine fertilizer-available P contents (P soluble in water, CA, or NAC+H_2O), it was possible to predict with high accuracy the P indices through PLS based on the ATR-FTIR spectra dataset (Table 3 and Figure 3), with R^2_{cal} and R^2_{cv} values higher than those reported by Ruangratanakorn et al. (2020), though the values of $RMSE_{cal}$ and $RMSE_{cv}$ were similar.

There are few literatures reporting the conjugated use of PLS regression and infrared spectroscopy to predict the total content of N, P, and K in OMFs. In this direction, the study carried out by Ruangratanakorn et al. (2020) should be highlighted since PLS regression based on the infrared spectroscopy to predict the N content in NPK mineral and organomineral fertilizers had a high prediction capacity considering the high values R^2_{cal} and R^2_{cv} of 0.98 and 0.97, and $RMSE_{cal}$ and $RMSE_{cv}$ of 1.91 and 2.00 g kg^{-1}. In this study, it was found values ~ 0.99 to R^2_{cal} and R^2_{cv} and $RMSE_{cal}$ and $RMSE_{cv}$ within the range of 1.8 to 2.4 g kg^{-1}, values of statistics parameters similar to those reported by Ruangratanakorn et al. (2020).

PLS regression and infrared spectroscopy also were effective in predicting N, P, and K total contents in swine, poultry, and beef cattle manures, with R^2_{cal} and R^2_{cv} ranging from 0.74-0.97, 0.50-0.91, and 0.63-0.95, respectively, as it was demonstrated by Chen et al. (2013) in an huge literature review. Evaluating the capacity of PLS regression to predict N, P, and K total content in mineral fertilizers, reported R^2_{cal} values of 0.90, 0.87, and 0.83, respectively, for N, P, and K in fertilizers originated from different production processes in China (Lin et al. 2018). Van Vuuren & Groenewald (2013) reported R^2_{cal} values of 0.92, 0.91, and 0.89, respectively, for N, P, and K in mineral fertilizers. Based on the results shown in Table 3, in this study, in the OMFs formulated with different proportions of P sources, CM and CH, the R^2_{cal} and R^2_{cv} values for N, P, and K total prediction was higher than those reported for regression models used to predict mineral and organic fertilizers properties and nutrient pools.

3.4 Economic and environmental implications

Chicken manure and coffee husk are organic residues massively produced in Brazil. CM has a pH > 7.0, and it is an enriched carbonate species and Ca chemical species, is an important source of N and K as well, while P contents on it are considered low to medium. CH is an important source of K among organic residues, though post-harvest coffee waste is poor in N and P and has a low liming value. Depending on the proportions, the mixture of CM and CH with MAP is suitable for producing high agronomic value OMFs as demonstrated in our study. Composting of CH and CM is not a suitable route to increase the solubilization of apatite, as well, a process to increase P agronomic indices of Low-grade P rock-derived OMFs. The use of organic residues in the synthesis of OMFs is a way to recycle nutrients while avoiding pollution of water and soil and the excessive use of non-renewable raw materials employed in the synthesis of soluble mineral fertilizers. Waste recycling through composting in the fertilizer

sector is a strategy to improve the agronomic value of soluble P sources such as MAP, potentially enhancing fertilization efficiency and crop yield (Maluf et al. 2018).

PLS regression models based on ATR-FTIR are an alternative, suitable and reliable technique to predict classical laboratory methods employed in the OMFs characterization. PLS regression based on infrared analysis has some advantages over the conventional lab methods, such as a lower time to infer OMFs properties, a lower cost per analysis, faster and non-invasive lab routine that does not employ chemical reagents; thus, it is an environmentally friendly analysis (Van Vuuren & Groenewald 2013; Chen et al. 2013; Higashikawa et al. 2014; Wang et al. 2014; Lin et al. 2018; Wang et al. 2019; Ruangratanakorn et al. 2020).

In Brazil, the complete analysis of OMFs properties in official and certified laboratories, on average, has the following prices: as a whole, analysis of pH, total C, N, P, and K contents, on average, costs US$ 18.66; EC: US$ 4.02 and each fertilizer-solubility index regarding P (P soluble in water or 2% citric acid or NAC+H_2O): US$ 6.77. thus, the total price per fertilizer sample analyzed is US$ 42.99, taking as standard the U.S. dollar in its current exchange ratio to the Brazilian currency, the Real (ESALQ. 2021). It is worth mentioning that carbon soluble in water is not determined as an index for fertilizers in commercial laboratories. Compared to the price of analysis per sample, the ATR-FTIR analysis price is about US$ 10.97 (IQSC-USP 2021), thus, lower than those values already mentioned for conventional lab analyses. Once the ATR-FTIR can be used to estimate the OMFs properties aforementioned though PLS regression, the cost per fertilizer full analysis was 3.92 folder lower than the wet lab and invasive routine methods adopted in Brazil. For this reason, PLS models based on ATR-FTIR can replace classical lab methods to evaluate a range of OMFs properties, contributing to a fast and accurate analysis of OMFs whose production and use in crop fields are increasing in Brazil.

4 Conclusion

The mixture and composting of soluble and low-grade P sources, chicken manure, and coffee husk produce organomineral fertilizers (OMFs) with contrasting nutrient pools, and chemical and physicochemical properties determined by the wet classical laboratory methods. The monoammonium phosphate-based OMFs had a higher agronomic value than low-grade phosphate-based OMFs. Partial least square (PLS) regression based on attenuated total reflection with Fourier Transform Infrared Spectroscopy (ATR-FTIR) predicted with robustness and accuracy the pH, electrical conductivity, C, P, N, and K total contents, and C and P soluble in water, as well as P soluble in citric acid (2%) or neutral ammonium citrate plus water. All PLS regression models used to estimate OMFs properties and nutrient pools were reliable, robust, and had no chance of correlation. PLS regression based on ATR-FTIR was an alternative new approach to assess key properties and nutrient pools in organomineral fertilizers in a simple, non-invasive and low-cost technique without the generation of lab wastes.

5 Acknowledgments

Many thanks to the Coordination for the Improvement of Higher Education Personnel (CAPES) (CAPES-PROEX/AUXPE 593/2018), National Council for Scientific and Technological Development (CNPq) (303899/2015-8 and 307447/2019-7 grants), and the Foundation for Research of the State of Minas Gerais (FAPEMIG) for financial support and scholarships provided. We are also grateful to Dr. Zuy M. Magriotis and Dr. Adelir A. Saczk from the Department of Chemistry/UFLA for providing the facilities and helping in the ATR-FTIR analysis. UFLA is an equal opportunity provider and employer.

6 References

Abd El-Mageed TA, Semida WM. 2015. Organo mineral fertilizer can mitigate water stress for cucumber production (*Cucumis sativus* L.). Agric Water Manag [Internet]. 159:1–10. https://linkinghub.elsevier.com/retrieve/pii/S0378377415300111

Berzina-Cimdina L, Borodajenko N. 2012. Research of Calcium Phosphates Using Fourier Transform Infrared Spectroscopy. In: Theophile T, editor. Infrared Spectrosc - Mater Sci Eng Technol [Internet]. Rijeka: InTech Europe; p. 123–148. https://www.intechopen.com/chapters/36171

Binh T, Zapata F. 2002. Standard characterization of phosphate rock samples from the FAO/IAEA phosphate project. In: Assess Soil Phosphorus Status Manag Phosphatic Fertil to Optim Crop Prod. Vienna: IAEA-TECDOC-1272; p. 9–23.

Brazil. 2017. Manual de métodos analíticos oficiais para fertilizantes e corretivos [Internet]. Brasil, editor. Brasília: MAPA. https://www.gov.br/agricultura/pt-br/assuntos/insumos-agropecuarios/insumos-agricolas/fertilizantes/legislacao/manual-de-metodos_2017_isbn-978-85-7991-109-5.pdf

Cancellier EL, Degryse F, Silva DRG, da Silva RC, McLaughlin MJ. 2018. Rapid and Low-Cost Method for Evaluation of Nutrient Release from Controlled-Release Fertilizers Using Electrical Conductivity. J Polym Environ [Internet]. 26(12):4388–4395. http://dx.doi.org/10.1007/s10924-018-1309-1

Chen L, Xing L, Han L. 2013. Review of the Application of Near-Infrared Spectroscopy Technology to Determine the Chemical Composition of Animal Manure. J Environ Qual [Internet]. 42(4):1015–1028. http://doi.wiley.com/10.2134/jeq2013.01.0014

Chien SH, Prochnow LI, Tu S, Snyder CS. 2011. Agronomic and environmental aspects of phosphate fertilizers varying in source and solubility: An update review. Nutr Cycl Agroecosystems. 89(2):229–255.

Erro J, Urrutia O, Baigorri R, Aparicio-Tejo P, Irigoyen I, Torino F, Mandado M, Yvin JC, Garcia-Mina JM. 2012. Organic Complexed Superphosphates (CSP): Physicochemical characterization and agronomical properties. J Agric Food Chem. 60(8):2008–2017.

ESALQ. 2021. Fertilizantes Minerais. Esalq-solos [Internet]. [accessed 2021 Sep 8]. https://www.esalqsolos.com.br/fertilizantes-minerais-categoria-18

FAO. 2017. World fertilizer trends and outlook to 2020: Summary report. Food Agric Organ United Nations [Internet].:38. http://www.fao.org/3/i6895e/i6895e.pdf

Fink JR, Inda AV, Tiecher T, Barrón V. 2016. Iron oxides and organic matter on soil phosphorus availability. Ciência e Agrotecnologia [Internet]. 40(4):369–379. www.editora.ufla.br%7Cwww.scielo.br/cagrohttp://dx.doi.org/10.1590/1413-70542016404023016%0Ahttp://dx.doi.org/10.1590/1413-70542016404023016

Frazão JJ, Benites V de M, Ribeiro JVS, Pierobon VM, Lavres J. 2019. Agronomic effectiveness of a granular poultry litter-derived organomineral phosphate fertilizer in tropical soils: Soil phosphorus fractionation and plant responses. Geoderma [Internet]. 337(October 2018):582–593. https://doi.org/10.1016/j.geoderma.2018.10.003

Gautam R, Vanga S, Ariese F, Umapathy S. 2015. Review of multidimensional data processing approaches for Raman and infrared spectroscopy. EPJ Tech Instrum [Internet]. 2(1):1–8. http://dx.doi.org/10.1140/epjti/s40485-015-0018-6

Higashikawa FS, Silva CA, Nunes CAÔ, Sánchez-Monedero MA. 2014. Fourier transform infrared spectroscopy and partial least square regression for the prediction of substrate maturity indexes. Sci Total Environ [Internet]. 470–471:536–542. http://dx.doi.org/10.1016/j.scitotenv.2013.09.065

Horwitz W, editor. 2000. Official methods of analysis of AOAC International. Food composition, additives, natural contaminants. 17th ed. Gaithersburg: AOAC.

IQSC-USP. 2021. Tabela de custo de análises–CAQI–IQSC–USP [Internet]. [accessed 2021 Sep 8]. http://caqi.iqsc.usp.br/revisar/tabela-de-custo-de-analises/

Kiralj R, Ferreira MMC. 2009. Basic validation procedures for regression models in QSAR and QSPR studies: Theory and application. J Braz Chem Soc. 20(4):770–787.

Kominko H, Gorazda K, Wzorek Z. 2017. The Possibility of Organo-Mineral Fertilizer Production from Sewage Sludge. Waste and Biomass Valorization. 8(5):1781–1791.

Liland KH, Mevik BH, Wehrens. 2021. pls: Partial Least Squares and Principal Component Regression [Internet]. https://cran.r-project.org/package=pls

Lin Z, Wang R, Wang Y, Wang L, Lu C, Liu Y, Zhang Z, Zhu L. 2018. Accurate and rapid detection of soil and fertilizer properties based on visible/near-infrared spectroscopy. Appl Opt [Internet]. 57(18):D69. https://www.osapublishing.org/abstract.cfm?URI=ao-57-18-D69

Lombi E, McLaughlin MJ, Johnston C, Armstrong RD, Holloway RE. 2005. Mobility, solubility and lability of fluid and granular forms of P fertiliser in calcareous and non-calcareous soils under laboratory conditions. Plant Soil [Internet]. 269(1–2):25–34. http://link.springer.com/10.1007/s11104-004-0558-z

Lu B, Liu N, Li H, Yang K, Hu C, Wang X, Li Z, Shen Z, Tang X. 2019. Quantitative determination and characteristic wavelength selection of available nitrogen in coco-peat by NIR spectroscopy. Soil Tillage Res [Internet]. 191:266–274. https://linkinghub.elsevier.com/retrieve/pii/S0167198718313102

Lu B, Liu N, Wang X, Hu C, Tang X. 2020. A feasibility quantitative analysis of NIR spectroscopy coupled Si-PLS to predict coco-peat available nitrogen from rapid measurements. Comput Electron Agric [Internet]. 173:105410. https://linkinghub.elsevier.com/retrieve/pii/S0168169920300648

Lustosa Filho JF, Barbosa CF, Carneiro JSDS, Melo LCA. 2019. Diffusion and phosphorus solubility of biochar-based fertilizer: Visualization, chemical assessment and availability to plants. Soil Tillage Res [Internet]. 194. https://www.scopus.com/inward/record.uri?eid=2-s2.0-85067666945&doi=10.1016%2Fj.still.2019.104298&partnerID=40&md5=dbb6f94d59f664ff738a93b048ec0ca2

Lustosa Filho JF, Penido ES, Castro PP, Silva CA, Melo LCA. 2017. Co-Pyrolysis of Poultry Litter and Phosphate and Magnesium Generates Alternative Slow-Release Fertilizer Suitable for Tropical Soils. ACS Sustain Chem Eng [Internet]. 5(10):9043–9052.

https://pubs.acs.org/doi/10.1021/acssuschemeng.7b01935

Ma F, Du CW, Zhou JM, Shen YZ. 2019. Investigation of soil properties using different techniques of mid-infrared spectroscopy. Eur J Soil Sci [Internet]. 70(1):96–106. https://onlinelibrary.wiley.com/doi/10.1111/ejss.12741

Maluf HJGM, Silva CA, de Morais EG, de Paula LHD. 2018. Is composting a route to solubilize low-grade phosphate rocks and improve MAP-based composts? Rev Bras Cienc do Solo [Internet]. 42. https://www.scopus.com/inward/record.uri?eid=2-s2.0-85042234113&doi=10.1590%2F18069657rbcs20170079&partnerID=40&md5=213bd78ab148fe3dd2d48a5f31921fc8

McLaughlin MJ, McBeath TM, Smernik R, Stacey SP, Ajiboye B, Guppy C. 2011. The chemical nature of P accumulation in agricultural soils-implications for fertiliser management and design: An Australian perspective. Plant Soil. 349(1–2):69–87.

Mumbach GL, Gatiboni LC, de Bona FD, Schmitt DE, Corrêa JC, Gabriel CA, Dall'Orsoletta DJ, Iochims DA. 2020. Agronomic efficiency of organomineral fertilizer in sequential grain crops in southern Brazil. Agron J. 112(4):3037–3049.

Pätzold S, Leenen M, Frizen P, Heggemann T, Wagner P, Rodionov A. 2020. Predicting plant available phosphorus using infrared spectroscopy with consideration for future mobile sensing applications in precision farming. Precis Agric [Internet]. 21(4):737–761. http://link.springer.com/10.1007/s11119-019-09693-3

R Core Team. 2020. R: A language and environment for statistical computing [Internet]. https://www.r-project.org/

Rose MT, Patti AF, Little KR, Brown AL, Jackson WR, Cavagnaro TR. 2014. A Meta-Analysis and Review of Plant-Growth Response to Humic Substances. In: Plant Soil [Internet]. [place unknown]; p. 37–89. http://linkinghub.elsevier.com/retrieve/pii/B9780128001387000024

Roy PP, Paul S, Mitra I, Roy K. 2009. On Two Novel Parameters for Validation of Predictive QSAR Models. Molecules [Internet]. 14(5):1660–1701. http://www.mdpi.com/1420-3049/14/5/1660

Ruangratanakorn J, Suwonsichon T, Kasemsumran S, Thanapase W. 2020. Installation design of on-line near infrared spectroscopy for the production of compound fertilizer. Vib Spectrosc [Internet]. 106:103008. https://linkinghub.elsevier.com/retrieve/pii/S0924203119301961

Silverstein RM, Webster FX, Kiemle DJ, Bryce D. 2005. Spectrometric identification of organic compounds. 7th ed. Hoboken: John Wiley & Sons.

Stevenson FJ. 1994. Humus chemistry: genesis, composition, reactions. New York: John Wiley & Sons.

Urrutia O, Erro J, Guardado I, San Francisco S, Mandado M, Baigorri R, Claude Yvin J, Ma Garcia-Mina J. 2014. Physico-chemical characterization of humic-metal-phosphate complexes and their potential application to the manufacture of new types of phosphate-based fertilizers. J Plant Nutr Soil Sci [Internet]. 177(2):128–136. https://onlinelibrary.wiley.com/doi/10.1002/jpln.201200651

Václavková Š, Šyc M, Moško J, Pohořelý M, Svoboda K. 2018. Fertilizer and Soil Solubility of Secondary P Sources—The Estimation of Their Applicability to Agricultural Soils. Environ Sci Technol [Internet]. 52(17):9810–9817. https://pubs.acs.org/doi/10.1021/acs.est.8b02105

Van Vuuren JAJ, Groenewald CA. 2013. Use of Scanning Near-Infrared Spectroscopy as a Quality Control Indicator for Bulk Blended Inorganic Fertilizers. Commun Soil Sci Plant Anal [Internet]. 44(1–4):120–135. http://www.tandfonline.com/doi/abs/10.1080/00103624.2013.736141

Wang C, Huang C, Qian J, Xiao J, Li H, Wen Y, He X, Ran W, Shen Q, Yu G. 2014. Rapid and Accurate Evaluation of the Quality of Commercial Organic Fertilizers Using Near Infrared Spectroscopy.Motta A, editor. PLoS One [Internet]. 9(2):e88279. https://dx.plos.org/10.1371/journal.pone.0088279

Wang LS, Wang RJ, Lu CP, Wang J, Huang W, Jian Q, Wang YB, Lin LZ, Song LT. 2019. Quantitative Analysis of Total Nitrogen Content in Monoammonium Phosphate Fertilizer Using Visible-Near Infrared Spectroscopy and Least Squares Support Vector Machine. J Appl Spectrosc [Internet]. 86(3):465–469. http://link.springer.com/10.1007/s10812-019-00842-0

Warnes GR, Bolker B, Bonebakker L, Gentleman R, Huber W, Liaw A, Lumley T, Maechler M, Magnusson A, Moeller S, et al. 2020. gplots: Various R Programming Tools for Plotting Data [Internet]. https://cran.r-project.org/web/packages/gplots/gplots.pdf

Yao S, Lu J, Li Junyan., Chen K, Li Jun, Dong M. 2010. Multi-elemental analysis of fertilizer using laser-induced breakdown spectroscopy coupled with partial least squares regression. J Anal At Spectrom. 25:1733–1738.

Zoca SM, Penn CJ, Rosolem CA, Alves AR, Neto LO, Martins MM. 2014. Coffee processing residues as a soil potassium amendment. Int J Recycl Org Waste Agric [Internet]. 3(4):155–165. https://www.scopus.com/inward/record.uri?eid=2-s2.0-84931045909&doi=10.1007%2Fs40093-014-0078-7&partnerID=40&md5=193d92e4674a797c7e473527a72b3b5a

Supplementary material 1. Mid-infrared spectral signatures and the main band signals of organomineral fertilizers formulated after the composting of multiple mixtures of P sources, chicken manure and coffee husk highlight each group according to each P source (Araxá, Bayóvar and Monoammonium phosphates). P: proportion of P source; CM: proportion of chicken manure; CH: proportion of coffee husk; overscribed numbers refer to the proportion (%) of each material used in OMFs mixture synthesis.

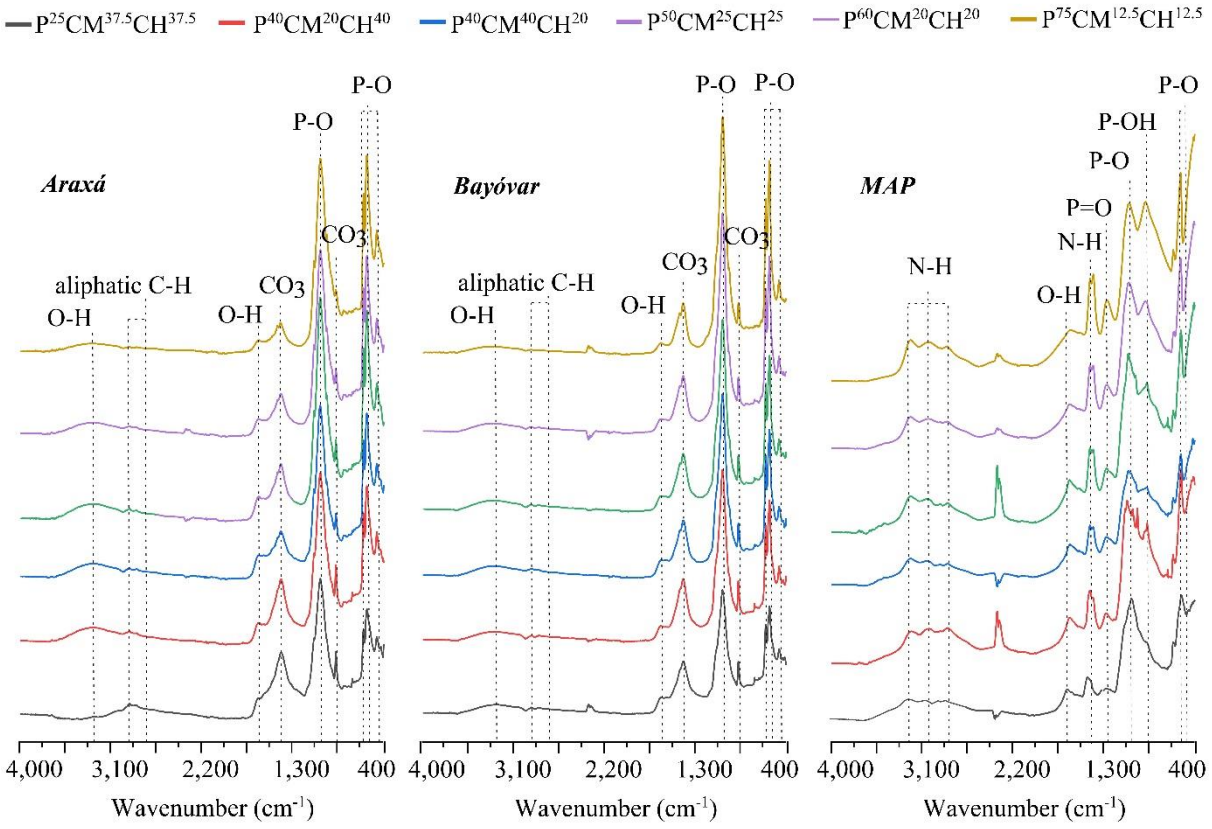

Supplementary material 2. Regression coefficient of partial least square regression to each variable measured according the Mid-infrared spectral signatures of organomineral fertilizers formulated after the composting of multiple mixtures of P sources, chicken manure and coffee husk. Variables mensured: pH, electrical conductivity (EC), content of water soluble C (C in H_2O), total carbon content (Total carbon), content of phosphorus soluble in water (P in H_2O), citric acid at 2% (P in CA) and neutral ammonium citrate plus water (P in NAC+H_2O), total content of phosphorus (Total P), nitrogen (Total N) and potassium (Total K).

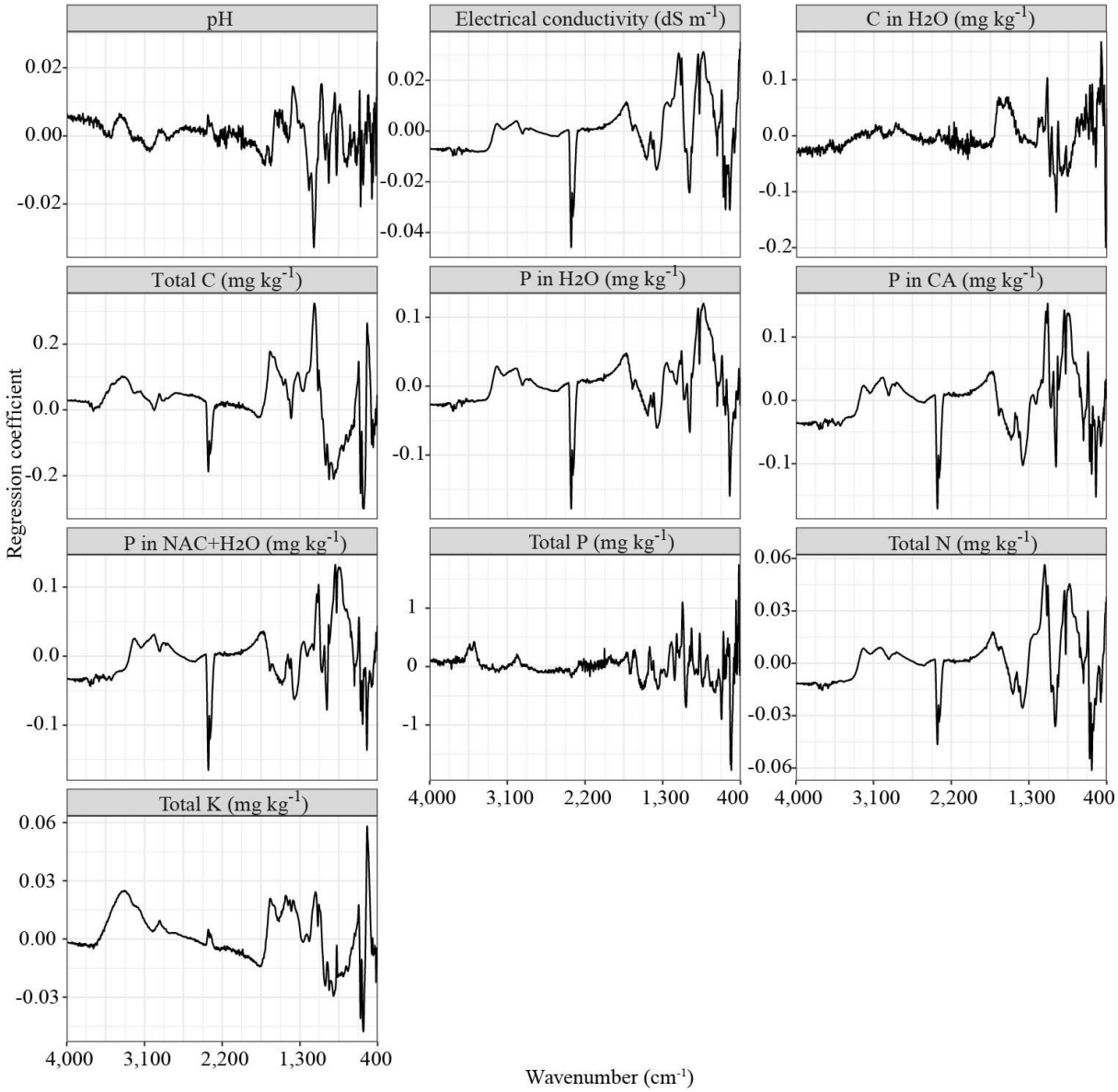

Preliminary version of manuscript edited following the rules of Waste and Biomass Valorization Journal

Effects of compost-based organomineral fertilizers on the kinetics of NPK release and maize growth in contrasting Oxisols

Everton Geraldo de Morais[1*], Carlos Alberto Silva[1], Henrique José Guimarães Moreira Maluf[2], Igor de Oliveira Paiva[1] and Leonardo Henrique Duarte de Paula[3]

[1]Departament of Soil Science, Federal University of Lavras, Av. Doutor Sylvio Menicucci 1001, zip code: 37200-000, Lavras-Minas Gerais, Brazil.
[2]Galvani Fertilizantes, Avenida Luís Eduardo Magalhães, 2071, Jardim das Acácias, zip code: 47.850-000, Luís Eduardo Magalhães-Bahia, Brazil.
[3]Departament of Agrarian Science, Federal Institute of Minas Gerais, Faz. Varginha - Rodovia Bambuí/Medeiros - Km 05, zip code: 38.900, Bambuí-Minas Gerais, Brazil.
* Corresponding author: evertonmoraislp@yahoo.com.br

Abstract

The composting of chicken manure (CM), coffee husk (CH), and monoammonium phosphate (MAP) in the correct proportion may create organomineral fertilizers (OMFs) with a gradual release of nutrients and higher agronomic performance in Oxisols. The study aimed to recycle CM and CH mixed with MAP through the composting in the production OMFs, characterizing them and evaluating agronomic performance. Four OMFs were produced and characterized by chemical and spectroscopic analysis using the mixture of four proportions between CM, CH, and MAP ($MAP^{25\%}CM^{37.5\%}CH^{37.5\%}$, $MAP^{40\%}CM^{40\%}CH^{20\%}$, $MAP^{50\%}CM^{25\%}CH^{25\%}$ and $MAP^{75\%}CM^{12.5\%}CH^{12.5\%}$). The mineralization of nitrogen (N) and phosphorus (P) and release of potassium (K) were evaluated in soil-OMFs incubated mixtures study, and NPK dynamics

of OMFs were evaluated in whole soil and its soil solution during maize (hybrid Pioneer 30F53) cultivation in greenhouse conditions for 36 days in two contrasting Oxisols. Nitrogen and P compounds and bonds identified in infrared analysis positively correlated with N and P forms in both OMFs and MAP sources. In a soil type-dependent way, an increase in the proportions of CH+CM over MAP in the OMFs promoted a more gradual release of N, P, and K. Reduction of readily N and P forms for maize increased the efficiency of OMFs over MAP in Oxisol with the lowest organic matter (OM) content, and the proportion in OMF of $MAP^{25\%}CM^{37.5\%}CH^{37.5\%}$ increased shoot biomass in approximately 26% and shoot P in 22% over MAP-fertilized maize plants. In the Oxisol with higher OM content, the N and P fertilizer-availability indices did not affect maize nutritional status and growth. The proportion of $MAP^{40\%}CM^{40\%}CH^{20\%}$ over MAP increased about 22 and 50 % of the shoot biomass and shoot P, respectively. Compared to MAP, the amount of N mineralized in the incubation-kinetics study only varies for OMFs added to soil with higher OM content, while the kinetics of P and K release rely on OMF type used to treat both Oxisols. The composting of CM, CH, and MAP was an alternative to improve the fertilization efficiency in tropical soils.

Graphical Abstract

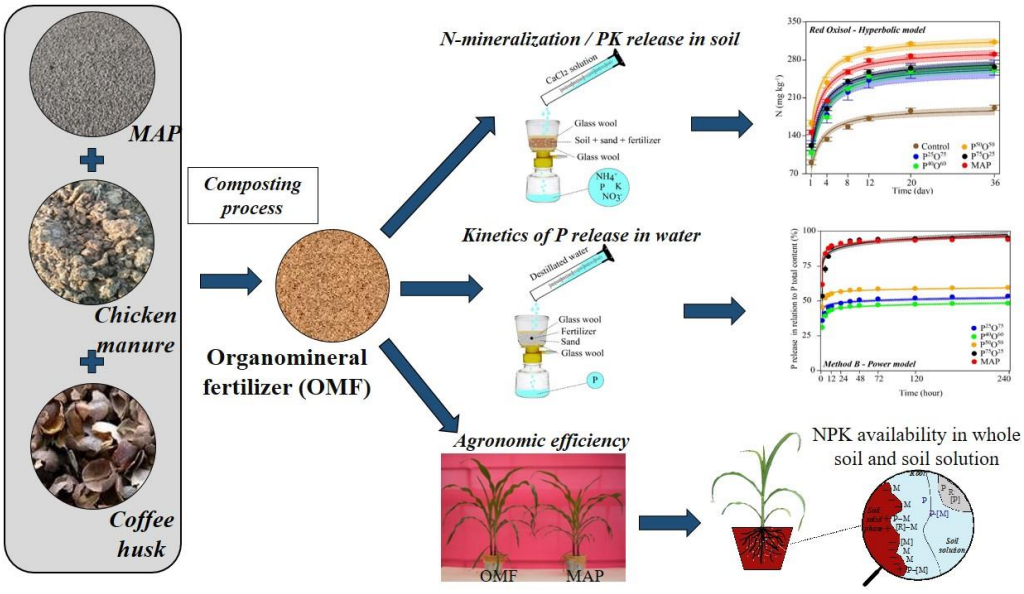

Statement of Novelty

Organomineral fertilizers (OMFs) based on MAP over isolated application of MAP has a higher fertilization efficiency in Oxisols. Coffee husks (CH) and chicken manure (CM) are organic residues produced in high quantities in Brazil with high potential for use in the production of MAP-OMFs; however, CH has a high Carbon: nitrogen ratio (C:N ratio), which can immobilize N, while chicken manure has high pH values that can reduce the availability of nutrients. The mixture and composting of CH, CM, and MAP in a correct proportion is a sustainable way of making OMFs with an adequate value of pH and C:N ratio and higher levels of N, phosphorus (P), and potassium (K) in forms with higher agronomic performance for plants cultivation.

Keywords: soil solution; composting-based fertilizers, nutrient cycling; highly weathered soils, N mineralization rate, kinetics of P and K release.

1 Introduction

Tropical soils as Brazilian soils, have low natural availability of nutrients, and nitrogen (N), phosphorus (P), and potassium (K) are the main nutrients used in fertilization practices to attend to the demand of plants, supplied mainly through mineral fertilizers; however, the mineral fertilizers have a low agronomic performance [1–3]. In soils rich in soil organic matter (SOM), part of the N required for plants may be supplied after the mineralization of SOM; however, in tropical soils, native OM is low [4]. In Brazilian soils, P availability is low, and phosphate is strongly adsorbed in Fe and Al oxides and low-activity mineral colloids, such as kaolinite, especially when soils are fertilized with mineral soluble P fertilizers [2, 3, 5, 6]. Soil K availability is low to medium in Brazilian soils, and most of the K added to the soil by mineral fertilizers tends to remain in solution due to the low cation exchange capacity of tropical soils making the K more prone to the leaching process [2, 7].

Increasing OM content in soils is a suitable long-term strategy for improving the use efficiency of P by plants due to OM is capable of blocking P fixation sites in tropical soils, increasing P availability for plants; however, achieving high levels of OM stored in tropical soils remains an enormous challenge [3, 5, 6]. In the short term, another strategy to achieve the beneficial effect of OM on soil P dynamics and availability is the mixture of mineral fertilizers with organic residues, hereafter named organomineral fertilizers (OMFs) [8–10]. OMFs combine the benefits of organic and inorganic nutrient sources resulting in stable forms and known nutrient concentrations, improving nutrient pools available in the short, medium and, long term [8, 9, 11]. Additionally, the synthesis of OMFs is an eco-friendly route to recycle wastes and organic residues to produce high-agronomic value inputs and fertilizers [12, 13].

In Brazil, chicken manure (CM) and coffee husk (CH) are available and have an enormous potential to produce OMFs, because CM is a source of N and P, and CH is a relevant source of K from Brazilian coffee plantations; however, CM has higher values of pH that may reduce the availability of the nutrients, and CH has a higher Carbon: N ratio (C:N ratio) that may immobilize N [14, 15]. Composting CM, CH, and monoammonium phosphate (MAP) in a correct mixture can be a suitable route to produce MAP-based OMFs with adequate properties and higher agronomic efficiency than the exclusive use of MAP to nourish plants [9, 16, 17]. Compared with mineral fertilizers, OMFs have slow-release nutrients, reducing NPK losses and increasing the use efficiency of NPK by crops, mainly for P, due to a more gradual release that reduces the specific P adsorption in tropical soils [5, 11, 18, 19]. Besides, organic ligands from organic residues from OMFs are capable of blocking phosphate-specific adsorption sites, and the formation of P-metal-organic ligand complexes in OMFs minimizes the specific P adsorption in tropical soils [6, 8, 20].

One of the main effects of OMFs is related to the forms in which nutrients are supplied to plants since both organic and mineral forms are simultaneously present in OMFs [16]. The

chemical bonds and compounds in OMFs may be identified by infrared spectroscopy analysis [21–23]. In addition, chemical analysis in OMFs is used to assess both organic N and mineral N forms, the solubility of P in different extractor solutions, as well as the fraction of organic N and P more prone to mineralized, controlling the capacity of OMFs to supply nutrient to crops [24–28]. Compared with mineral fertilizers, OMFs maintain high levels of nutrients; however, the nutrients are gradually released for crops [29, 30], which may promote a higher nutrient residual effect across different cropping seasons [11, 31, 32]. Besides, the soil type and its properties control the OMFs effects, and among soil properties, native OM content is a key factor controlling OMFs effects since organic compounds linked to soil native OM may hinder the positive role played by exogenous organic ligands found in OMFs [8, 9, 12, 17, 33].

Thus, we hypothesized that recycling of CM and CH and production of compost-based OMFs through the composting in the correct proportion of MAP, CM, and CH mixtures, have a higher agronomic performance and gradual NPK release over the exclusive use of MAP-KCl on the maize growth in a soil type-dependent way. This study aimed to: i) evaluate the chemical properties and kinetics of P release from OMFs and MAP; ii) identify the main N and P chemical forms present in OMFs through the spectroscopy analysis (ATR-FTIR); iii) evaluate the effects of OMFs on maize growth in two contrasting Oxisols; iv) elucidate how OMFs properties affect the kinetics of NPK release across soils and their solutions, as well as to relate fertilizer nutrient pools with maize nutritional status and biomass production, and; v) evaluate the dynamics of mineralization/release of NPK from OMFs incubated in contrasting Oxisols.

2 Material and Methods

2.1 OMFs characterization

OMFs were produced through the composting of mixtures of different proportions of MAP, CM, and CH in three repetitions over 150 days; once the input of organic residues and

their ratios in mixing during the synthesis of OMFs control the properties, pools, and nutrient availability of the resulting OMFs. Characterization of organic residues and MAP were described in **Table 1**, and more details of the synthesis of OMFs are described in Maluf et al. [16]. Besides OMFs, MAP was tested and evaluated regarding properties, such as forms and agronomic value of their N and P pools. The OMFs investigated were: $P^{25}O^{75}$ (25% MAP + 37.5% CM + 37.5% CH), $P^{40}O^{60}$ (40% MAP + 40% CM + 20% CH), $P^{50}O^{50}$ (50% MAP + 25% CM + 25% CH) and $P^{75}O^{25}$ (75% MAP + 12.5% CM + 12.5% CH).

Table 1. Nutrient contents, pools and P availability of matrices used in organomineral fertilizers synthesis.

Material	pH ($CaCl_2$)	Total N	Total K	P			
				Total	Water	Citric acid	NAC+H_2O
		g kg^{-1}					
MAP	4.1	110.0	-	237.0	219.0	225.0	235.0
CM	7.1	30.2	28.4	34.2	5.4	23.9	17.9
CH	4.6	17.3	42.4	1.2	1.0	1.1	1.2

pH was determined in CaC_2 solution at a ratio of 1:5 (w/v); *Modified from Maluf et al. [16]. Water, citric acid NAC+H2O: soluble P in water or in citric acid at 2% or in neutral ammonium citrate plus water, respectively.

The pH of OMFs and MAP was determined in a 0.01 mol L^{-1} $CaCl_2$ solution, and the total N content was determined by the Kjeldahl method after the digestion of samples in sulfuric acid [24]. Total P and K contents of fertilizers were determined, respectively, using the vanadomolybdate and flame photometry methods after the digestion of samples in a nitric-perchloric (4:1) solution [24]. Mineral N was extracted with a 2 mol L^{-1} KCl solution (10 mL extractant: 1 g fertilizer) [34, 35], and N as N-$NH_4^+$and N-NO_3^- contents were determined by distillation followed by titration. OMFs organic N content was determined by subtracting the N-NH_4^+ amount from the total N content determined through the Kjeldahl method [35].

In OMFs and MAP samples, the content of soluble P in water was extracted by successive washing with distilled water of one gram fertilizer samples placed on filter paper, P soluble in neutral ammonium citrate plus water (NAC+H_2O) was extracted by boiling the sample with a NAC solution, and P soluble in citric acid (CA) was extracted by shaking fertilizer samples in a 2% CA solution [24]. P contents in extracts were determined by the vanadomolybdate method [36]. The compare the N and P pools related to the N forms and solubility of P fertilizer samples, N or P indices were calculated according to N forms (N-mineral and N-organic) (Eq. 1) and soluble P (Eq. 2) fractions (water or CA or NAC+H_2O or FA) according to respectively nutrient total content:

$$\text{N index (\%)} = \left(\frac{\text{N-form content } \left(\text{g kg}^{-1}\right)}{\text{Total N content } \left(\text{g kg}^{-1}\right)} \right) \times 100 \quad \text{(Eq. 1)}$$

$$\text{P index (\%)} = \left(\frac{\text{Soluble P content } \left(\text{g kg}^{-1}\right)}{\text{Total P content } \left(\text{g kg}^{-1}\right)} \right) \times 100 \quad \text{(Eq. 2)}$$

2.2 Kinetics of P release

Two methodologies were tested to evaluate the kinetics of P release by OMFs and MAP. In both methodologies, a completely randomized design was adopted with three repetitions. Firstly (Method A), one gram of each dry fertilizer was mixed with 200 ml of distilled water and, agitated on a horizontal shaker at 80 rpm up to 240 h at 25°C. The kinetics of P released were assessed by analyzing water leachates collected at 0.25, 0.5, 1, 6, 12, 24, 48, 72, 120, and 240 hours. An aliquot of 2 mL of supernatant from each flask was collected and filtered (<0.45 μm) for the quantification of P concentration in the supernatant of each kinetics sampling time [30].

In the second kinetics method, Method B, OMFs and MAP were incubated with sand in a mini-lysimeter regularly leached with distilled water. Each mini-lysimeter

(Supplementary material 1) was prepared and filled from the bottom to its top as follows: In the lysimeter bottom, it was inserted a 0.45 μm pore filter; in another layer, in sequence, was packed 2 cm of glass wool over the filter; in layers, it was packed 20 g sand; 200 mg P fertilizer based on dry weight (inserted in the mini-lysimeter center); 20 g sand; and, finally, 2 cm of glass wool to eliminate the direct contact of water with sand, aiming to avoid preferential water flow in mini-lysimeters [37]. The sand and glass wool were pre-washed with hydrochloric acid, then repeatedly washed with distilled water. Initially, 50 ml of distilled water were passed through each experimental unit, setting the initial leaching time, 0 h; then, the incubated samples were periodically leached with water at 4, 8, 12, 24, 36, 48, 72, 120, 168 and 240 hours, in a water flow equivalent to 7 ml h^{-1}.

In both kinetics methods (A and B), the P concentration in leachates sampled was determined by the vanadomolybdate method [36]. In the kinetic of P release, the amount of P released was reported as the percentage of P in leachates over the total P total content in each fertilizer. In the leachates collected, electrical conductivity (EC) was determined in an EC Meter-Toledo bench meter, aiming to correlate EC with P content in the mass of fertilizer (g kg^{-1}) as proposed by Maluf et al. [16].

2.3 Spectroscopy analysis

ATR-FTIR analysis (attenuated total reflectance with Fourier transform infrared spectroscopy) was performed, and spectra were generated in the middle spectral range of 4000 to 650 cm^{-1}, with 2 cm^{-1} resolution, using an Agilent Cary 630 FTIR spectrometer. Identifying FTIR bands was performed based on group assignments described in Maluf et al. [16] and Stuart [38]. For each FTIR spectrum, a pre-processing step was performed aiming at correcting the baseline, as well as separating N and P chemical groups recorded in the fertilizer spectra. Thus,

a simultaneous normalization of the bands and peaks was performed to allow comparison among spectra and their peaks [38].

FTIR spectra and N and P groups were normalized in relation to the total area of N and P chemical groups bond peaks recorded in spectra for each fertilizer. In this direction, the relative peak area was calculated as follows (Eq. 3):

$$\text{N or P area (\%)} = \left(\frac{\text{Specific peak area of N or P } \left(\text{g kg}^{-1}\right)}{\text{Total peak area of N or P } \left(\text{g kg}^{-1}\right)} \right) \times 100 \qquad \text{(Eq. 3)}$$

Where specific peak areas for N is related to peaks features and areas between 3350-2650 or 1490-1340 cm^{-1}, while total peak area for N groups in spectra is assigned as the sum of peak areas of N chemical species and groups already mentioned, specific peak of P chemical species is the area recorded between 1340-1180, or 1180-1950, or 950-750 cm^{-1}. Total peak area for P chemical groups present in fertilizers is the sum of peak area of P compounds assegnded for the IR regions aforementioned.

2.4 Maize cultivation

Maize plants (hybrid Pioneer 30F53) were grown in greenhouse conditions for 36 days after sowing in two Oxisols with contrasting chemical and physicochemical properties (**Table 2**). In the Red Oxisol (RO) (*Dystrophic Red Latosol* [39]; *Typic Hapludox* [40]), soil samples were incubated for 30 days with $CaCO_3$ and $MgCO_3$ pure *per analysis reagents* (p.a.), respectively, at a 4:1 ratio to achieve a target soil pH of 6.2, as well as to increase in the soil the exchangeable Ca and Mg contents to allow plentiful maize growth. Soil carbonate solubilization for soil acidity correction was achieved by keeping soil moisture close to 60% of the maximum soil water-holding capacity (MWHC). In the Yellow Oxisol (YO) (*Dystrophic Yellow Latosol* [39]; *Typic Hapludox* [40]), pH and Ca^{2+} content were already at levels considered optimum for maximum maize growth; thus, liming was not performed, and 30 mg kg^{-1} of Mg was

provided to maize plants at the sowing fertilization. The limed soil samples were dried and passed through a 4 mm sieve for further analysis.

Table 2. Main chemical and physicochemical properties and texture of Oxisols used to cultivate maize.

Oxisol	pH	N-total	$N\text{-}NH_4^+$	$N\text{-}NO_3^-$	P	K	P-rem
		——————mg kg^{-1}——————			——mg kg^{-1}——		mg L^{-1}
Red	4.1	2,010	71.1	1.1	11.7	30.4	13.2
Yellow	6.0	329	4.1	-	6.1	2.5	11.7

Oxisol	Ca^{2+}	Mg^{2+}	Al^{3+}	C	Clay	Silt	Sand
	——————$cmol_c$ kg^{-1}——————			——————g kg^{-1}——————			
Red	0.3	0.1	1.1	24.0	625	95	280
Yellow	1.9	0.1	0.1	4.5	460	85	455

pH was determined in H_2O at a ratio of 1:2.5 (w/v); P: soil available P determined by the resin soil test~; available K determined by the Mehlich-1 soil test; P-rem: remaining phosphorous; Ca^{2+}, Mg^{2+} and Al^{3+} determined after the use of a1 mol^{-1} KCl as soil extractant; C: total C determined (dry combustion) in an automatic carbon analyzer; clay, silt and sand were determined by the Boyoucos method. All analytical protocols are described in details in Teixeira et al. [41] and Raij et al. [42].

Initially, 10 seeds were sown in a pot (diameter of 14 cm and height of 16 cm) filled with 1.8 kg of soil in each experimental unit, and after 7 days, the thinning was performed, leaving two maize plants per pot. In each Oxisol (RO and YO), six P treatments were tested, and a completely randomized design was adopted with three repetitions. The treatments tested were: four OMFs ($P^{25}O^{75}$, $P^{40}O^{60}$, $P^{50}O^{50,}$ and $P^{75}O^{25}$), the exclusive use of MAP as mineral N and P source, and control (no P added to the soil). When fertilizers were used, it was applied phosphorous (300 mg kg^{-1}) was homogeneously mixed with the whole soil in pots based on the P solubility of fertilizer in NAC+H_2O following the Brazilian legislation to recommend soluble MAP fertilizers [24].

The fertilizers investigated in this study had different N and K total contents; thus, N supplied as NH_4NO_3 and K as KCl were added complementarily to furnish the same amount of N and K added to the soil by OMFs, regardless of the nutrient source used in each treatment. In the standardization of N recommendation, the total amount of N applied was based on the amount suggested to compare OMFs with mineral N sources [12]. During maize sowing fertilization, it was provided to plants 120, 40, 0.8, 1.3, 3.7, 0.2, 4, and 1.6 mg kg^{-1}, respectively, of K, S, B, Cu, Mn, Mo, Zn, and Fe. Additionally, in YO, Mg was supplied to plants at 30 mg kg^{-1}. The top-dressing fertilization was carried out 20 days after maize planting by adding to soil 100 mg kg^{-1} N as NH_4NO_3. All nutrients were supplied to plants as *pure per analysis* reagents and according to the recommendation of nutrients for the plentiful growth of plants in pots [43].

One day after maize planting, an aliquot of 20 ml of soil solution was collected with the *Suolo Acqua*® sampler installed in the middle section of the pot [44]. Twelve hours before the soil solution sampling, soil water content was kept at 70% soil MWHC. Soil solution was collected between 07:00-09:00 a.m. and, in sequence, filtered (<0.45 μm). Soil solution samples were characterized for pH using a pH bench meter, and $N\text{-}NH_4^+$ and $N\text{-}NO_3^-$ contents through the distillation method followed by titration [35]. N-mineral content in soil solution (solution N-mineral) was determined by summing $N\text{-}NH_4^+$ and $N\text{-}NO_3^-$ contents in soil solution. Contents in the soil solution of P (solution P) and K (solution K) were determined in an inductively coupled plasma optical emission spectrometer (ICP-OES).

After the solution sampling, 30 g of the whole soil was collected, dried and passed through a 2 mm sieve for further analysis. In the whole soil, pH was determined in water at a ratio of 1:2.5 (w/v) (soil pH) [41], $N\text{-}NH_4^+$ and $N\text{-}NO_3^-$ were determined by the distillation method followed by titration (soil N-mineral) after extraction of soil mineral N with a 1 mol L^{-1} KCl solution (10 mL extractor solution: 1 g soil) [35, 41]. Available contents of K were

determined by flame photometry after extraction of K using the Mehlich-1 soil test (soil K) [41], and soil available P was determined using the resin soil test (soil P-resin)[42].

At the end of the experiment (36 days after planting), the threshold period from which conduction would be limited by pot size, plants were harvested and separated into shoot and root, then dried in a laboratory oven at 60º C until constant weight.Thus, shoot (SDM) and root (RDM) dry matter were determined, and total dry matter production (TDM) was calculated as the sum of SDM and RDM. N content in maize shoot was determined by the Kjeldahl method after the sulfuric acid digestion of plant tissues. P and K contents were determined in an ICP-OES machine after the digestion of plants in a nitric-perchloric acid solution (ratio of 4:1)[45]. The N, P and K accumulated in the shoot were calculated as Eq. 4. After the maize cultivation, the residual effect of fertilization was evaluated by sampling soil solution and, again, the whole soil, following the same protocols and analytical procedures aforementioned for determination of nutrients in the soil solution and the whole phase collected at the beginning of maize cultivation (one day after maize sowing).

Nutrient accumulated (mg pot^{-1})=SDM (g pot^{-1})×nutrient content in shoot (mg g^{-1}) (Eq. 4)

2.5 Mineralization and release of N, P, and K in OMF-Oxisols mixtures

As references the amounts of OMFs and MAP added to soils for maize fertilization, mineralization of N and P and K from OMFs, and nutrients released from MAP incubated in the two contrasting Oxisols were determined. In the kinetics study, the same statistical design and environmental conditions adopted for the maize cultivation experiment were used to set up the kinetics experiment. Fertilizers were mixed with 50 g soil and 50 g sand (pre-washed with hydrochloric acid, followed by distilled water washing). Excluding the amount of N added to soil, the amounts of all nutrients were standardized according to levels previously used to fertilize maize plants grown in pots. The amount of N was not standardized; thus, N

mineralization from soil or OMFs was correctly evaluated. The soil+sand mixed with fertilizer samples were incubated for 36 days in a mini-lysimeter **(Supplementary material 2)**. During the incubation, the sand-fertilizer mixtures kept their moisture kept at 60% MWHC.

At 1, 4, 8, 12, 20, and 36 days of incubation, the leaching phase was performed using 100 ml of 0.01 mol L^{-1} $CaCl_2$ solution [46]. The leached volume of each experimental unit and time were measured, then leachates were filtered (< 0.45 μm) and, in sequence, N-NH_4^+ and N-NO_3^- contents were determined by the distillation method followed by the titration of N evolved from samples an ammonia [35]. P and K contents in leachates were determined in an ICP-OES machine. The N mineralized and, P, and K leached were calculated as Eq. 5, and accumulated amounts of N, P, and K leached were related to the soil mass incubated and depicted as a function of incubation time.

$$\text{Nutrient leached}\left(\text{mg kg}^{-1}\right)=\left(\frac{\text{Leached volume}\left(\text{mg kg}^{-1}\right)\times\text{nutrient content in leachate}\left(\text{mg L}^{-1}\right)}{\text{Soil amount in each experimental unit (Kg)}}\right) \quad \text{(Eq. 5)}$$

2.6 Statistical analysis

All statistical analysis was carried out using the R software through the stats, base, tidyverse agricolae, corrplot, factoextra, FactoMineR, nlstools, and Metrics packages [47–54]. The dataset of fertilizer properties and maize traits were subjected to analysis of variance, and when significant differences were verified (p<0.05), the treatment means were compared by the Duncan test (p<0.05). The Pearson correlation analysis was performed to verify the relationship between N forms and P-fertilizer solubility indices with the FTIR spectra normalized dataset. Mathematical models were adjusted to the P release dataset as a function of EC for the two kinetics methods investigated. The principal component analysis (PCA) was performed to evaluate the relationship between nutrient availability (sampled at the sowing phase) in soil and solution, N, P, and K accumulated in the shoot, SDM, RDM and TDM, and N and P forms supplied to maize by fertilizers. The Pearson correlation analysis was also

performed to verify the statistical significance of variables used as inputs and the cluster shown in the PCA diagram.

The dataset of the kinetic of P release and NPK mineralization/release studies were adjusted to different non-linear mathematical models as an output of the relationship between incubation time versus the amount of nutrient released or mineralized from each fertilizer [30, 55, 56]. The mathematical models adjusted to the kinetics of the nutrients release dataset were the Elovich model (Eq. 6), the simple exponential model (Eq. 7), the power function model (Eq. 8), and the hyperbolic model (Eq. 9).

$$Pt=a+b\ln t \quad \text{(Eq. 6)}$$

$$Pt=N0\left(1-e^{-kt}\right) \quad \text{(Eq. 7)}$$

$$Pt=a*t^{b} \quad \text{(Eq. 8)}$$

$$Pt=\frac{N0*t}{(N0*b+t)} \quad \text{(Eq. 9)}$$

Where Nt: fraction of nutrient released or leached in time-analyzed; a, the initial nutrient released or leached; b, nutrient released or leached constant rate, t, time of nutrient release or mineralization/leaching; N0, the maximum amount of nutrient released or leached over sampling time. The selection of the model that best fitted to dataset was performed based on the highest value of the coefficient of determination (R^2), the lowest value of root-mean-square error (rmse), and lowest value of the Akaike Information Criterion (AIC) [57]. Mathematical models generated for each fertilizer with its nutrient dynamics evaluated were compared by adopting a 95% bootstrap confidence interval, using 1000 bootstrap interactions.

3 Results

3.1 OMFs and MAP characterization

Chemical properties and NPK availability indices of OMFs and MAP were described in **Table 3**. Mixing of organic residues (CM and CH) with MAP increased organic over mineral N content and forms in OMFs over MAP. Mineral N related according to total N content increased by MAP over OMFs, and between OMFs, $P^{25}O^{75}$ had lower proportions of mineral N over other OMFs. As the proportions of organic residues in OMFs increased, the fertilizer-P water index diminished for $P^{25}O^{75}$, $P^{40}O^{60}$ and $P^{50}O^{50}$ compared to MAP. The fertilizer P-CA index increased as follows: MAP > $P^{75}O^{25}$ > $P^{25}O^{75}$ > $P^{50}O^{50}$ = $P^{40}O^{60}$, while the fertilizer P-NAC+H_2O index follows this sequence: $P^{40}O^{60}$ < $P^{50}O^{50}$ < $P^{25}O^{75}$ < $P^{75}O^{25}$ = MAP.

Table 3. Nutrient contents, pools and P availability indices of organomineral fertilizers (OMF) and MAP.

Fertilizer	pH ($CaCl_2$)	N (g kg^{-1})			K (g kg^{-1})*
		Total*	N-NH_4^+	N-Organic	
$P^{25}O^{75}$	5.92 ± 0.05	51.3 ±1.2	31.3 ±0.8	20.0 ±1.0	32.3 ± 1.6
$P^{40}O^{60}$	5.59 ± 0.06	69.8 ±1.0	54.0 ±2.3	15.8 ±1.3	24.1 ± 0.3
$P^{50}O^{50}$	4.94 ± 0.01	76.0 ±1.1	62.3 ±1.1	13.7 ±1.9	19.9 ± 0.8
$P^{75}O^{25}$	4.43 ± 0.01	97.2 ±1.2	82.9 ±0.9	14.3 ±2.1	7.5 ± 0.1
MAP	3.86 ± 0.01	113.7 ±2.1	113.4 ±1.8	0.0 ± 0.1	0.0 ± 0.0

Fertilizer	P (g kg^{-1})			
	Total	Water	Citric acid	NAC+H_2O
$P^{25}O^{75}$	97.0 ±1.0	47.9 ±0.9	64.6 ±3.1	81.5 ±0.5
$P^{40}O^{60}$	173.4 ±1.0	90.0 ±1.6	96.3 ±0.4	116.6 ±0.6
$P^{50}O^{50}$	178.4 ±2.1	108.9 ±2.8	104.7 ±2.7	127.6 ±1.9
$P^{75}O^{25}$	186.5 ±1.3	169.3 ±1.9	149.0 ±3.8	183.3 ±1.2
MAP	236.7 ±1.1	225.8 ±0.6	223.1 ±0.4	233.6 ±1.5

Fertilizer	N-index (%)		P index (%)		
	Mineral	Organic	H_2O	Citric acid	NAC+H_2O
$P^{25}O^{75}$	61.0 ±1.4 D	39.0 ±1.4 A	49.4 ±1.1 D	66.7 ±3.4 C	84.0 ±0.8 B
$P^{40}O^{60}$	77.2 ±2.2 C	22.8 ±2.2 B	50.1 ±0.7 D	55.6 ±0.2 D	67.3 ±0.6 D
$P^{50}O^{50}$	82.0 ±2.3 BC	18.0 ±2.3 BC	61.0 ±1.6 C	58.7 ±2.0 D	71.5 ±1.9 C
$P^{75}O^{25}$	85.4 ±2.0 B	14.6 ±2.0 C	90.8 ±0.6 B	79.9 ±2.5 B	98.3 ±0.6 A
MAP	99.8 ±0.1 A	0.0 ±0.1 D	95.4 ±0.7 A	94.3 ±0.6 A	98.7 ±1.1 A

*Modified from Maluf et al. [16]. Means with standard error followed by the same letter in each column are not different by the Duncan test ($p<0.05$). Organomineral fertilizers ($P^{25}O^{75}$, $P^{40}O^{60}$, $P^{50}O^{50}$ and $P^{75}O^{25}$) were produced from the mixture of different proportions of coffee husk, chicken manure, and monoammonium phosphate (MAP).

3.2 Kinetics of fertilizer P release in water

Considering the lower values of rmse and AIC combined with higher values of R^2 to evaluate the mathematical models that best fitted the P released dataset, for the kinetics method A, the Elovich model (**Supplementary material 3**) was the one that best fitted the dataset. For

kinetics method B, the power model was the one that best adjusted to the P-released dataset. The fertilizer with higher total P content released a greater amount of P soluble in water over the mass of fertilizer for both methods A and B used to study the kinetics of P release (**Supplementary material 4)**. The P released according to fertilizer mass over time was accurately predicted using the leachate EC (**Fig. 1**).

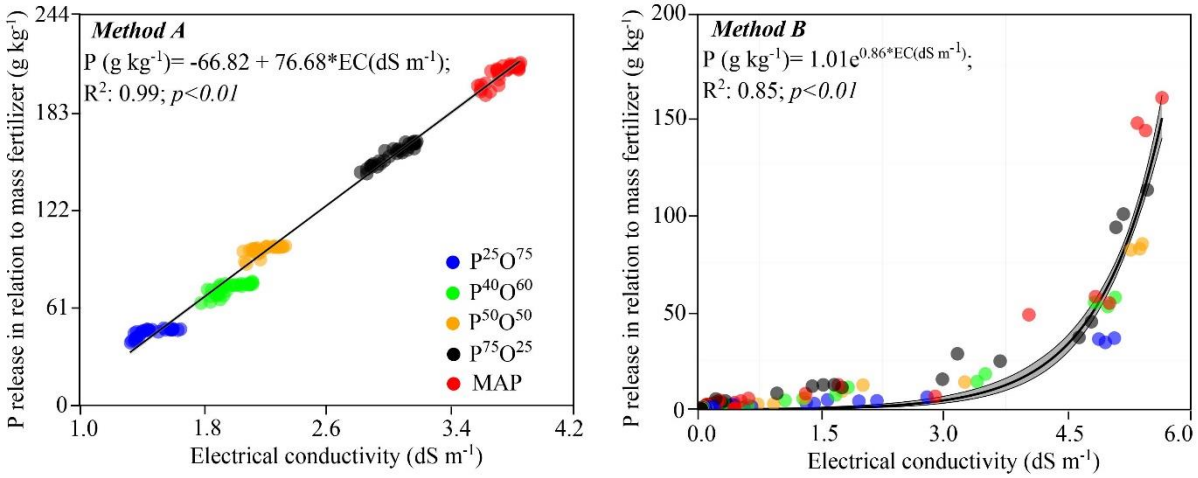

Figure 1. Relation of P release in the kinetics of P release and electrical conductivity (EC) from organomineral and monoammonium phosphates (MAP) fertilizers.

When P released was calculated as a function of total P content in OMFs and MAP, the adequate method to cluster the different sources of P with different total P content was the kinetics Method A. The initial and final amount of P released was higher for MAP than OMFs, following this decreasing order of P release: $P^{75}O^{25} > P^{50}O^{50} > P^{25}O^{75} > P^{40}O^{60}$ (**Fig. 2**). When kinetics method B was used, $P^{75}O^{25}$ over MAP had a lower initial released of P, though after 12 hours, OMF samples had a similar P release pattern up to the sampling time of 240 hours (**Fig. 2**). $P^{40}O^{60}$ had a lower P release than $P^{25}O^{75}$, though, in the range of 4 to 8 hours, the P release of both OMFs was similar, after 8 hours, the $P^{40}O^{60}$ was the OMF with the lower P release rate. In both methods A and B, the b parameter allowed to infer the P release constant rate, showing that the $P^{75}O^{25}$ had a lower release rate constant over MAP, $P^{50}O^{50}$ was higher

over MAP, and $P^{25}O^{75}$ and $P^{40}O^{60}$ did not differ in relation to MAP (**Supplementary material 5**). Using method A, the EC of leachates increased over the incubation time of both OMFs and MAP (**Supplementary material 6**), though, for method B, the EC of leachates decreased as the incubation evolved (**Supplementary material 7**).

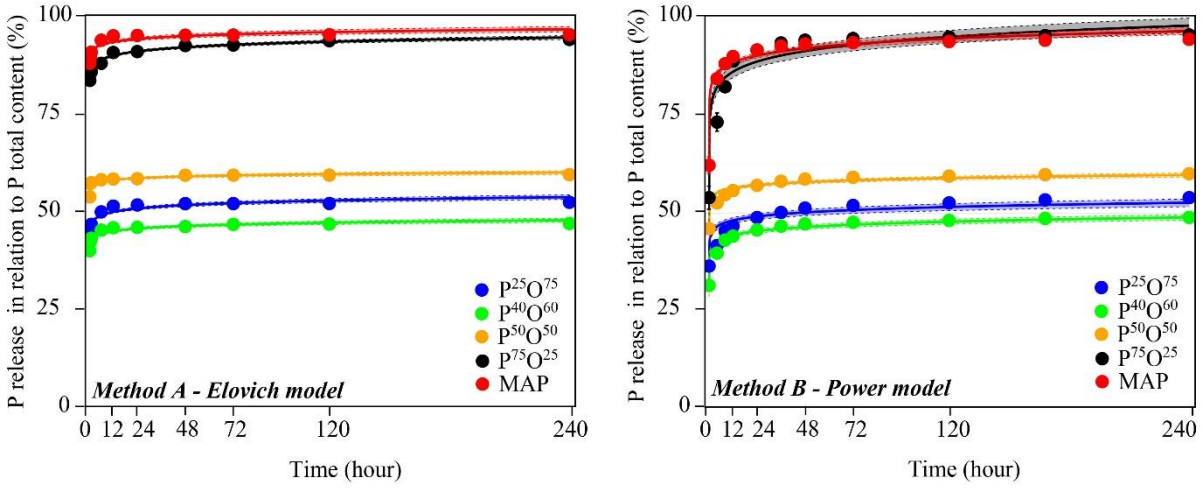

Figure 2. Kinetics of P release of organomineral fertilizers ($P^{25}O^{75}$, $P^{40}O^{60}$, $P^{50}O^{50,}$ and $P^{75}O^{25}$) and monoammonium phosphate (MAP) as related to methods used in the evaluated.

3.3 Infrared spectroscopy and correlation analysis

FTIR analysis revealed that the prominent N peaks were assigned as N-H bonds recorded between 3350 and 2650 cm^{-1} ($N\text{-}H^{3350\text{-}2650}$), whose areas increased in spectra as the proportion of organic residues over MAP increased in OMFs. N bonds between 1490 and 1340 cm^{-1} ($N\text{-}H^{1490\text{-}1340}$) were favored due to the increased MAP proportions in OMFs (**Fig. 3**). FTIR bonds recorded in the region between 3350 and 2650 cm^{-1} were assigned to N in the form of organic groups, while those between 1490 and 1340 cm^{-1} regions were used to characterize N in mineral forms in fertilizers.

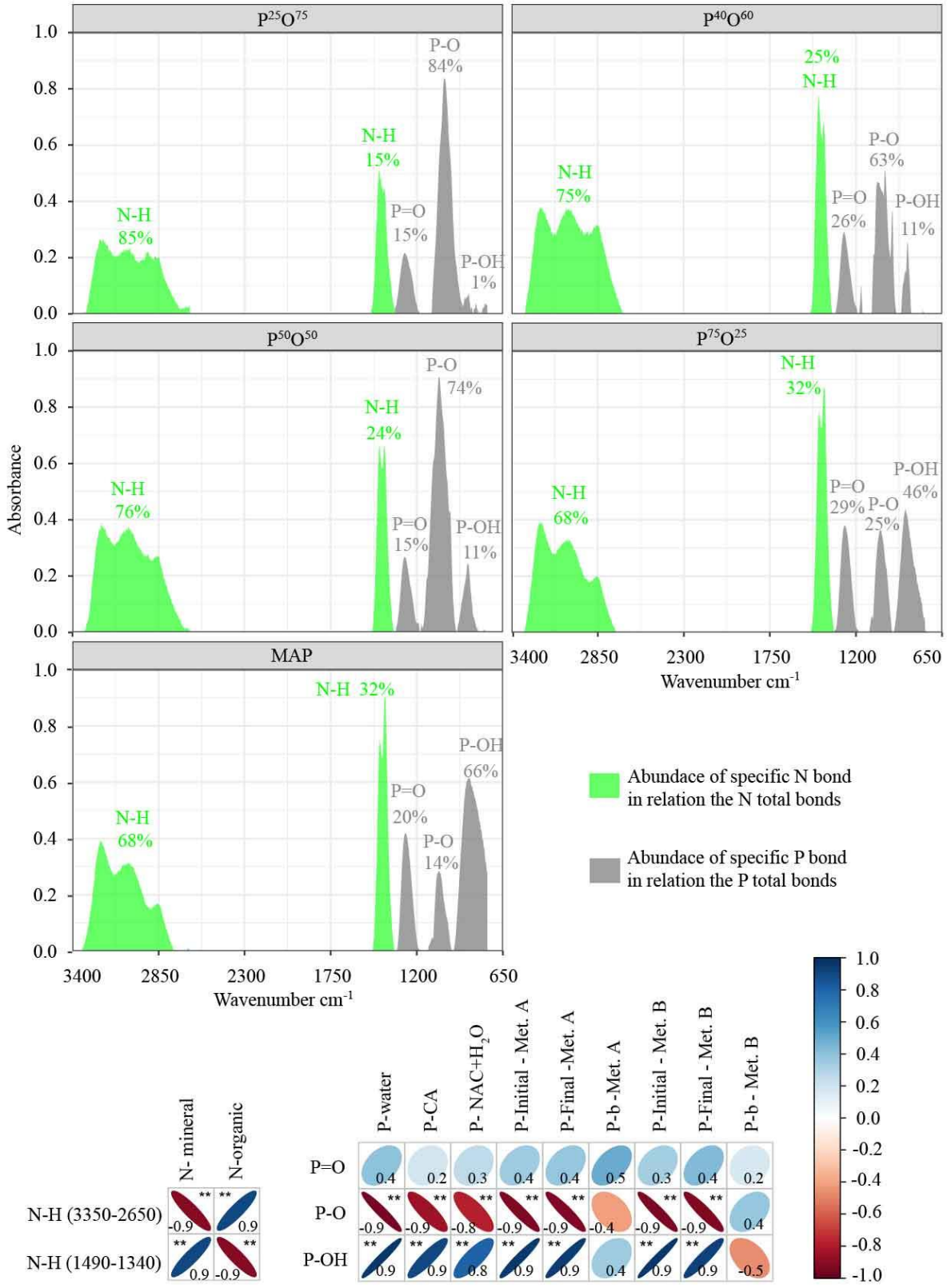

Figure 3. Absorption peaks areas and P and N chemical groups recorded in FTIR spectrum after pre-processing for each OMFs ($P^{25}O^{75}$, $P^{40}O^{60}$, $P^{50}O^{50,}$ and $P^{75}O^{25}$) and monoammonium phosphate (MAP) and correlation analysis between N and P groups and chemical forms **: significant correlation (p<0.01). P-water, P-CA, and P-NAC+H2O: P solubility index in water,

in citric acid at 2%, and in neutral ammonium citrate solution plus water, respectively; P-initial - Met. A, P-final – Met. A, P-b – Met. A: initial, final and constant rate release from kinetic of P release, respectively, according to method A; P-initial - Met. B, P-final – Met. B P-b – Met. B: initial, final and constant rate release from kinetic of P release, respectively, according to method B.

Phosphorus FTIR P group peaks were mainly recorded for regions between 1340-1180, 1180-950, and 950-750 cm^{-1}, which are assigned to P=O, P-O, and P-OH bonds, respectively (**Fig. 3**). Regarding P total area in FTIR spectrum, a decreased of P-O and an increased of P-OH bonds area related to the enrichment of OMFs with MAP (over organic residues in the composting mixtures), compared to the analysis of pure MAP. The P=O area bonds did not follow the same trend for P-OH, considering that the highest percentage area was recorded for P chemical species for $P^{75}O^{25}$. Fertilizer-P availability indices, such as P in water, CA, and NAC+H_2O, and initial and final P released by OMFs and MAP were positively correlated with P-OH chemical groups and negatively related to P-O chemical groups (**Fig. 3**). Constant rate of P release had no relationship with P chemical groups identified by FTIR spectroscopy analysis.

3.4 Maize cultivation and soil properties

3.4.1 N and P forms used in maize fertilization

Fixing the amount of P added to soil based on fertilizer-NAC+H_2O solubility and total N content in OMFs, the OMFs with higher proportions of MAP increased the amount applied of fertilizer-P soluble in H_2O, as well as N-mineral forms, and reduced the organic N amounts added to the soil (**Table 4**). Due to the lower proportion of P soluble in NAC+H_2O according to total P content, the highest amount of P applied per pot was reported for the $P^{40}O^{60}$ and $P^{50}O^{50}$ sources. The amount of P soluble in CA added in each pot was higher for MAP than OMFs.

Table 4. Amounts of P and N supplied by organomineral fertilizers ($P^{25}O^{75}$, $P^{40}O^{60}$, $P^{50}O^{50}$ and $P^{75}O^{25}$) and monoammonium phosphate (MAP) to maize grown in Oxisols.

Fertilizer	N (mg pot^{-1})		P (mg pot^{-1})		
	Mineral	Organic	Total	Water	Citric acid
$P^{25}O^{75}$	387.5 ±5.7 D	137.6 ±5.7 A	642.8 ±6.1 C	317.2 ±4.4 D	428.2 ±18.6 B
$P^{40}O^{60}$	432.2 ±9.1 C	92.8 ±9.1 B	803.0 ±7.4 A	402.5 ±6.8 C	446.2 ±4.2 B
$P^{50}O^{50}$	466.8 ±9.0 B	58.3 ±9.0 C	755.8 ±19.9 B	461.2 ±14.7 B	443.1 ±9.7 B
$P^{75}O^{25}$	483.0 ±6.2 B	42.1 ±6.2 C	549.3 ±3.5 D	498.6 ±3.0 A	438.9 ±11.9 B
MAP	525.0 ± 0.4 A	0.0 ±0.4 D	547.2 ±5.9 D	522.0 ±2.5 A	515.7 ±2.3 A

Means followed by the same letter in each column did not differ by the Duncan test ($p<0.05$).

3.4.2 Soil solution

OMFs affected soil solution properties in a soil type-dependent way (**Fig. 4**). Compared to MAP, in RO, the initial solution pH increased in response to the addition of $P^{25}O^{75}$, while mineral N forms were similar for $P^{75}O^{25}$, though they reduced following this order: $P^{50}O^{50}$ = no-P fertilization > $P^{40}O^{60}$ > $P^{25}O^{75}$. Initial solution P content in RO was reduced by about 40% for all OMFs compared to MAP. Soil solution initial K content was not affected by the sources or nutrients investigated. In YO, initial solution pH was lower for control (no-P added to the soil) and $P^{75}O^{25}$ over MAP (**Fig. 4**). Solution initial mineral N contents in YO was greater for $P^{50}O^{50}$ (+28%) and $P^{75}O^{25}$ (+44%) over MAP, lower for $P^{25}O^{75}$ (-40%) over MAP, and similar to $P^{40}O^{60}$. In YO, the content of initial solution P was similar for $P^{50}O^{50}$ and MAP, while the other OMFs had P in soil solution lower than MAP, a reduction of about 57%. Initial solution K was greater (66%) for $P^{75}O^{25}$ over MAP and similar to $P^{25}O^{75}$, $P^{40}O^{60}$, and $P^{50}O^{50}$, compared to MAP.

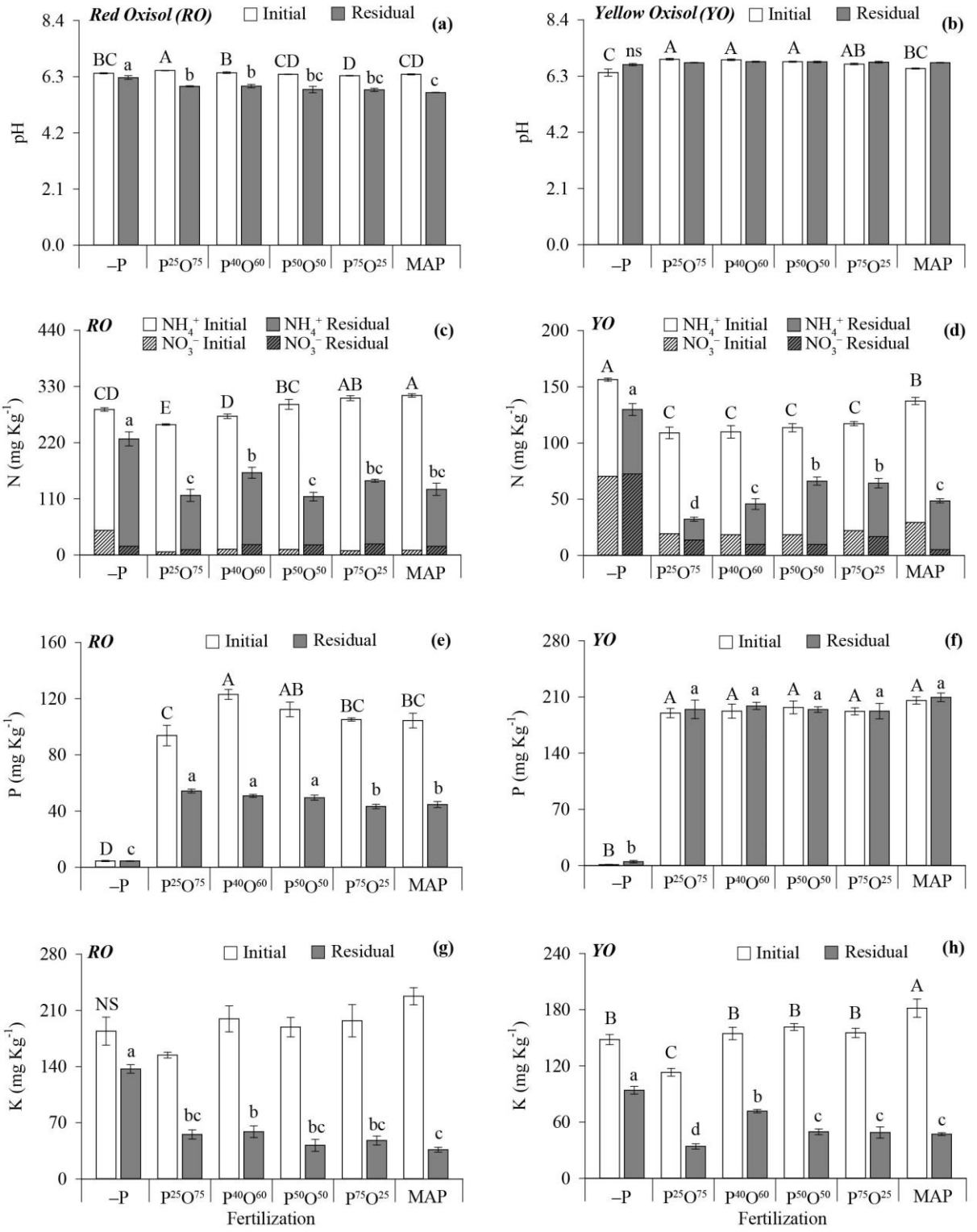

Figure 4. Initial and residual soil solution pH (a, b) and contents of N (c, d), P (e, f) and K (g, h) as a function of organomineral fertilizers ($P^{25}O^{75}$, $P^{40}O^{60}$, $P^{50}O^{50}$ and $P^{75}O^{25}$) and monoammonium phosphate (MAP) used to nourish maize grown in contrasting Oxisols. Bars with standard error followed by the same uppercase or minuscule letters did not differ, respectively, regarding initial and residual pH and attributes compared by the Duncan test ($p<0.05$). NS or ns: not significant by the Anova F-test ($p>0.05$). –P: no-P fertilization.

After the maize cultivation, soil solution pH was higher for all OMFs compared to MAP in RO (**Fig. 4**). Residual solution mineral N verified after maize cultivation (N residual) was similar among fertilizers (OMFs and MAP) and lower for fertilizers over control (no P added). No residual solution P (solution content after maize cultivation) was verified for control, $P^{75}O^{25}$, and MAP. In RO, residual P in the solution was ranked in the following order: $P^{40}O^{60} > P^{50}O^{50} > P^{25}O^{75}$. A higher residual solution K (K verified after maize cultivation) contents were verified for control (no-P), and only $P^{40}O^{60}$ increased solution K over MAP. In YO, solution pH after maize cultivation was not affected by using OMFs and MAP. Residual solution N-mineral and available K were higher when P was not added to soils (control) compared to P-fertilized soils. Compared to MAP, residual solution mineral N in YO was higher of about 69% for $P^{50}O^{50}$ over MAP, and lower for $P^{25}O^{75}$ and $P^{40}O^{60}$, over MAP, a reduction of 83%. At least in the YO solution, the residual effect of P was not verified for OMFs and MAP used to fertilize maize plants.

3.4.3 Whole soil properties

Initial pH in RO increased to $P^{25}O^{75}$ and $P^{40}O^{60}$ over MAP and to the addition of $P^{25}O^{75}$, $P^{40}O^{60,}$ and $P^{50}O^{50}$ to YO (**Fig. 5**). In RO, compared to MAP, $P^{75}O^{25}$ had similar mineral N contents, and the use of $P^{50}O^{50}$, $P^{40}O^{60,}$ and $P^{25}O^{75}$ in RO reduced the mineral N of about 18, 13 and 6% respectively for $P^{50}O^{50}$, $P^{40}O^{60,}$ and $P^{25}O^{75}$ compared to MAP as a source of N to maize. $P^{40}O^{60}$ treated RO soil had a greater initial P-resin level than MAP-treated samples with an increase of 18%; for the other OMFs, soil P-resin contents were similar to MAP. Initial soil K was not affected by OMF and MAP applied to RO. In YO, all OMFs reduced the initial solution mineral N compared to MAP, with an average reduction of 18%. Initial soil P-resin increased in response to P fertilization over control. All OMFs reduced the initial soil K over MAP, with lower available K contents verified for soils treated with $P^{25}O^{75}$, a reduction of 38%.

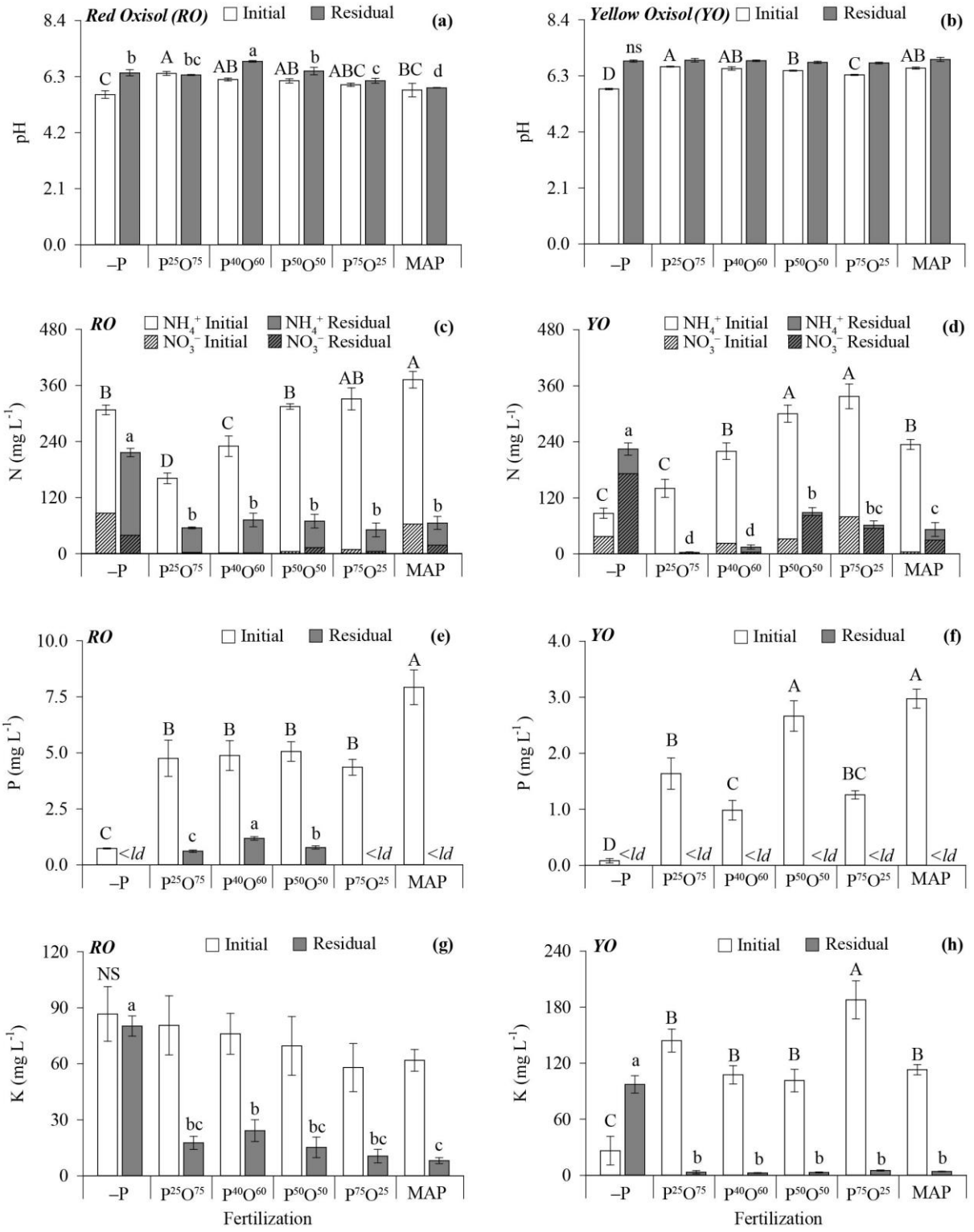

Figure 5. Initial and residual whole soil pH (a, b) and available contents of N (c, d), P (e, f) and K (g, h) as affected by organomineral ($P^{25}O^{75}$, $P^{40}O^{60}$, $P^{50}O^{50}$ and $P^{75}O^{25}$) and monoammonium phosphate (MAP) fertilization for maize cultivated in contrasting Oxisols. Bars with standard error followed by the same uppercase or minuscule letters did not differ, respectively, regarding initial and residual pH and attributes compared by the Duncan test (p<0.05). NS or ns: not significant by the Anova F-test (p>0.05). –P: no-P fertilization.

At the end of maize cultivation, in RO, pH was greater for control (no-P addition), $P^{25}O^{75}$ and $P^{40}O^{60}$ over MAP, while in YO soil pH after maize cultivation was not affected by P sources investigated (**Fig. 5**). Residual soil N-mineral verified after maize cultivation was higher in control (no P) over P-fertilized soils; however, OMFs did not differ over MAP regarding soil residual P. In RO, $P^{25}O^{75}$, $P^{40}O^{60}$, and $P^{50}O^{50}$ increased about 15% of the residual soil P after maize cultivation over MAP; however, in YO, the availability of P did not differ for OMFs and MAP. After maize cultivation, a higher residual soil K was verified when P was not added to both Oxisols. $P^{40}O^{60}$ increased of about 57% residual soil K over MAP in both Oxisols, while $P^{25}O^{75}$ decreased residual soil K in RO, a reduction of 28%.

3.4.4 Maize nutritional status and growth

No-P fertilization reduced the biomass production, and N, P, and K accumulated in the shoot of maize plants grown in both Oxisols (**Fig. 6**). Among P fertilizers, the OMFs effects on maize growth relied on the Oxisol type. In RO, the SDM, RDM, and TDM reduced in response to the use of $P^{25}O^{75}$ to fertilize maize, a reduction of 20, 13, and 10%, respectively for SDM, RDM, and TDM; while $P^{40}O^{60}$ and $P^{50}O^{50}$ increased SDM and TDM of about 20 and 40% respectively compared to MAP. In YO, $P^{25}O^{75}$ and $P^{40}O^{60}$ increased RDM and TDM over MAP an average of about 118 and 53%, respectively, while SDM only increased in $P^{25}O^{75}$-treated soil, with an increase of 26%. Compared to MAP, N in shoot increased in response to $P^{40}O^{60}$, $P^{50}O^{50,}$ and $P^{75}O^{25}$ with an increment of about 29%, and P and K in shoot relied on the use of $P^{40}O^{60}$ and $P^{50}O^{50}$ with an average increment of the two OMFs of 48 and 52% for P and K, respectively. In YO, P in the shoot reduced when plants were fertilized with $P^{75}O^{25}$ (reduction of 23%). However, the P accumulated in the shoot by OMFs did not differ in relation to MAP-treated plants. N and K accumulated in the shoot of maize grown in YO did not show any statistical differences between OMFs and MAP-fertilized plants.

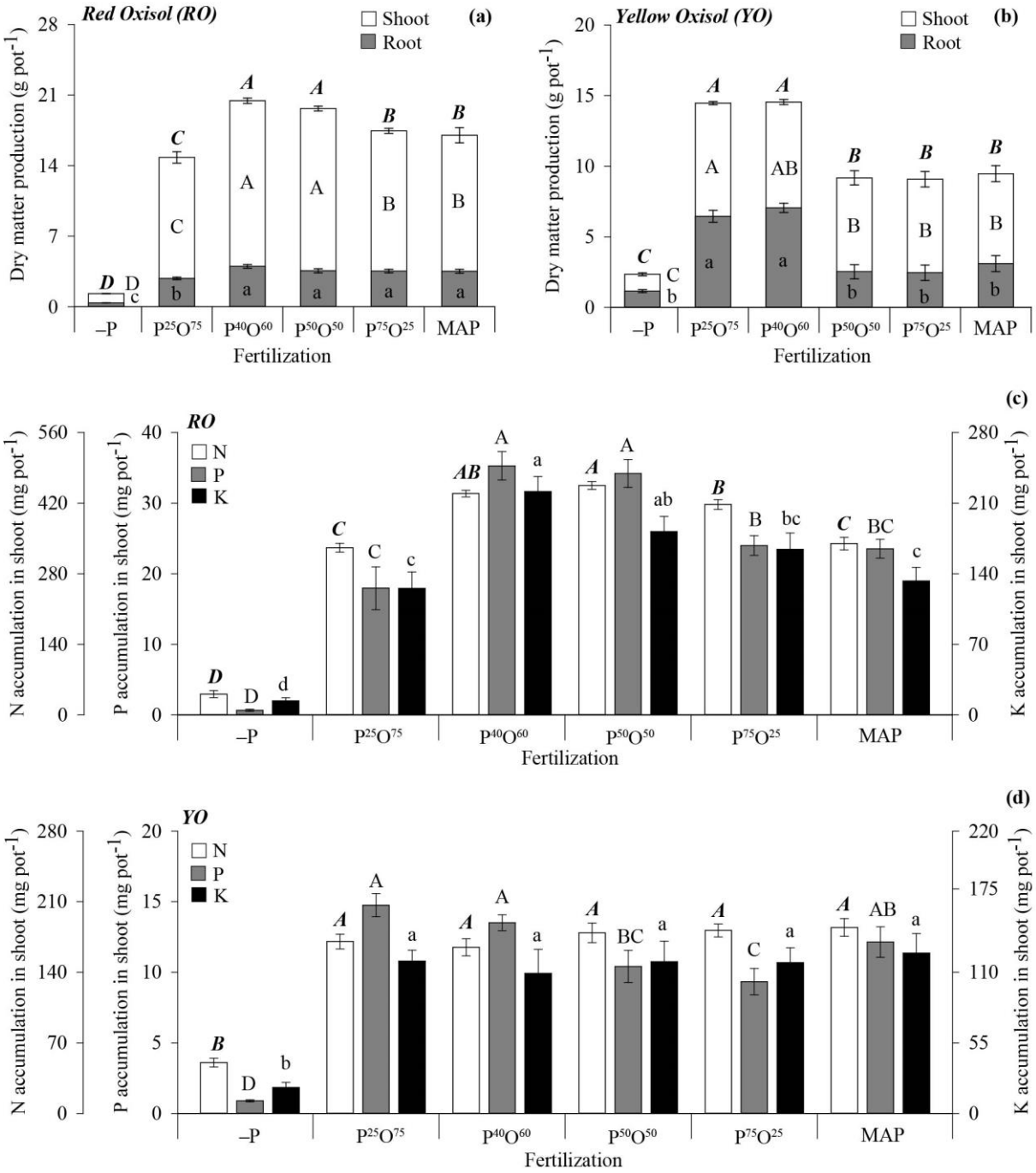

Figure 6. Total (TDM) (full bar), shoot (SDM) and root (RDM) dry matter production (a, b) and N, P and K accumulated (c, d) in shoot according to organomineral ($P^{25}O^{75}$, $P^{40}O^{60}$, $P^{50}O^{50}$ and $P^{75}O^{25}$) and monoammonium phosphate (MAP) fertilization for maize cultive in contrasting Oxisols. Bars with standard error followed by same italic-bold-uppercase or uppercase or minuscule letter not differentiate, respectively the TDM, SDM and RDM in dry matter production of N, P and K accumulation in the shoot by Duncan test ($p<0.05$). –P: no-P fertilization.

3.4.5 Principal component analysis

The variation explained by PCA in RO was 74.5% (PC1+PC2) and in YO was 62.9% (PC1+PC2) (**Fig. 7**). In both Oxisols, the increase of N-mineral forms applied via fertilizers increased the solution N-mineral, as well as the whole soil mineral N contents, which was confirmed by Pearson correlation analysis (p<0.05) (**Supplementary material 8 and 9**). In pots, the increase of fertilizer-P water or CA availability indices increased P in RO solution, though P in soil solution was only correlated with the amount of fertilizer-P CA index (p<0.05). The total P added to RO positively related to soil P-resin and biomass production (TDM, SDM, and RDM), besides controlling N, P, and K accumulated in the shoot, mirroring the Pearson correlation analysis (p<0.05). Soil pH of both Oxisols and solution pH of RO was positively correlated with the organic N amount added to the soil (p<0.05) (**Supplementary material 8**). In YO, soil P-resin and solution P were not related to the amount of total P or P soluble in water added to soil; however, solution P was regulated by the fertilizer-P-solubility CA index (p<0.05). The Reduction of P soluble in water in fertilizers increased maize biomass production (TDM, SDM, and RDM), and P accumulated in the shoot of plants grown in YO. In YO, whole soil and solution K contents and K in maize shoot were slightly explained by variables depicted in the PCA diagrams.

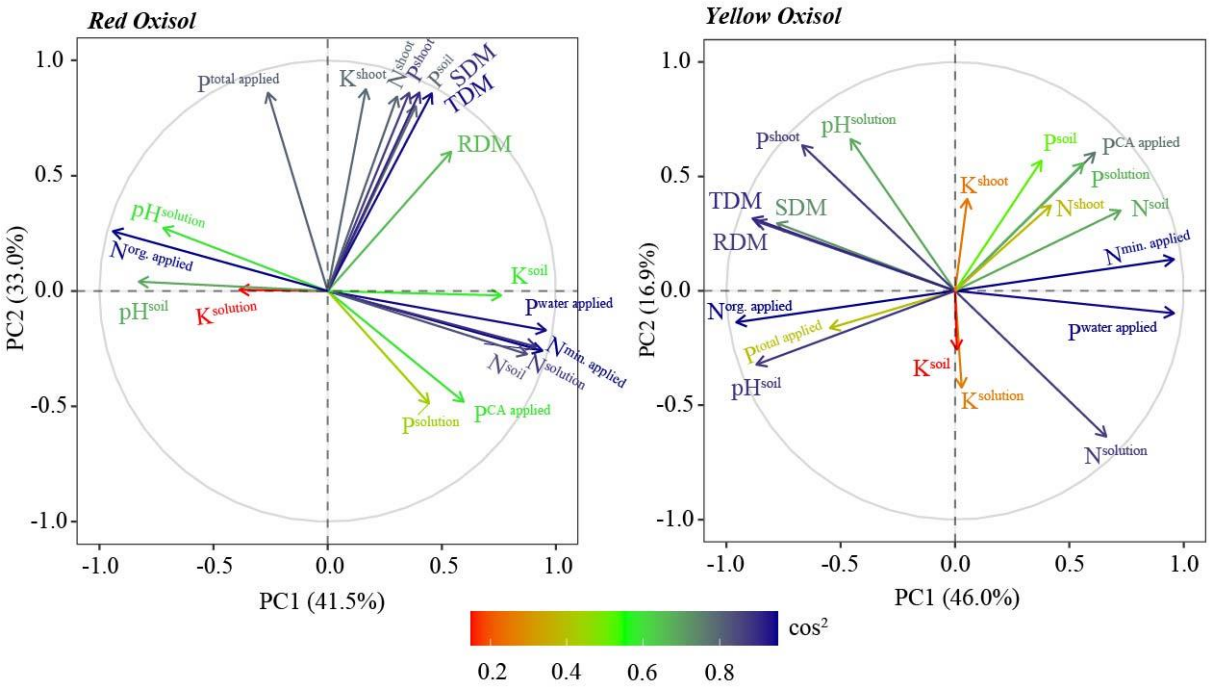

Figure 7. Principal component analysis by maize growing in contrasting Oxisols. $N^{solution}$, $P^{solution}$ and $K^{solution}$: soil solution contents of N-mineral, P and K respectively; $pH^{solution}$: pH in soil solution; N^{soil}, P^{soil} and K^{soil}: soil availability of N, P and K respectively; pH^{soil}: pH in soil; TDM, SDM and RDM: total, shoot and root dry matter production respectively; N^{shoot}, P^{shoot} and K^{shoot}: Shoot accumulation of N, P and K respectively; $N^{min.\ applied}$ and $N^{org.\ applied}$: N-mineral and N-organic forms applied added in soil though fertilizers respectively; $P^{water\ applied}$, $P^{CA\ applied}$ and $P^{total\ applied}$: Amounts of P added in soil though fertilizers based on solubility in water, and citric acid at2 % and total P contents respectively.

3.5 Mineralization and release of NPK from OMFs incubated in Oxisols

Mathematical models adjusted to mineralized N and kinetics models for P and K released over time for fertilizers incubated in Oxisols were chosen based on the highest values of R^2, and lowest values of rmse and AIC (**Supplementary materials 10 and 11**). N mineralized, P and K leached in RO, and N mineralized and P leached in YO were best fitted to the hyperbolic model. K released in YO was best fitted to the Elovich model (**Fig. 8**). In RO, initial and final mineralized N contents followed this order: $P^{50}O^{50}$ > MAP > $P^{75}O^{25}$ = $P^{25}O^{75}$ = $P^{40}O^{60}$, while the N mineralization rate constant did not differ among OMFs and MAP (**Supplementary material 12**). However, among OMFs, $P^{50}O^{50}$ was characterized by the

lowest N mineralization constant rate in RO (**Supplementary material 12**). Amounts of P released in RO presented the following order: MAP > $P^{40}O^{60}$ > $P^{75}O^{25}$ = $P^{25}O^{75}$ > $P^{50}O^{50}$, while $P^{50}O^{50}$ had a lower P leaching rate constant than MAP. $P^{25}O^{75}$ released a greater K content over other fertilizer sources added to RO. K release constant rate in RO did not differ among fertilizers and control (no-P added to the soil).

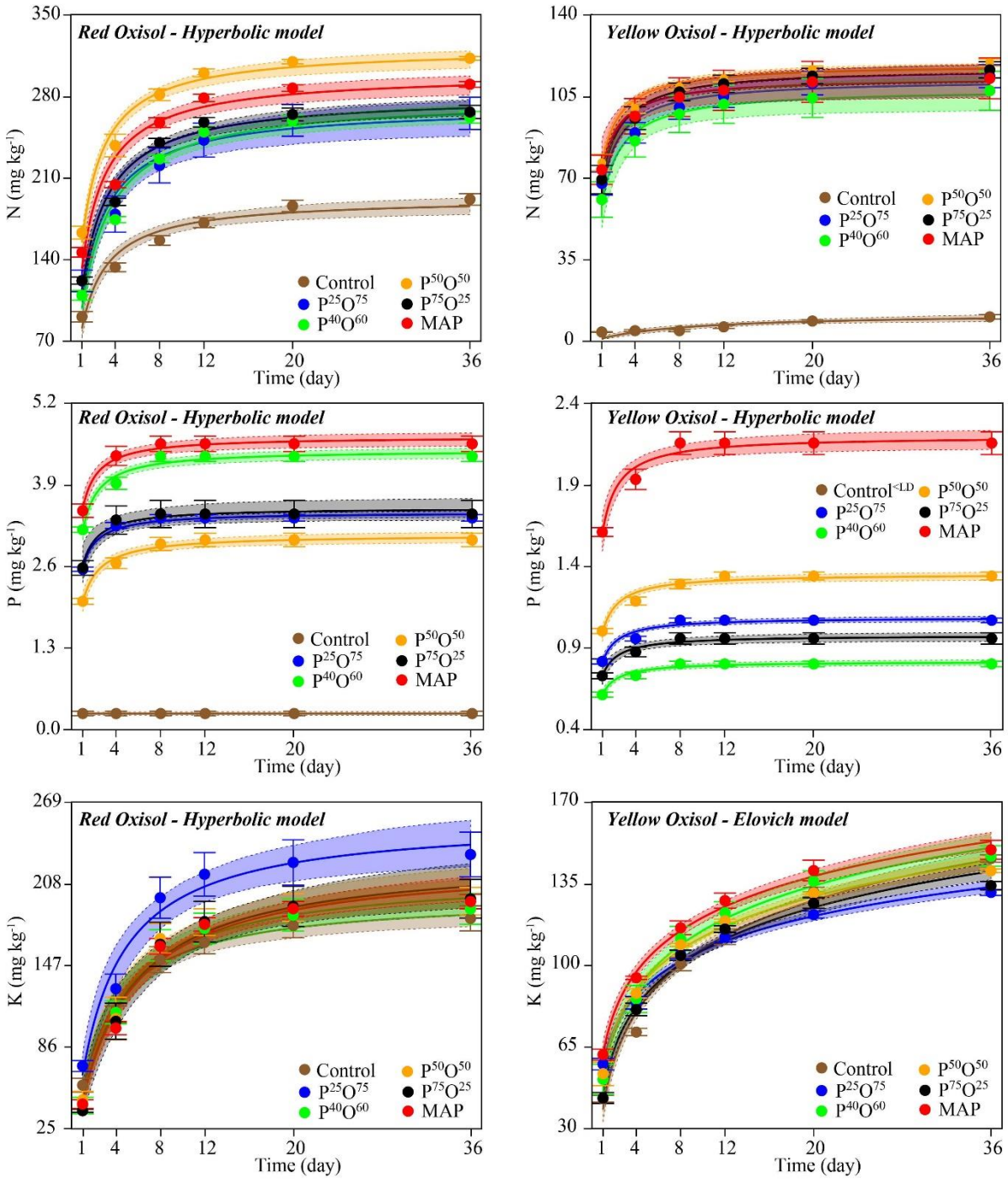

Figure 8. Leaching of N, P and K according to the organomineral ($P^{25}O^{75}$, $P^{40}O^{60}$, $P^{50}O^{50}$ and $P^{75}O^{25}$) and monoammonium phosphate (MAP) fertilizers in contrasting Oxisols. $^{<LD}$: the content is lower than which detection limit of the ICP-OES machine.

Initial and final N mineralized in YO, as well as N mineralization constant rate, was not affected by OMFs, compared to MAP (**Fig. 8 and Supplementary material 12**). P leached

was not verified for P not treated soil (control) in YO; however, when P was verified in leachates, P had a higher amount of P released in leachates as follows: MAP > $P^{50}O^{50}$ > $P^{25}O^{75}$ > $P^{75}O^{25}$ > $P^{40}O^{60}$. MAP had a lower P leaching constant rate due to the higher amount leached. The initial amount of K leached in YO was lower for $P^{75}O^{25}$ and control compared to the other nutrient sources. Final leached K was higher for $P^{25}O^{75}$ and $P^{75}O^{25}$ over other treatments. Among treatments studied, $P^{25}O^{75}$ had a lower K-leached constant rate.

4 Discussion

4.1 OMFs and MAP characterization and P release

The main benefits of OMFs over mineral fertilizers are partly explained by their specific nutrient pools and forms, availability, and gradual release to crops [8, 16, 31]. The proportion of mineral and organic N in OMFs depends on the proportion of mixtures between MAP, CH, and CM during composting, and an increase in MAP proportions in OMF mixtures increased mineral N according to total N content (**Table 3**). In OMFs, the proportion of N forms regulates the N supplying to crops, being N-NH_4^+ and N-NO_3^- are readily available to crops, while N organic from OMFs needs to be converted into mineral N; thus, the organic N forms in OMFs are to release N to crops in a lower rate than mineral N forms [4, 26, 28].

The fertilizer FTIR spectral signature can also infer forms and fertilizer-N and P availability indices [21, 22]. FTIR analysis revealed that the $N\text{-}H^{1490\text{-}1340}$ area increased and the $N\text{-}H^{3350\text{-}2650}$ decreased due to an increase in MAP in OMFs (**Fig. 3**). As the organic matrix increased in the OMFs, a sharp increase in the 2920 and 2850 cm^{-1} peak areas were recorded in the fertilizer FTIR spectra, peaks more evident in $P^{25}O^{75}$ and assigned to C in aliphatic methylene chains in organic molecules [58]. The main features of the FTIR spectra related to $N^{3350\text{-}2650}$ bonds (**Fig. 3**) were probably linked to the N-organic compounds as the primary amine salts identified in the region between 3200 and 2800 cm^{-1} [59].

Amine salts are formed by reactions between mineral N and organic C compounds with carboxylic acid groups [59]. Thus, the N from the MAP and the C from the organic residues probably react during composting, with the subsequent formation of primary amine salts (R-NH_3^+) in OMFs, with H atoms of N- NH_4^+ from the MAP being replaced by organic groups (aliphatic methylene groups) present in the organic residues (CM and CH). The formation of more amine salts than amines promotes the synthesis of more soluble N forms, however less soluble than mineral N forms [23]. Thus, a fraction of the N from MAP was possibly incorporated into the OMF organic matrix, reducing the levels of N readily available to plants. However, due to the overlapping areas and peaks in the FTIR spectra, the assignment of N chemical species and functional groups could be a possible limitation of the FTIR technique to infer the chemical nature of N compounds present in OMFs.

The P contents available to plants were strongly related to the fertilizer-P solubility indices, and CA and NAC+H_2O solubility predict the amounts of P capable of being acquired by roots, while the P soluble in water mirrors P forms readily available to plants [60, 61]. A combination of different fertilizer-P availability indices is a strategy to increase the agronomic efficiency of P sources; once the same amount of NAC+H_2O-soluble P was added to soils, a reduction of water-soluble P may decrease the phosphate-specific adsorption in tropical soils [16, 20]. The highest amount of P soluble in NAC+H_2O, CA, and water as a % of total P content in fertilizer were found for MAP and $P^{75}O^{25}$, the compost-based OMF most enriched in MAP (**Table 3**). The lowest P-CA and P-NAC+H_2O fertilizer indices were found for $P^{40}O^{60}$ and $P^{50}O^{50}$, followed by $P^{25}O^{75}$. P solubility in water (P water index) decreased as the proportion of CM+CH increased in the OMFs, and this effect occurred due to an increase in the free soluble P forms as the proportion of MAP increased in the formulated OMFs [16].

Regarding the total P area in the FTIR spectra, the P-O bond signal decreased, and the P-OH bond area increased as the proportion of MAP in OMFs increased (**Fig. 3**). The fertilizer-

P solubility indices (water, CA, and NAC+H_2O) was positively correlated with the P-OH chemical groups and negatively correlated with P-O groups from OMFs and MAP (**Fig. 3**). Depending on the waste composted, an increase in the pH of the compost-based OMFs [16] leads to the conversion of $H_2PO_4^-$ into HPO_4^{2-} as one electron is donated to the latter phosphate group [62], which decreases the fertilizer-P solubility indices (**Erro! Fonte de referência não encontrada.3**). This effect promoted an increase in the relative abundance of P-O over P-OH and may be associated with the deprotonation of P groups during composting. The effect observed related to P groups in the FTIR spectrum was also related to the kinetics of P release study, with a positive correlation between P-OH groups and the initial and final kinetics of P release (**Fig. 3**).

The amount of P released according to both kinetics methods can be predicted by measuring the fertilizer EC of leachates collected over time (**Fig. 1**) as proposed by the use of EC to estimate soluble P contents in fertilizers has previously been proposed and used by Maluf et al. [16]. The behavior and amounts of P in the kinetics study depended on the proportion of CM+CH+MAP in OMFs and the method evaluated (**Fig. 2 and Supplementary material 5**). The dynamics of P release in water for both the kinetics methods investigated (A and B) were similar for $P^{25}O^{75}$, $P^{40}O^{60}$, $P^{50}O^{50}$, and MAP and different for the $P^{75}O^{25}$. Method A is a closed system, and in a closed system, no reactants or products can enter or escape, limiting the reaction rate; in contrast, in an open system (Method B), the products are free to escape, so that a new chemical equilibrium can be established during the formation of new products [63]. The open system method is similar to nutrient uptake for plants from soil solution and equilibrium formed between the solid and liquid phases [3].

The initial and final P release in water was reduced for all the OMFs compared with MAP in Method A (**Fig. 2**). In method B, the reduction was only verified for $P^{25}O^{75}$, $P^{40}O^{60}$, and $P^{50}O^{50}$ over MAP. Using method B, the initial P release from $P^{75}O^{25}$ was lower than that of

MAP, although the final P releases from $P^{75}O^{25}$ and MAP were similar, indicating that $P^{75}O^{25}$ had a more gradual release of P than MAP (**Fig. 2 and Supplementary material 5**). A more gradual release of P but compatible with nutritional demand of plants is suitable a strategy to reduce P fixation, increase soil P availability, and increase P uptake for plants [19, 56, 61].

4.2 Agronomic performance and mineralization/release of NPK

The differential properties of OMFs over MAP resulted in at least one of OMFs being more efficient than MAP in nourishing maize plants in soil type-dependent effect (**Fig. 6**). Fertilizers that gradually release P have a higher agronomic performance than the fully soluble P fertilizers to nourish plants [19]. The effects of OMFs on plants were related to effects on nutrient pools and contents in the soil solid phase and soil solution, especially in Oxisols, which have inherent and characteristic low levels of P in the liquid phase and high P fixation [2, 3, 6]. While nutrient present in mineral fertilizers is soluble and readily available to crops, in OMFs, the presence of organic compounds protect nutrient from negatively interacting with tropical soil components, as happened with P, while reducing nutrient losses through leaching (K and N), improving the efficient use of nutrients by crops [5, 8–10, 12, 17, 33, 64].

Additionally, during OMF synthesis, it is possible to convert waste and nutrients contained in them into inputs of high agronomic value to be used in crop fields as fertilizers contributing to reducing soil and water pollution and the impact of inadequate disposal of wastes in the environment [9, 12, 13]. The production of OMFs with CH may also be a suitable and effective source of K for crops [16], as observed in our study; because despite the little effect on dynamics of K on maize cultivated by OMFs over MAP (**Fig. 7**), the CH used in OMFs synthesis supplied the K required for maize plants (**Table 3 and Fig. 6**).

Although potassium is massively found in soil in the ionic form (K^+), the nutrient mineralization kinetics study indicated that a potential loss of K through soil leaching processes

could be anticipated even when soils are treated with OMFs [7]. As observed by higher K contents in leachates observed for OMF enriched in organic residues ($P^{25}O^{75}$) over MAP addition to composted piles in RO and the reduction of final amount leached of K by $P^{25}O^{75}$ and $P^{75}O^{25}$ over MAP in YO (**Fig. 8**). In line with results mentioned the pattern of K release are relevant to improve the management of K fertilizers, including the definition of rate, time and number of topdressing fertilization and longevity of K sources in the soil-plant system [7].

Due to the different pools and solubility of N forms in OMFs may positively interact with P and N, promoting greater fertilizer use efficiency, especially for crops responsive to N (e.g., maize) [17, 29]. Readily available forms of N (N-mineral) from the OMFs and MAP fertilization contributed to increasing the soil N-mineral and solution N-mineral in RO (**Fig. 7 and Supplementary materials 8 and 9**), an effect favored by an increase in the MAP proportion used during OMF synthesis (**Table 3**). In YO (with the lower OM content), the N accumulation in the shoots was favored by the more available N forms applied via fertilizers (**Fig. 7**) due to the low contribution from the naturally occurring N in soil (**Fig. 8**).

In RO, due to higher levels of OM and N content (**Table 2**), there were higher available contents of N, as observed in the soil N-mineral and by natural mineralization of N in this soil (**Fig. 8**), and consequently, the N accumulated by maize was higher in RO than in YO (**Fig. 7**). Thus, in the RO, OM contributed to an increase in the amount of N mineralized, while in YO (with the lowest OM content), the amount of N mineralized and the rate of N mineralization did not differ among the OMFs in relation to MAP nitrogen supplying (**Fig. 8**). The soil contribution to the N supply is highly related to the OM content [3], and the N mineralization rate is a process regulated by the interaction between OMFs and soil components biotic and abiotic factors controlled by OM decomposition [4, 27, 28], as observed in our study.

In RO, in addition to the high contributions to the N mineralized from the soil native OM, OMFs differed from MAP in their capacity to mineralize; thus, $P^{50}O^{50}$ increased the

amounts of N mineralized, and $P^{25}O^{75}$, $P^{40}O^{60}$, and $P^{75}O^{25}$ decreased N mineralization compared with MAP fertilization. Effect in part explained by different amounts of N added to the soils in mineralization study when were applied 189, 180, 179, 157, and 146 mg kg^{-1} of total N and N mineral concentrations of 115, 139, 147, 134, and 146 mg kg^{-1}, respectively for by $P^{25}O^{75}$, $P^{40}O^{60}$, $P^{50}O^{50}$, $P^{75}O^{25}$ and MAP (**Fig. 8**). Reduced mineralization rate of N from OMFs over mineral fertilizers reported in this study has also already been reported to OMFs over urea, and most N mineralized is limited up to 30 days of OMF incubation in soils [28]. Specific N mineralization rates for the OMFs in soil resembled the P release dynamics reported by Grohskopf et al. [27]. The role played by phosphate in retaining N is related to the temporary retention of $N\text{-}NH_4^+$ followed by the increase of the electronegative potential of soil when P is bounded to adsorption exchangeable sites of Fe and Al oxides present in tropical soils [27].

The main effects observed of OMFs over MAP were related to the dynamics of P. By adjusting the amount of P added to soils as a function of $NAC+H_2O$-soluble P fractions and total N in OMFs, an increase in the proportion of MAP in the OMFs increases the applied amount of P soluble in water added to the soil (**Table 4**). P soluble in water was negatively correlated with biomass production, and P accumulated in the maize shoot (**Fig. 7**). Reducing P soluble in water in fertilizers with high levels of P soluble in $NAC+H_2O$ is a suitable strategy to prevent the negative reactions of P with soil colloids that reduce the efficiency of P fertilizers [20].

Besides, applying OMFs or soil enrichment with OM has organic molecules that can reduce the specific adsorption of P into soil minerals [6, 8, 33]. Because organic molecules block specific P adsorption sites on the solid phase of tropical soils, altering the surface charge of iron oxides, and promoting the electrostatic repulsion of phosphates [5, 6], preventing P fixation and increasing the use efficiency of P fertilizers by crops [8]. The effect of organic molecules input in soil with lower OM was observed in YO when the OMF nutrient sources

containing higher proportions of organic residues ($P^{25}O^{75}$ and $P^{40}O^{50}$) improved the total and root maize biomass production, and the use of $P^{25}O^{75}$ increased shoot biomass over MAP application (**Fig. 6**).

In RO, with a higher OM content and, consequently, more natural protection for the P species, the $P^{25}O^{75}$ formulation, which contained a lower amount of water-soluble P applied (**Table 4**), reduced maize growth without affecting the N, P, and K levels in the maize shoots (**Fig. 6**). This decrease in maize growth is explained in part by the short interval available for the rapidly growing annual crops to acquire P, as well as by the high P requirement of the crops and the high P solubility of the fertilizers [5]. In clay Oxisols, the slow P release due to the low water-soluble P content of the OMFs compared with the mineral fertilizers seems to be the reason for the lower production of maize biomass [11]. However, a more gradual P release is predicted to increase P availability compared with fully solubilized mineral P fertilizers in the long term (residual P) due to the P derived from the OMFs [31], and this prediction is mirrored by the data shown in this study.

$P^{40}O^{60}$ and $P^{50}O^{50}$ applications in RO increased the total P applied (**Table 4**), favoring maize biomass production and N, P, and K levels accumulated in the shoot (**Figs. 5, 6, and 7**). A higher OM content than YO characterizes RO, and the OM is supposed to enrich the soil with different organic compounds, including organic acids that can block soil P adsorption sites [5, 6]. Besides, organic acids may interact with humic molecules in OMFs fragmenting them, and, consequently, increasing nutrient release for plants [65]. This is a possible explanation for the high P resin contents verified in RO but not in YO (Oxisol with the lowest OM content). The effect of higher production of biomass due to a higher amount of total P applied in OMFs based on the recommendation in P soluble in NAC+H_2O seems to explain the effects of chicken litter-based OMF over MAP on maize growth and another P-OMF on soybean growth, showed positive effects of OMF application on maize growth but not on soybean growth [64].

For maize growth, an OMF with a P-NAC+H_2O solubility index of 79% was used and compared with the positive control (triple superphosphate (TSP) with a P-NAC-H_2O solubility index of 96%)). Overall, the OMF added more total P to soil than TSP, e.g., for the recommended application of 52 kg ha^{-1} of P, the total P applied was 14 kg ha^{-1} greater for OMF than that of the TSP application. However, in the soybean experiment, the OMF used had a solubility index of 95% in NAC+H_2O, a value close to that of TSP. Thus, based on previous studies by Frazão et al. [64] and in results of this study, liming favors P mineralization, and the release of organic acids by soil OM may contribute to the availability of P, which a NAC+H_2O extractor test may not assess. Therefore, this additional P may have contributed to the greater P accumulation in the maize shoot, and increased P availability in soil.

The aforementioned effect appears more related to a higher P availability throughout maize growth, as the readily available P measured in the soil solution (solution P) was decreased for both by $P^{40}O^{60}$ and $P^{50}O^{50}$ and by other OMFs over MAP (**Fig. 4**). Although the P concentration in the soil solution is low compared with the P levels in the solid phase, both soil phases are in equilibrium with each other [3, 5], and the soil solution is the compartment from which plants take up nutrients [5, 6].

Similar effects and higher agronomic efficiency and maize growth of OMFs produced from poultry litter were observed over plants fertilized with MAP and grown in two Oxisols. Maize biomass production was higher in the clay loam Oxisol with higher OM content than the sandy loam Oxisol [9]. In this direction, a positive effect of OMFs on plants over P mineral sources was dependent on the soil type in which wheat plants were cultivated by Erro et al. [8], and the soil OM content was the key factor determining the potential response of plants to OMFs. In this study, the effects of OMFs on fertilizer P solubility depended on soil type.

In addition to the main effect on the crops, fertilizers with a more gradual release have a higher residual effect, thus increasing P levels in soils' successive cultivation

cycles [11, 31, 32]. However, the higher residual effect of the OMFs over the mineral fertilizers may be due to the lower growth rate of the plants that consequently extracted fewer nutrients from the production system [11, 31], as observed by the application of $P^{25}O^{75}$ in RO and reduction of maize growth, but with a higher residual effect on P availability in whole soil and soil solution (**Figs. 4, 5, and 6**). When a higher total amount of P from OMFs was applied to RO, a higher maize biomass production was verified, and a higher nutrient residual effect on solution P and soil P-resin over MAP fertilization. The residual P effect of OMFs was not verified in YO.

In studies performed in Oxisol samples to evaluate the OM mineralization dynamics, $N\text{-}NH_4^+$ and $N\text{-}NO_3^-$ mineralized and K^+ leached are easily moved by $CaCl_2$ solution[46]. However, due to the specific adsorption of P in tropical soils, the $CaCl_2$ solution is not strong enough to remove all forms of P possibly released by fertilizers [3, 5, 6]. Thus, the use of $CaCl_2$ solution only simulated elucidates the potential losses of P through leaching in Oxisols, and it was observed that MAP promotes a higher amount of P in leachates of the kinetics study over MAP (**Fig. 8**). P leaching is not a severe issue in highly weathered soils, such as Oxisols, due to the specific phosphate adsorption in kaolinite and Fe and Al (oxi) hydroxides colloids of tropical soils [5, 6]. High and soluble amounts of P in leachates from MAP mini-lysimeters are explained due to the high amount of P applied in free forms ($H_2PO_4^-$) in soluble P fertilizers, whose P chemical species are more susceptible to being lost in leachates, mainly in sandy soils.

5 Conclusion

Synthesis of organomineral fertilizers (OMFs) by mixing monoammonium phosphate (MAP) with coffee husk and chicken manure generated fertilizers with a wide range of OMFs with different N, P, and K contents, forms, and release rates. In a soil type-dependent way, the kinetics of K release slightly relied on the OMF type, while contents of N mineralized relied on

OMF tested and organic matter content of the Oxisol incubated. P release rates were lower for OMFs over MAP. Soluble P was rapidly released in MAP-treated soils, and P released in soils highly depended on the MAP proportion in OMFs. The amount of N mineralized from OMFs relied on soil type, being strongly regulated by soil OM content. Regardless of the kinetics method investigated, electrical conductivity was a suitable and fast index to predict soluble P released from the composted-based OMFs and MAP. The abundance of N and P bonds and assignments of peaks of N and P groups recorded in ATR-FTIR spectra were suitable indices to predict mineral and organic N forms and fertilizer-P availability indices, and available and residual P in soils. Proportions of MAP over organic residues (Chicken manure and coffee husk) in OMFs were key factors controlling the availability of N, P, and K in whole soil and its solution, as well as the residual P-resin, and maize nutritional status and growth. Compared to the exclusive use of MAP, maize biomass, mainly that related to root, was favored by plant fertilization with OMFs with higher proportions of organic residues over MAP. Maize biomass production, agronomic value, and capacity of OMFs in supplying NPK to plants strongly relied on soil type. Maize biomass (shoot+root) was approximately 31% greater for plants fertilized with $P^{40}O^{60}$-OMF over MAP+KCl fertilized plants in Red Oxisol. In the sandy soil (YO), maize biomass was 55% for OMF over MAP-nourished plants, surprisingly, for the OMF with only 25% MAP in the composted mixture. As this was a greenhouse study, further studies must be carried out for validation at the field level, testing different agricultural managements and crops and evaluating the main and residual effects.

6 Acknowledgments

Many thanks to the Coordination for the Improvement of Higher Education Personnel (CAPES) (CAPES-PROEX/AUXPE 593/2018), National Council for Scientific and Technological Development (CNPq) (303899/2015-8 and 307447/2019-7 grants), and the

Foundation for Research of the State of Minas Gerais (FAPEMIG) for financial support and scholarships provided. UFLA is an equal opportunity provider and employer.

Declaration of conflict of interest

The authors declare no conflict of interest.

7 References

1. FAO: World fertilizer trends and outlook to 2020: Summary report. Food Agric. Organ. United Nations. 38 (2017)
2. Lopes, A.S., Guilherme, L.R.G.: A career perspective on soil management in the Cerrado region of Brazil. Elsevier Inc. (2016)
3. Marschner, P.: Marschner's Mineral Nutrition of Higher Plants. Elsevier, Oxford (2012)
4. Rigby, H., Clarke, B.O., Pritchard, D.L., Meehan, B., Beshah, F., Smith, S.R., Porter, N.A.: A critical review of nitrogen mineralization in biosolids-amended soil, the associated fertilizer value for crop production and potential for emissions to the environment. Sci. Total Environ. 541, 1310–1338 (2016). https://doi.org/10.1016/j.scitotenv.2015.08.089
5. McLaughlin, M.J., McBeath, T.M., Smernik, R., Stacey, S.P., Ajiboye, B., Guppy, C.: The chemical nature of P accumulation in agricultural soils-implications for fertiliser management and design: An Australian perspective. Plant Soil. 349, 69–87 (2011). https://doi.org/10.1007/s11104-011-0907-7
6. Fink, J.R., Inda, A.V., Tiecher, T., Barrón, V.: Iron oxides and organic matter on soil phosphorus availability. Ciência e Agrotecnologia. 40, 369–379 (2016). https://doi.org/10.1590/1413-70542016404023016
7. Najafi-Ghiri, M., Boostani, H.R., Hardie, A.G.: Investigation of biochars application on potassium forms and dynamics in a calcareous soil under different moisture conditions. Arch. Agron. Soil Sci. 0, 1–15 (2020). https://doi.org/10.1080/03650340.2020.1834083
8. Erro, J., Urrutia, O., Baigorri, R., Aparicio-Tejo, P., Irigoyen, I., Torino, F., Mandado, M., Yvin, J.C., Garcia-Mina, J.M.: Organic Complexed Superphosphates (CSP): Physicochemical characterization and agronomical properties. J. Agric. Food Chem. 60, 2008–2017 (2012). https://doi.org/10.1021/jf204821j
9. Sá, J.M., Jantalia, C.P., Teixeira, P.C., Polidoro, J.C., Benites, V. de M., Araújo, A.P.: Agronomic and P recovery efficiency of organomineral phosphate fertilizer from poultry litter in sandy and clayey soils. Pesqui. Agropecu. Bras. 52, 786–793 (2017). https://doi.org/10.1590/S0100-204X2017000900011
10. Kominko, H., Gorazda, K., Wzorek, Z.: The Possibility of Organo-Mineral Fertilizer Production from Sewage Sludge. Waste and Biomass Valorization. 8, 1781–1791 (2017). https://doi.org/10.1007/s12649-016-9805-9
11. Sakurada, R., Batista, L.M.A., Inoue, T.T., Muniz, A.S., Pagliar, P.H.: Organomineral

phosphate fertilizers: Agronomic efficiency and residual effect on initial corn development. Agron. J. 108, 2050–2059 (2016). https://doi.org/10.2134/agronj2015.0543

12. Antille, D.L., Godwin, R.J., Sakrabani, R., Seneweera, S., Tyrrel, S.F., Johnston, A.E.: Field-scale evaluation of biosolids-derived organomineral fertilizers applied to winter wheat in England. Agron. J. 109, 654–674 (2017). https://doi.org/10.2134/agronj2016.09.0495

13. Mumbach, G.L., Gatiboni, L.C., Bona, F.D., Schmitt, D.E., Dall'Orsoletta, D.J., Gabriel, C.A., Bonfada, É.B.: Organic, mineral and organomineral fertilizer in the growth of wheat and chemical changes of the soil. Rev. Bras. Ciências Agrárias - Brazilian J. Agric. Sci. 14, 1–7 (2019). https://doi.org/10.5039/agraria.v14i1a5618

14. Santos Dalólio, F., da Silva, J.N., Carneiro de Oliveira, A.C., Ferreira Tinôco, I. de F., Christiam Barbosa, R., Resende, M. de O., Teixeira Albino, L.F., Teixeira Coelho, S.: Poultry litter as biomass energy: A review and future perspectives. Renew. Sustain. Energy Rev. 76, 941–949 (2017). https://doi.org/10.1016/j.rser.2017.03.104

15. Janissen, B., Huynh, T.: Chemical composition and value-adding applications of coffee industry by-products: A review. Resour. Conserv. Recycl. 128, 110–117 (2018). https://doi.org/10.1016/j.resconrec.2017.10.001

16. Maluf, H.J.G.M., Silva, C.A., Morais, E.G. de, Paula, L.H.D. de: Is Composting a Route to Solubilize Low-Grade Phosphate Rocks and Improve MAP-Based Composts? Rev. Bras. Ciência do Solo. 42, (2018). https://doi.org/10.1590/18069657rbcs20170079

17. Frazão, J.J., Benites, V. de M., Ribeiro, J.V.S., Pierobon, V.M., Lavres, J.: Agronomic effectiveness of a granular poultry litter-derived organomineral phosphate fertilizer in tropical soils: Soil phosphorus fractionation and plant responses. Geoderma. 337, 582–593 (2019). https://doi.org/10.1016/j.geoderma.2018.10.003

18. Grohskopf, M.A., Corrêa, J.C., Fernandes, D.M., de Melo Benites, V., Teixeira, P.C., Cruz, C.V.: Phosphate fertilization with organomineral fertilizer on corn crops on a Rhodic Khandiudox with a high phosphorus content. Pesqui. Agropecu. Bras. 54, e00434 (2019). https://doi.org/10.1590/S1678-3921.PAB2019.V54.00434

19. Everaert, M., Warrinnier, R., Baken, S., Gustafsson, J.P., De Vos, D., Smolders, E.: Phosphate-Exchanged Mg-Al Layered Double Hydroxides: A New Slow Release Phosphate Fertilizer. ACS Sustain. Chem. Eng. 4, 4280–4287 (2016). https://doi.org/10.1021/acssuschemeng.6b00778

20. Urrutia, O., Erro, J., Guardado, I., San Francisco, S., Mandado, M., Baigorri, R., Claude Yvin, J., Ma Garcia-Mina, J.: Physico-chemical characterization of humic-metal-phosphate complexes and their potential application to the manufacture of new types of phosphate-based fertilizers. J. Plant Nutr. Soil Sci. 177, 128–136 (2014). https://doi.org/10.1002/jpln.201200651

21. Lu, B., Liu, N., Li, H., Yang, K., Hu, C., Wang, X., Li, Z., Shen, Z., Tang, X.: Quantitative determination and characteristic wavelength selection of available nitrogen in coco-peat by NIR spectroscopy. Soil Tillage Res. 191, 266–274 (2019). https://doi.org/10.1016/j.still.2019.04.015

22. Ruangratanakorn, J., Suwonsichon, T., Kasemsumran, S., Thanapase, W.: Installation design of on-line near infrared spectroscopy for the production of compound fertilizer. Vib. Spectrosc. 106, 103008 (2020). https://doi.org/10.1016/j.vibspec.2019.103008

23. Ouellette, R.J., Rawn, J.D.: Amines and Amides. In: Ouellette, R.J. and RAWN, J.D. (eds.) Organic chemistry: structure, mechanism, and synthesis. pp. 803–842. Elsevier, San Diego (2014)

24. Brazil: Manual de métodos analíticos oficiais para fertilizantes e corretivos. MAPA, Brasília (2017)

25. Chien, S.H., Prochnow, L.I., Tu, S., Snyder, C.S.: Agronomic and environmental aspects of phosphate fertilizers varying in source and solubility: An update review. Nutr. Cycl. Agroecosystems. 89, 229–255 (2011). https://doi.org/10.1007/s10705-010-9390-4

26. Russo, M.A., Belligno, A., Wu, J.Y., Sardo, V., others: Comparing mineral and organic nitrogen fertilizer impact on the soil-plant-water system in a succession of three crops. Recent Res. Sci. Technol. 2, 14–22 (2010)

27. Grohskopf, M.A., Corrêa, J.C., Fernandes, D.M., Teixeira, P.C., Mota, S.C.A.: Mobility of Nitrogen in the Soil Due to the Use of Organomineral Fertilizers with Different Concentrations of Phosphorus. Commun. Soil Sci. Plant Anal. 51, 208–220 (2020). https://doi.org/10.1080/00103624.2019.1705321

28. Antille, D.L., Sakrabani, R., Godwin, R.J.: Nitrogen Release Characteristics from Biosolids-Derived Organomineral Fertilizers. Commun. Soil Sci. Plant Anal. 45, 1687–1698 (2014). https://doi.org/10.1080/00103624.2014.907915

29. Mumbach, G.L., Gatiboni, L.C., de Bona, F.D., Schmitt, D.E., Corrêa, J.C., Gabriel, C.A., Dall'Orsoletta, D.J., Iochims, D.A.: Agronomic efficiency of organomineral fertilizer in sequential grain crops in southern Brazil. Agron. J. 112, 3037–3049 (2020). https://doi.org/10.1002/agj2.20238

30. Liang, Y., Cao, X., Zhao, L., Xu, X., Harris, W.: Phosphorus Release from Dairy Manure, the Manure-Derived Biochar, and Their Amended Soil: Effects of Phosphorus Nature and Soil Property. J. Environ. Qual. 43, 1504–1509 (2014). https://doi.org/10.2134/jeq2014.01.0021

31. Sakurada, R.L., Muniz, A.S., Sato, F., Inoue, T.T., Neto, A.M., Batista, M.A.: Chemical, Thermal, and Spectroscopic Analysis of Organomineral Fertilizer Residue Recovered from an Oxisol. Soil Sci. Soc. Am. J. 83, 409–418 (2019). https://doi.org/10.2136/sssaj2018.08.0294

32. Martins, D.C., Resende, Á.V. De, Galvão, J.C.C., Simão, E.D.P., Ferreira, J.P.D.C., Almeida, G.D.O.: Organomineral Phosphorus Fertilization in the Production of Corn, Soybean and Bean Cultivated in Succession. Am. J. Plant Sci. 08, 2407–2421 (2017). https://doi.org/10.4236/ajps.2017.810163

33. Borges, B.M.M.N., Abdala, D.B., Souza, M.F. de, Viglio, L.M., Coelho, M.J.A., Pavinato, P.S., Franco, H.C.J.: Organomineral phosphate fertilizer from sugarcane byproduct and its effects on soil phosphorus availability and sugarcane yield. Geoderma. 339, 20–30 (2019). https://doi.org/10.1016/j.geoderma.2018.12.036

34. Omar, L., Ahmed, O.H., Majid, N.M.A.: Improving Ammonium and Nitrate Release from Urea Using Clinoptilolite Zeolite and Compost Produced from Agricultural Wastes. Sci. World J. 2015, 1–12 (2015). https://doi.org/10.1155/2015/574201

35. Bremner, J.M., Keeney, D.R.: Determination and Isotope-Ratio Analysis of Different Forms of Nitrogen in Soils: 3. Exchangeable Ammonium, Nitrate, and Nitrite by Extraction-Distillation Methods. Soil Sci. Soc. Am. J. 30, 577–582 (1966). https://doi.org/10.2136/sssaj1966.03615995003000050015x

36. Kitson, R.E., Mellon, M.G.: Colorimetric Determination of Phosphorus as Molybdivanadophosphoric Acid. Ind. Eng. Chem. Anal. Ed. 16, 379–383 (1944). https://doi.org/10.1021/i560130a017

37. Maluf, H.J.G.M.: Technologies for the efficient use of phosphorus in the plantsoil-fertilizer system, http://repositorio.ufla.br/bitstream/1/37366/1/TESE_Technologies for the efficient use of phosphorus in the plantsoil-fertilizer system.pdf, (2017)

38. Stuart, B.H.: Infrared Spectroscopy: Fundamentals and Applications. (2004)

39. Embrapa: Sistema brasileiro de classificação de solos. Embrapa, Brasília (2018)

40. Staff, S.S.: Keys to soil taxonomy. United States Department of Agriculture, Washington (2014)

41. Teixeira, P.C., Donagemma, G.K., Fontana, A., Teixeira, W.G. eds: Manual de métodos de análise de solo. Embrapa, Brasília (2017)

42. Raij, B. V., Quaggio, J.A., da Silva, N.M.: Extraction of phosphorus, potassium, calcium, and magnesium from soils by an ion-exchange resin procedure. Commun. Soil Sci. Plant Anal. 17, 547–566 (1986). https://doi.org/10.1080/00103628609367733

43. Novais, R.F.., Neves, J.C.L.., Barros, N.F.: Ensaio em ambiente controlado. In: Oliveira, A.J.., Garrido, W.E.., Araújo, J.D.., and Lourenço, S. (eds.) Métodos de pesquisa em fertilidade do solo. p. 189−253. Embrapa-SEA, Brasília (1991)

44. Carmo, D.L. do, Silva, C.A., Lima, J.M. de, Pinheiro, G.L.: Electrical Conductivity and Chemical Composition of Soil Solution: Comparison of Solution Samplers in Tropical Soils. Rev. Bras. Ciência do Solo. 40, (2016). https://doi.org/10.1590/18069657rbcs20140795

45. Silva, F.C. ed: Manual de análises químicas de solos, plantas e fertilizantes. Embrapa Informação Tecnológica, Brasília (2009)

46. Stanford, G., Smith, S.J.: Nitrogen Mineralization Potentials of Soils 1 GEORGE STANFORD AND S. J. SMITH 2. Soil Sci. Soc. Am. J. 36, 465–472 (1972)

47. Lê, S., Josse, J., Husson, F.: FactoMineR : An R Package for Multivariate Analysis. J. Stat. Softw. 25, (2008). https://doi.org/10.18637/jss.v025.i01

48. Kassambara, A., Mundt, F.: factoextra: Extract and Visualize the Results of Multivariate Data Analyses, https://cran.r-project.org/package=factoextra, (2020)

49. R Core Team: R: A language and environment for statistical computing, https://www.r-project.org/, (2020)

50. Mendiburu, F.: agricolae: Statistical Procedures for Agricultural Research, https://cran.r-project.org/package=agricolae, (2020)

51. Wickham, H., Averick, M., Bryan, J., Chang, W., McGowan, L., François, R., Grolemund, G., Hayes, A., Henry, L., Hester, J., Kuhn, M., Pedersen, T., Miller, E., Bache, S., Müller, K., Ooms, J., Robinson, D., Seidel, D., Spinu, V., Takahashi, K., Vaughan, D., Wilke, C., Woo, K., Yutani, H.: Welcome to the Tidyverse. J. Open Source Softw. 4, 1686 (2019). https://doi.org/10.21105/joss.01686

52. Baty, F., Ritz, C., Charles, S., Brutsche, M., Flandrois, J.-P., Delignette-Muller, M.-L.: A Toolbox for Nonlinear Regression in R : The Package nlstools. J. Stat. Softw. 66, (2015). https://doi.org/10.18637/jss.v066.i05

53. Wei, T., Simko, V.: R package “corrplot”: Visualization of a Correlation Matrix,

https://github.com/taiyun/corrplot, (2017)

54. Hamner, B., Frasco, M.: Metrics: Evaluation Metrics for Machine Learning, https://cran.r-project.org/package=Metrics, (2018)

55. Dou, Z., Toth, J.D., Jabro, J.D., Fox, R.H., Fritton, D.D.: Soil nitrogen mineralization during laboratory incubation: Dynamics and model fitting. Soil Biol. Biochem. 28, 625–632 (1996). https://doi.org/10.1016/0038-0717(95)00184-0

56. Lustosa Filho, J.F., Penido, E.S., Castro, P.P., Silva, C.A., Melo, L.C.A.: Co-Pyrolysis of Poultry Litter and Phosphate and Magnesium Generates Alternative Slow-Release Fertilizer Suitable for Tropical Soils. ACS Sustain. Chem. Eng. 5, 9043–9052 (2017). https://doi.org/10.1021/acssuschemeng.7b01935

57. Akaike, H.: A Bayesian Extension of the Minimum AIC Procedure of Autoregressive Model Fitting. Biometrika. 66, 237 (1979). https://doi.org/10.2307/2335654

58. Smidt, E., Schwanninger, M.: Characterization of Waste Materials Using FTIR Spectroscopy: Process Monitoring and Quality Assessment. Spectrosc. Lett. 38, 247–270 (2005). https://doi.org/10.1081/SL-200042310

59. Lin-Vien, D., Colthup, N.B., Fateley, W.G., Grasselli, J.G.: The handbook of infrared and Raman characteristic frequencies of organic molecules. Elsevier (1991)

60. Binh, T., Zapata, F.: Standard characterization of phosphate rock samples from the FAO/IAEA phosphate project. In: Assessment of Soil Phosphorus Status and Management of Phosphatic Fertilizers to Optimize Crop Production. pp. 9–23. IAEA-TECDOC-1272, Vienna (2002)

61. Erro, J., Urrutia, O., San Francisco, S., Garcia-Mina, J.M.: Development and agronomical validation of new fertilizer compositions of high bioavailability and reduced potential nutrient losses. J. Agric. Food Chem. 55, 7831–7839 (2007). https://doi.org/10.1021/jf0708490

62. Cerozi, B. da S., Fitzsimmons, K.: The effect of pH on phosphorus availability and speciation in an aquaponics nutrient solution. Bioresour. Technol. 219, 778–781 (2016). https://doi.org/10.1016/j.biortech.2016.08.079

63. Pelton, A.D.: Phase Diagrams and Thermodynamic Modeling of Solutions. Elsevier, Amsterdam (2019)

64. Frazão, J.J., Benites, V.D.M., Pierobon, V.M., Ribeiro, S.: A Poultry Litter-Derived Organomineral Phosphate Fertilizer Has Higher Agronomic Effectiveness Than Conventional Phosphate Fertilizer Applied to Field-Grown Maize and Soybean. Sustainability. (2021). https://doi.org/10.3390/su132111635

65. Morais, E., Silva, C.A., Maluf, H.J.G.M.: UV-visible Spectroscopy as a New Tool to Predict the Bioactivity of Humic Fragments Induced by Citric/ Oxalic Acids on Eucalyptus Nutrition and Growth. Commun. Soil Sci. Plant Anal. 51, 2830–2845 (2020). https://doi.org/10.1080/00103624.2020.1849266

Supplementary material 1. Kinetics of P release scheme.

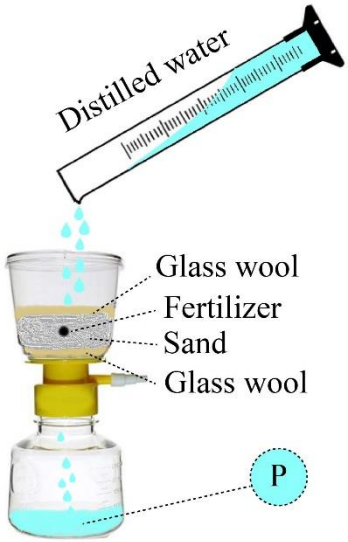

Supplementary material 2. Scheme of mineralization/lixiviation of N, P and K in Oxisols.

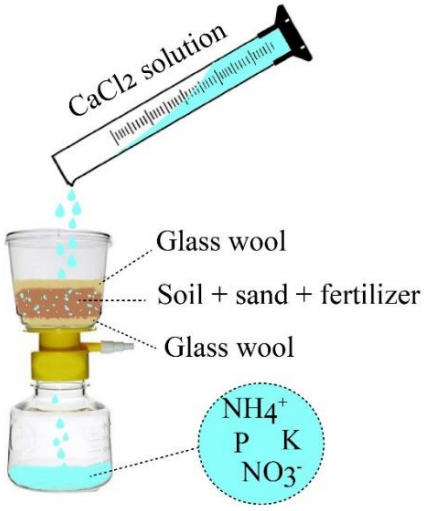

Supplementary material 3. Parameters of models adjusted to the kinetics of P release from organomineral and monoammonium phosphates (MAP) fertilizers.

The kinetics of P release as related to mass fertilizer (mg kg^{-1})												
Method A – Agitation												
Treat.	Elovich			Exponential			Power			Hyperbolic		
	R^2	rmse	AIC	R^2	rmse	AIC	R^2	rmse	AIC	R^2	rmse	AIC
$P^{25}O^{75}$	0.89	0.96	89	0.52	2.06	134	0.88	1.02	92	0.85	1.12	144
$P^{40}O^{60}$	0.86	1.49	115	0.61	2.47	145	0.85	1.54	117	0.88	1.35	109
$P^{50}O^{50}$	0.74	1.52	116	0.78	1.39	111	0.73	1.53	117	0.88	1.02	92
$P^{75}O^{25}$	0.95	1.52	116	0.37	5.31	191	0.95	1.54	117	0.68	3.78	171
MAP	0.83	2.61	149	0.49	4.55	182	0.83	2.66	150	0.83	2.62	154
Method B – Mini-lysimeter												
Treat.	Elovich			Exponential			Power			Hyperbolic		
	R^2	rmse	AIC	R^2	rmse	AIC	R^2	Rmse	AIC	R^2	rmse	AIC
$P^{25}O^{75}$	0.80	2.31	155	0.52	3.57	184	0.84	2.09	148	0.73	11.02	258
$P^{40}O^{60}$	0.87	3.16	176	0.67	5.09	208	0.89	2.90	170	0.83	9.53	248
$P^{50}O^{50}$	0.76	3.94	190	0.57	5.26	209	0.77	3.84	188	0.78	13.90	273
$P^{75}O^{25}$	0.88	8.13	238	0.70	12.98	269	0.90	7.53	233	0.88	16.42	284
MAP	0.96	4.09	193	0.87	7.71	234	0.96	4.39	197	0.93	18.86	294

Kinetics of P release as related to P total content (%)												
Method A – Agitation												
Treat.	Elovich			Exponential			Power			Hyperbolic		
	R^2	rmse	AIC	R^2	rmse	AIC	R^2	rmse	AIC	R^2	rmse	AIC
$P^{25}O^{75}$	0.89	0.99	91	0.52	2.12	136	0.88	1.05	94	0.85	1.16	100
$P^{40}O^{60}$	0.86	0.86	82	0.61	1.42	112	0.85	0.87	84	0.88	0.78	76
$P^{50}O^{50}$	0.74	0.85	82	0.78	0.78	76	0.73	0.86	82	0.88	0.57	58
$P^{75}O^{25}$	0.95	0.82	79	0.38	2.85	154	0.95	0.83	80	0.67	2.02	134
MAP	0.83	1.10	97	0.49	1.92	130	0.83	1.12	98	0.82	1.12	103
Method B – Mini-lysimeter												
Treat.	Elovich			Exponential			Power			Hyperbolic		
	R^2	rmse	AIC	R^2	rmse	AIC	R^2	rmse	AIC	R^2	rmse	AIC
$P^{25}O^{75}$	0.80	2.39	158	0.52	3.68	186	0.84	2.15	150	0.73	10.70	256
$P^{40}O^{60}$	0.89	1.68	134	0.69	2.85	169	0.91	1.52	127	0.82	16.57	285
$P^{50}O^{50}$	0.90	1.32	118	0.67	2.35	156	0.91	1.22	113	0.66	25.00	312
$P^{75}O^{25}$	0.88	4.36	197	0.70	6.95	227	0.90	4.03	192	0.88	30.64	326
MAP	0.96	1.72	136	0.87	3.25	177	0.96	1.85	140	0.93	44.72	351

R^2: coefficient of determination; rmse: root-mean-square error (mg kg^{-1} or %); AIC: The Akaike information criterion. Treat: Treatment studied; $P^{25}O^{75}$: (25% MAP + 37.5% CM (chicken manure) + 37.5% CH (coffee husk)); $P^{40}O^{60}$: (40% MAP + 40% CM + 20% CH), $P^{50}O^{50}$: (50% MAP + 25% CM + 25% CH) and $P^{75}O^{25}$: (75% MAP + 12.5% CM + 12.5% CH).

Supplementary material 4. The kinetics of P release from organomineral and monoammonium phosphates (MAP) fertilizers.

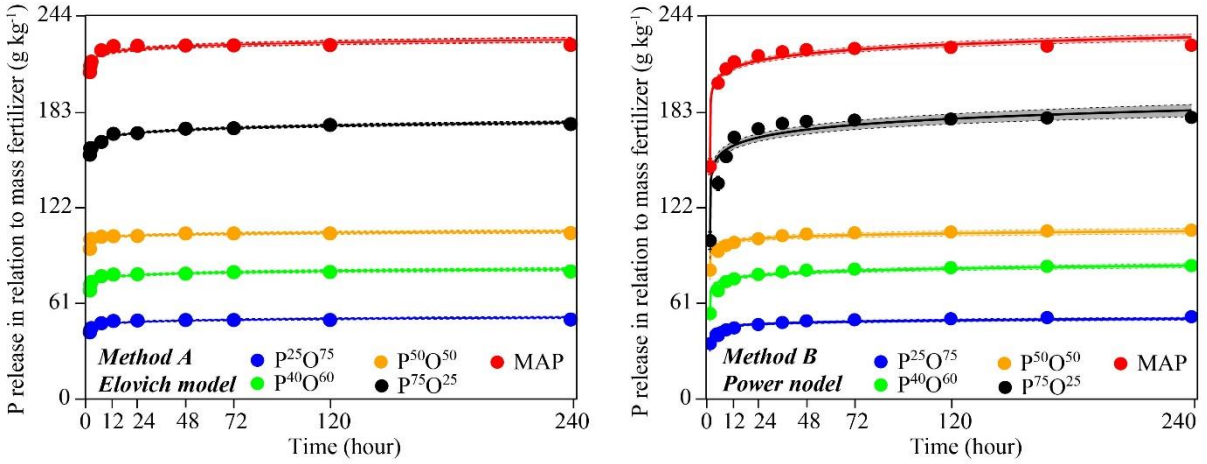

$P^{25}O^{75}$: (25% MAP + 37.5% CM (chicken manure) + 37.5% CH (coffee husk)); $P^{40}O^{60}$: (40% MAP + 40% CM + 20% CH), $P^{50}O^{50}$: (50% MAP + 25% CM + 25% CH) and $P^{75}O^{25}$: (75% MAP + 12.5% CM + 12.5% CH).

Supplementary material 5. Parameters of models related to the velocity of the kinetics of P release in water according to organomineral and monoammonium phosphates (MAP) fertilizers.

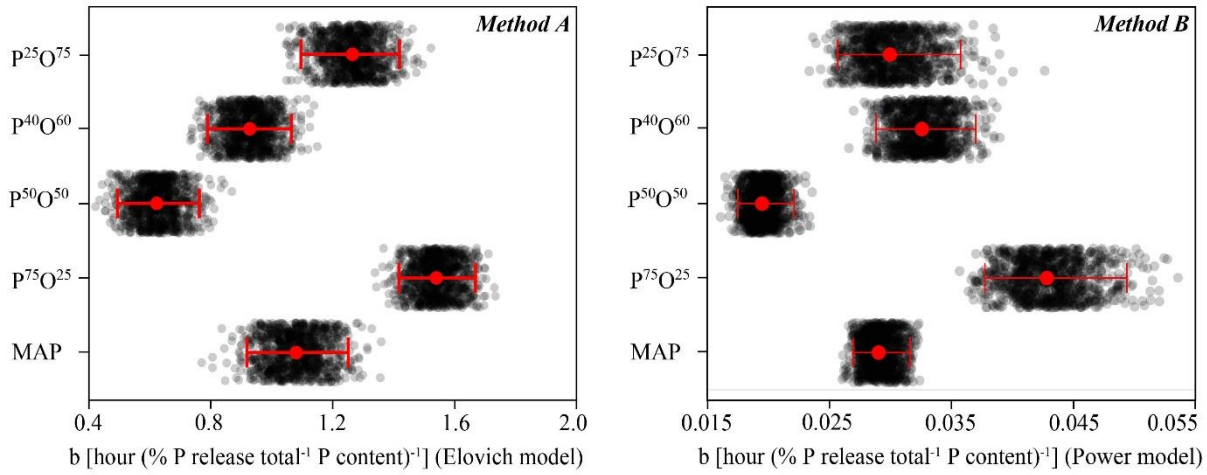

Supplementary material 6. Electrical conductivity of samples in the study of the kinetics of P release from organomineral and monoammonium phosphates (MAP) fertilizers in Method A (Agitation method).

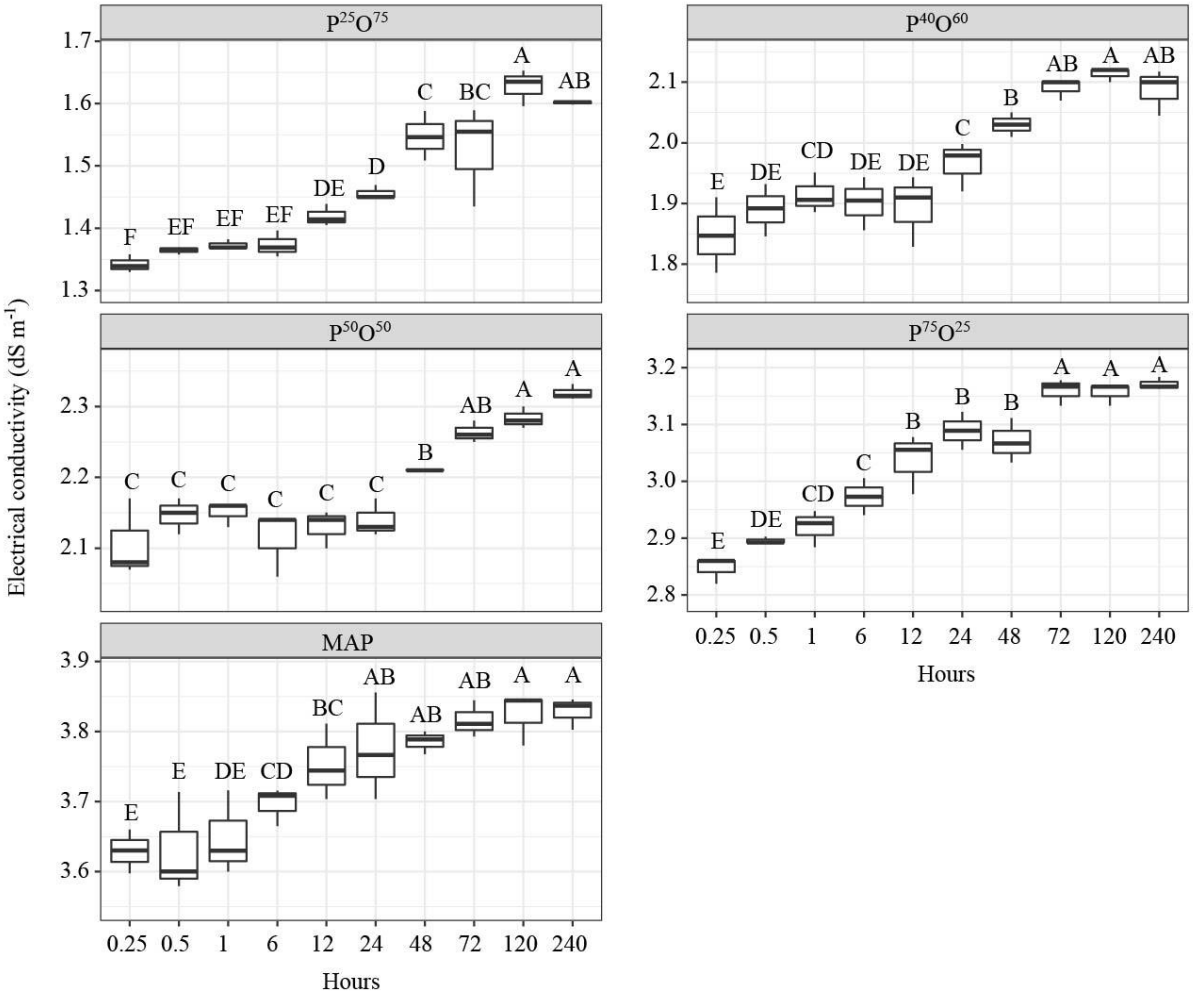

$P^{25}O^{75}$: (25% MAP + 37.5% CM (chicken manure) + 37.5% CH (coffee husk)); $P^{40}O^{60}$: (40% MAP + 40% CM + 20% CH), $P^{50}O^{50}$: (50% MAP + 25% CM + 25% CH) and $P^{75}O^{25}$: (75% MAP + 12.5% CM + 12.5% CH). The means followed by same capital letter did not differ by the Duncant test ($p<0.05$).

Supplementary material 7. Electrical conductivity of samples in the study of the kinetics of P release from organomineral and monoammonium phosphates (MAP) fertilizers in Method B (Mini-lysimeter method).

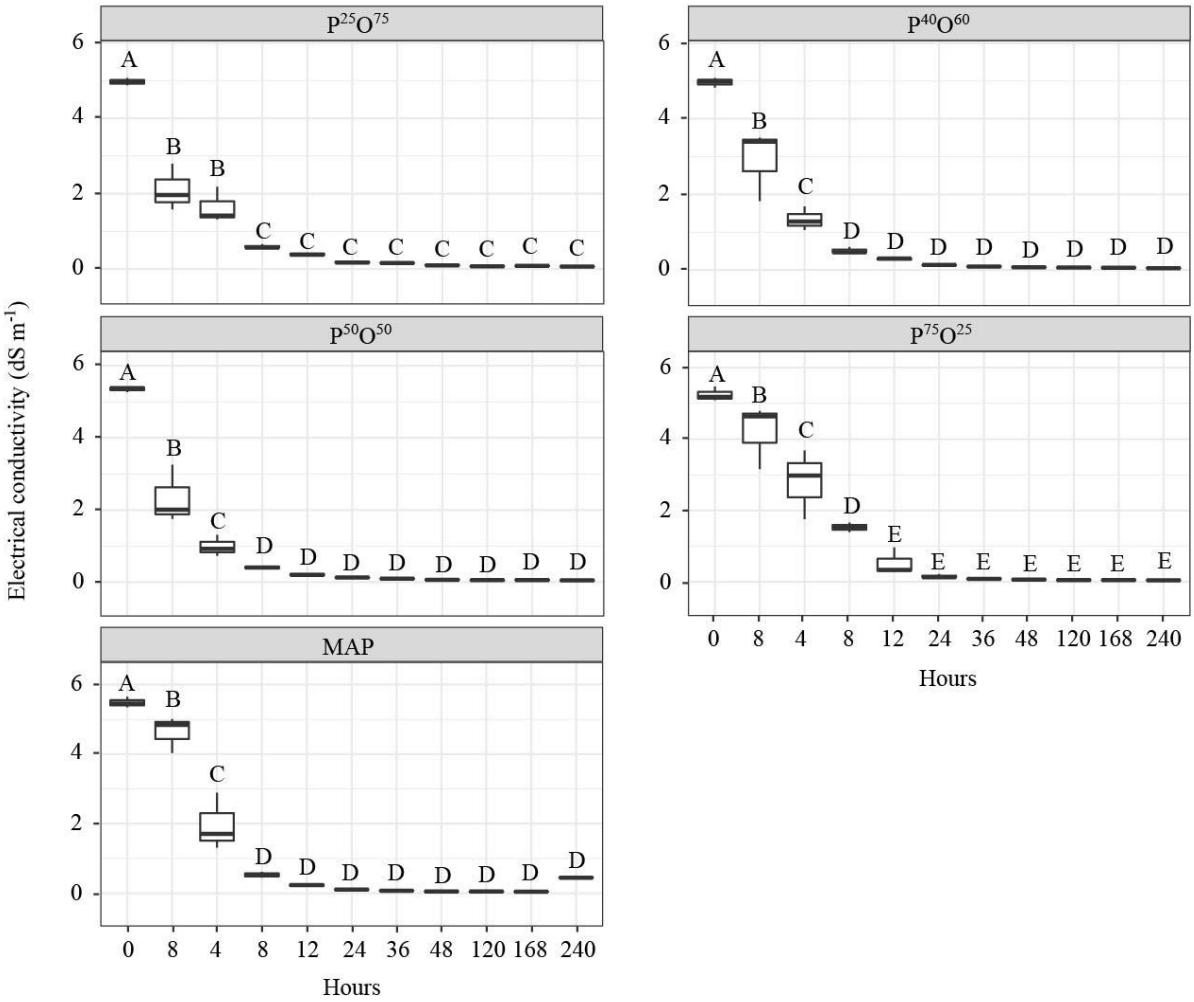

$P^{25}O^{75}$: (25% MAP + 37.5% CM (chicken manure) + 37.5% CH (coffee husk)); $P^{40}O^{60}$: (40% MAP + 40% CM + 20% CH), $P^{50}O^{50}$: (50% MAP + 25% CM + 25% CH) and $P^{75}O^{25}$: (75% MAP + 12.5% CM + 12.5% CH). The means followed by same capital letter did not differ by the Duncant test ($p<0.05$).

Supplementary material 8. Pearson correlation analysis in Red Oxisol to maize growing.

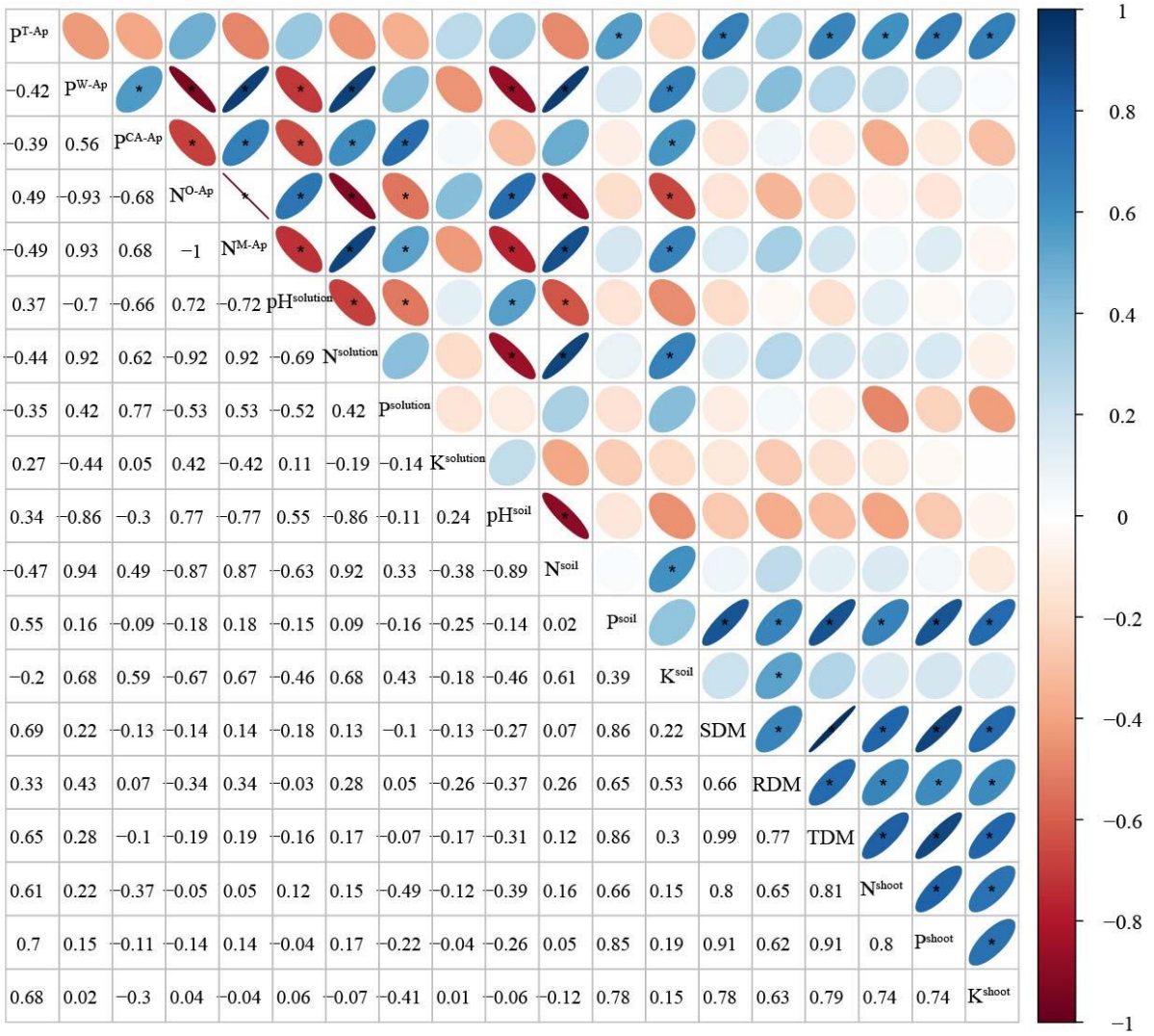

*Significant Pearson correlation analysis (p<0.05). $P^{T\text{-}Ap}$, $P^{W\text{-}AP}$ and $P^{CA\text{-}Ap}$: Amounts of P added in soil though fertilizers based on total conents, solubility in water, and citric acid at 2% respectively. $N^{O\text{-}Ap}$ and $N^{M\text{-}Ap}$: N-organic and N-mineral forms applied added in soil though fertilizers respectively; $N^{solution}$, $P^{solution}$ and $K^{solution}$: soil solution contents of N-mineral, P and K respectively; $pH^{solution}$: pH in soil solution; N^{soil}, P^{soil} and K^{soil}: soil availability of N, P and K respectively; pH^{soil}: pH in soil; TDM, SDM and RDM: total, shoot and root dry matter production respectively; N^{shoot}, P^{shoot} and K^{shoot}: Shoot accumulation of N, P and K respectively.

Supplementary material 9. Pearson correlation analysis in Yellow Oxisol to maize growing.

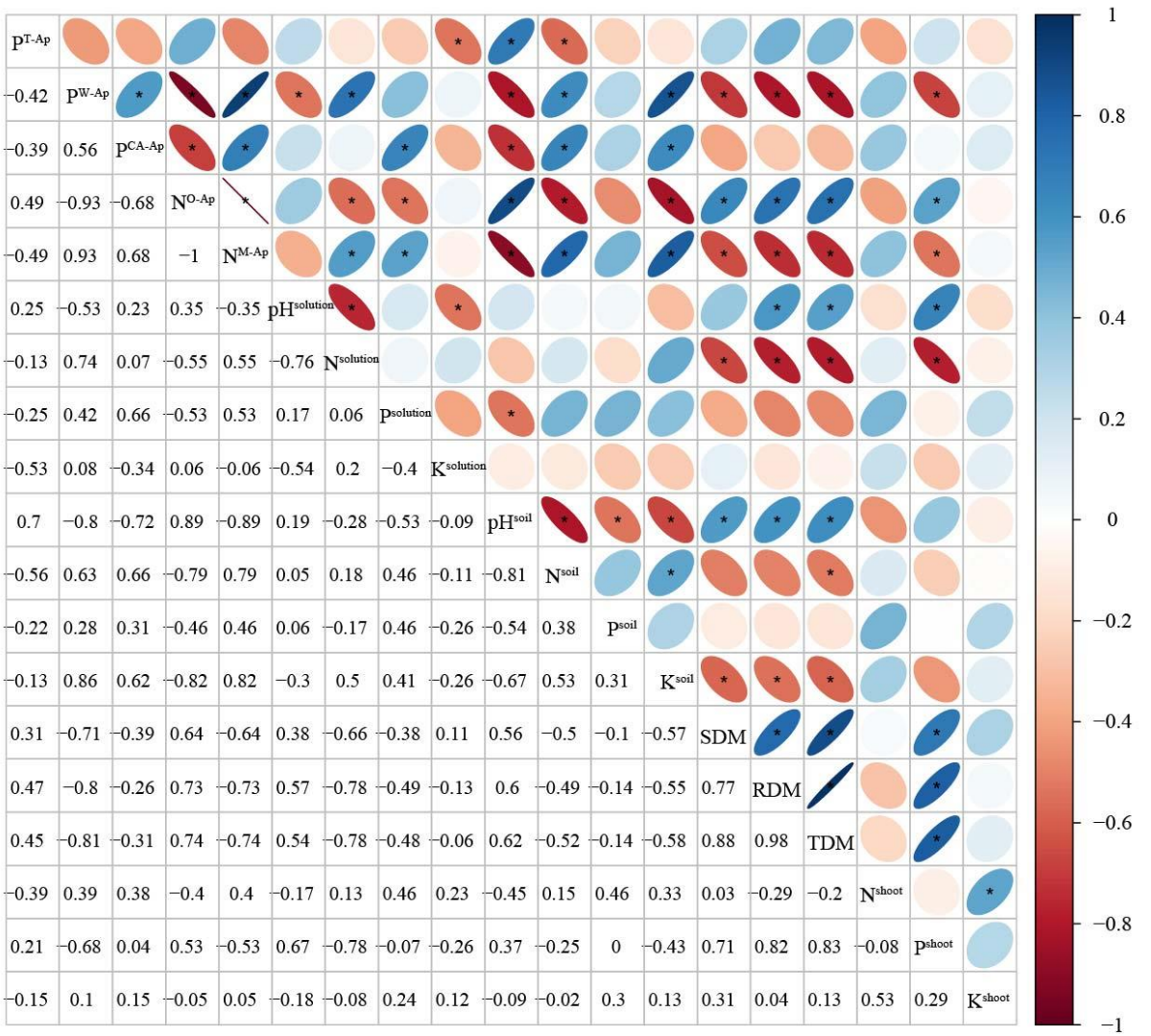

*Significant Pearson correlation analysis (p<0.05). $P^{T\text{-}Ap}$, $P^{W\text{-}AP}$ and $P^{CA\text{-}Ap}$: Amounts of P added in soil though fertilizers based on total conents, solubility in water, and citric acid at 2% respectively. $N^{O\text{-}Ap}$ and $N^{M\text{-}Ap}$: N-organic and N-mineral forms applied added in soil though fertilizers respectively; $N^{solution}$, $P^{solution}$ and $K^{solution}$: soil solution contents of N-mineral, P and K respectively; $pH^{solution}$: pH in soil solution; N^{soil}, P^{soil} and K^{soil}: soil availability of N, P and K respectively; pH^{soil}: pH in soil; TDM, SDM and RDM: total, shoot and root dry matter production respectively; N^{shoot}, P^{shoot} and K^{shoot}: Shoot accumulation of N, P and K respectively.

Supplementary material 10. Parameters of models adjusted to mineralization of N and release of P and K in Red Oxisol according to organomineral and monoammonium phosphates (MAP) fertilizers application.

Nitrogen												
Treat.	Elovich			Exponential			Power			Hyperbolic		
	R^2	rmse	AIC	R^2	rmse	AIC	R^2	rmse	AIC	R^2	rmse	AIC
Control	0.95	7.57	130	0.80	16.77	159	0.92	9.79	139	0.93	9.74	139
$P^{25}O^{75}$	0.85	21.13	167	0.76	28.69	178	0.81	23.35	171	0.84	22.04	168
$P^{40}O^{60}$	0.93	14.34	153	0.93	17.89	161	0.88	19.61	164	0.96	10.78	143
$P^{50}O^{50}$	0.92	15.05	155	0.86	21.45	167	0.87	19.17	163	0.96	10.76	143
$P^{75}O^{25}$	0.91	15.40	156	0.91	17.94	161	0.86	20.08	165	0.96	10.27	141
MAP	0.93	13.66	151	0.84	23.19	170	0.89	17.63	160	0.94	12.63	148
Phosphorus												
Treat.	Elovich			Exponential			Power			Hyperbolic		
	R^2	rmse	AIC	R^2	rmse	AIC	R^2	rmse	AIC	R^2	rmse	AIC
Control	0.00	0.05	-50	0.00	0.05	-50	0.00	0.05	-50	0.00	0.05	-50
$P^{25}O^{75}$	0.70	0.17	-7	0.93	0.08	-34	0.67	0.18	-5	0.93	0.08	-33
$P^{40}O^{60}$	0.78	0.21	1	0.83	0.19	-3	0.74	0.23	4	0.91	0.13	-16
$P^{50}O^{50}$	0.75	0.19	-3	0.77	0.18	-4	0.71	0.20	0	0.86	0.14	-13
$P^{75}O^{25}$	0.39	0.33	18	0.53	0.29	13	0.37	0.34	18	0.52	0.30	13
MAP	0.63	0.26	9	0.80	0.19	-3	0.60	0.27	10	0.81	0.18	-4
Potassium												
Treat.	Elovich			Exponential			Power			Hyperbolic		
	R^2	rmse	AIC	R^2	rmse	AIC	R^2	rmse	AIC	R^2	rmse	AIC
Control	0.90	14.47	153	0.92	14.01	152	0.84	18.51	162	0.93	12.32	147
$P^{25}O^{75}$	0.83	25.09	173	0.87	22.64	169	0.77	29.54	179	0.88	22.41	169
$P^{40}O^{60}$	0.87	19.72	164	0.91	16.91	159	0.78	25.69	174	0.91	16.26	157
$P^{50}O^{50}$	0.86	20.72	166	0.92	16.39	158	0.78	26.29	174	0.90	17.62	160
$P^{75}O^{25}$	0.85	23.36	170	0.87	21.45	168	0.76	29.33	178	0.88	20.85	166
MAP	0.93	14.99	155	0.98	8.75	135	0.85	22.07	168	0.96	11.02	143

R^2: coefficient of determination; rmse: root-mean-square error (mg kg^{-1}); AIC: The Akaike information criterion. Treat: Treatment studied; Control: no P-fertilization; $P^{25}O^{75}$: (25% MAP + 37.5% CM (chicken manure) + 37.5% CH (coffee husk)); $P^{40}O^{60}$: (40% MAP + 40% CM + 20% CH), $P^{50}O^{50}$: (50% MAP + 25% CM + 25% CH) and $P^{75}O^{25}$: (75% MAP + 12.5% CM + 12.5% CH).

Supplementary material 11. Parameters of models adjusted to mineralization of N and release P and K in Yellow Oxisol according to organomineral and monoammonium phosphates (MAP) fertilizers application.

Nitrogen												
Treat.	Elovich			Exponential			Power			Hyperbolic		
	R^2	rmse	AIC	R^2	rmse	AIC	R^2	rmse	AIC	R^2	rmse	AIC
Control	0.66	1.48	71	0.73	1.71	76	0.79	1.19	63	0.70	1.61	74
$P^{25}O^{75}$	0.82	7.28	129	0.66	9.97	140	0.79	7.74	131	0.80	7.61	130
$P^{40}O^{60}$	0.63	11.80	146	0.58	12.63	148	0.60	12.26	147	0.66	11.32	144
$P^{50}O^{50}$	0.92	4.25	109	0.81	6.49	124	0.89	4.98	115	0.94	3.58	103
$P^{75}O^{25}$	0.82	7.32	129	0.76	8.47	134	0.78	8.02	132	0.86	6.34	124
MAP	0.54	11.98	146	0.50	12.48	148	0.52	12.24	147	0.60	11.57	145
Phosphorus												
Treat.	Elovich			Exponential			Power			Hyperbolic		
	R^2	rmse	AIC	R^2	rmse	AIC	R^2	rmse	AIC	R^2	rmse	AIC
Control	-	-	-	-	-	-	-	-	-	-	-	-
$P^{25}O^{75}$	0.80	0.04	-56	0.79	0.04	-55	0.78	0.05	-54	0.90	0.03	-69
$P^{40}O^{60}$	0.74	0.04	-61	0.78	0.04	-64	0.71	0.04	-59	0.86	0.03	-73
$P^{50}O^{50}$	0.84	0.05	-50	0.76	0.06	-43	0.81	0.06	-47	0.89	0.04	-57
$P^{75}O^{25}$	0.64	0.06	-46	0.68	0.05	-48	0.62	0.06	-45	0.76	0.05	-53
MAP	0.70	0.12	-19	0.71	0.12	-20	0.67	0.13	-17	0.80	0.10	-27
Potassium												
Treat.	Elovich			Exponential			Power			Hyperbolic		
	R^2	rmse	AIC	R^2	rmse	AIC	R^2	rmse	AIC	R^2	rmse	AIC
Control	0.98	5.25	117	0.95	10.44	142	0.97	6.39	124	0.97	7.06	127
$P^{25}O^{75}$	0.98	3.59	103	0.84	11.48	145	0.96	5.24	117	0.94	6.51	125
$P^{40}O^{60}$	0.94	7.92	132	0.89	12.70	149	0.91	9.89	140	0.93	9.09	137
$P^{50}O^{50}$	0.98	3.89	106	0.90	10.87	143	0.95	6.68	125	0.96	5.88	121
$P^{75}O^{25}$	0.98	4.78	113	0.96	8.03	132	0.93	8.60	135	0.98	4.13	108
MAP	0.97	5.10	116	0.86	13.08	150	0.95	7.07	127	0.94	7.76	131

R^2: coefficient of determination; rmse: root-mean-square error (mg kg^{-1}); AIC: The Akaike information criterion. Treat: Treatment studied; Control: no P-fertilization; $P^{25}O^{75}$: (25% MAP + 37.5% CM (chicken manure) + 37.5% CH (coffee husk)); $P^{40}O^{60}$: (40% MAP + 40% CM + 20% CH), $P^{50}O^{50}$: (50% MAP + 25% CM + 25% CH) and $P^{75}O^{25}$: (75% MAP + 12.5% CM + 12.5% CH).

Supplementary material 12. Parameters of models related to the velocity of the kinetics of mineralization of N and release of P and K adjusted to release process in Red and Yellow Oxisols according to organomineral and monoammonium phosphates (MAP) fertilizers application.

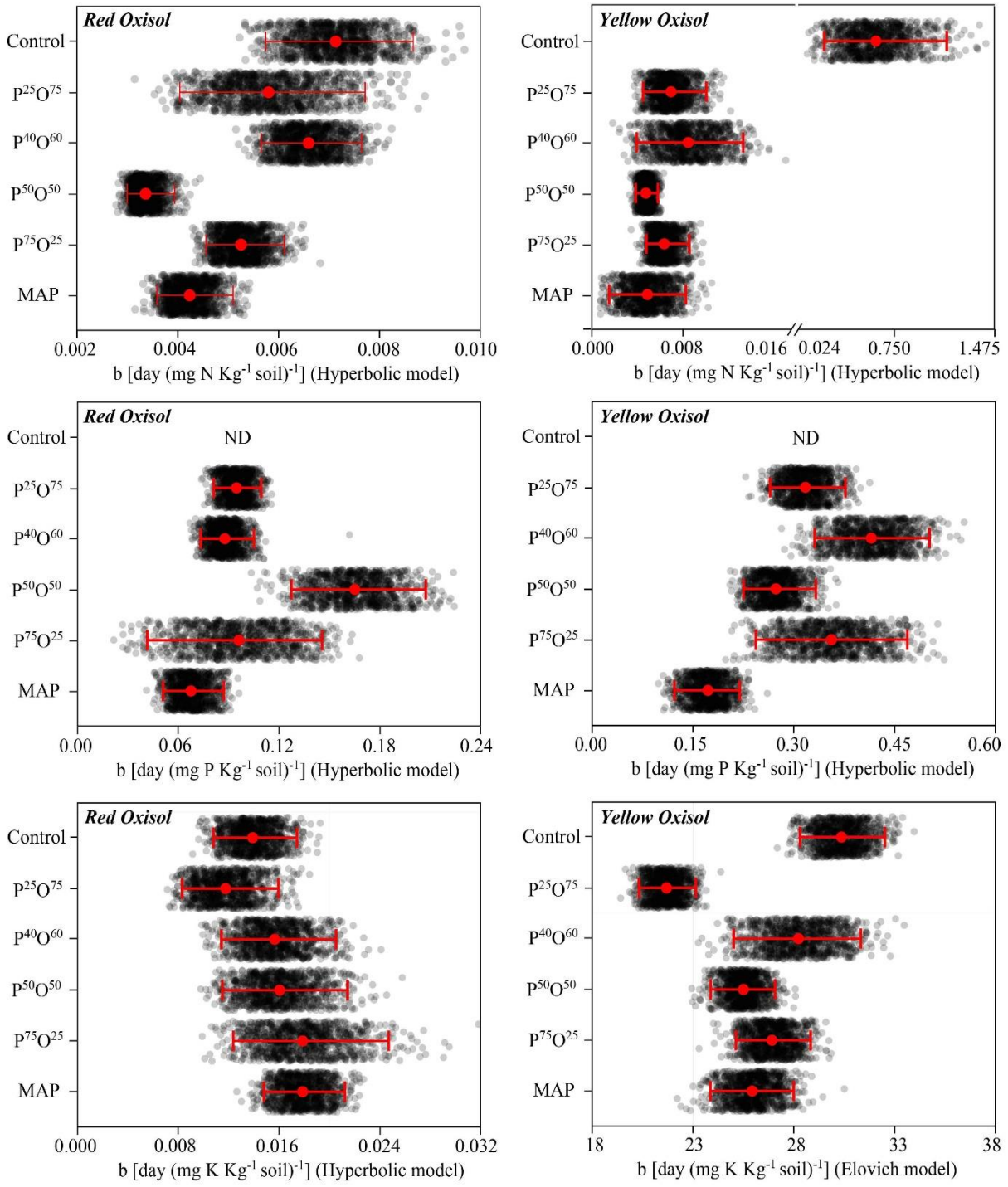

$P^{25}O^{75}$: (25% MAP + 37.5% CM (chicken manure) + 37.5% CH (coffee husk)); $P^{40}O^{60}$: (40% MAP + 40% CM + 20% CH), $P^{50}O^{50}$: (50% MAP + 25% CM + 25% CH) and $P^{75}O^{25}$: (75% MAP + 12.5% CM + 12.5% CH); control: no-P fertilization.

Preliminary version of manuscript edited following the rules of Science of The Total Environment Journal

Biochar-based phosphate fertilizers: synthesis, properties, kinetics of P release, and recommendation basis for successively grown maize and brachiaria in contrasting Oxisols

Everton Geraldo de Morais[1*] and Carlos Alberto Silva[1]

[1]Departament of Soil Science, Federal University of Lavras, Av. Doutor Sylvio Menicucci 1001, ZIP code: 37200-900, Lavras-Minas Gerais, Brazil.
* Corresponding author: evertonmoraislp@yahoo.com.br

Abstract

Biochar-based fertilizers (BBFs) were produced by acidulation of phosphate rock with different acids, with or no addition of magnesium (Mg), using coffee husk as the feedstock for biochar production. Properties of BBFs produced were assessed by different chemical methods, infrared spectroscopy, and the kinetics of phosphorus (P) release in water or citric acid (CA). To evaluate the agronomic performance, maize plants and, in sequence, brachiaria were grown in pots filled with two Oxisols with contrasting texture and soil organic matter (SOM) contents. P recommendation for plants was based on the total P content of fertilizers. In both maize and brachiaria cultivation, it was evaluated the P availability in the whole soil and its solution, plant biomass, and P accumulated in the shoot. Using the same chemical stoichiometric ratio, nitric acid was more effective than hydrochloric and sulfuric acids in solubilizing P from P-apatite. Regarding the kinetics of P release, the addition of soluble Mg reduced the amounts of P released in water and maintained or increased P released in CA. The kinetics of P release in water did not explain the variation of P accumulated by maize or brachiaria plants in two

Oxisols; however, when CA was used as the extractor solution, a significant correlation was verified. The higher proportions of P soluble in neutral ammonium citrate plus water (NAC+H_2O) in BBFs increased maize biomass production in Oxisols. The higher residual effect of P for brachiaria growth was found for BBFs produced with the solubilization using nitric acid in Oxisol with the higher SOM. BBFs production by acidulation of low-grade phosphate rock combined with the addition of Mg is an alternative to improve the efficiency of P fertilization in tropical soils. P recommendation for maize and brachiaria should be based on BBFs soluble P content in NAC+H_2O.

Keywords: the kinetics of P release; organomineral fertilizer; soil solution; P-Mg interaction; phosphorus residual effect, P-fertilizer availability chemical index.

Graphical abstract

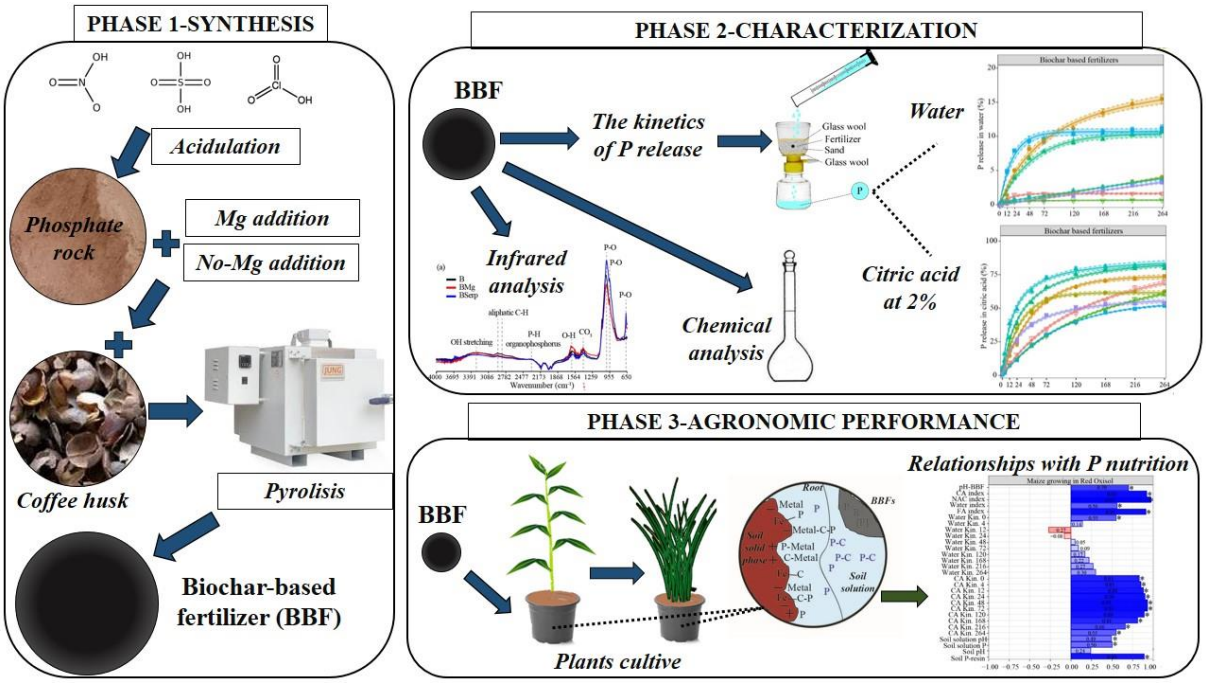

1 Introduction

Tropical Brazilian soils are highly weathered, have low availability of phosphorus (P), and P is prone to be specifically adsorbed in Fe and Al oxides and low-activity mineral colloids, such as kaolinite, which reduces the efficiency of phosphate fertilizers, mainly soluble phosphate fertilizers (Fink et al., 2016; McLaughlin et al., 2011; Withers et al., 2018). Among strategies to increase the efficiency of phosphate fertilization, the increase of the content of soil organic matter (SOM) levels is very effective because organic molecules from SOM can block P fixation sites, and SOM contains humic substances that can form a bond between metal-organic ligand-P, forming new P complexed compounds with higher agronomic performance (Erro et al., 2012). However, increasing SOM levels takes a long time and is an enormous challenge in the tropical landscape due to the high SOM decomposition rate and low input of organic residues in crop fields of most tropical soils (Fink et al., 2016; McLaughlin et al., 2011).

A strategy to ensure beneficial effects of organic molecules on the soil P availability is the production of fertilizers containing both a mineral and an organic matrix, hereafter named organomineral fertilizers (OMFs), with greater agronomic performance in nourishing plants with P than soluble P mineral fertilizers (Erro et al., 2012; Frazão et al., 2021; Lustosa Filho et al., 2017; Martins et al., 2017; Sakurada et al., 2016, 2019). OMFs may be produced through different routes, including mixing of low-grade or acidified P sources with biochar that comes from different feedstocks charring under the pyrolysis process, with the subsequent synthesis of biochar-based fertilizers (BBFs) (Lustosa Filho et al., 2019, 2017). BBFs may be produced with the pyrolysis of biomass rich in nutrients and a mixture between nutrient mineral sources, including low-grade P rocks, and organic residues and wastes (Lustosa Filho et al., 2017; Rose et al., 2019; Tumbure et al., 2020; Wang et al., 2012).

The mixture between phosphoric acid or triple superphosphate with coffee husk results in BBFs with a more gradual P release in water due to the formation of P stable forms during

pyrolysis (Lustosa Filho et al., 2017). Synthesis routes, including the mixture of organic residues and igneous phosphate rock, were tested for the production of BBFs and this route is not adequate to solubilize the apatite during the pyrolysis process because only a small portion of P from phosphate rock are solubilized and becomes available to crops (Tumbure et al., 2020). In addition, pyrolysis, by nature, is a process that involves the production of high pH charred matrices. Therefore, biochar is supposed to have in most cases a pH in the alkaline range, and this is not an adequate condition for complete solubilization of apatite, hence the need to acidify charred matrices to solubilize apatite (Tumbure et al., 2020).

The low efficiency of pyrolysis in solubilizing low-grade phosphate rock is due to the high recalcitrance and composition of phosphate rocks, which requires a crucial step of phosphate acidulation to produce high agronomic value P fertilizers (UNIDO and IFDC, 1998). Different acids could be used for this purpose, such as nitric, sulfuric and hydrochloric, resulting in fertilizers with different properties and agronomic performance (UNIDO and IFDC, 1998). In addition, inorganic acids can be mixed in the production of BBFs, before pyrolysis (Lustosa Filho et al., 2017). When inorganic acids interact with the biochar, there is a chemical activation of the biochar matrix, functionalizing its organic matrix compounds, and effect whose magnitude relies on the acid type used (Sahin et al., 2017).

When phosphate rock is acidulated and converted into highly water-soluble mineral fertilizer P chemical species, the P solubilized presents low efficiency in the soil-plant system of most soils (Withers et al., 2018). However, when the acidulation process is followed by mixing of organic compounds with P solubilized chemical species, soluble phosphate reacts with carbon (C) compounds, forming P-organic complexes with higher agronomic performance than single superphosphate (Erro et al., 2012). In addition, other metals (Mg) can be added in the BBFs synthesis the fertilizers produced have new properties as the formation of struvite promotes a more gradual release of P to crops; besides, there is a synergistic effect between P

and Mg on the uptake of both nutrients , mainly P, by plants (An et al., 2021; Lustosa Filho et al., 2017; Suwanree et al., 2022; Talboys et al., 2016).

Pyrolysis has already been used to synthesize biochar-based phosphate fertilizers, which presented a more gradual release of P over acidulated mineral P fertilizers with or without addition of Mg (Lustosa Filho et al., 2017). Fertilizers with a gradual P release may present a higher agronomic performance than readily soluble P sources, increasing P availability in whole soil and its solution in crop stages of high nutritional demand, thus, reducing P losses in soil through specific adsorption, precipitation, formation of low-soluble Ca phosphates etc. (An et al., 2021; Ghodszad et al., 2021). However, in BBFs, if P release is too slow and does not meet plant nutritional demand, growth may be hampered for crops with a short window to grow and uptake P, such as maize (Lustosa Filho et al., 2017). Dynamics of P-fertilizer release is anticipated by P kinetics release studies. In most P kinetics release studies, water is used as the extractant solution, though 0.01 M $CaCl_2$ solutions are also employed to leachate soluble phosphate (Baird et al., 2019; Carneiro et al., 2021; Lustosa Filho et al., 2017). The relationship between P released in water and nutrient plant uptake was mathematical modeled for mineral fertilizers, and its use for OMFs may be limited due to the unique properties of OMFs, as the presence of nutrients in mineral and organic forms. For this reason, it is necessary to verify the correlation between the amounts of P in water released in the kinetic studies, plant P uptake, and other test solutions to leachate P in kinetics release studies.

Organic acids are capable to simulate the capacity of plants to acquire P; thus, P-BBF kinetics release can correlate with P-fertilizer organic acid indices since plant roots can release organic acids such as citric (CA), malic and oxalic acids to mobilize P chemical species in the rhizosphere (Adeleke et al., 2017). Use of CA, neutral ammonium citrate plus water ($NAC+H_2O$) and formic acid (FA) solutions are proposed to estimate the P solubility indices in OMFs and their relation with P uptake by plants (Duboc et al., 2022; Rose et al., 2019; Wang

et al., 2012). These P-fertilizer indices aforementioned extract different pools of P in OMFs, though some chemical species of P can not be assessed by these extractant solutions, though they may be available when plants are successively cultivated (Sakurada et al., 2016; Wang et al., 2012). Even for the main crop, P pools in BBFs not assessed by fertilizer chemical solubility indices may be partially responsible for possible greater agronomic performance of OMFs over mineral fertilizers. A higher P uptake by maize was linked to the use of OMF over MAP due to a lower proportion of contents of P soluble in NAC+H_2O concerning total P, which resulted in forms of applied P not assessed by NAC+H_2O solution since the recommendation was based on soluble P contents in NAC+H_2O, already in soybean cultivated using an OMF with a high proportion of soluble P in NAC+H_2O, there was no difference in P uptake by the use of OMFs over MAP (Frazão et al., 2021).

Fertilizer P pools can be assessed both by chemical analytical methods or predicted by infrared spectroscopy (Duboc et al., 2022; Lustosa Filho et al., 2017; Wang et al., 2012). Due to a more gradual release of P from different forms of P in organic-based fertilizers, OMFs can promote a higher residual effect (residual P) than mineral fertilizers (Martins et al., 2017; Sakurada et al., 2016). The first and second crops need to be successively grown and evaluated to assess the P residual effect for the subsequent crop. The effect of OMFs is highly dependent on soil properties, relying mainly on SOM content since certain pools of organic compounds in soils are capable of improving the use efficiency of fertilizer P by crops, thus, masking less evident the potential effect of the OMF organic matrix on the soil P chemistry and availability (Erro et al., 2012; Fink et al., 2016). In this study, we hypothesized that the production of BBFs from the mixture of coffee husk and the acidification of Araxá phosphate rock (APR) combined with Mg addition and the formation of biochar produce the BBFs with spectroscopy properties, and with contrasting P-fertilizer indices, which controls the P release and agronomic efficiency of BBFs by maize-brachiaria successively grown in two Oxisol with contrasting texture and

SOM contents. The aims of this study were: I) To produce BBFs with different chemical properties and P solubility indices; II) To decrease P soluble in water by mixing coffee husk biochar and Mg in the synthesis of BBFs; III) to investigate lab protocols to evaluate the kinetics of P release using water and CA as extractant solutions; IV) To correlate P pools with the amounts of P released in the kinetics of P release study with the P uptake by maize and brachiaria successively grown in two contrasting Oxisols; V) To evaluate in soils residual P effect of BBF over triple superphosphate and low-grade Araxá phosphate.

2 Material and Methods

2.1 Biochar-based fertilizers synthesis

Twelve organomineral fertilizes based on pyrolysis of a mixture of the coffee husk (CH), APR, inorganic acids and addition or no of Mg were performed. Coffee husk and APR were mixed at a ratio of 2:1 (mass of CH: mass of APR). Coffee husk and APR were dried and passed through a 1 and 0.25 mm mesh sieves, respectively. CH used had 17.3 and 42.4 g kg^{-1} to N and K total contents, and 1.2, 1.0, 1.2, 1.1 and 1.1 g kg^{-1}, respectively, of P total, P soluble in water, in NAC+H_2O, in citric acid at 2% (CA), and formic acid at 2% (FA). APR used had 126.22, 0.10, 6.52, 16.96 and 15.53 g kg^{-1}, respectively, contents of P total, P soluble in water, in NAC+H_2O, in CA and in FA. Before pyrolysis, initially, the no-acidulation or acidulation of APR was performed using three different inorganic acids (H_2SO_4-98%), hydrochloric (HCl-37%) and nitric (HNO_3-65%) acids (Reagent grade, Synth). In sequence, CH and APR were without (no Mg) or mixed with Mg supplied as a soluble Mg source (MgCl) (Reagent grade, Synth) or as a low-grade serpentinite rock.

The proportion of inorganic acid was based on the H_2SO_4 amount used to solubilize the low-grade P rocks in the phosphate fertilizer industry, as follows: 0.58:1 (w:w) ratio of H_2SO_4 to AR low-grade rock (UNIDO and IFDC, 1998). Based on the stoichiometric ratio used

to mix H_2SO_4 with AR, the amounts of HCl and HNO_3 was also determined considering the chemistry basis used by Sahin et al. (2017) to evaluate the chemical activation, as well as in the same stoichiometry ratio to solubilize phosphate rocks by different acids (UNIDO and IFDC, 1998). Mg was incorporated at a 1:1 mol P:Mg ratio (Lustosa Filho et al., 2017). After the pre-treatment, the mixtures were dried at 60 ^{o}C until constant weight and pyrolysis were performed using a muffle furnace whose temperature was set to 300 °C at a heating rate of 10 °C min^{-1}, maintaining the target temperature for 30 min. The pyrolysis and BBFs production were performed with three repetitions. The treatments studied were shown and described in **Table 1**.

Table 1. Acronyms of treatments used in the production of biochar-based fertilizers (B).

Acronyms	Acid type	Mg source
B	No acidulation	No Mg addition
BMg		MgCl
BSerp		Serpentinite
BSA	Sulfuric acid	No Mg addition
BSAMg		MgCl
BSASerp		Serpentinite
BHA	Hydrochloric acid	No Mg addition
BHAMg		MgCl
BHASerp		Serpentinite
BNA	Nitric acid	No Mg addition
BNAMg		MgCl
BNASerp		Serpentinite

2.2 BBFs chemical characterization

Biochar samples were passed through a 1 mm sieve. The pH of biochar samples was determined in water at a ratio of 1:10 (w:v) through a pH digital Toledo Meter (Singh et al., 2017). After sulfuric digestion, total nitrogen (N) content was determined through the Kjeldahl method (Phares et al., 2020). Ammonium (NH^{4+}) and nitrate (NO_3^-) contents in biochar were extracted with 2 mol L^{-1} KCl solution (10 mL extractant g^{-1} of biochar) and determined by

distillation followed by titration (Singh et al., 2017). N loss during pyrolysis was calculated due to the use of nitric acid in feedstockpre-treatment as follows (Eq. 1):

$$\text{N loss}=\left(100-\left\{100\times\left[\frac{(\text{DWBc (g)}\times\text{N-Bc (mg g}^{-1}))}{((\text{DWBm(g)}\times\text{N-Bm(mg g}^{-1}))+(\text{DWAdd(g)}\times\text{N-Add (mg g}^{-1}))}\right]\right\}\right) \quad \text{(Eq. 1)}$$

Where: DWBc, DWBm and DWAdd are, respectively, the biochar mass, dry weight biomass and dry weight additive (Mg and acid); N-Bc, N-Bm and N-Add are, respectively, N contents in biomass, biomass mass, and the amount of additive (Mg or acid).

Total P and potassium (K) contents were determined through the nitric-perchloric acid analytical method (Enders and Lehmann, 2012). P soluble in water was extracted by successive washing of 1 g of BBFs using a paper filter with distilled water until reaching a final volume of 250 ml in a volumetric flask (Brazil, 2017). The P content soluble in CA was extracted by stirring 1 g of fertilizer with 100 ml of CA solution at 2% for 30 min (Brazil, 2017). The P content soluble in NAC+H_2O was extracted by boiling 1 g of fertilizer in 50 ml of NAC+H_2O solution (Brazil, 2017). Based on the method recommended by P available in biochar, the content of P soluble in FA solution at 2% was also determined; thus, 0.35 g of biochar were mixed with 35 ml of 2% FA, ultrasonicated for 10 min, then shaked for 30 min (Singh et al., 2017). The P contents extracted by water, CA, NAC+H_2O and FA were determined using the vanadomolybdate method (Kitson and Mellon, 1944). To compare the P solubility of BBFs, a P index was calculated, taking into account the ratio of soluble P fractions water or CA or NAC+H_2O or FA and total P content in BBFs, as follows (Eq. 2):

$$\text{P index (\%)}=\left(\frac{\text{Soluble P content }\left(\text{g kg}^{-1}\right)}{\text{Total P content }\left(\text{g kg}^{-1}\right)}\right)\times 100$$

(Eq. 2)

2.3 Infrared spectroscopy

Twelve OMFs synthetized samples were scanned in the medium infrared region, the main peak in spectra were identified, bonds, functional groups, features and spectroscopic signatures determined as well. The infrared spectrum was obtained using the Attenuated Total Reflectance (ATR) Fourier Transform Infrared (FTIR) spectroscopy technique in an Agilent® Cary 630 spectrometer. Measurements and spectra were generated at 4000 to 650 cm^{-1} wavenumber range with a resolution of 4 cm^{-1}. In each FTIR spectrum, pre-processing (normalization) of the dataset was performed (Gautam et al., 2015). The main peaks were identified and interpreted according to the infrared library available elsewhere and assignments for the main peaks (Maluf et al., 2018; Singh et al., 2017; Socrates, 2004; Stuart, 2004; Y. Wang et al., 2014).

2.4 The kinetics of P release

Based on BBFs properties and spectroscopy analysis, a cluster analysis was performed, and eight BBFs were selected and, together with APR and TSP properties, were evaluated regarding their role in nourishing crops successively grown as well as related to the kinetics of P release dataset and parameter of mathematical equations to predict P released. OMFs samples produced with CH and serpentinite were not evaluated. The TSP used had 196.13, 175.00, 185.37, 175.33 and 177.62 mg kg^{-1}, respectively, of P total, P soluble in water, in NAC+H_2O, in CA and in FA contents. Two extraction solutions were chosen to evaluate the kinetics of P release; therefore, water and CA were used at 2% as extractant solutions. The fertilizers were incubated with sand in a mini-lysimeter with periodic leaching of incubated BBFs, using distilled water (for more details, see manuscript 2 of thesis) or a CA solution at 2%, hereafter defined as a new method to evaluate the dynamics of P in leachates of the sand incubated BBFs. In the mini-lysimeter, it was added 200 mg kg^{-1} of P based on the total P content of each BBF.

Initially, 50 ml of distilled water or CA solution was passed through each fertilizer incubated, delimiting this leaching time as 0 h, then the volume of water or CA solution used in each leaching and leachates were sampled in the following incubation time: 0, 4, 12, 24, 48, 72, 120, 168, 216 and 264 hours. Leaching solutions were added to the sand-fertilizer mixture at a cumulative equivalent rate of 7 mL h^{-1}. P concentration in solutions leached was determined by the vanadomolybdate method (Kitson and Mellon, 1944). The kinetics of P release in water or in CA was normalized according to the total P content of each fertilizer packed added.

2.5 BBFs agronomic performance

To verify the agronomic efficiency of eight BBFs synthetized over APR and TSP, maize plants and, in sequence, brachiaria were grown in Red (RO) and Yellow (YO) Oxisols with contrasting texture and soil organic matter contents (**Table 2**). Plants were grown in pots filled with 0.8 kg Oxisol and 300 mg kg^{-1} P, which was based on the total P content of each fertilizer and homogenously mixed with the whole soil in each pot. Eleven treatments were studied in a completely randomized design with three repetitions for each Oxisol. One treatment in which plants were cultivated without P application (negative control), and ten treatments related to P fertilizers as follows: APR, TSP, B, BMg, BSA, BSAMg, BHA, BHAMg, BNA, BNAMg. All fertilizers were only added to Oxisols at the beginning of maize cultivation.

Table 2. Main chemical, physicochemical, and texture of Oxisols used in maize-brachiaria growing.

Oxisol	pH	C	Clay	Silt	Sand	P-rem
		——————g kg^{-1}——————				mg L^{-1}
Red	4.9	19.8	770	100	130	15.5
Yellow	6.2	4.5	460	85	455	11.7

Oxisol	Total N	P	K	Ca^{2+}	Mg^{2+}	Al^{3+}
	————mg kg^{-1}————			————$cmol_c$ kg^{-1}————		
Red	2,580	8.3	16.6	0.2	0.1	0.8
Yellow	329	6.1	2.5	1.9	0.1	0.1

pH was determined in H_2O at a ratio of 1:2.5 (w/v); P: available phosphorus determined by resin soil test, K: available potassium determined by Mehlich-1 soil test; P-rem: remaining phosphorus; exchangeable calcium (Ca^{2+}), exchangeable magnesium (Mg^{2+}) and aluminum (Al^{3+}) determined by KCl 1 mol^{-1} soil test; C: carbon determined (dry combustion) in an automatic TOC analyzer; clay, silt and sand assessed by the Boyoucos method. All methodologies are described in details in Teixeira et al. (2017).

Liming was performed in RO, aiming to raise pH to 6-6.5 and increase the contents of exchangeable calcium (Ca) and Mg using carbonates ($CaCO_3$ and $MgCO_3$ at the 4:1 ratio using Reagent grade, Synth). After mixing with carbonate, soil samples were incubated for 30 days, and soil moisture was kept close to 70% of the soil maximum water holding capacity (MWHC). In YO, soil acidity correction was not performed as the pH and Ca^{2+} contents were already at optimum levels for plentiful maize growth. Mg in YO was provided at the sowing fertilization. According to the difference in total contents of N and K found in BBFs fertilizers, there was a standardization of N and K amount applied, using in maize planting fertilization 100 mg kg^{-1} of N and 200 mg kg^{-1} of K. N and K supplied in the sowing fertilization were supplied to plants as NO_4NO_3 and KCl (Reagent grade, Synth). In the maize planting fertilization, it was also provided 30, 40, 0.81, 2, 7.3, 0.15, 5 and 10 mg kg^{-1} respectively of Mg, sulfur (S), boron (B), copper (Cu), manganese (Mn), molybdenum (Mo), zinc (Zn) and iron (Fe), which were respectively supplied to plants with $MgSO_4.7H_2O$, H_3BO_3, $CuSO_4.5H_2O$, $MnCl_2.4H_2O$, $(NH_4)_6Mo_7O_{24}.4H_2O$, $ZnSO_4.7H_2O$ and $FeCl_3.6H_2O$ (Reagent grade, Synth).

After the sowing fertilization, soil moisture was maintained close to 70% MWHC, then, five maize seeds were sowed per pot. Five days after planting, thinning was performed to grow only one maize plant per pot. Maize top-dressing fertilization was carried out at 14 and 21 days after planting, adding to soil 125 mg kg^{-1} N supplied as NH_4NO_3 (Reagent grade, Synth), and maize was grown for 30 days. After the maize cultivation, in each experimental unit, ten seeds of brachiaria were sowed per pot. Ten days after planting, thinning was performed, and two brachiaria plants were grown per pot. The Brachiaria planting fertilization was carried out using 50 mg kg^{-1} N and 100 mg kg^{-1} K, which were supplied as NO_4NO_3 and KCl (Reagent grade, Synth). Brachiaria top-dressing fertilization was carried out at 15, 25, 35 and 45 days after planting using 100 mg kg^{-1} N provided as NH_4NO_3 (Reagent grade, Synth). To evaluate fertilizers P residual effects in Oxisols, brachiaria, in sequence, was grown for 55 days.

After 12 hours of planting, an aliquot of the soil solution (20 ml) was collected through the *Suolo Acqua* sampler (Carmo et al., 2016). The soil solution sampler were inserted in the middle of the pot during the filling of the pot with soil. The soil solution samples was filtered through a 0.45 µm pore membrane, and solution pH was determined through a bench pH meter; the content of P in soil solution (solution P) was determined by the vanadomolybdate method (Kitson and Mellon, 1944). After 18 hours of planting, the 30 g samples of whole soil were collected in each experimental unit using a pot soil auger; then, soil samples were dried and sieved (2-mm) and stored for further analyses. In whole soil, it was determined pH at a ratio of 1g of soil to 2.5 ml of water (soil pH) and available P content by the ion-exchange resin method (soil P-resin test) (Teixeira et al., 2017).

After maize and brachiaria cultivation, plants were harvested, separated into shoot and root, and then dried in a laboratory oven at 60°C until constant weight. The dried biomass was weighed, and shoot (SDM) and root (RDM) dry matter were determined. Total dry matter (TDM) was obtained by adding SDM to RDM. SDM was sieved (1-mm), and samples were

digested in a mixture of nitric and perchloric acids at a 4:1 ratio; P in the shoot was determined by the molybdenum blue method (Silva, 2009). According to the SDM and P content in plant tissue of each experimental unit, P accumulated in the shoot (P in shoot) was calculated as follows (Eq. 3):

$$\text{P in shoot} = \text{shoot dry matter (g)} \times \text{P content in the shoot tissue (mg g}^{-1}\text{)} \quad \text{(Eq. 3)}$$

2.6 Statistical analysis

All statistical analysis was carried out using the following R Software packages: stats, base, tidyverse, agricolae, factoextra, FactoMineR, pvclust and corrplot (Kassambara and Mundt, 2020; Lê et al., 2008; Mendiburu, 2020; R Core Team, 2020; Suzuki et al., 2019; Wei and Simko, 2017; Wickham et al., 2019). In the characterization of the twelve OMFs produced, mean of N losses and soluble P indices were compared by the Duncan test ($p<0.05$), considering that the assumptions of analysis of variance (ANOVA) were attained and the significant difference was verified ($p<0.05$). The whole dataset of pH and P in whole soil and its solution, besides maize and brachiaria biomass production and P in both crops shoot were also compared by the Duncan test ($p<0.05$).

The dataset of the kinetics of P release in water or CA was adjusted to different non-linear mathematical models as an output of the relationship between incubation time versus the amount of P released from each fertilizer (Dou et al., 1996; Liang et al., 2014; Lustosa Filho et al., 2017). The following mathematical models were adjusted to P kinetics dataset: Linear model (Eq. 4), Elovich model (Eq. 5), simple exponential model (Eq. 6), power function (Eq. 7), parabolic model (Eq. 8) and hyperbolic model (Eq. 9).

$$Pt = a + bt \quad \text{(Eq. 4)}$$

$$Pt=a+b\ln t$$

(Eq. 5)

$$Pt=N0\left(1-e^{-kt}\right)$$

(Eq. 6)

$$Pt=a*t^{b}$$ (Eq. 7)

$$Pt=a+\left(bt^{0.5}\right)$$

(Eq. 8)

$$Pt=\frac{N0*t}{(N0*b+t)}$$

(Eq. 9)

Where: Pt: fraction of P released from fertilizer in the leaching time evaluated; a, initial P content released from fertilizer; b, P release rate constant for each fertilizer, t, time of release (hour); N0, the maximum amount of P released from fertilizer during the whole kinetics study.

The best model was selected according to the higher value of the coefficient of determination (R^2), the lowest value of root-mean-square error (rmse), and the lowest value of the Akaike Information Criterion (AIC) (Akaike, 1979). Mathematical models fitted to each fertilizer rate of nutrient release were compared using a 95% confidence interval and 1000 bootstrap interactions.

The synthetized BBFs were grouped in two ways, considering their chemical attributes or Middle infrared spectral signature. Initially, the dataset was scaled, and the cluster analysis was based on the matrix of Euclidean distances among samples, using the Ward's algorithm hierarchical clustering (Ward, 1963). Each dendrogram branch was calculated using the bootstrap support. To determine the relationship between the chemical properties of BBBs synthesized (excluding dataset of BBFs produced with serpentinite) and the P nutrition status of maize and brachiaria grown in the two contrasting Oxisols. Initially, it was removed from

the dataset the data related to plants fertilized with TSP, APR and non-fertilized with P; using this new and processed dataset, the Pearson's correlation analysis was performed.

3 Results

3.1 BBFs chemical properties

Fertilizer pH and NPK pools were shown in **Table 3**. During pyrolysis, a higher losses of N occurred when nitric acid was used in pre-treatment (88.5% of N added was volatilized during pyrolysis) (**Supplementary material 1**). Addition of MgCl increased N losses during pyrolysis in non-acidified and hydrochloric acid pre-treated feedstock. According to pH and NPK pools, the cluster analysis formed five groups (clusters) of fertilizers (**Figure 1**). The BNA formed the group with intermediate values of P soluble in water and higher values of P soluble in CA, FA and NAC+H_2O, a high value of N-Total and N-mineral contents. The second group was formed by BNAMg and BNASerp, which had properties similar to group I; however, the main difference of BBFs of group II was their lower N-mineral content over fertilizers from group I. Group III was formed by BHASerp, BHA, BHAMg and BSAMg. The BBFs of group III over other BBFs grouped had intermediate values of P soluble in CA, FA and NAC+H_2O, and lower contents of total N. The main properties of group IV formed by BSASerp and BSA were their higher contents of P soluble in water over other OMFs; however, over other BBFs produced by acidulation of apatite, fertilizer from this specific group has a lower proportion of P soluble in CA, FA and NAC+H_2O. BBFs enclosed in group V with lower contents of P soluble in water, CA, FA and NAC+H_2O (B, BMg and BSerp).

Table 3. pH, nitrogen (N), phosphorus (P), and potassium (K) pools and contents in biochar-based fertilizers (B).

Fertilizer	pH	N^{Total}	$N\text{-}NH_4^+$	$N\text{-}NO_3^-$	K^{Total}
		g kg^{-1}			
B	5.3 ±0.1	10.72 ±0.49	0.035 ±0.005	0.058 ±0.002	34.90 ±1.74
BMg	4.3 ±0.1	7.67 ±0.23	0.038 ±0.007	0.038 ±0.007	35.81 ±1.39
BSerp	5.4 ±0.1	8.99 ±0.35	0.033 ±0.002	0.066 ±0.003	33.15 ±0.13
BSA	2.9 ±0.2	9.71 ±0.13	0.058 ±0.003	-	36.62 ±1.51
BSAMg	5.3 ±0.1	9.42 ±0.05	0.118 ±0.007	-	36.49 ±0.48
BSASerp	3.6 ±0.2	7.73 ±0.06	0.146 ±0.003	-	32.84 ±1.57
BHA	4.4 ±0.2	10.74 ±0.29	0.155 ±0.007	-	28.52 ±0.15
BHAMg	5.6 ±0.2	9.30 ±0.13	0.240 ±0.003	-	29.16 ±1.05
BHASerp	4.8 ±0.2	7.97 ±0.10	0.170 ±0.005	-	28.08 ±2.13
BNA	6.8 ±0.3	21.05 ±0.14	0.054 ±0.003	2.702 ±0.089	34.08 ±3.89
BNAMg	7.5 ±0.1	15.88 ±0.33	0.057 ±0.003	0.114 ±0.007	32.84 ±2.00
BNASerp	10.3 ±0.1	14.55 ±0.06	0.053 ±0.004	-	29.34 ±2.60

Fertilizer	P^{Total}	P^{H_2O}	P^{CA}	P^{NAC+H_2O}	P^{FA}
	g kg^{-1}				
B	51.91 ±1.58	1.15 ±0.10	9.88 ±0.31	4.73 ±0.16	12.26 ±0.15
BMg	51.25 ±0.49	0.78 ±0.01	9.03 ±0.15	4.09 ±0.15	9.02 ±0.15
BSerp	50.16 ±1.15	0.94 ±0.04	8.71 ±0.11	3.91 ±0.07	10.80 ±0.17
BSA	54.64 ±3.66	4.79 ±0.14	7.01 ±0.23	12.83 ±0.26	6.96 ±0.03
BSAMg	57.31 ±2.55	6.06 ±0.28	20.39 ±0.05	20.50 ±0.23	20.01 ±0.21
BSASerp	52.51 ±0.65	5.18 ±0.15	9.67 ±0.09	9.74 ±0.21	10.64 ±0.37
BHA	56.16 ±0.71	1.94 ±0.02	23.14 ±1.19	21.96 ±0.04	21.64 ±0.12
BHAMg	54.96 ±0.38	3.91 ±0.19	25.47 ±0.11	24.09 ±0.21	22.39 ±0.22
BHASerp	58.73 ±2.11	2.50 ±0.09	12.32 ±0.05	14.93 ±0.03	11.27 ±0.07
BNA	58.84 ±0.65	4.31 ±0.02	30.69 ±0.26	31.79 ±0.54	29.69 ±0.46
BNAMg	48.03 ±0.44	3.61 ±0.02	29.14 ±0.29	31.54 ±0.31	27.76 ±0.63
BNASerp	52.94 ±0.55	1.03 ±0.04	25.12 ±0.36	25.80 ±0.24	27.09 ±1.19

Not detected or low limit of detection of method. N^{Total}, $N\text{-}NH_4^+$ and $N\text{-}NO_3^-$: contents of nitrogen total, ammonium and nitrate respectively; K^{Total}: total contents of potassium; P^{Total}, N^{H_2O}, N^{CA}, $N^{NAC+H_2O}$and N^{FA}: contents of total phosphorus (P), P soluble in water, in citric acid at 2%, in neutral ammonium citrate plus water, and in formic acid at 2% respectively. More details of the BBFs acronyms were shown in Table 1.

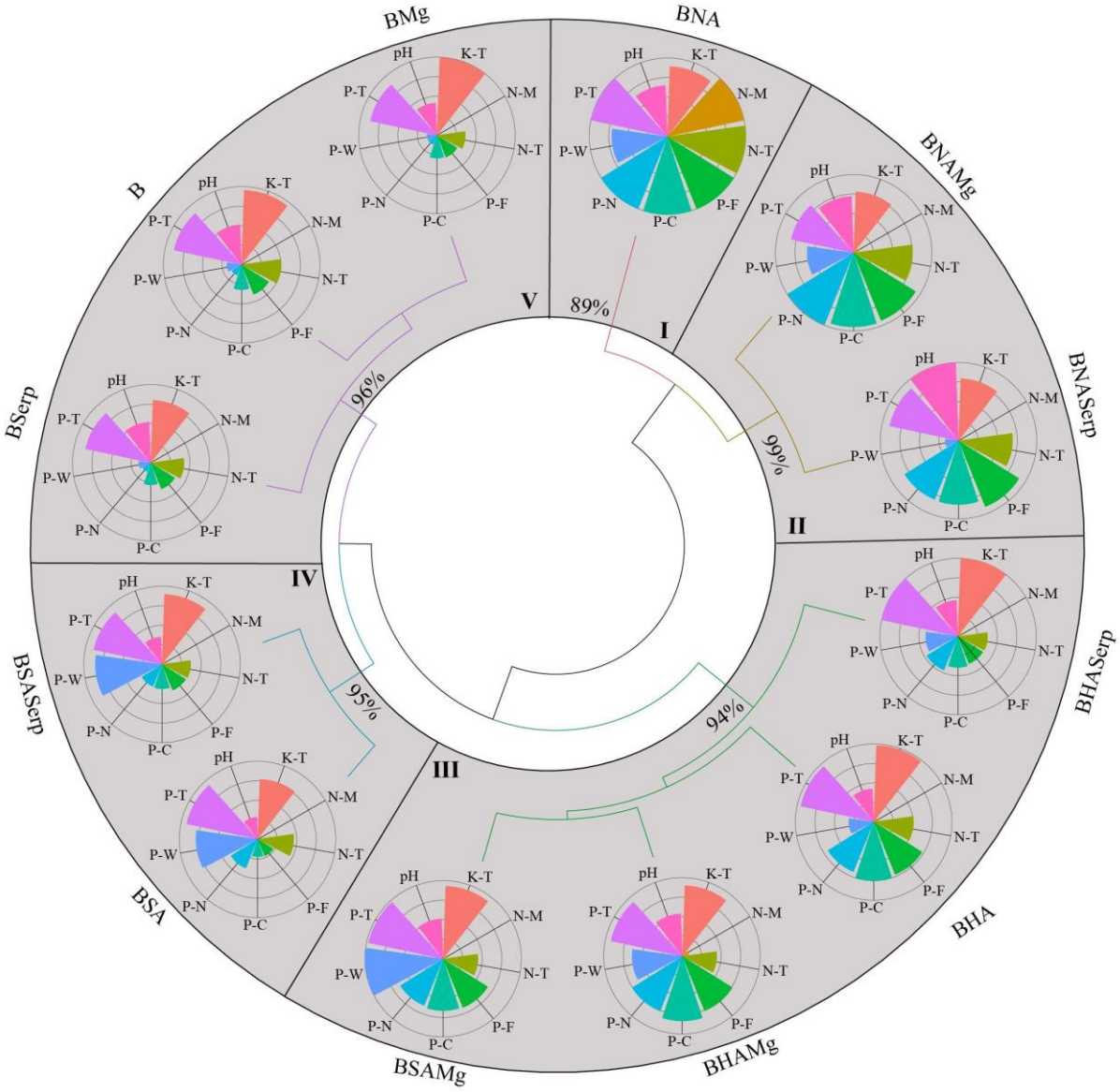

Figure 1. Cluster analysis between all biochar-based fertilizers (BBFs) synthetized. Percentage means the similarity within each group formed by cluster analysis. K-T: total content of potassium; N-M and N-T: contents of N-mineral and N-total; P-F, P-C, P-N, and P-W: the content of P soluble in formic acid at 2%, in citric acid at 2%, in neutral ammonium citrate plus water and water respectively; P-T: total content of P. The radar charts at the tip of terminal branches display the ratio of value variable in each biochar/maximum valor of variable found in all OMFs for each variable measured rescaled to vary between 0 and 1 (maximum across all samples). More details of the BBFs acronyms were shown in Table 1.

The P solubility index related to contents of P soluble by different extractant solutions as a percentage of total P content in BBF had a higher proportion of P soluble in CA, FA and NAC+H_2O by nitric acid-based BBFs, followed by hydrochloric acid and sulfuric acid (**Figure 2**). Compared to the exclusive use of nitric, hydrochloric or sulfuric acids, Mg addition as

magnesium chloride increased all fertilizer-P solubility indices. Thus, serpentinite as an Mg source was not effective in increasing fertilizer-P solubility indices. A higher P soluble in water index was verified when sulfuric acid was mixed with coffee husk and MgCl before pyrolysis in order to produce BSAMg.

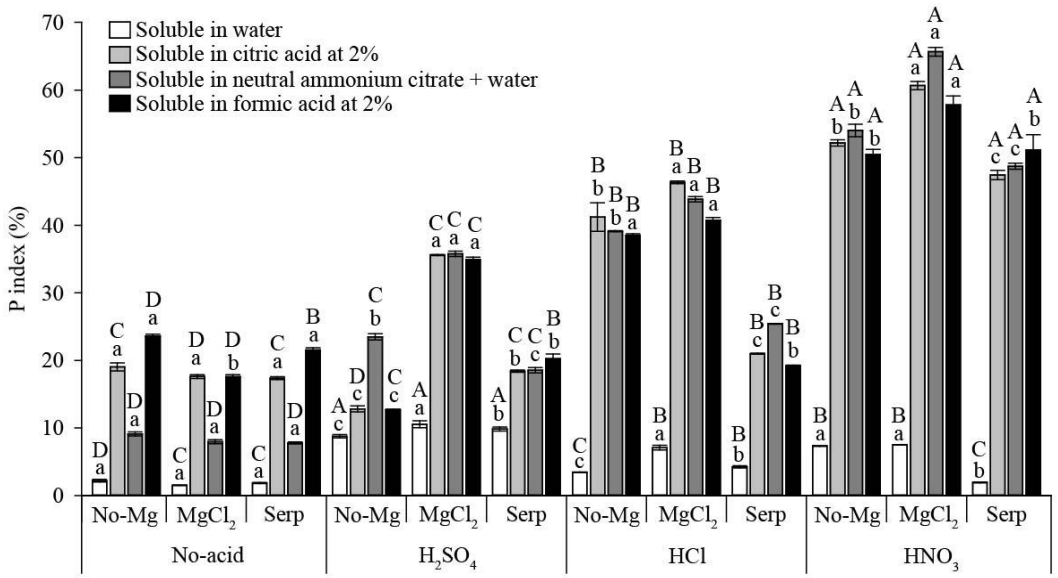

Figure 2. Amounts of fertilizer-P solubility index different extractant solutions as a percentage of total P content (P index) in fertilizers according to different acid and Mg source were used before pyrolysis to produce BBFs. The bars with standard error followed by the same capital letter did not differ the acid treatment in each Mg condition tested according to the Duncan test ($p<0.05$). The bars with standard error followed the same minuscule letter and did not differ the Mg condition in each acid treatment tested according to the Duncan test ($p<0.05$). No-Mg: no-Mg addition; $MgCl_2$: Mg added via magnesium chloride; Serp: Mg added via serpentinite. More details of the BBFs acronyms were shown in Table 1.

3.2 Infrared spectroscopy

The Mg sources used in BBFs synthesis did not generate new peaks in FTIR spectrum (**Figure 3**). The OH stretching was founded for all BBFs at different IR spectrum, including between 3400 and 3200 cm^{-1} for non-acidified fertilizers, at 3380 and 3250 cm^{-1} for hydrochloric and nitric acids used previous to biochar production, and at 3620 and 3550 cm^{-1} for sulfuric acid-derived BBFs; in fact, for sulfuric acid-derived biochars, the OH stretching

was related to tertiary alcohols. Aliphatic C groups were recorded at 2915 and 2850 cm^{-1} for all BBFs. O-H bonds were also verified for all BBFs at 1615, 1620, 1625 and 1640 cm^{-1}, respectively, to non-acidified, sulfuric, hydrochloric and nitric acid-derived BBFs.

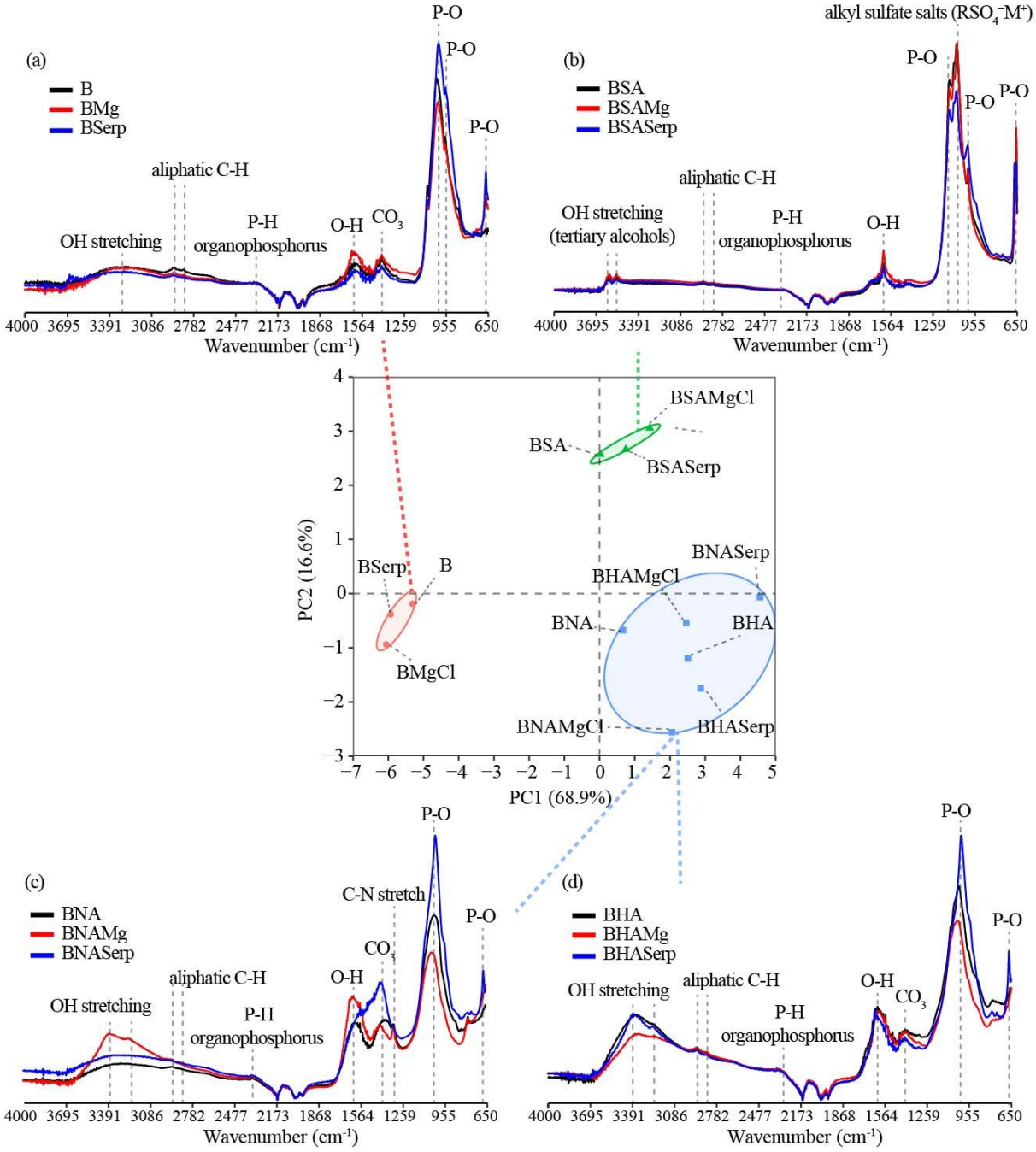

Figure 3. Attenuated Total Reflectance Fourier Transform Infrared spectrum of biochar based-fertilizers (BBFs) and its division by cluster analysis. More details of the BBFs acronyms were shown in Table 1.

The P-H organophosphorus groups were found at 2353 cm^{-1} for all BBFs. The P-O groups were founded in no-acid (1025, 960 and 670 cm^{-1}), sulfuric (1150, 960 and 670 cm^{-1}), hydrochloric (1040 and 670 cm^{-1}) and nitric-derived (1040 and 670 cm^{-1}) biochars. Peaks related to the CO_3 groups were found in non-acidified (1420 cm^{-1}), hydrochloric (1425 cm^{-1}) and nitric acids-based BBFs. When sulfuric acid was used to treat coffee and produce BBFs, the charred matrices had a peak at 1080 cm^{-1}, which was related to RSO_4^+M alkyl sulfate salts. When nitric acid was used before pyrolysis, resulting BBFs showed a peak at 1350 cm^{-1}, related to the C-N stretch. Based on FTIR spectrum, three groups regarded the type of acid employed before the pyrolysis and BBFs production. According to BBFs FTIR spectral signature and PCA, three clusters were formed: group I (B, BMg and BSerp), group II (BSA, BSAMg and BSASerp) and group III (BNA, BNAMg, BNASerp, BHA, BHAMg and BHASerp).

3.3 The kinetics of P release

The models chosen to fit P released over time (kinetics study) were based on the lower values of RMSE, the highest value of the coefficient of determination and lower values of AIC (**Supplementary materials 2 and 3**). For P released in water, the exponential model was the best that fitted to P released by TSP, B, BSA and BNA, while the linear model explained most of the variation of P released by BSAMg, BHAMg and BNAMg. The hyperbolic model fitted better to explain P released by APR, BMg and BHA. When kinetics of P release was performed using CA solution, the Power model was the one that best fitted to TSP and APR leached P, while the hyperbolic model fitted better for B, BMg, BSAMg, BNA and BNAMg of P in leachates, and the exponential model was the best one to explain variation of P released from BSA, BHA and BHAMg.

Not acidified fertilizers (B and BMg) had a lower amount of P release in water among BBFs (**Figure 4**). For P released in water, when Mg was added via MgCl, previously pyrolysis,

the P release in water was reduced and a gradually and continuously released over leaching time (linear model). Considering time of 264 hours, the amount of 3.3, 4.1 and 3.6% of total P in BBFs, respectively, were released by BSAMg, BHAMg and BNAMg. When Mg not was used in BBFs synthesis, up to 36 hours, the amount of P released by BNA and BHA were similar. After 36 hours, BHA had a higher amount of P over BNA. From 72 to 96 hours, BHA had similar amounts released compared. After 96 hours, BHA releases higher amounts of P than other BBFs synthetized. Initially, the higher amount of P released in water was higher than BSA, and from 72 hours, the amount of P released was constant. After 156 hours, the amounts released of P by BSA and BNA were similar and lower than BHA.

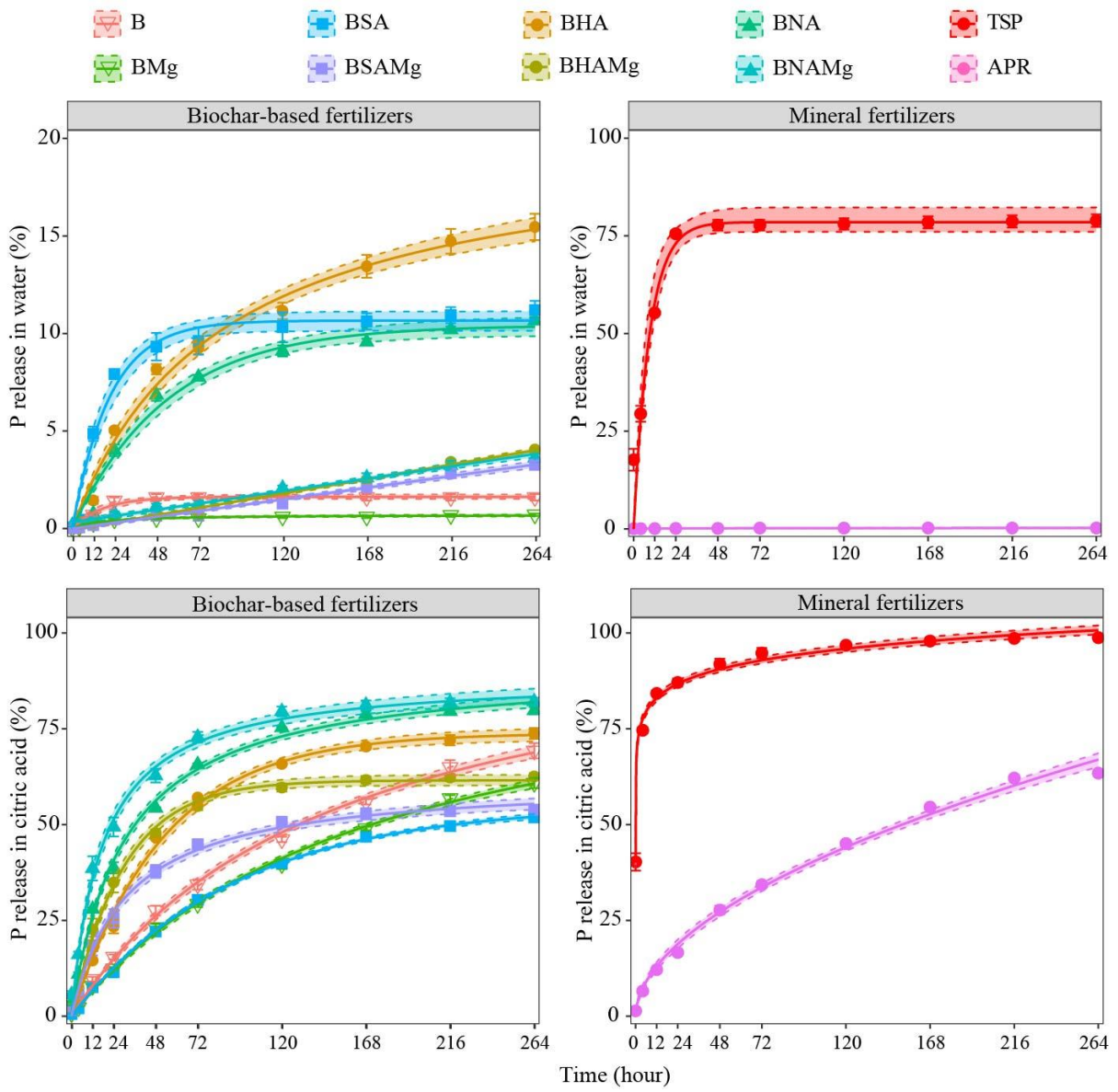

Figure 4. The kinetics of P release in water and citric acid at 2% as related to total P content of biochar based-fertilizers (BBFs) and mineral fertilizers (TSP: triple superphosphate; APR: Araxá phosphate rock). More details of the BBFs acronyms were shown in Table 1.

The TSP had a higher and faster release of P in water than BBFs; about 76% of the total P content in TSP was released up to 24 hours. After 24 hours, the release of P from the TSP tended to stabilize, reaching values of 78.9% at the end of the kinetics study using water. The released of P in the water of APR was the lowest among fertilizers, inferior to 0.3% of total P content. At 264 hours of the kinetics of P release in water, the amounts of P released were:

1.6, 0.7, 11.2, 3.3, 15.5, 4.1, 10.7, 3.6, 0.2, and 78.9, respectively, for B, BMg, BSA, BSAMg, BHA, BHAMg, BNA, BNAMg, AR and TSP.

When the kinetics of P release was performed using CA solution, the pattern of P release was different among BBFs. Amounts of P released in CA increased when nitric acid was used previously for BBFs production regardless of the Mg addition. A higher initial P release was found for BNAMg; however, after 168 hours, the P release was similar for BNA and BNAMg (**Figure 4)**. Higher initial P release amounts were also verified due to Mg addition when hydrochloric acid was used to produce BBFs; however, after 72 hours of incubation, the amounts of BHA were higher than BHAMg. The lower P amounts after 264 hours were verified for sulfuric acid-derived BBFs. Initially, Mg addition increased the P released; however, up to 264 hours, the amounts of P released by BSA and BSAMg were similar. Unlikely the kinetics of P release in water, when CA was used, P release was higher for B, BMg and APR. P released in CA by TSP was higher and faster than P amounts released by BBFs, reaching values close to 92% at 48 hours of accumulated leaching time, while at 264 hours, the P release was about 99% of TSP total P. Comparing the confidence interval of models (95%) up to 264 hours, the amounts of P release in CA followed this order: TSP (99.0%) > BNAMg (79.8%) = BNA (82.0%) > BHA (73.8%) > B (69.3%) = FA (63.4%) > BHAMg (62.6%) = BMg (60.9%) >BSAMg (53.9%) = BSA (51.9%).

3.4 BBFs agronomic efficiency: maize nutrition and growth

P availability in whole soil evaluated by the P soil resin method showed higher values for TSP over BBFs in both Oxisols (**Figure 5**). In RO, among BBFs, the soil P-resin contents followed this decreasing order: BNA = BNAMg > BHAMg = BHAMg > BSAMg; however, compared to TSP, there was a reduction in soil P-resin of approximately 42, 39, 47, 48 and 60%, respectively, for BNA, BNAMg, BHAMg, BHAMg and BSAMg. B, BMg and BA did

not increase the soil P-resin over APR for maize grown in RO. In YO, the acidulation process before pyrolysis increased the soil P-resin over APR as follows: BNAMg > BNA > BHAMg > BHA > BSAMg > BSA; however, the soil P-resin was lower over TSP added to YO. Reduction of soil P-resin were, respectively, 21, 29, 42, 47, 52 and 70% for BNAMg > BNA > BHAMg > BHA > BSAMg > BSA, compared to TSP.

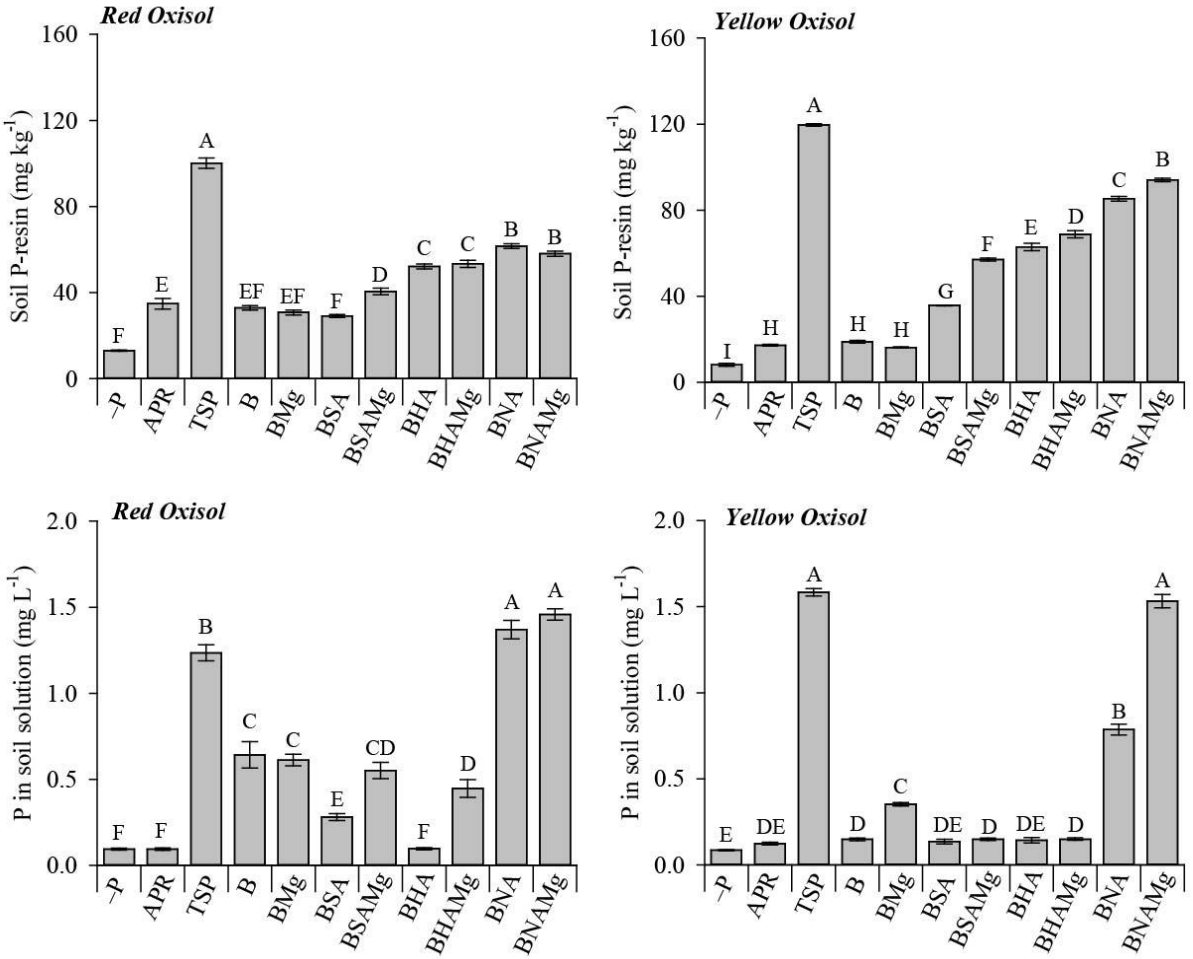

Figure 5. Available Phosphorus (P) in whole soil assessed by the resin soil test, and contents of P in soil solution for maize grown in the Red and Yellow Oxisols. Bars with standard error followed by the same letter did not differ the treatments according to the Duncan test (p<0.05). –P: no P fertilizer to plants; TSP: triple superphosphate; APR: Araxá phosphate rock. More details of the BBFs acronyms were shown in Table 1.

The P content in soil solution in RO was higher for BNAMg and BNA over TSP, increasing ~14.5% (**Figure 5**). The other BBFs reduced the solution P over TSP addition to

RO. BBFs with lower P content in soil solution in RO than TSP, B, BMg, BSAMg, BHAMg and BSA increased the solution P over APR application in RO. When maize was cultivated in YO, TSP and BNAMg had a higher soil solution P than the other BBFs and APR. Compared to APR, the following BBFs: BNA, BMg, BHAMg, BSAMg, and B increased the soil solution P contents, although they were lower than solution P in TSP-treated soils.

Considering the recommendation of P to crops based on the fertilizer total P content, TSP was the source of P that produced the highest maize biomass (SDM, RDM and TDM) in both Oxisols (**Figure 6**). Among BBFs used to treat RO, the BNAMg promoted a higher SDM and TDM than APR, and BSAMg, BHA, BHAMg and BNA had similar values regarding SDM and TDM. The P in the shoot of maize grown in RO was higher by nitric acid-derived BBFs regardless of Mg addition via $MgCl_2$ (BNA and BNAMg) than APR; however, the values were lower than TSP; on average, 51 and 59% less P accumulated in the maize shoot fertilized with BNA and BNAMg. Compared to APR in RO, the BSAMg, BHA, and BHAMg showed similar values, and B, BMg and BSA decreased the P accumulated in the maize shoot. In YO with the lowest OM, BSA, BSAMg, BHA, BHAMg, BNA, and BNAMg had higher SDM, RDM, TDM and P in maize shoot, with a higher increase of to BSAMg, BNA and BNAMg. However, compared to TSP, the BBFs reduced the P in maize shoot, with values of about 57, 44, 51 and 57% of the maize in the shoot of TSP, respectively, to BSAMg, BHAMg, BNA and BNAMg.

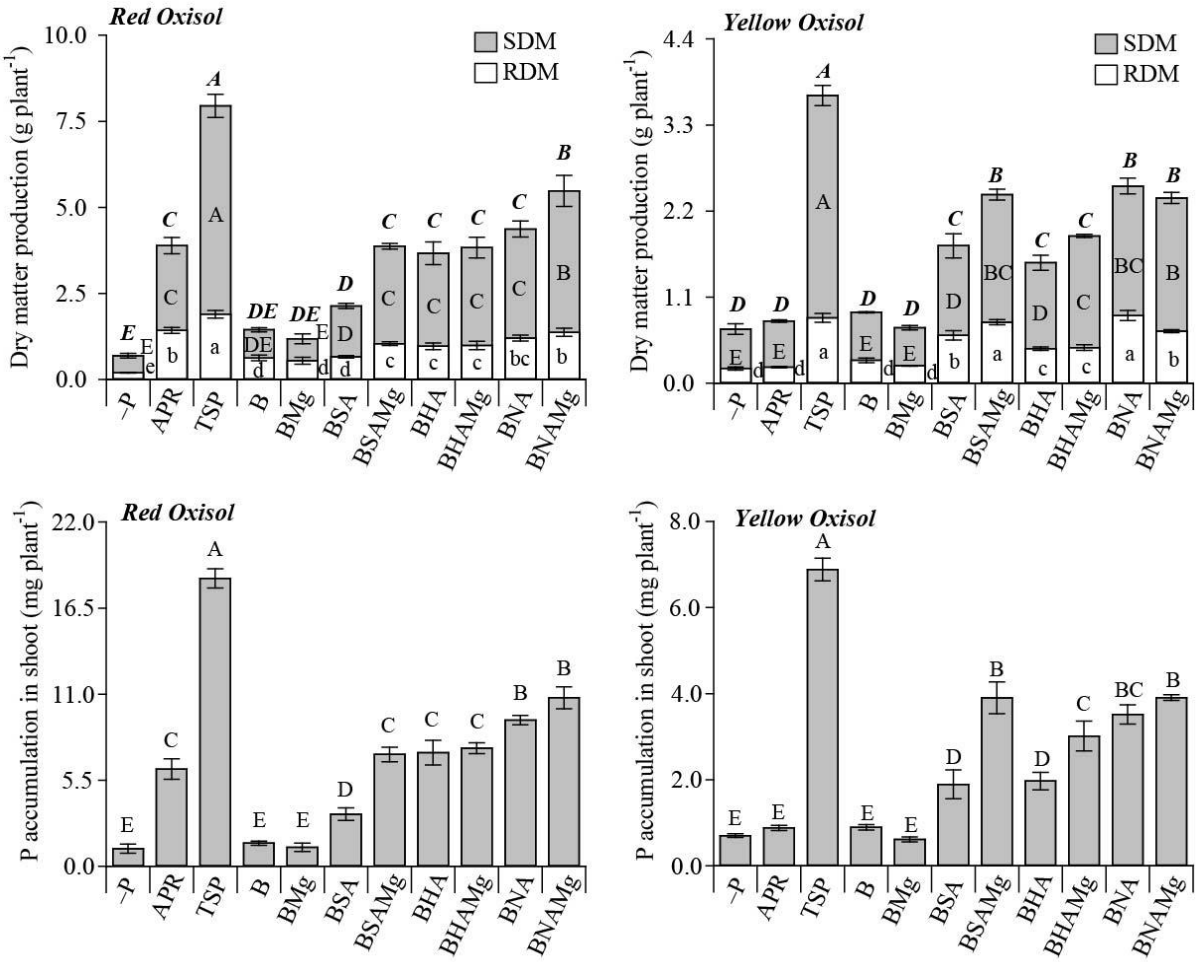

Figure 6. Biomass production and phosphorus (P) accumulated in maize shoot for maize growing in Red and Yellow Oxisols. The bars with standard error followed by the same bold italic, capital, and minuscule letter did not differ the treatments respectively for total (full bar), shoot (SDM), and root (RDM) dry matter production according to the Duncan test (p<0.05). The bars with standard error followed by the same capital letter did not differ the treatments for p accumulated in maize shoot according to the Duncan test (p<0.05). –P: no P fertilizer application; TSP: triple superphosphate; APR: Araxá phosphate rock. More details of the BBFs acronyms were shown in Table 1.

3.5 BBFs P residual effect on brachiaria nutrition and growth

In RO, evaluating the residual effect on soil P-resin, BHA, BHAMg, BNA, and BNAMg had higher soil P-resin than TSP. Thus, soil P-resin increased about 40, 40, 26 and 36%, respectively, for BHA, BHAMg, BNA and BNAMg-treated soils (**Figure 7**). Residual effect of BSA and TSP on soil P-resin was similar in RO. Among treatments with P application for maize grown in RO, the soil P-resin residual effect on brachiaria was lower for APR, B and

BMg over other BBFs. TSP had a higher soil P-resin residual effect in YO, followed by BNAMg = BNA > BHAMg > BHA = BSAMg > BSA, with a reduction of 25, 28, 38, 43, 45 and 64 %, respectively for P-resin in BNAMg, BNA, BHAMg, BHA, BSAMg and BSA-treated soils, compared to TSP. A higher residual effect of BBF on the content of P in the soil solution of RO was verified for BNAMg, BNA and BSAMg over TSP, with an increase for BNA and BNAMg of ~ 87% over TSP (**Figure 7**). In YO, the BSAMg, BSA, BNA and BNAMg increased ~60% the content of P in soil solution over TSP-treated soils.

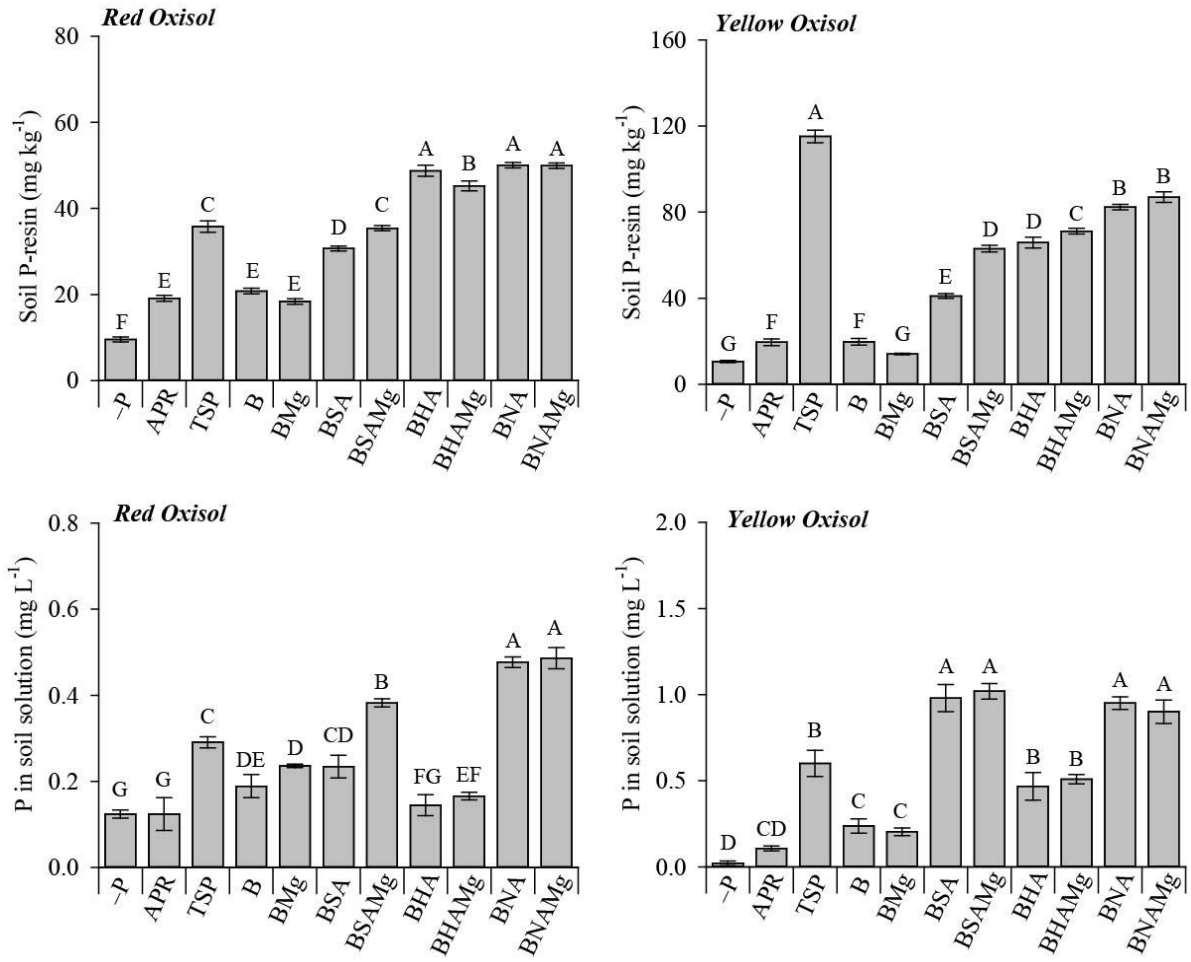

Figure 7. Phosphorus (P) residual available in whole soil by resin method and contents of P in soil solution for brachiaria growing in Red and Yellow Oxisols. The bars with standard error followed by the same letter did not differ the treatments according to the Duncan test (p<0.05). –P: no P fertilizer application; TSP: triple superphosphate; APR: Araxá phosphate rock. More details of the BBFs acronyms were shown in Table 1.

Despite the little effect on maize growth, the BSA, BNA and BNAMg showed the positive residual effects of P on brachiaria biomass production (**Figure 8**). In RO, BSA, BNA and BNAMg had lower SDM and TDM than TSP, reaching 51-74% and 61-96 % respectively to SDM and TDM compared to TSP. However, the RDM was similar to BSA and BNAMg and higher to BNA (increase about 32%) than TSP applied to RO. When P in brachiaria shoot was evaluated in RO, the BNA had similar values to TSP. BSA, BHA and BNAMg increased the B in brachiaria shoot over APR applied in RO, reaching values about 57, 61 and 61 % respectively to BSA, BHA and BNAMg compared to TSP. In YO, the brachiaria biomass production (SDM, RDM and TDM) and P in brachiaria shoot of BBFs and APR were very low compared to the TSP, and the BNA with higher biomass production and P in maize shoot, compared to other BBFs, only reached respectively to 15, 21, 18 and 21% of SDM, RDM, TDM and P in the shoot compared to TSP.

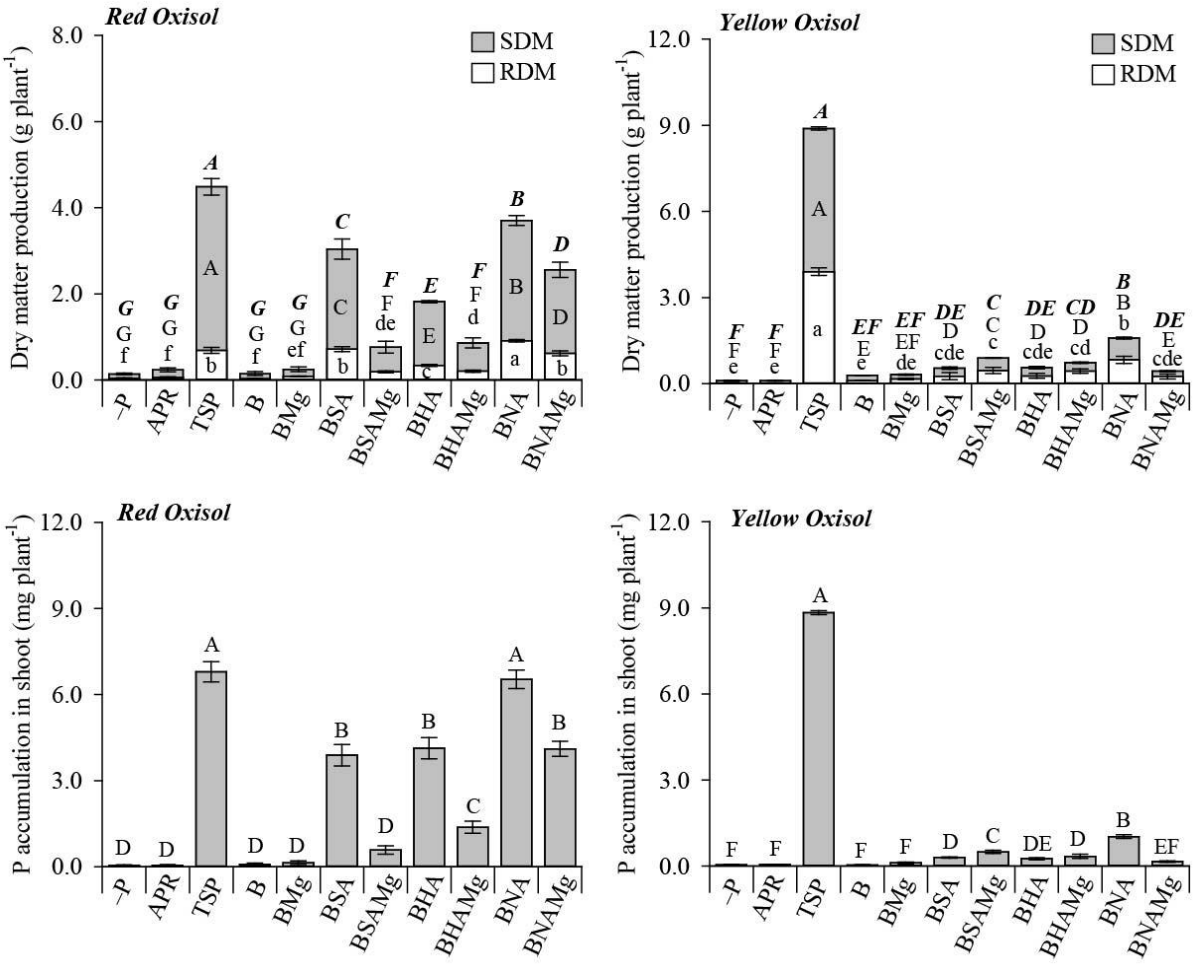

Figure 8. Biomass production and phosphorus (P) accumulated in brachiaria shoot for brachiaria growing in Red and Yellow Oxisols after maize cultivation. The bars with standard error followed by the same bold italic, capital, and minuscule letter did not differ the treatments respectively for total (full bar), shoot (SDM), and root (RDM) dry matter production according to the Duncan test (p<0.05). The bars with standard error followed by the same capital letter did not differ the treatments for P accumulated in brachiaria shoot according to the Duncan test (p<0.05). –P: no P fertilizer application; TSP: triple superphosphate; APR: Araxá phosphate rock. More details of the acronyms of BBFs were described in Table 1.

3.6 Correlation matrix analysis

When maize was grown in RO and YO, significant correlations were found between P in maize shoot and the pH of BBFs, soluble P index (CA, water, NAC+H2O and FA) (**Figure 9**). Higher correlation coefficients for BBFs chemical properties were observed between NAC+H_2O and P accumulated in maize shoot, respectively, with r equal to 0.97 and 0.85 for RO and YO, respectively. The kinetics of P release in water was not correlated with P in maize

shoot in both Oxisols. Amounts of P released in kinetics study using a 2% CA solution positively correlated with P in maize shoot, and the higher coefficient of correlation was observed between P in shoot and the amount of P released up to 48-72 hours for RO (r: 0.93) and between 12-24 hours in YO (r: 0.79-0.80). An increase in soil solution pH, soil solution P and soil P-resin contents due to BBFs application positively correlated with P in maize shoot for both Oxisols, and it was related to soil pH and P in maize shoot in YO. The highest coefficients of correlation were verified for Soil P-resin and P in maize shoot (r = 0.85-0.89).

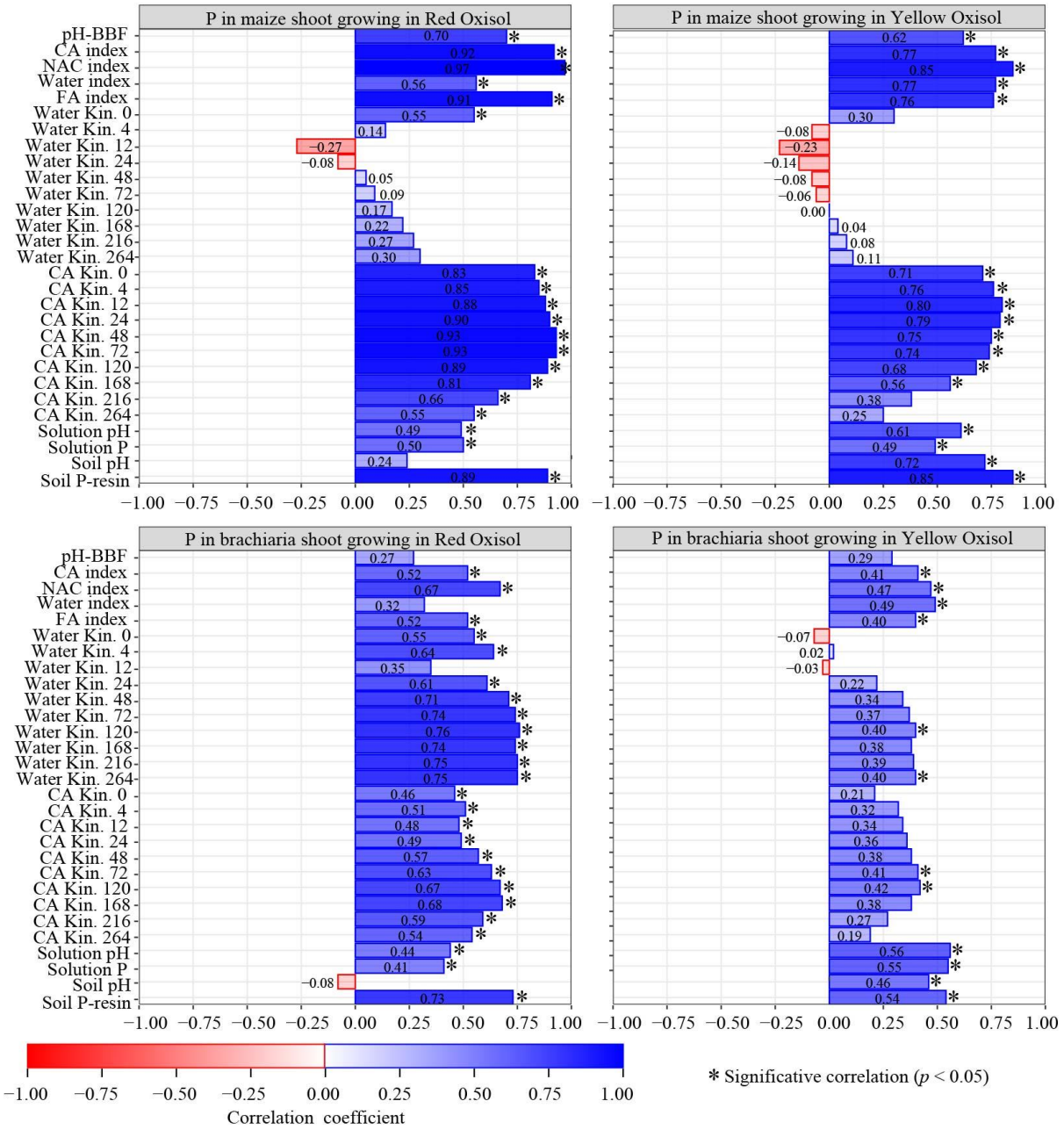

Figure 9. Pearson's correlation analysis between phosphorus (P) accumulated in maize or brachiaria shoot and biochar based-fertilizers (BBFs) properties or whole soil and its solution properties. pH-BBFs: pH of BBFs, CA, NAC, Water, FA: index of P soluble in citric acid (2%), neutral ammonium citrate plus water, water, and formic acid (2%), respectively; Water Kin. 0, 4, 12, 24, 48, 72, 120 168, 216 and 264: amounts of P release in kinetics of P release in water at 0, 4, 12, 24, 48, 72, 120 168, 216, and 264 hours, respectively; CA Kin. 0, 4, 12, 24, 48, 72, 120 168, 216 and 264: amounts of P release in the kinetics of P release in citric acid (2%) at 0, 4, 12, 24, 48, 72, 120 168, 216 and 264 hours, respectively; Solution pH and soil pH: pH determined in whole soil and its solution, respectively; Solution P and soil P-resin: P available determined in whole soil and its solution, respectively.

When brachiaria was grown after maize, the same significant correlations were found for P in brachiaria shoot and CA, NAC+H_2O and FA soluble P index (**Figure 9**). The relation between the water-soluble P fertilizer index and P in brachiaria shoot was observed only for plants grown in YO. Coefficients of correlation between soluble P indexes and P in the shoot were lower for brachiaria than maize plants. For the brachiaria grown in RO, the kinetics of P release in water or CA correlated positively with P in the plant shoot, with a higher correlation of P with amounts of P released in water. The P in brachiaria shoot only positively correlated with amounts of P released in water up to 120 and 264 hours; for P in brachiaria shoot, P released in CA between 72-120 hours was the best correlated with P in shoot. In the brachiaria experiment, an increase in soil solution pH, solution P, and Soil P-resin also positively correlated with P in maize shoot in both Oxisols, as well as with soil pH and P in maize shoot in YO. A higher correlation coefficient (r) was observed between soil P-resin and P in maize shoot; thus, in this case, r was 0.75 for plants grown in RO and 0.54 for YO-cultivated plants.

4 Discussion

4.1 BBFs chemical and spectroscopic characterization

Organic residues can be mixed after the synthesis of mineral fertilizers or even during the synthesis creating a organomineral fertilizers (OMFs), which potentially might have a higher agronomic performance than mineral fertilizers, depending on fertilizer properties, as happened with using biochar in OMFs synthesis (Carneiro et al., 2021; Erro et al., 2012; Frazão et al., 2021; Lustosa Filho et al., 2017; Maluf et al., 2018; Sakurada et al., 2016). For this reason, we synthesized different OMFs called biochar-based fertilizers (BBFs) with different chemical properties and nutrient pools (**Table 3**). The pH of BBFs varied from 2.9 to 10.3, which is relevant because fertilizer pH is an important property determining fertilizer solubilization and reactions of nutrient with components in the soil-fertilizer interface. At the same time, chemical

forms and pools of nutrients evaluated by different extractant solutions control the nutrient release kinetics in the soil-fertilizer interface, determining, thus, agronomic efficiency and capacity of OMFs in nourishing plants (Binh and Zapata, 2002; Lombi et al., 2005; Urrutia et al., 2014).

Based on P pools in BBFs, evaluating the P soluble in different extractor methods, when APR and CH were mixed to produce BBFs using the pyrolysis process without acidulation, a lower soluble P content was verified in relation to total P in BBFs over acidulated-rock phosphate derived BBFS (**Figure 2**). The mixture between Dorowa phosphate rock and maize residue pyrolysed at 450 ^{o}C was not effective in destabilizing the phosphate rock and solubilize P (Tumbure et al., 2020). Thus, in this study, pyrolysis at 300 ^{o}C without acidulation of APR was also not effective solubilizing P from apatite. The BBFs produced without acidulation regardless of Mg addition formed one group through cluster analysis of chemical or FTIR spectrum (**Figures 1 and 3**).

Due to the low natural availability of P in phosphate rocks, commonly in the synthesis of phosphate fertilizers, phosphate rock is commonly converted into highly soluble mineral fertilizers through the acidulation process using inorganic acids, which has a low agronomic performance of fertilizers produced and is therefore unsustainable (Withers et al., 2018). However, the addition of organic matrix during the synthesis of fertilizers may increase the agronomic performance of fertilizers by generating OMFs with P complex (Erro et al., 2012). Besides, when inorganic acids are contacted with biochar, inorganic acids may disestablish biochar structure, promoting the chemical activation (Sahin et al., 2017), effects indicated by changes observed in infrared analysis (**Figure 3**).

The same stoichiometric ratio used in acidulation of P-phosphate rock or activation of biochar allows comparing the efficacy of different acids on the final fertilizer properties (Sahin et al., 2017; UNIDO and IFDC, 1998). Based on the same stoichiometry (mol of acid: g of P-

APR), the nitric and hydrochloric acids promote a higher P solubilization of APR over sulfuric acid (**Figure 2**). P-apatite rock dissolves readily when nitric acid is mixed with low-grade phosphate as it happens in the nitrophosphate production route (UNIDO and IFDC, 1998). When sulfuric acid is mixed with P-rock phosphate, initially, there is a fast reaction, with subsequent formation of phosphoric acid (H_3PO_4) and calcium sulfate ($CaSO_4$). In sequence, in a much slower process the phosphoric acid formed in first step of apatite solubilization reacts again with the P-rock forming monocalcium phosphate ($Ca(H_2PO_4).H_2O$). Although the reactions take place simultaneously, the second step is slower and occurs after several days or weeks of sulfuric acid-rock phosphate incubation. Thus, the material is stored in piles for the final curing process from 2-6 weeks (UNIDO and IFDC, 1998). In our process of BBF synthesis, a curing process was not required, since the reaction is instantaneous, which explains a lower amount of soluble P in CA, NAC+H_2O and FA when sulfuric acid was used in the acidulation process (**Table 3**).

Although the main effects on the P solubility index were related to the type of acid used during the acidulation step, the Mg addition also showed different effects in a Mg source depend-effect (**Figure 2**). Serpentinite could not promote changes that would allow it to differentiate the resulting BBFs when no-Mg was added or Mg added via magnesium chloride, as demonstrated by grouping always similar to the no-Mg added or Mg added via magnesium chloride (**Figure 1**). When compared to different sources of Mg, the Mg provided via serpentinite over magnesium chloride reduced the proportion of P soluble in both solution extractor methods evaluated (water, CA, NAC+H_2O and FA) (**Figure 2**). The lower proportion of soluble P when serpentinite was used, regardless of the type of acid in the acidulation process, is due to the need for acid solubilization of serpentinite so that Mg in stable and insoluble forms can be solubilized to soluble forms of Mg more prone to chemical reactions with other chemical compounds and ions (Teir et al., 2007; Vieira et al., 2022). In summary, part of the acid used

to solubilize apatite was consume in phosphate rock solubilization, while the remaining acid possibly was consumed in serpentinite solubilization, thus, the effectiveness of the P solubilization from APR reduces.

When Mg was supplied as magnesium chloride, a soluble source of Mg, all the added acid could be used to solubilize P from APR. The Mg added via magnesium chloride had the best results increasing the contents of P soluble in CA, NAC+H2O and FA when combined with the acidulation process regardless type of acid (**Figure 2**). However, the higher increase was observed in sulfuric acid plus Mg over isolated sulfuric acid treatment, increasing about 177, 52 and 174 %, respectively, to P soluble in CA, NAC+H_2O and FA. The Mg added via magnesium chloride also increases the P soluble in water to acidulation using sulfuric and hydrochloric acids. Mg added during synthesis of P-biochar reacts with phosphates forming magnesium pyrophosphate ($Mg_2P_2O_7$) or struvite ($NH_4MgPO_4.6H_2O$), composts with low-solubility in water but soluble in other extractors as the citric acid solution (Lustosa Filho et al., 2017; Suwanree et al., 2022; Talboys et al., 2016), being CA which is an extractor that simulates the capacity of roots acquired P (Binh and Zapata, 2002) with high potential to be used in studies of P release kinetics, although there are no studies. The effect of Mg addition on the reduction of P soluble in water was observed in the kinetics of P release in water; however, the Mg addition increased the kinetics of P release in citric acid, effects regardless type of acid used in acidulation (**Figure 4**).

The main effects observed due to the type of acid used in the acidulation process were also confirmed by dividing groups from the cluster analysis based on the FTIR spectrum (**Figure 3**). The hydrochloric and nitric acids were the most effective in the acidulation process and formed the same groups through cluster analysis based on the FTIR spectrum. The group formed by hydrochloric and nitric acids had similarities in the behavior of some functional groups as follows: higher intensities of absorption of OH groups, more prominent peaks of CO_3

and reduction of the intensity of P-O groups, groups that P-O that also decreased in the following order of Mg addition (serpentinite > non-Mg > MgCl). Besides, the hydrochloric and nitric acids cluster group had higher absorbance intensity related to aliphatic C-H groups over no-acidulation or acidulation with sulfuric acid.

OH stretching found at 3400-3200 cm^{-1} in non-acidified fertilizer, and hydrochloric and nitric acids-derived BBFs are related to 3500-3250 cm^{-1} -OH stretching vibration in phenolic groups (Lago et al., 2021). The e peak of OH stretching when sulfuric acid was used in acidulation was related to tertiary alcohols (3620 and 3550 cm^{-1})(Socrates, 2004), and OH-stretching from tertiary alcohols over from phenolic groups apparently contributed to the increase of P solubility in water. The CO_3 groups found in BBFs are related to the IR assignments peaks already found in raw APR, and C-aliphatic groups found in all BBFs are derived from organic material (coffee husk) used in the biochar production (Maluf et al., 2018). The maintenance or increase of C-aliphatic groups is a new property of organomineral fertilizers, and its presence indicates a possible biostimulant role of organomineral fertilizers. The role of C-aliphatic groups as plant biostimulants due to the application of humic materials (humic acid) promotes stimulation of plasma membrane H^+-ATPase (Aguiar et al., 2013), a proton pump that has an important role in the process that triggers plant nutrient uptake (Marschner, 2012). Thus, organomineral fertilizers can act as both nutrient sources and plant biostimulants. Among the synthesized BBFs, those produced with the acidification of apatite with nitric acid may have a more important biostimulant role due to the higher intensity of C-aliphatic groups (FTIR spectral signature) over FRIR spectra of other BBFs.

It was observed that a part of P from APR was incorporated into the biochar matrix as observed by the formation of P-H organophosphorus in BBFs, peaks already described at 2353 cm^{-1} (Y. Wang et al., 2014) and not found in coffee husk before pyrolysis (Maluf et al., 2018). The P-O peaks at 960 cm^{-1}, verified in non-acid and acidulation using sulfuric acid, and

reduction in the intensity of P-O peaks at 1040 cm^{-1} may be related to the lower proportions of soluble P in the different extractors because the BBFs with this tendency of P groups had lower proportions of soluble P in CA, NAC+H_2O and FA (**Figures 2 and 3**).

The group formed in the infrared analysis when sulfuric acid during the acidulation process had a different peak than the other BBFs, a peak related to an alkyl sulfate salts (RSO_4^- M), showing an interaction between organic radicals from coffee husk pyrolysis, S from sulfuric acid and Ca from APR ($Ca_5(PO_4)_3(Cl/F/OH)$). Thus, new C-SO_4Ca compounds were produced, which, together with the peaks of OH from tertiary alcohols, seem to have contributed to the increase of soluble P in water over other synthetized BBFs. A higher losses of N was observed due to acidulation using nitric acid before pyrolysis; however, part of N was incorporated into biochar structure as observed by C-N stretch in BNA, BNA Mg and BNAMg (**Figure 3**).

4.2 BBFs agronomic efficiency as related to P pools and the kinetics of P release

Based on the cluster analysis, the following BBFs were chosen to fertilize plants: B, BMg, BSA, BSAMg, BHA, BHAMg, BNA, and BNAMg. The BBFs were compared using TSP and APR as positive and negative controls to plants. Phosphorus recommendation was based on the BBFS total P contents. Over P soluble in water, a higher biomass production was verified for fertilizers with greater proportions of soluble P in NAC+H2O, CA, and FA (**Figures 6 and 8**), fertilizer P indices that are supposed to simulate P acquired by plants (Binh and Zapata, 2002; Duboc et al., 2022; Santos et al., 2019; Singh et al., 2017).

When only BBFs were used to fertilizer plants, a higher correlation between P in NAC+H_2O and P in maize and brachiaria shoots (in both Oxisols), compared to P extracted with CA, FA or water (**Figure 9**). Evaluating seventy-nine P-rich wastes and fertilizers added to three soils (alkaline and two acid soils) cultivated with rye (*Secale cereal* L.), the extraction of P by NAC+H_2O extractor solution had a correlation coefficient of 0.52 for the acid soil with

294 g kg^{-1} clay and 0.19 for acid soil with 101 g kg^{-1} clay (Duboc et al., 2022). However, due to the high diversity of fertilizers in the Duboc's study (Duboc et al., 2022), better statistical approaches could be made to divide fertilizers into groups with common properties because the P extraction methods had different chemical reactions. These chemical reactions interact with the fertilizer properties, thus determining their efficiency in simulating the P plant uptake.

Different chemical extractors may or not extract larger amounts of P depending on the type of fertilizer; as an example, we have that P from rock phosphates as APR can be partially solubilized by acidification when using CA or FA; however, the NAC+H_2O extraction involves strong cation complexation (mainly Ca and Fe) inducing P co-dissolution (Duboc et al., 2022; Santos et al., 2019). The extractant solution effect was higher values for P soluble in CA and FA of B and Mg of lower solubility in P soluble NAC+H_2O (**Figure 2)**. In biochar, the FA extraction solution with an ultrasonication process is the recommended technique because the ultrasonication improves the wetting of the biochar, allowing, in some cases, higher extractions of P from biochar (Singh et al., 2017). In addition to the extractors, the P soluble in water shows the P readily available for plants (Brazil, 2017).

Despite the high correlation of NAC+H_2O and P accumulated by maize and brachiaria in our study, the NAC+H_2O solution use is limited in the kinetics of P study studies due to preheating samples such as NAC+H_2O extractor solution (Brazil, 2017; Duboc et al., 2022) cannot be done in the proposed kinetics of P release scheme. Thus, CA is an excellent alternative to extract P in the kinetics of P release over time, given its significant correlation with P uptake by maize and brachiaria plants (**Figure 9**) due to its simple preparation and use. The P release in CA evaluated by the new proposed method of the kinetics of P release showed a high correlation with the accumulated amounts of P in maize and Brachiaria plants in both Oxisols (**Figure 9**), being 48-72 and 12-24 hours for maize cultivate in RO and YO

respectively, 120 or 264, and 72-120 hours to brachiaria cultivated in RO and YO respectively. Thus, a new method to study the rate of P released from OMFs was proposed in this study.

Other solution extractors as a solution of 0.01 M $CaCl_2$ adjusted to pH > 6 with 0.1 M NaOH were indicated to simulate the P availability of mineral fertilizer for temperate climate soils to represent better the ionic strength conditions of the soil solution (Baird et al., 2019). However, there is not a suitable solution to study the kinetics of P release from fertilizers for tropical soils and for BBFs, BBFs that have different properties over mineral fertilizers due to the presence of P-mineral and P-organic in BBFs. Due to the high potential of root exudation of organic acids as citric, malic, and oxalic acids (Adeleke et al., 2017), CA is a potential extractor to use in the kinetics of P release studies, mainly due to the greater practicality and lower cost of CA solutions combined with high efficiency to estimate the P accumulated by maize and brachiaria plants due to BBFs application as shown in our study (**Figure 9**) and as observed in relation of P soluble in CA and P uptake by ryegrass plants (Rose et al., 2019).

In both kinetics of P release performed (using water or CA), it was verified that TSP has high and faster P release compared to BBFs (**Figure 4**), results similar to those found by Lustosa Filho et al., (2017) compared the kinetics of P release in the water of P-biochar over TSP. The gradual release is a property of fertilizers that reduces P loss, as happens with P-BBFs with more gradual P release, which contributes to increasing the soil available P (An et al., 2021; Ghodszad et al., 2021). In the kinetics of P release of BBFs, it was observed that the acidulation process found the higher values using water as an extractor without the addition of Mg. The addition of Mg +acidulation promotes slow and lower P release in water over acidulation without Mg added via magnesium chloride. The slow P release of biochar produced by the addition of Mg before pyrolysis is controlled by the dissolution of $Mg_2P_2O_7$ crystals formed during pyrolysis (Suwanree et al., 2022). Contrary behavior was observed using CA as extractor solution when Mg addition or no-Mg addition had similar amounts of P release when

nitric and sulfuric acids were used in acidulation; however, the lower P release was verified when used hydrochloric acid.

Mg added over no-Mg added during acidulation, in the no-Mg BBFs had slow P release in CA (**Figure 4**). When Mg was added during the production of BBFs from the mixture of poultry litter (PL) and TSP or phosphoric acid (H_3PO_4) or monoammonium phosphate (MAP), the P release in water was lower, reducing the P release from 99.8 to 31.6, 86.0 to 28.9 % and 37.0% to 9.1% respectively to Mg addition over no-Mg on PLxTSP, PLx H3PO4 and PLxMAP (Lustosa Filho et al., 2017). The rapid release of P from fertilizer may promote strongly adsorbed by Fe and Al oxides in Oxisols due to high P fixation capacity in tropical soils, and a smart approach to increase fertilizer efficiency is the fertilizers with high solubility in extractors that simulate nutrient uptake capacity of the root as NAC+H_2O solution extractor, with low solubility in water (Fink et al., 2016; Maluf et al., 2018; Urrutia et al., 2014). The effect is reached when Mg is added during BBFs synthesis (**Figures 2 and 4**).

The relationship found in our study proves that P soluble in FA from biochar is a sensitive indicator of P bioavailability for plants (**Figure 9**), also was found by Wang et al., (2012). However, in general, the higher response of BBF was related to higher amounts of P soluble in NAC+H_2O that improve the soil P-resin; consequently, it improves the maize and brachiaria growth and P nutrition (**Figures 2, 5, 6, 7, 8, and 9**). In three successive resin extractions, the P extracted by resin method was efficient similar to the P accumulation capacity in Italian ryegrass (*Lolium multiflorum* Lam.) (T. Wang et al., 2014). However, in the aforementioned model that relates soil P resin and P accumulation, there is a mixture in the dataset of data from mineral sources of P (calcium dihydrogen phosphate) and P-biochar sources, which can compromise applications due to the unique properties of OMFs over mineral fertilizers, as observed by an apparent higher influence on the data point of source data on the

created model (T. Wang et al., 2014). Thus, the best option would be to establish relationships only for the BBFs dataset without mineral sources.

The properties of BBFs interact with the soil, and the effects of biochar on the soil are due to changes in physical, chemical, and microbiological properties of soil, thus affecting the P chemical by interaction with mineral and organic soil components (Ghodszad et al., 2021). The P available in soil increases due to biochar application by the following mechanism: increase of cations adsorption of soil into biochar, consequently reducing the P sorption and precipitation with these cations; increase of water retention capacity, improving the P diffusion process; an increase of soil pH that increases the stronger anionic repulsion and improves the P contents in soil solution; competitive reactions between P and C organic molecules from biochar by adsorption sites, thus blocking P adsorption sites; more gradual release of P, increase of fertilizer efficiency when biochar is the mixture with mineral fertilizers, and this effects may increase the yield of crops in effect dependent of rate and properties (temperature, feedstock, C:N ratio) of biochar and its interaction with soil and plant type (An et al., 2021; Bai et al., 2022; Carneiro et al., 2021; Ghodszad et al., 2021; Johan et al., 2021).

When analyzing the P contents in the soil solution during the first crop using maize as a test plant, different trends were observed compared to P available in whole soil determined by the soil resin test method (**Figure 5**). At the beginning of the maize cultive, the solution P in RO increased by 14% for BNA and BNAMg over TSP. Two hypotheses may be related to the higher solution P values observed; the first includes the formation in BNA and BNAMg of compounds such as calcium nitrate with higher hydrophobicity and solubility since nitrate-containing compounds are generally higher soluble and hygroscopic (Nasiraee et al., 2021). Thus, the higher hygroscopicity may have increased hydration and consequently the dissolution of BNA and BNAMg, especially in soil with greater water retention capacity (RO), due to the higher SOM levels of RO over YO (**Table 2**). In addition, the FTIR spectrum was observed

with the interaction of P from APR and organic matrix (**Figure 3**), and the presence of these bonds may favor a higher P availability, as already demonstrated by the interaction between a reactive organic matrix (humic acid), Ca and P forming Ca-P-humic acid complex (Erro et al., 2012).

In YO during maize cultive, BBFs did not increase solution P over TSP (**Figure 5**). Only BNAMg had similar values of solution P compared to TSP. Among the BBFs, the BNA increased the soil solution P values, and Mg addition in BBFs improved solution P. Mg increasing soil solution P was also observed in BHAMg over BHA and BSAMg over BSA; thus, Mg showed the synergic effect of magnesium and phosphate of BBFs. The presence of Mg in BBFs having a synergistic effect on P uptake due to the application of Mg-enriched BBFs has already been demonstrated (Carneiro et al., 2021); however, our work shows that initially, this effect is related to changes in P availability in the whole soil and its solution.

These effects of BBFs on soil solution could not promote gains of maize biomass production for both Oxisol compared to TSP, and within the BBFs, the ones that obtained the highest yields were BNA in RO and BSA, BNA and BNAMg in YO (**Figure 6**). The main effect on maize growth and P was conditioned by the fraction of P soluble in chemical extractors (CA, NAC+H_2O, and CA) and by the amount of P release in the kinetics of release in CA. These effects on the soil solution are promising and should be better studied in other research using the standardization of P applied preferentially by the solubility of P in NAC+H_2O. The standardization of P recommendation based on the soluble contents of P in NAC+H_2O was used to compare TSP and P-biochar produced by different routes with addition or no-Mg addition. It was observed that P-biochar reduced the maize biomass production P in shoot compared to TSP, an effect that seems to be related to the low solubility of P in water (less than 2%) due to the formation of P stable forms during pyrolysis and once that for high P-demanding crops, such as maize, if P is not released at the right time and amount, the initial plant growth is reduced

and consequently grain yield as well (Lustosa Filho et al., 2019, 2017; Rose et al., 2019). Thus, the ideal BBFs with intermediate solubility of P in water and high solubility in NAC+H2O. In addition to the main effect on the first crops observed, fertilizers with a more gradual release have a higher residual effect, thus increasing P levels in soils during successive cultivation cycles; thus, OMFs over mineral fertilizers had a potential nutrient residual effect (nutrient residual) across different crop seasons (Martins et al., 2017; Sakurada et al., 2016, 2019). For this reason, we used a second brachiaria crop after the maize crop. The gradual release of P, as happens in OMFs, e.g., BBFs, can either positively affect the short and long-term during cultivation (Carneiro et al., 2021). The more P nutrient residual is due to a more gradual P release in OMFs that may increase P availability than fully solubilized mineral P fertilizers in the long term (residual P), as shown by Sakurada et al., (2019). Due to the residual effect of OMFs, after the first cultivation, mainly due to nutrient forms in OMFs, there is the need to be evaluated P availability in the soil to check if the residual nutrient effect is enough to meet the nutritional demand of plants grown in sequence to the crash crop (Sakurada et al., 2016, 2019).

The residual effect of P (soil P resin) in RO for brachiaria was higher for BHA, BHAMg, BNA, and BNAM over TSP (**Figure 7**). However, in YO, the soil P resin is higher by TSP over BBFs, showing the influence of soil type controlling the residual effect of fertilizer. When evaluating the soil solution in the RO, it was observed that the same pattern of increasing levels in the soil solution was greater, about 66% for BNA and BNAMg over TSP. In YO, BSA, BSAMg, BNA, and BNAMg had higher soil P resin (**Figure 7**). In YO, solution P and soil P resin effects do not reflect in higher production of brachiaria biomass or P in the shoot, and TSP with higher residual soil P resin had higher brachiaria biomass production and P in the shoot. However, in RO, BNA residual effect allows maintaining the same P accumulation in the brachiaria shoot with a lower brachiaria biomass production over TSP.

Thus, it is observed that the residual effect of fertilizers was highly dependent on soil properties. As observed in our study, P-HA-based OMFs were highly dependent on soil properties, with SOM the key factor conditioning the effect of OMFs (Erro et al., 2012). In the study evaluating the combination application of humic acid plus zinc sulfate over isolated application of zinc sulfate for maize-brachiaria growing in the same soil used in our study, YO had a high residual effect for brachiaria and the observed effects of increasing Zn in the soil solution in YO due to the humic acid+zinc sulfate promotes higher brachiaria biomass production and P accumulated in the shoot (Morais et al., 2021). In our work, the effects on soil solution P were also correlated with brachiaria and P in brachiaria shoot when TSP, APR, and no-P fertilization treatments were excluded from the dataset (**Figure 9**).

4.3 Study limitations and future perspectives

Our study proposed and evaluated the synthesis routes of BBFs produced from the acidulation and mixing of phosphate rock with coffee husk. We provide a basis for choosing the best fertilizer solubility indices and extractants and agronomic basis for the recommendation of BBFs to nourish a maize-brachiaria succession. Furthermore, we propose a new method to evaluate the kinetics of P release. However, in future studies, for a better comparison between BBFs and mineral fertilizers, the amount of P recommended to crops should be based on the soluble contents of in NAC+H_2O. Since experiments under controlled conditions have shown the potential of these new BBFs fertilizers to nourish plants, it is necessary to test the carbon-based fertilizers under field conditions across different crops and soils. We have shown the potential of using nitric acid in the synthesis of BBFs; however, due to high N losses during pyrolysis, other strategies of acidulation with nitric acid should be investigated.

5 Conclusion

Acidulation of Araxá phosphate rock (APR) with different acids and subsequent mixing with coffee husk and OMF production by pyrolysis creates biochar based-fertilizers (BBFs) with different chemical properties, NPK pools, and infrared spectral signature. The Mg addition via magnesium chloride before pyrolysis was more effective than serpentinite in promoting positive changes in BBFs properties. The Mg addition during acidulation of APR aiming at the production of BBFs reduced the amounts of P release in water and increased the P released in citric acid (2%). The new kinetics of P release in citric acid proposed was an effective approach to investigate the agronomic performance of BBFs on cultive of maize and brachiaria in sequence in contrasting Oxisols. The main effect on maize and residual P effect on brachiaria growth was conditioned by BBFs properties and its interaction with P pools in Oxisols. P residual effect of BBFs was higher in the Oxisol with the highest organic matter content. The P content soluble in neutral ammonium citrate plus water (NAC+H_2O) was the best fertilizer-P index for maize and brachiaria plants cultivated in Oxisols. Plant growth and P nutrition were the main plant traits related to with the P amounts added to soil based on P in neutral ammonium solution. For the correct comparison of BBFs and mineral fertilizers, P recommendation to plants should be based on the soluble contents of P in NAC+H_2O, considering that the agronomic recommendation based on fertilizer total P content was not a factor governing plant P uptake and growth.

6 Acknowledgments

Many thanks to the Coordination for the Improvement of Higher Education Personnel (CAPES) (CAPES-PROEX/AUXPE 593/2018), National Council for Scientific and Technological Development (CNPq) (303899/2015-8 and 307447/2019-7 grants), and the

Foundation for Research of the State of Minas Gerais (FAPEMIG) for financial support and scholarships provided. UFLA is an equal opportunity provider and employer.

7 References

Adeleke, R., Nwangburuka, C., Oboirien, B., 2017. Origins, roles and fate of organic acids in soils: A review. South African J. Bot. 108, 393–406. https://doi.org/10.1016/j.sajb.2016.09.002

Aguiar, N.O., Novotny, E.H., Oliveira, A.L., Rumjanek, V.M., Olivares, F.L., Canellas, L.P., 2013. Prediction of humic acids bioactivity using spectroscopy and multivariate analysis. J. Geochemical Explor. 129, 95–102. https://doi.org/10.1016/j.gexplo.2012.10.005

Akaike, H., 1979. A Bayesian Extension of the Minimum AIC Procedure of Autoregressive Model Fitting. Biometrika 66, 237. https://doi.org/10.2307/2335654

An, X., Wu, Z., Liu, X., Shi, W., Tian, F., Yu, B., 2021. A new class of biochar-based slow-release phosphorus fertilizers with high water retention based on integrated co-pyrolysis and co-polymerization. Chemosphere 285, 131481. https://doi.org/10.1016/j.chemosphere.2021.131481

Bai, S.H., Omidvar, N., Gallart, M., Kämper, W., Tahmasbian, I., Farrar, M.B., Singh, K., Zhou, G., Muqadass, B., Xu, C.-Y., Koech, R., Li, Y., Nguyen, T.T.N., van Zwieten, L., 2022. Combined effects of biochar and fertilizer applications on yield: A review and meta-analysis. Sci. Total Environ. 808, 152073. https://doi.org/10.1016/j.scitotenv.2021.152073

Baird, R., da Silva, R.C., Degryse, F., McLaughlin, M.J., 2019. A column perfusion test to assess the kinetics of nutrient release by soluble, sparingly soluble and coated granular fertilizers. J. Plant Nutr. Soil Sci. 182, 763–771. https://doi.org/10.1002/jpln.201800666

Binh, T., Zapata, F., 2002. Standard characterization of phosphate rock samples from the FAO/IAEA phosphate project, in: Assessment of Soil Phosphorus Status and Management of Phosphatic Fertilizers to Optimize Crop Production. IAEA-TECDOC-1272, Vienna, pp. 9–23.

Brazil, 2017. Manual de métodos analíticos oficiais para fertilizantes e corretivos. MAPA, Brasília.

Carmo, D.L. do, Silva, C.A., Lima, J.M. de, Pinheiro, G.L., 2016. Electrical Conductivity and Chemical Composition of Soil Solution: Comparison of Solution Samplers in Tropical Soils. Rev. Bras. Ciência do Solo 40. https://doi.org/10.1590/18069657rbcs20140795

Carneiro, J.S.S., Andrade Ribeiro, I.C., Nardis, B.O., Barbosa, C.F., Lustosa Filho, J.F., Azevedo Melo, L.C., 2021. Long-term effect of biochar-based fertilizers application in tropical soil: Agronomic efficiency and phosphorus availability. Sci. Total Environ. 760. https://doi.org/10.1016/j.scitotenv.2020.143955

Dou, Z., Toth, J.D., Jabro, J.D., Fox, R.H., Fritton, D.D., 1996. Soil nitrogen mineralization during laboratory incubation: Dynamics and model fitting. Soil Biol. Biochem. 28, 625–632. https://doi.org/10.1016/0038-0717(95)00184-0

Duboc, O., Hernandez-Mora, A., Wenzel, W.W., Santner, J., 2022. Improving the prediction of fertilizer phosphorus availability to plants with simple, but non-standardized extraction techniques. Sci. Total Environ. 806, 150486. https://doi.org/10.1016/j.scitotenv.2021.150486

Enders, A., Lehmann, J., 2012. Comparison of Wet-Digestion and Dry-Ashing Methods for Total Elemental Analysis of Biochar. Commun. Soil Sci. Plant Anal. 43, 1042–1052. https://doi.org/10.1080/00103624.2012.656167

Erro, J., Urrutia, O., Baigorri, R., Aparicio-Tejo, P., Irigoyen, I., Torino, F., Mandado, M., Yvin, J.C., Garcia-Mina, J.M., 2012. Organic Complexed Superphosphates (CSP): Physicochemical characterization and agronomical properties. J. Agric. Food Chem. 60, 2008–2017. https://doi.org/10.1021/jf204821j

Fink, J.R., Inda, A.V., Tiecher, T., Barrón, V., 2016. Iron oxides and organic matter on soil phosphorus availability. Ciência e Agrotecnologia 40, 369–379. https://doi.org/10.1590/1413-70542016404023016

Frazão, J.J., Benites, V.D.M., Pierobon, V.M., Ribeiro, S., 2021. A Poultry Litter-Derived Organomineral Phosphate Fertilizer Has Higher Agronomic Effectiveness Than Conventional Phosphate Fertilizer Applied to Field-Grown Maize and Soybean. Sustainability. https://doi.org/10.3390/su132111635

Gautam, R., Vanga, S., Ariese, F., Umapathy, S., 2015. Review of multidimensional data processing approaches for Raman and infrared spectroscopy. EPJ Tech. Instrum. 2, 1–8. https://doi.org/10.1140/epjti/s40485-015-0018-6

Ghodszad, L., Reyhanitabar, A., Maghsoodi, M.R., Asgari Lajayer, B., Chang, S.X., 2021. Biochar affects the fate of phosphorus in soil and water: A critical review. Chemosphere 283, 131176. https://doi.org/10.1016/j.chemosphere.2021.131176

Johan, P.D., Ahmed, O.H., Omar, L., Hasbullah, N.A., 2021. Phosphorus Transformation in Soils Following Co-Application of Charcoal and Wood Ash. Agronomy 11, 2010. https://doi.org/10.3390/agronomy11102010

Kassambara, A., Mundt, F., 2020. factoextra: Extract and Visualize the Results of Multivariate Data Analyses.

Kitson, R.E., Mellon, M.G., 1944. Colorimetric Determination of Phosphorus as Molybdivanadophosphoric Acid. Ind. Eng. Chem. Anal. Ed. 16, 379–383. https://doi.org/10.1021/i560130a017

Lago, B.C., Silva, C.A., Melo, L.C.A., Morais, E.G. de, 2021. Predicting biochar cation exchange capacity using Fourier transform infrared spectroscopy combined with partial least square regression. Sci. Total Environ. 794, 148762. https://doi.org/10.1016/j.scitotenv.2021.148762

Lê, S., Josse, J., Husson, F., 2008. FactoMineR : An R Package for Multivariate Analysis. J. Stat. Softw. 25. https://doi.org/10.18637/jss.v025.i01

Liang, Y., Cao, X., Zhao, L., Xu, X., Harris, W., 2014. Phosphorus Release from Dairy Manure, the Manure-Derived Biochar, and Their Amended Soil: Effects of Phosphorus Nature and Soil Property. J. Environ. Qual. 43, 1504–1509. https://doi.org/10.2134/jeq2014.01.0021

Lombi, E., McLaughlin, M.J., Johnston, C., Armstrong, R.D., Holloway, R.E., 2005. Mobility, solubility and lability of fluid and granular forms of P fertiliser in calcareous and non-calcareous soils under laboratory conditions. Plant Soil 269, 25–34. https://doi.org/10.1007/s11104-004-0558-z

Lustosa Filho, J.F., Barbosa, C.F., Carneiro, J.S. da S., Melo, L.C.A., 2019. Diffusion and phosphorus solubility of biochar-based fertilizer: Visualization, chemical assessment and availability to plants. Soil Tillage Res. 194, 104298. https://doi.org/10.1016/j.still.2019.104298

Lustosa Filho, J.F., Penido, E.S., Castro, P.P., Silva, C.A., Melo, L.C.A., 2017. Co-Pyrolysis of Poultry Litter and Phosphate and Magnesium Generates Alternative Slow-Release Fertilizer Suitable for Tropical Soils. ACS Sustain. Chem. Eng. 5, 9043–9052. https://doi.org/10.1021/acssuschemeng.7b01935

Maluf, H.J.G.M., Silva, C.A., de Morais, E.G., de Paula, L.H.D., 2018. Is composting a route to solubilize low-grade phosphate rocks and improve MAP-based composts? Rev. Bras. Cienc. do Solo 42. https://doi.org/10.1590/18069657rbcs20170079

Marschner, P., 2012. Marschner's Mineral Nutrition of Higher Plants. Elsevier, Oxford. https://doi.org/10.1016/C2009-0-63043-9

Martins, D.C., Resende, Á.V. De, Galvão, J.C.C., Simão, E.D.P., Ferreira, J.P.D.C., Almeida, G.D.O., 2017. Organomineral Phosphorus Fertilization in the Production of Corn, Soybean and Bean Cultivated in Succession. Am. J. Plant Sci. 08, 2407–2421.

https://doi.org/10.4236/ajps.2017.810163

McLaughlin, M.J., McBeath, T.M., Smernik, R., Stacey, S.P., Ajiboye, B., Guppy, C., 2011. The chemical nature of P accumulation in agricultural soils-implications for fertiliser management and design: An Australian perspective. Plant Soil 349, 69–87. https://doi.org/10.1007/s11104-011-0907-7

Mendiburu, F., 2020. agricolae: Statistical Procedures for Agricultural Research.

Morais, E.G. de, Silva, C.A., Jindo, K., 2021. Humic Acid Improves Zn Fertilization in Oxisols Successively Cultivated with Maize–Brachiaria. Molecules 26, 4588. https://doi.org/10.3390/molecules26154588

Nasiraee, M., Mousavi, S.M., Saljoughi, E., Kiani, S., Razmgar, K., 2021. Production of calcium nitrate crystals via membrane distillation crystallization using polyvinylidene fluoride/sorbitan trioleate membranes. Adv. Powder Technol. 32, 1463–1471. https://doi.org/10.1016/j.apt.2021.02.043

Phares, C.A., Atiah, K., Frimpong, K.A., Danquah, A., Asare, A.T., Aggor-Woananu, S., 2020. Application of biochar and inorganic phosphorus fertilizer influenced rhizosphere soil characteristics, nodule formation and phytoconstituents of cowpea grown on tropical soil. Heliyon 6, e05255. https://doi.org/10.1016/j.heliyon.2020.e05255

R Core Team, 2020. R: A language and environment for statistical computing.

Rose, T.J., Schefe, C., Weng, Z. (Han), Rose, M.T., van Zwieten, L., Liu, L., Rose, A.L., 2019. Phosphorus speciation and bioavailability in diverse biochars. Plant Soil 443, 233–244. https://doi.org/10.1007/s11104-019-04219-2

Sahin, O., Taskin, M.B., Kaya, E.C., Atakol, O., Emir, E., Inal, A., Gunes, A., 2017. Effect of acid modification of biochar on nutrient availability and maize growth in a calcareous soil. Soil Use Manag. 33, 447–456. https://doi.org/10.1111/sum.12360

Sakurada, R., Batista, L.M.A., Inoue, T.T., Muniz, A.S., Pagliar, P.H., 2016. Organomineral phosphate fertilizers: Agronomic efficiency and residual effect on initial corn development. Agron. J. 108, 2050–2059. https://doi.org/10.2134/agronj2015.0543

Sakurada, R.L., Muniz, A.S., Sato, F., Inoue, T.T., Neto, A.M., Batista, M.A., 2019. Chemical, Thermal, and Spectroscopic Analysis of Organomineral Fertilizer Residue Recovered from an Oxisol. Soil Sci. Soc. Am. J. 83, 409–418. https://doi.org/10.2136/sssaj2018.08.0294

Santos, W.O., Mattiello, E.M., Barreto, M.S.C., Cantarutti, R.B., 2019. Acid ammonium citrate as P extractor for fertilizers of varying solubility. Rev. Bras. Cienc. do Solo 43, 1–12. https://doi.org/10.1590/18069657rbcs20180072

Silva, F.C. (Ed.), 2009. Manual de análises químicas de solos, plantas e fertilizantes, 2. ed. ed. Embrapa Informação Tecnológica, Brasília.

Singh, B., Camps-Arbestain, M., Lehmann, J., CSIRO (Australia), 2017. Biochar: A Guide to Analytical Methods, Csiro publishing.

Socrates, G., 2004. Infrared and Raman characteristic group frequencies: tables and charts. John Wiley \& Sons.

Stuart, B.H., 2004. Infrared Spectroscopy: Fundamentals and Applications, Infrared Spectroscopy: Fundamentals and Applications. https://doi.org/10.1002/0470011149

Suwanree, S., Knijnenburg, J.T.N., Kasemsiri, P., Kraithong, W., Chindaprasirt, P., Jetsrisuparb, K., 2022. Engineered biochar from sugarcane leaves with slow phosphorus release kinetics. Biomass and Bioenergy 156, 106304. https://doi.org/10.1016/j.biombioe.2021.106304

Suzuki, R., Terada, Y., Shimodaira, H., 2019. pvclust: Hierarchical Clustering with P-Values via Multiscale Bootstrap Resampling.

Talboys, P.J., Heppell, J., Roose, T., Healey, J.R., Jones, D.L., Withers, P.J.A., 2016. Struvite: a slow-release fertiliser for sustainable phosphorus management? Plant Soil 401, 109–123. https://doi.org/10.1007/s11104-015-2747-3

Teir, S., Revitzer, H., Eloneva, S., Fogelholm, C.J., Zevenhoven, R., 2007. Dissolution of natural serpentinite in mineral and organic acids. Int. J. Miner. Process. 83, 36–46. https://doi.org/10.1016/j.minpro.2007.04.001

Teixeira, P.C., Donagemma, G.K., Fontana, A., Teixeira, W.G. (Eds.), 2017. Manual de métodos de análise de solo, 3rd ed. Embrapa, Brasília.

Tumbure, A., Bishop, P., Bretherton, M., Hedley, M., 2020. Co-Pyrolysis of Maize Stover and Igneous Phosphate Rock to Produce Potential Biochar-Based Phosphate Fertilizer with Improved Carbon Retention and Liming Value. ACS Sustain. Chem. Eng. 8, 4178–4184. https://doi.org/10.1021/acssuschemeng.9b06958

UNIDO, IFDC, 1998. Fertilizer manual, 1st ed. Kluwer Academic Publishers, Dordrecht.

Urrutia, O., Erro, J., Guardado, I., San Francisco, S., Mandado, M., Baigorri, R., Claude Yvin, J., Ma Garcia-Mina, J., 2014. Physico-chemical characterization of humic-metal-phosphate complexes and their potential application to the manufacture of new types of phosphate-based fertilizers. J. Plant Nutr. Soil Sci. 177, 128–136. https://doi.org/10.1002/jpln.201200651

Vieira, K.R.M., Arce, G.L.A.F., Luna, C.M.R., Facio, V.O., Carvalho, J.A., Neto, T.G.S., Ávila, I., 2022. Understanding the Acid Dissolution of Serpentinites (Tailings and Waste

Rock) for Use in Indirect Mineral Carbonation. South African J. Chem. Eng. 40, 270. https://doi.org/10.1016/j.sajce.2022.02.005

Wang, T., Camps-Arbestain, M., Hedley, M., 2014. The fate of phosphorus of ash-rich biochars in a soil-plant system. Plant Soil 375, 61–74. https://doi.org/10.1007/s11104-013-1938-z

Wang, T., Camps-Arbestain, M., Hedley, M., Bishop, P., 2012. Predicting phosphorus bioavailability from high-ash biochars. Plant Soil 357, 173–187. https://doi.org/10.1007/s11104-012-1131-9

Wang, Y., Yin, R., Liu, R., 2014. Characterization of biochar from fast pyrolysis and its effect on chemical properties of the tea garden soil. J. Anal. Appl. Pyrolysis 110, 375–381. https://doi.org/10.1016/j.jaap.2014.10.006

Ward, J.H., 1963. Hierarchical Grouping to Optimize an Objective Function. J. Am. Stat. Assoc. 58, 236–244. https://doi.org/10.1080/01621459.1963.10500845

Wei, T., Simko, V., 2017. R package "corrplot": Visualization of a Correlation Matrix.

Wickham, H., Averick, M., Bryan, J., Chang, W., McGowan, L., François, R., Grolemund, G., Hayes, A., Henry, L., Hester, J., Kuhn, M., Pedersen, T., Miller, E., Bache, S., Müller, K., Ooms, J., Robinson, D., Seidel, D., Spinu, V., Takahashi, K., Vaughan, D., Wilke, C., Woo, K., Yutani, H., 2019. Welcome to the Tidyverse. J. Open Source Softw. 4, 1686. https://doi.org/10.21105/joss.01686

Withers, P.J.A., Rodrigues, M., Soltangheisi, A., de Carvalho, T.S., Guilherme, L.R.G., Benites, V. de M., Gatiboni, L.C., de Sousa, D.M.G., Nunes, R. de S., Rosolem, C.A., Andreote, F.D., Oliveira, A. de, Coutinho, E.L.M., Pavinato, P.S., 2018. Transitions to sustainable management of phosphorus in Brazilian agriculture. Sci. Rep. 8, 2537. https://doi.org/10.1038/s41598-018-20887-z

Supplementary material 1. Nitrogen losses during pyrolysis and biochar-based fertilizers production.

Materials used in biochar synthesis	N loss (%)
Coffee husk	20.5 ±2.1 Bb
Coffee husk + MgCl	36.5 ±1.0 Ba
Coffee husk + Serpentinite	17.5 ±1.2 Bb
Coffee husk + H_2SO_4	17.6 ±1.9 BCa
Coffee husk + MgCl + H_2SO_4	14.3 ±0.2 Da
Coffee husk + Serpentinite + H_2SO_4	16.0 ±0.6 Ba
Coffee husk + HCl	14.7 ±0.8 Cb
Coffee husk + MgCl + HCl	19.2 ±2.7 Ca
Coffee husk + Serpentinite + HCl	15.3 ±0.2 Bb
Coffee husk + HNO_3	87.9 ±0.5 Aa
Coffee husk + MgCl + HNO_3	88.2 ±0.4 Aa
Coffee husk + Serpentinite + HNO_3	89.5 ±0.1 Aa

The bars with standard error followed by the same capital letter did not differ the acid treatment in each Mg condition tested according to the Duncan test (p<0.05). The bars with standard error followed the same minuscule letter did not differ the Mg condition in each acid treatment tested according to the Duncan test (p<0.05).

Supplementary material 2. Coefficients of the kinetics of P release in water for each fertilizers studied.

Fertilizer	Linear			Elovich			Exponential			Power			Parabolic			Hyperbolic		
	R^2	rmse	AIC	R^2	Rmse	AIC	R^2	rmse	AIC	R^2	Rmse	AIC	R^2	rmse	AIC	R^2	rmse	AIC
APR	0.72	0.04	-68	0.57	0.05	-60	0.94	0.02	-91	0.90	0.02	-89	0.89	0.02	-86	0.94	0.02	-94
TSP	0.38	17.18	177	0.75	10.95	159	0.97	5.95	134	0.83	9.02	151	0.62	13.51	167	0.94	6.80	139
B	0.40	0.50	35	0.61	0.41	27	0.92	0.19	-4	0.75	0.33	18	0.62	0.40	26	0.89	0.22	3
BMg	0.64	0.14	-17	0.62	0.14	-16	0.90	0.08	-41	0.87	0.08	-37	0.82	0.10	-30	0.91	0.07	-45
BSA	0.56	2.70	102	0.66	2.38	97	0.97	0.76	52	0.87	1.49	79	0.78	1.93	89	0.96	0.83	55
BSAMg	0.97	0.18	-5	0.32	0.93	60	-	-	-	0.97	0.18	-5	0.89	0.37	23	-	-	-
BHA	0.87	2.05	91	0.50	3.97	118	0.98	0.75	51	0.97	1.06	65	0.97	1.02	64	0.99	0.68	47
BHAMg	0.99	0.15	-13	0.31	1.16	69	-	-	-	0.99	0.13	-20	0.90	0.45	31	-	-	-
BNA	0.77	1.96	90	0.52	2.83	104	0.98	0.57	41	0.92	1.14	68	0.92	1.18	69	0.98	0.65	45
BNAMg	0.97	0.21	-1	0.39	0.95	61	0.98	0.20	-0.66	0.98	0.23	-2	0.95	0.26	9	0.98	0.22	-1

R^2: regression coefficient; rmse: root mean squared error; AIC: Akaike Information Criterion; TSP: triple superphosphate; APR: Araxá phosphate rock. More details of the BBFs acronyms were shown in Table 1.

Supplementary material 3. Coefficients of the kinetics of P release in citric acid at 2% for each fertilizer studied.

Fertilizer	Linear			Elovich			Exponential			Power			Parabolic			Hyperbolic		
	R^2	rmse	AIC	R^2	Rmse	AIC	R^2	rmse	AIC	R^2	rmse	AIC	R^2	rmse	AIC	R^2	rmse	AIC
APR	0.93	5.84	133	0.50	15.52	172	0.99	2.41	98	0.99	1.83	87	0.99	1.91	89	0.99	2.00	91
TSP	0.50	9.40	152	0.91	3.90	117	0.82	17.97	178	0.95	3.03	107	0.73	6.88	140	0.87	17.57	177
B	0.94	5.73	133	0.47	17.70	178	0.99	1.95	89	0.99	2.04	91	0.99	2.40	98	0.99	1.59	81
BMg	0.95	4.72	125	0.45	15.83	173	1.00	1.42	77	0.99	1.71	84	0.99	2.26	95	0.99	1.17	69
BSA	0.90	6.04	135	0.48	13.82	168	0.99	0.79	53	0.98	2.88	105	0.98	2.75	103	0.99	1.10	66
BSAMg	0.71	10.39	156	0.62	11.87	162	0.99	2.07	92	0.94	4.84	126	0.90	6.16	135	0.99	2.01	91
BHA	0.78	13.04	165	0.54	18.80	180	0.99	1.91	89	0.94	6.87	140	0.93	7.38	143	0.99	2.99	107
BHAMg	0.66	12.88	165	0.64	13.34	166	0.99	2.05	91	0.92	6.20	136	0.87	8.11	146	0.99	2.22	95
BNA	0.73	14.61	170	0.63	16.95	176	0.99	2.77	104	0.95	6.16	135	0.91	8.25	147	0.99	2.00	90
BNAMg	0.64	16.18	174	0.70	14.98	171	0.98	4.31	121	0.94	6.79	139	0.86	10.20	156	0.99	2.88	105

R^2: regression coefficient; rmse: root mean squared error; AIC: Akaike Information Criterion; TSP: triple superphosphate; APR: Araxá phosphate rock. More details of the BBFs acronyms were shown in Table 1.

Supplementary material 4. pH of whole soil and its solution for maize and brachiaria grown in Red and Yellow Oxisols.

Maize cultivation				
Treatments	Whole soil		Soil solution	
	RO	YO	RO	YO
– P	6.0 ±0.02 E	5.9 ±0.06 C	5.9 ±0.04 EF	6.4 ±0.08 B
APR	6.0 ±0.01 E	5.9 ±0.06 C	5.9 ±0.04 EF	6.3 ±0.05 B
TSP	6.1 ±0.04 CD	5.9 ±0.06 C	5.9 ±0.06 DEF	6.3 ±0.08 B
B	6.3 ±0.02 B	6.0 ±0.06 C	6.3 ±0.03 B	6.3 ±0.08 B
BMg	6.1 ±0.04 C	6.0 ±0.04 C	6.0 ±0.02 DE	6.2 ±0.08 B
BSA	5.9 ±0.04 E	6.0 ±0.04 C	5.8 ±0.03 F	6.3 ±0.07 B
BSAMg	6.0 ±0.04 E	6.3 ±0.03 B	6.1 ±0.07 CD	6.4 ±0.05 B
BHA	6.0 ±0.03 DE	6.3 ±0.01 B	5.9 ±0.06 EF	6.3 ±0.06 B
BHAMg	6.0 ±0.01 E	6.3 ±0.04 B	6.2 ±0.07 CD	6.3 ±0.09 B
BNA	6.4 ±0.01 A	6.8 ±0.04 A	6.5 ±0.02 AB	6.8 ±0.04 A
BNAMg	6.4 ±0.01 A	6.8 ±0.05 A	6.6 ±0.07 A	6.8 ±0.06 A

Brachiaria cultivation				
Treatments	Whole soil		Soil solution	
	RO	YO	RO	YO
– P	6.4 ±0.01 A	6.4 ±0.09 B	5.5 ±0.03 F	6.3 ±0.05 A
APR	6.3 ±0.02 B	6.4 ±0.05 B	5.5 ±0.05 F	6.3 ±0.03 A
TSP	6.1 ±0.02 C	6.4 ±0.09 B	6.0 ±0.04 CD	6.5 ±0.12 A
B	6.4 ±0.04 A	6.3 ±0.06 B	6.1 ±0.09 BC	6.4 ±0.08 A
BMg	6.3 ±0.02 B	6.3 ±0.05 B	5.8 ±0.03 DE	6.4 ±0.08 A
BSA	5.9 ±0.03 D	6.4 ±0.06 B	5.7 ±0.03 E	6.3 ±0.09 A
BSAMg	6.0 ±0.02 D	6.3 ±0.11 B	6.0 ±0.03 CD	6.5 ±0.06 A
BHA	6.0 ±0.01 D	6.5 ±0.04 B	5.9 ±0.02 DE	6.6 ±0.01 A
BHAMg	6.0 ±0.03 D	6.4 ±0.06 B	5.8 ±0.05 E	6.4 ±0.05 A
BNA	6.3 ±0.03 B	6.8 ±0.06 A	6.4 ±0.06 A	6.7 ±0.07 A
BNAMg	6.3 ±0.02 B	6.7 ±0.04 A	6.2 ±0.07 BC	6.5 ±0.20 A

The means with standard error followed by the same letter did not differ the treatments according to the Duncan test ($p<0.05$). –P: no P fertilizer application; TSP: triple superphosphate; APR: Araxá phosphate rock. More details of the BBFs acronyms were shown in Table 1.

Preliminary version of manuscript edited following the rules of Science of The Total Environment Journal

Novel NPK-slow release biochar-based fertilizer produced from the coffee post-harvest residues-derived biochar and acidulated low-grade phosphate rock

Everton Geraldo de Morais[1*] and Carlos Alberto Silva[1]

[1]Departament of Soil Science, Federal University of Lavras, Av. Doutor Sylvio Menicucci 1001, ZIP code: 37200-900, Lavras-Minas Gerais, Brazil.
* Corresponding author: evertonmoraislp@yahoo.com.br

Abstract

Biochar-based fertilizers (BBFs) containing nitrogen (N), phosphorus (P), and potassium (K) may have higher use efficiency of NPK by plants than mineral fertilizers. Our study aimed to synthesize BBFs containing NPK with a gradual release, characterizing and evaluating the agronomic performance. BBFs were produced by acidulating Araxá phosphate rock whose mixture with coffee post-harvest-derived biochar formed a composite. BBFs were characterized for N forms, P and K solubility in different extractors, the kinetics of P release, and tested as NPK source for maize grown in pots filled with Oxisol. BBFs contained N and P in organic forms and K with lower water solubility than mineral fertilizers. The main effect of BBFs on maize biomass was related to P nutrition, and BBFs over mineral fertilizers improved P accumulated in the maize shoot. BBFs had a more gradual release of P over mineral fertilizers, which initially reduced the P in the soil solution; however, at the phase of the higher required evaluated (25 days), the BBFs increased the P in the soil solution, effect positively correlated with P accumulated in the shoot. BBFs with a more gradual release of P was an effective strategy to increase the use efficiency of P in Oxisol.

Keywords: organomineral fertilizers, soil solution, composites, apatite solubilization.

1 Introduction

Tropical soils naturally have low levels of nitrogen (N), phosphorus (P), and potassium (K), which hamper plant growth and yield (FAO, 2017; Lopes and Guilherme, 2016). In addition, tropical soils have a specific P adsorption in Fe and Al oxides and low-activity mineral colloids, such as kaolinite, reducing the P availability in the soil (Fink et al., 2016). P fertilization is essential to increase crop yield in tropical soils like Oxisols, and the highly soluble mineral fertilizers are generally used in fertilization practices with a low recuperation of P added (5-25%) (McLaughlin et al., 2011; Withers et al., 2018). One of the strategies used to increase the efficiency of P fertilization is to increase the soil organic matter (SOM) content in tropical soils; however, SOM is achieved in few crop fields in the long term and it is a challenge overcome in tropical regions due to scarcity and lousy distribution of precipitation and high mean temperature (Fink et al., 2016; Gmach et al., 2020; McLaughlin et al., 2011).

Another strategy to increase the efficiency of P use is the use of organic fertilizers; however, organic fertilizers generally have a low concentration of P, which requires high rates to fulfill P plant demand (Mumbach et al., 2020). Organomineral fertilizers (OMFs) are a class of fertilizers that combine higher nutrient concentrations over organic fertilizers, with a more gradual release and positive effects of the organic matrix over soluble mineral fertilizers (Bai et al., 2022; Gwenzi et al., 2018; Piash et al., 2022; Suwanree et al., 2022). Different routes, organic matrix and mineral sources of nutrients can use to produce OMFs; and among synthesis routes, biochar-based fertilizers (BBFs) is promising in synthesizing fertilizers with higher agronomic performance (Barbosa et al., 2022; Fachini et al., 2022; Gwenzi et al., 2018; Johan et al., 2021; Piash et al., 2022; Suwanree et al., 2022). Biochars are rich C and stable matrices produced through the pyrolysis of organic wastes in the absence of oxygen (Singh et al., 2017).

In BBFs, the diversity of nutrient pools controls the dynamics and release rate of P and other nutrients (Shi et al., 2020; Suwanree et al., 2022). Regarding N forms, when mineral N is mixed with biochar, part of the mineral N interacts with the pyrolyzed matrix, forming organic N-containing compounds, N also may be adsorbed in the surface of charred matrices; in addition, biochar may already contain organic N (Barbosa et al., 2022; Shi et al., 2020; Wang et al., 2012). Thus, in BBFs, there are mineral and organic N chemical species, pools that control the supply to plants (Wang et al., 2012). Potassium can interact with the biochar by weak interaction through negative charges in organic functional groups, physical protection of K inside micropores, besides being trapped in the hydrophobic radicals of biochars, which difficult K dissolution and release (Fachini et al., 2022; Mukherjee et al., 2011).

Fertilizers with a gradual release of P may have higher agronomic performance than soluble mineral P fertilizers (Everaert et al., 2016). When P interacts with the biochar, it is gradually released by BBFs, and P losses due to specific adsorption are reduced; consequently, soil P availability is enhanced (Bai et al., 2022; Ghodszad et al., 2021). A more gradual release of P is mirrored by the amounts of P soluble in water and through kinetics of P release in water (Carneiro et al., 2021; Suwanree et al., 2022). Besides, other extractor solution as citric acid acting dissolving phosphates in OMFs have a potential to be used in the kinetics of P release studies (Johan et al., 2021). In OMFs, P is complexed in organic forms, consequently it is less prone to precipitated with Ca and other cations found in soils; in addition to organic ligands from OMFs compete with P for specific sites of fixation in soils, which increases P in the soil solution (An et al., 2021; Bai et al., 2022; Ghodszad et al., 2021; Johan et al., 2021).

Nutrient pools and properties of BBFs are influenced by their synthesis route (An et al., 2021; Lustosa Filho et al., 2019; Piash et al., 2022). When poorly soluble P sources such as low-grade phosphate rocks and plant residues were mixed, BBFs synthesized did not increase their agronomic value over the raw phosphate rock (Tumbure et al., 2020). Thus, BBF synthesis

routes that include poorly soluble phosphate rocks require previous acidulation of rock as happened in the route used to produce soluble mineral P fertilizers (UNIDO and IFDC, 1998). When phosphate rocks are acidulated and mixed with organic compounds, the P chemical species solubilized reacts with carbon (C), forming P-organic complexes with higher agronomic performance than mineral fertilizers (Erro et al., 2012).

Thus, we hypothesize that the novel NPK synthesis routes of BBFs through acidulation of low-grade phosphate to formulate a new BBF in which N, P, and K are gradually released with higher agronomic performance on maize growth. The aims of this study were: i) to propose a novel synthesis route of NPK based on the mixing of acidulated apatite with coffee post-harvest residues; ii) To characterize the novel BBFs and to study the kinetics release of NPK; iii) to evaluate the effect of BBFs on soil nutrient availability and maize growth as well.

2 Material and Methods

2.1 Biochar-based fertilizers (BBFs) synthesis

The routes of BBFs production were developed and patented at the BR1020220127840 deposit patent (Silva and Morais, 2022). Briefly, BBFs synthesis involves the acidulation of Araxá phosphate rock (APR) using two proportions of inorganic acid; it shaking the mixture in a horizontal shaker for 30 min at 120 rpm for one hour. After the acidulation process, samples were immediately mixed with coffee post-harvest residues-derived biochars produced at low (300^{o}C) and high temperature (500^{o}C). Pyrolysis was performed in a muffle furnace at a heating rate of 10 °C min^{-1} and pyrolysis of feedstock at the target temperature for 60 min. After the mixture of inorganic acid + phosphate rock + biochar, the final fertilizers was left to rest for 30 min; then, charred samples were dried in an oven at 60° C until constant weight, with the subsequent production of four BBFs (**Table 1**). BBFs were produced using three repetitions.

Table 1. Acronyms of process used in the production of biochar-based fertilizers (BBFs).

Acronyms	Description
BBF1	Acid proportion 1 + APR + biochar produced at low temperature
BBF2	Acid proportion 2 + APR + biochar produced at low temperature
BBF3	Acid proportion 1 + APR + biochar produced at high temperature
BBF4	Acid proportion 2 + APR + biochar produced at high temperature

APR: Araxá phosphate rock. Acid proportions and biochar properties and conditions during BBFs synthesis were patented at the BR1020220127840 deposit patent (Silva and Morais, 2022).

2.2 BBFs chemical characterization

Four BBFs synthetized and conventional sources of NPK were characterized. Mineral sources of nutrients were: ammonium nitrate, triple superphosphate, and potassium chloride. BBFs and mineral fertilizers samples were passed through a 1 mm sieve, dried, and stored for further analysis. The pH of BBFs was determined in a 0.01 mol L^{-1} $CaCl_2$ solution at a ratio of 1g biochar:10 ml $CaCl_2$ solution (Brazil, 2017; Singh et al., 2017). Mineral (ammonium ($N\text{-}NH_4^+$) and nitrate ($N\text{-}NO_3^-$)) N contents were extracted using a 2 mol L^{-1} KCl extractant solution, and determined by distillation followed by titration (Singh et al., 2017). Total N was determined following the Kjeldahl method after sulfuric digestion (Brazil, 2017; Phares et al., 2020). Due to the high contents of $N\text{-}NO_3^-$, total N content was determined by adding N-Kjeldahl to $N\text{-}NO_3^-$.

Total P and K contents were determined by the nitro-perchloric acid method (Brazil, 2017; Enders and Lehmann, 2012). P and K contents soluble in water were extracted by successive washed of 1 g of fertilizer samples with distilled water until a volume of 250 ml (Brazil, 2017). One g of fertilizer samples was stirred with 100 ml of citric acid (CA) solution at 2% for 30 min extracting the P and K contents soluble in CA (Brazil, 2017). One g of fertilizers samples was boiling in 50 ml of neutral ammonium citrate plus water ($NAC+H_2O$) solution extracting the P and K content soluble in $NAC+H_2O$ (Brazil, 2017). Based on the method recommended by P and K available in biochar, the content of P and K soluble in formic

acid (FA) solution at 2% was also measured; 0.35 g of biochar were mixed with 35 ml of 2% AF, ultrasonicate for 10 min, then was shaken for 30 min (Singh et al., 2017).

The P contents extracted by water, CA, NAC+H_2O, and FA were determined by the vanadomolybdate method (Kitson and Mellon, 1944) and K contents determined by the flame photometry method (Fox, 1951). To compare the NPK pools related to the N forms and solubility of P and K in BBFs samples, N or P or K indices were calculated according to N forms (N-mineral and N-organic) (Eq. 2) and soluble P (Eq. 2) and K (Eq.3) fractions (water or CA or NAC+H_2O or FA) according to respectively nutrient total content:

$$\text{N index (\%)} = \left(\frac{\text{N-form content } \left(\text{g kg}^{-1}\right)}{\text{Total N content } \left(\text{g kg}^{-1}\right)} \right) \times 100 \quad \text{(Eq. 1)}$$

$$\text{P index (\%)} = \left(\frac{\text{Soluble P content } \left(\text{g kg}^{-1}\right)}{\text{Total P content } \left(\text{g kg}^{-1}\right)} \right) \times 100$$

(Eq. 2)

$$\text{K index (\%)} = \left(\frac{\text{Soluble K content } \left(\text{g kg}^{-1}\right)}{\text{Total K content } \left(\text{g kg}^{-1}\right)} \right) \times 100$$

(Eq. 3)

2.3 Infrared spectroscopy analysis

Two biochar produced (low and high temperature), and four BBFs samples were scanned in a medium infrared region identifying the main peaks and spectroscopic signatures. The infrared spectrum was obtained at 4000 to 650 cm^{-1} wavenumber range with a resolution of 4 cm^{-1} by Attenuated Total Reflectance Fourier transform infrared (FTIR) spectroscopy using an Agilent® Cary 630 spectrometer. Pre-processing (normalization) of the dataset was performed in each FTIR spectrum (Gautam et al., 2015). The main peaks in FTIR spectra were identified and interpreted according to the infrared library already described (Kennedy et al.,

2004; Lustosa Filho et al., 2017; Singh et al., 2017; Trivedi and Dahryn Trivedi, 2015; Wang et al., 2014). The FTIR spectra of biochars are shown in **Supplementary material 1**.

2.4 BBF agronomic performance

The agronomic performance of four BBFS synthetized was tested in Sandy Loam Oxisol. Maize was used as a plant test cultivated for 25 days under greenhouse conditions in a new model involving plant growth in a mini-lysimeter filled with 0.550 kg of soil (**Supplementary material 2**). Six treatments were tested in a completely randomized design with three repetitions, as follows: four BBFs synthetized, positive control (NPK added via mineral fertilizers), and negative control (without NPK fertilization). The soil used had 230, 25, 745 g kg^{-1} respectively to clay, silt, and sand, 6.98 g kg^{-1} of total carbon determined in a dry combustion carbon analyzer (Elementar, model Vario TOC Cube, Germany), 496 mg kg^{-1} of N-total (Kjeldahl method), 6.1 to pH in water (1:2.5 ratio - w:v). In addition the soil contained 1.3, 0.50 and 0.10 $cmol_c$ kg^{-1} respectively to Ca^{2+}, Mg^{2+} and Al^{3+} evaluated by KCl 1 mol^{-1} extraction method. The contents available of K, Zn, Fe, Mn, and Cu evaluated by the Mehlich-1 soil test method were respectively 49.8, 0.5, 24.3, 11.8, and 0.25 mg kg^{-1}. Besides, the soil contained 0.13 mg kg^{-1} of B (hot water method) and 2.2 mg kg^{-1} of S (monocalcium phosphate in acetic acid method). All protocols are described in detail in Teixeira et al., (2017).

The phosphorus was applied homogeneously in whole soil at 200 mg kg^{-1} of P based on recommendation in P soluble in NAC+H_2O (Paper 5 of the thesis). The mineral fertilizers used to add NPK were ammonium nitrate, triple superphosphate, and potassium chloride. There was no standardization of the amount of N and K applied by BBFs; thus, in BBFs, additional fertilization with mineral fertilizers was not used. The amount of N and K applied via mineral fertilizers was based on the average amount of N and K provided by the BBFs and amounts based on plants fertilization in pots experiment (Novais et al., 1991); thus, 200 and 150 mg kg^{-1} was applied respectively for N and K. The application of N via ammonium nitrate and K via

potassium chloride was divided during maize cultivation, with 20% applied at planting fertilization and 80% at top-dressing fertilization 13 days after planting. The N forms and P and K solubility in different extractors applied during maize cultivation were different by treatments, as shown in **Supplementary material 3**. In the planting fertilization also was provided at 30, 40, 0.81, 2, 7.3, 0.15, 5, and 10 mg kg^{-1}, respectively, to Mg, S, B, Cu, Mn, Mo, Zn, and Fe, through $MgSO_4.7H_2O$, H_3BO_3, $CuSO_4.5H_2O$, $MnCl_2.4H_2O$, $(NH_4)_6Mo_7O_{24}.4H_2O$, $ZnSO_4.7H_2O$, and $FeCl_3.6H_2O$ (Reagent grade, Synth).

Before and after maize cultivation (25 days) 15 g of the whole soil in each experimental unit) was collected. The soil samples were dried and passed through a 2 mm sieve. In the whole soil samples, soil pH was determined in water at a ratio of 1:2.5 (w/v) (Teixeira et al., 2017), $N\text{-}NH_4^+$ and $N\text{-}NO_3^-$ were extracted with a 1 mol L^{-1} KCl solution (10 mL extractor solution: 1 g of soil), and N mineral contents determined through the distillation followed by titration (soil N-mineral) (Bremner and Keeney, 1966; Teixeira et al., 2017). The K availability contents were extracted by Mehlich-1 solution and determined by flame photometry (Teixeira et al., 2017), and P available in the soil was extracted by the resin soil test (Raij et al., 1986) and determined by the molybdenum blue method (Murphy and Riley, 1962).

The soil solution was collected in each mini-lysimeter at 1, 7, 15, and 25 days after maize planting during maize cultivation. During the collection of soil solution, the soil moisture was maintained at 70% of MWHC (overnight). After 12 hours, the soil solution was removed through the bottom of the mini-lysimeter using the vacuum process. The vacuum was performed using a vacuum pump model 12 CFM 110V-220V double stage SURYHA®. The vacuum was performed individually in each mini-lysimeter, using the pump's maximum power for 1 min. (time required for the end of the soil solution flow from the bottom of the mini-lysimeter), then 10 ml of soil solution was removed and stored. The rest of the soil solution collected was replaced on the top of the mini-lysimeter aimed at the return of this solution in each

experimental unit. The soil solution samples were filtered (<0.45 µm), and pH was determined in a pH bench meter; contents of $N\text{-}NH_4^+$ and $N\text{-}NO_3^-$ contents were determined through the distillation method followed by titration (Bremner and Keeney, 1966), P contents determined by molybdenum blue method (Murphy and Riley, 1962) and K contents determined by flame photometry method (Fox, 1951).

After maize cultivation, plants were harvested, separated into shoot and root, and dried at 60 ^oC until constant weight until samples were weighted, determining shoot (SDM) and root (RDM) dry matter production. The total dry matter production was obtained by the sum of SDM and RDM. In shoot tissues, the N content was determined by the Kjeldahl method, and P and K were determined by nitric perchloric acid digestion followed by determination of P contents by molybdenum blue method and K contents by flame photometry method (Silva, 2009). The nutrient accumulation of N or P o K (NuAc) in the shoot was calculated as follows (Eq. 4):

$$NuAc\ (mg\ pot^{-1}) = shoot\ dry\ matter\ (g\ pot^{-1}) * nutrient\ concentration\ in\ shoot\ (mg\ g^{-1}) \quad \text{(Eq. 4)}$$

2.5 The kinetics of P release

Based on the same amount applied for maize growing in a mini-lysimeter scheme, two studies of the kinetics of P release of four BBFs and TSP was carried out, related to two extractors, water or CA at 2% (Paper 5 of the thesis). The scheme of mini-lysimeter used was described in detail in paper 2 of the thesis. Briefly, the BBFs and TSP were mixed and incubated in a mini-lysimeter with sand (pre-washed with hydrochloric acid), and periodic leaching was carried out, thus determining the release of P in water or CA. In time 0, 50 ml of distilled water or CA solution, depending on the study, was passed in each mini-lysimeter, and from that, the solution was passed in a cumulative volume equivalent to 7 mL h^{-1} at 0, 4, 12, 24, 48, 72, 120, 168, 216 and 264 hours. The P release was calculated by volume leached, and P concentration in leachates determined by the vanadomolybdate method (Kitson and Mellon, 1944).

2.6 Statistical analysis

All statistical analysis was performed in R software (R Core Team, 2020), using the base, stats, corrplot nlstools, tidyverse, Metrics, emmeans packages (Baty et al., 2015; Hamner and Frasco, 2018; R Core Team, 2020; Russel, 2021; Wei and Simko, 2017; Wickham et al., 2019). The NPK indexes were compared between each BBF and the reference mineral fertilizer according to nutrient studied through the Dunnett test (p<0.05) after basic assumptions of analysis variance (normality, homoscedasticity, additivity, and independence of residuals) were attained, and the significance of the analysis of variance (ANOVA) was reached (p<0.05). The dataset related to maize cultivation was compared by the Duncan test (p<*0.05*) after ANOVA showed a significant difference (p<0.05) and the basic assumptions of analysis variance attended. In the dataset from the soil solution, the split-plot experiment was used is 4 x 6 (four-time of cultivation x 6 fertilizers treatments) to compare the treatments.

In the kinetics of P release studies, different nonlinear models were adjusted to the dataset of P released for each fertilizer (Dou et al., 1996; Liang et al., 2014; Lustosa Filho et al., 2017). The chosen mathematical model of kinetics of P released dataset was based on the highest value of the coefficient of determination (R^2), the lowest value of root-mean-square error (RMSE), and the Akaike information criterion (AIC) (Akaike, 1979). Mathematical models adjusted to kinetics of P release of each P source were compared by confidence interval generated through a 95% bootstrap confidence interval using 1000 bootstrap interactions. The mathematical models adjusted were the Elovich model (Eq. 5), simple exponential model (Eq. 6), power function (Eq. 7), and hyperbolic model (Eq. 9), as follows:

$$Pt=a+b \ln t$$

(Eq. 5)

$$Pt=N0\left(1-e^{-kt}\right) \quad \text{(Eq. 6)}$$

$$Pt=a*t^{b} \quad \text{(Eq. 7)}$$

$$Pt=\frac{N0*t}{(N0*b+t)} \quad \text{(Eq. 8)}$$

Where: Pt: fraction of P released from fertilizer in leaching time evaluated; a, initial P content released from fertilizer; b, P release rate constant of fertilizer, t, leaching nutrient release time (hour); N0, the maximum amount of P released from fertilizer during the whole kinetics study.

The data of cultivation without NPK fertilization was removed from the dataset; then biomass production and NPK in the shoot were correlated with amounts of nutrients applied and available contents in whole soil and its solution using the Pearson correlation (p<0.05).

3 Results

3.1 BBFs and mineral fertilizers characterization

The main properties and features of BBFs synthetized and mineral fertilizers were shown in **Table 2**. Compared to mineral fertilizers (**Table 3**), the BBFs had a lower proportion of mineral N (ammonium+nitrate) according to total N content. In relation to total P, all BBFs had lower proportion of P soluble in water and FA than TSP. Compared to TSP, BBF1, BBF3, and BBF4 had a lower proportion of P soluble in CA and NAC+H_2O. BBF2 and TSP had a similar proportion of P soluble in CA and NAC+H_2O. Contents of K soluble in water, CA, and FA according to total K content were lower for BBFs over KCl. However, the proportion of K soluble in NAC+H_2O was only reduced in BBF4 over KCl, while BBF1, BBF2, and BB3 had similar proportion of K soluble in NAC+H_2O compared to KCl.

Table 2. pH and nitrogen (N), phosphorus (P), and potassium (K) contents and forms in biochar-based fertilizers (BBFs) and mineral fertilizers used to nourish maize.

Fertilizer	pH	N^{Total}	$N\text{-}NH_4^+$	$N\text{-}NO_3^-$	$N^{organic}$
		g kg^{-1}			
BBF1	3.23 ±0.01	78.8 ±0.9	0.40 ±0.04	36.8 ±0.87	41.7 ±0.19
BBF2	2.62 ±0.01	84.9 ±1.1	0.69 ±0.10	47.6 ±0.71	36.6±0.87
BBF3	3.52 ±0.03	50.5±0.7	0.21 ±0.13	39.0 ±0.47	11.2 ±0.15
BBF4	2.32 ±0.01	57.7 ±1.6	0.04 ±0.02	51.8 ±1.42	5.83 ±0.22
NA	-	345 ±0.01	172.7 ±0.03	172.4 ±0.03	-
TSP	-	-	-	-	-
KCl	-	-	-	-	-

Fertilizer	P^{Total}	P^{H_2O}	P^{CA}	P^{NAC+H_2O}	P^{FA}
	g kg^{-1}				
BBF1	53.4 ±0.33	10.2 ±0.21	39.1 ±0.76	38.9 ±0.39	36.3 ±0.90
BBF2	44.8 ±0.26	34.0 ±0.13	38.0 ±0.58	44.2 ±0.33	35.3 ±0.69
BBF3	60.1 ±0.72	6.67 ±0.15	39.7 ±0.61	36.9 ±0.60	37.6 ±0.95
BBF4	48.2 ±0.48	25.7 ±0.26	31.2 ±0.60	35.6 ±0.26	27.0 ±0.34
NA	-	-	-	-	-
TSP	196 ±2.35	175 ±1.1	175 ±0.57	185 ±0.12	178 ±0.94
KCl	-	-	-	-	-

Fertilizer	K^{Total}	K^{H_2O}	K^{CA}	K^{NAC+H_2O}	K^{FA}
	g kg^{-1}				
BBF1	27.3 ±0.33	20.4 ±0.18	20.7±0.17	25.8 ±0.60	21.5 ±0.71
BBF2	24.1 ±0.25	19.6 ±0.06	18.7 ±0.33	23.5 ±0.80	19.0 ±0.21
BBF3	34.1 ±1.01	26.9 ±0.41	27.0 ±0.33	33.9 ±0.38	23.1 ±1.01
BBF4	28.4 ±0.33	20.6 ±0.46	18.8 ±0.40	25.4 ±0.40	21.0 ±0.93
NA	-	-	-	-	-
TSP	-	-	-	-	-
KCl	524 ±0.05	523 ±0.03	524 ±0.02	524 ±0.02	524 ±0.05

-Not detected or below the method limit of detection; NA: ammonium nitrate; TSP: triple superphosphate; KCl: potassium chloride; N^{Total}, $N\text{-}NH_4^+$, $N\text{-}NO_3^-$ and $N^{organic}$: , respectively, contents of total N, and N as ammonium, nitrate and in organic forms; P^{Total}, P^{H_2O}, P^{CA}, P^{NAC+H_2O}, and $P^{FA,}$ respectively, contents of total P, P soluble in water, in citric acid, in neutral ammonium citrate plus water and in formic acid; K^{Total}, K^{H_2O}, K^{CA}, K^{NAC+H_2O}, and K^{FA}, respectively, contents of total K, K soluble in water, in citric acid, in neutral ammonium citrate plus water and in formic acid.

Table 3. Index of nitrogen (N) forms, and phosphorus (P) and potassium (K) solubility in the different extractors for biochar-based fertilizers (BBFs) and mineral fertilizers according to the total content of N, P, and K respectively.

	Index (%)									
	N^{min}	$N^{organic}$	P^{H_2O}	P^{CA}	P^{NAC+H_2O}	P^{FA}	K^{H_2O}	K^{CA}	K^{NAC+H_2O}	K^{FA}
BBF1	47*	53*	19*	73*	73*	68*	75*	76*	95	79*
BBF2	57*	43*	76*	85	99	79*	81*	77*	97	79*
BBF3	78*	22*	11*	66*	61*	63*	79*	79*	99	68*
BBF4	90*	10*	53*	65*	74*	56*	72*	66*	89*	74*
NA	100	0	-	-	-	-	-	-	-	-
TSP	-	-	89	89	98	95	-	-	-	-
KCl	-	-	-	-	-	-	100	100	100	100

*: the means differed from the standard fertilizer used in comparison with the standard fertilizer by the Dunnett test ($p<0.05$), the standard fertilizer for N forms was ammonium nitrate (NA), for P solubility index was triple superphosphate (TSP) and for K solubility index was potassium chloride (KCl). -Not detected or low limit of detection of method; N^{min} and $N^{organic}$: respectively index of N mineral (ammonium+nitrate) and N organic according to total N contents; P^{H_2O}, P^{CA}, P^{NAC+H_2O}, and P^{FA}: respectively index of P soluble in water, in citric acid, in neutral ammonium citrate plus water and in formic acid according to total P contents; K^{Total}, K^{H_2O}, K^{CA}, K^{NAC+H_2O}, and K^{FA}: respectively index of K soluble in water, in citric acid, in neutral ammonium citrate plus water and in formic acid according to total K contents.

3.2 Infrared spectroscopy

FTIR spectrum of biochar showed the peaks related to OH stretching, C-H stretching of aliphatic groups, COO- carboxylate anions, C-H deformation from CH_2 groups, C-H bending, OH (phenolic groups), C-O stretching (**Supplementary material 1A**). APR showed peaks related to the CO_3 groups and P-O bonds (**Supplementary material 1B**). In the FTIR spectrum of BBFs were observed peaks related to OH stretching (3415 cm^{-1}) and carbon groups related to C-H stretching of aliphatic groups (2905 cm^{-1}), C-H deformation from CH_2 groups (1380 cm^{-1}). It was verified N groups related to N-H bonds (3240 cm^{-1}), N-H flexural of acid amides (1634 cm^{-1}), and NO_3 asymmetric stretching (1340 cm^{-1}). P peaks found in the FTIR spectrum of BBFs were related to P-O bonds (740, 820, 950, and 1040 cm^{-1}), P=O bonds (1235 cm^{-1}), ionic bond P^{+}-O^{-} in acid phosphate esters (1080 cm^{-1}) and P-H organophosphorus (2353

cm^{-1}) (**Figure 1**). All BBFs showed similar FTIR peaks but with different absorbance intensities.

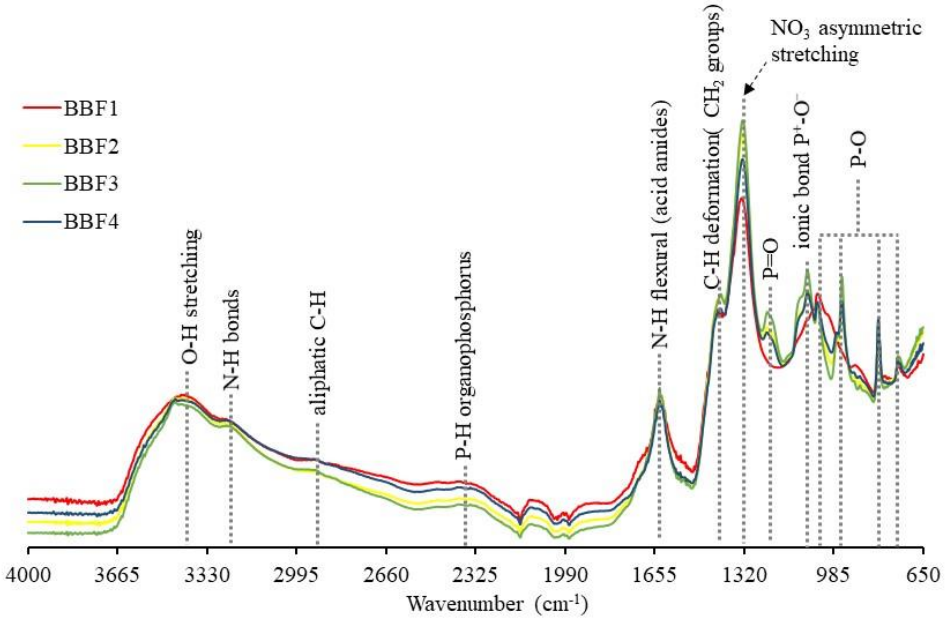

Figure 1. Normalized FTIR spectra of biochar-based fertilizers (BBFs) identifying the main peaks and groups.

Compared to Biochar used in the synthesis, the BBFs reduced the absorbance intensity of aliphatic groups, and peaks related to COO-carboxylate anions and OH (phenolic groups) from biochar disappeared in BBFs. The mains different between BBFs was related to higher absorbance in NO_3 asymmetric stretching as follows BBF3 > BBF2 > BBF4 > BBF1. The increased absorbance area between 1500 and1740 cm^{-1} related to the N-H flexural of acid amides was in the opposite direction of the NO_3 asymmetric stretching. P^{+}-O^{-} in acid phosphate esters and P=O bonds was higher as follows by BBFs: BBF3 > BBF4 = BBF2 > BBF1. Peaks related to P-O groups were higher in BBF1 than in other BBFs. P-H organophosphorus and aliphatic C was higher by BBF1 and BBF4 compared to BBF2 and BBF3.

3.3 BBFs agronomic performance

Values of pH analyzed in whole soil and soil solution was shown in **Supplementary material 4**. The main difference in maize growing and nutrition due the pH of soil solution was verified at 25 days when BBFs had higher pH values in soil solution compared to TSP. The negative control treatment where there was no NPK fertilization reduced the mineral N and the available levels of P and K over fertilization treatments (**Figure 2**). Due to the splitting of N and K in mineral fertilizers the lower values of N-mineral in the whole soil and soil K-Mehlich was verified when compared BBFs. Among the BBFs, BBF4 had higher N-mineral contents, and BBF3 had the highest soil K-Mehlich over other BBFs. The soil P-resin increased by BBF1, BBF3, and BB4 over TSP with higher increase for BBF1 (+28%) and BBF3 (+22%) over TSP. After maize cultivation, the higher N-mineral values were verified by no-NPK fertilization over fertilization treatments. Soil P-resin contents after maize cultivation were higher for BBF1 (+29%), BBF2 (+15%), and BBF3 (+43%) over TSP. K added via mineral fertilizer showed higher values of soil K-Mehlich over BBFs after maize cultivation increased of about 79%.

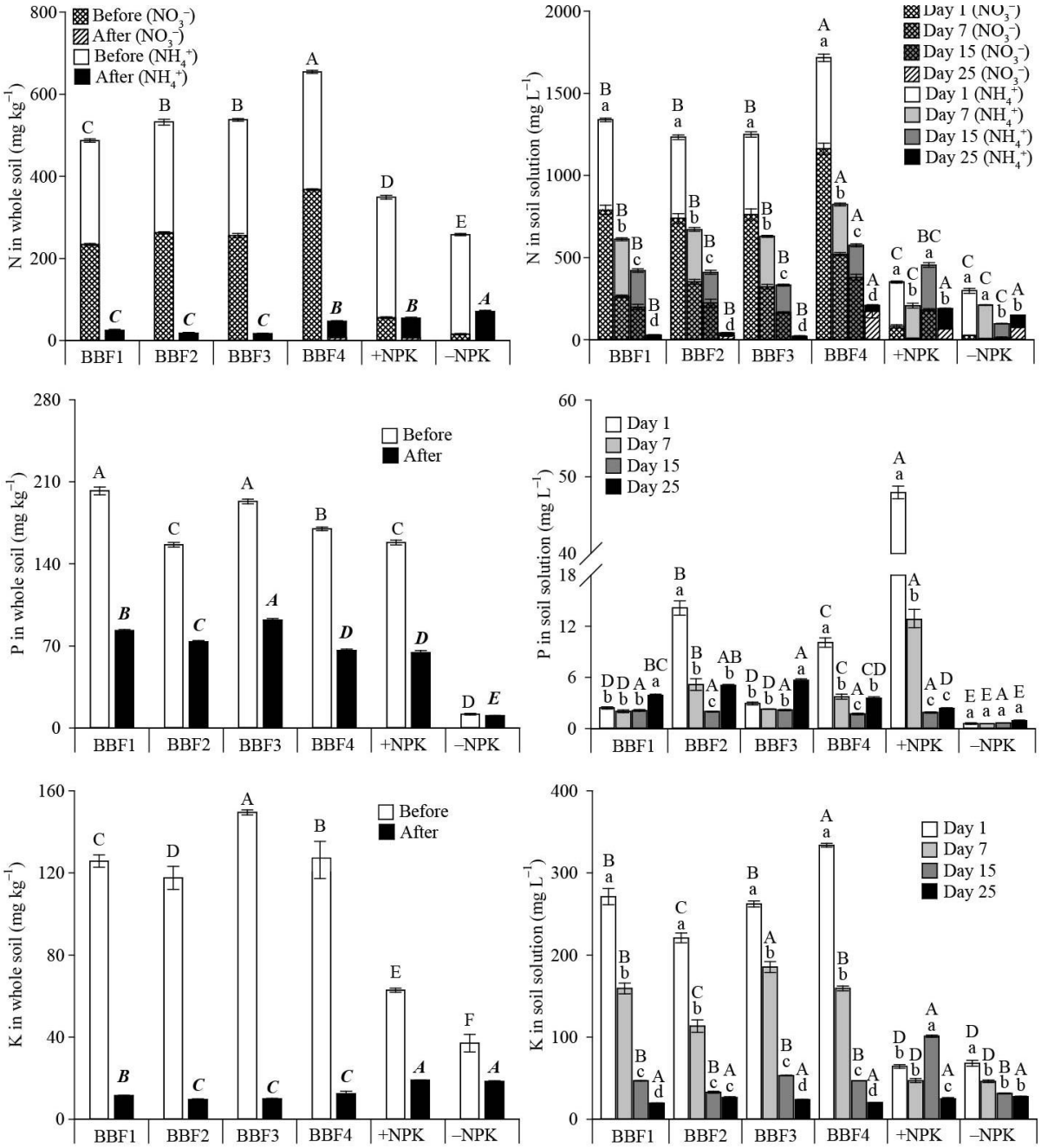

Figure 2. Contents of nitrogen mineral (N-mineral), phosphorus (P) available by the resin method, and potassium (K) available by the Mehlich-1 soil test method before and after maize cultivation; and N-mineral (NH_4^++NO_3^-), P, and K contents in the soil solution according to biochar-based fertilizers (BBFs), NPK added via mineral fertilizers (+NPK) and maize cultivation without NPK application (-NPK) at different times of soil solution collection. The bars with standard error followed by the same capital letter did not differ fertilizer treatment in each time evaluated (before or after cultivation or day 1, 7, 15, and 25) according to the Duncan test (p<0.05). The bars with standard error followed the same minuscule letter and did not differ the time evaluated in each fertilizer treatment tested according to the Duncan test (p<0.05).

Due to the splitting of N and K with the rest of fertilization applied at 13 days, in the soil solution collected at 1 and 7 days, there were higher solution contents of N-mineral and K by the BBFs over mineral fertilizers. Between BBFs, BBF4 had higher solution N- mineral at 1 and 7 days over other BBFs increases of about 24% and 20% respectively. For K in the soil solution among the BBFs, BBF4 had the higher values at day 1 (+23%) and BBF3 at day 7 (+20%). Evaluating the content of K in the soil solution at 15 days, NPK added via mineral fertilizers over BBFs increased of about 125% the K content; at 25 days, there was no difference between BBFs and NPK added via mineral fertilizers. For N-mineral and K in the soil solution there was a decrease according to the time evaluated from 1 to 25 days for all BBFs.

The TSP initially released a higher amount P for the soil solution compared to BBFs; however, there was a reduction of P the soil solution to TSP throughout the time of cultivation. BBFs, on the other hand, reduced the initial contents of P in the soil solution (-85%) over TSP, with higher reductions for BBF1 and BBF3, reduction of about 95% compared to TSP. At 15 days, there was no difference between the P contents in the soil solution for BBFs and TSP. At the final time evaluated (25 days), BBF1, BBF2, and BBF3 had higher contents of P in the soil solution over TSP, increase of about of 105% for BBFs over TSP.

When maize was not fertilized with NPK, the SDM, RDM, TDM, and accumulation of NPK in the shoot were lower over plants fertilizers with mineral fertilizers or BBFs (**Figure 3**). BBF1, BBF3 and BBF4 increased of about 24% SDM over TSP. All BBFs over TSP increased TDM (+25%) and RDM (+37%) over TSP. The accumulation of N in the shoot did not differ between BBFs and TSP. P accumulated in the shoot was higher for all BBFs over TSP, with a higher accumulated of P for BBF3, increase of about 46%. The K accumulated in the shoot was similar between BBF3, BBF4, and TSP, and this group increased of about 35% of K accumulated in shoot compared to BBF1 and BBF2.

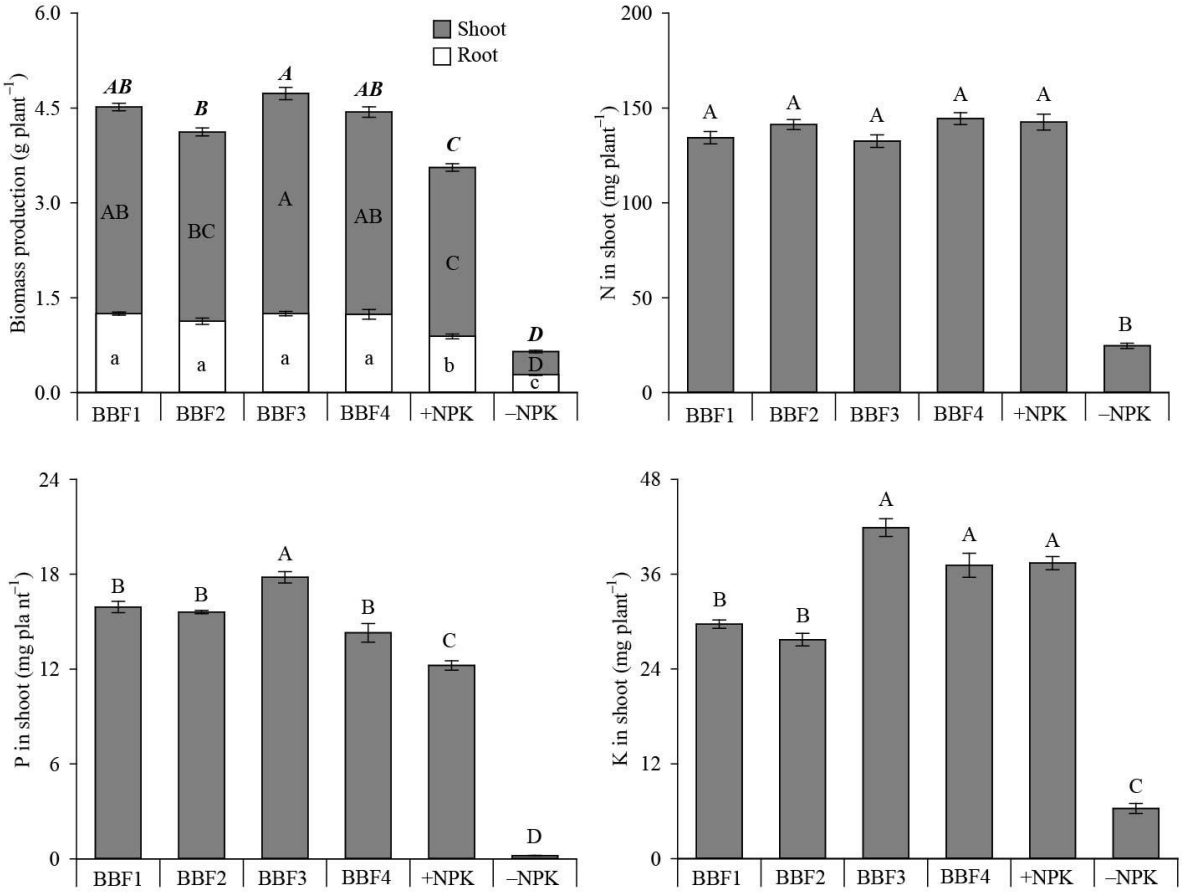

Figure 3. Biomass production and nitrogen (N), phosphorus (P), and potassium (K) accumulated in the maize shoot. The bars with standard error followed by the same bold italic, capital, and minuscule letter did not differ the fertilization treatments respectively for total (full bar), shoot, and root dry matter production according to the Duncan test ($p<0.05$). The bars with standard error followed by the same capital letter did not differ the fertilization treatments for N or P or P accumulated in maize shoot according to the Duncan test ($p<0.05$).BBF: Biochar based-fertilizer; +NPK: NPK added to soil via ammonium nitrate, triple superphosphate, and potassium chloride; –NPK: maize cultivated without NPK fertilization.

3.4 The kinetics of P release

In the study of the kinetics of P release, the equivalent amount used for maize cultivation was used (110 mg of P per pot based on the P solubility in NAC+H_2O); thus, the total P content applied was different between fertilizers, applying 151.0, 111.4, 179.4, 148.8 and114.6 mg of total P by mini-lysimeter (experimental unit), respectively by BBF1, BBF2, BBF3, BBF4, and TSP. The power model was best fitted for all fertilizers for P released in water (**Supplementary**

material 5). For P released in CA, the power model was the best model for BBF2, BBF4, and TSP, while the hyperbolic model for BBF1 and BBF3 (**Supplementary material 5**).

TSP had higher amounts of P released in water, about 81.2 mg until 12 hours with constant release from that 12 hours, equivalent to 71% of the total P applied (**Figure 4**). At the end of the kinetics study (264 hours), BBF4 and BBF2 had similar P released in water close to 74 mg of P, equivalent to 67% and 49% of the total P applied, respectively for BBF2 and BBF4. The P release in water for BBF2 and BBF4 was lower than TSP and higher over BBF1 and BBF3. Between BBF4 and BBF2, the P released from BBF2 was more gradual than BBF4. Initially, BBF1 and BBF3 had similar P released in water; however, during the time evaluated, BBF3 released lower amounts, closed to 26.7 mg (15% of the total P content) at 264 hours, compared to the amounts released from 31.5 mg to BBF1 (21% of total P content).

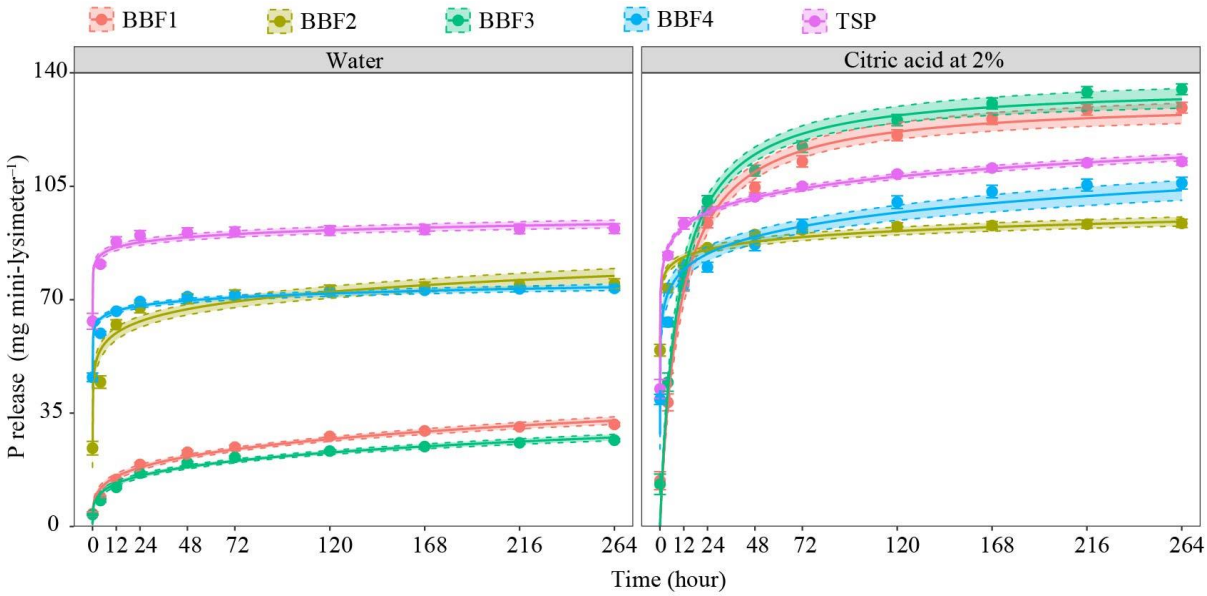

Figure 4. The kinetics of P release in water and citric acid at 2% as related to the total P content of biochar based-fertilizers (BBFs) and triple superphosphate (TSP).

In the kinetics of P release in CA, BBF1 and BBF3 initially released the lower amounts of P in CA; however, with the evaluation of time, this release was higher, reaching values of 129.3 and 135.0 mg of P at 264 hours, respectively for BBF1 and BBF3, values higher than the other fertilizers, equivalent to the released of 86 and 75% of the total P applied for BBF1 and BBF3. Initially, the P released in CA by TSP, BBF2, and BBF4 was similar at about 45.1 mg of P; however, with the evaluation of time, the P released from TSP was faster and higher than BBF2 and BBF4, reaching values close to 112.6 mg (98% of total P content applied) at 264 hours. Despite the faster initial releasesdof BBF2 and BBF4 over the other BBFs, both had the lowest released amounts of P in CA up to 264 hours, with BBF2 having the lowest amount released at 93.6 mg of P (84% of total P content), compared to the released amount of 106.0 mg of P (71% of total P content) using BBF4.

3.5 Correlation analysis

SDM, RDM, and TDM positively correlated ($p<0.05$) with P accumulated in the maize shoot, with coefficient of correlation of 0.85, 0.73, and 0.85, respectively, for SDM, RDM, and TDM, and not correlated ($p>0.05$) with N or K accumulated in the shoot. It was observed that the properties of whole soil and soil solution and N forms applied or evaluated in whole soil and its soil solution did not affect the N accumulated in the maize shoot (**Figure 5**). The P accumulated in the maize shoot positively correlated with solution pH at 25 days, amounts of total P applied and contents soluble in CA, soil P-resin before and after cultivation, and contents of P in soil solution at 25 days. There were negative correlation between P accumulated in the shoot and amounts of P release in water of kinetic of P release at all times evaluated, as well as the amounts of P release in the kinetics of P release study in CA at 0, 4, and 12 hours, the P contents in soil solution at 1 and 7 days, and amounts of P applied soluble in water. K

accumulated in the shoot positively correlated with K forms applied in soil (total K content, content of K soluble in water, in CA, in FA, and in NAC+H_2O).

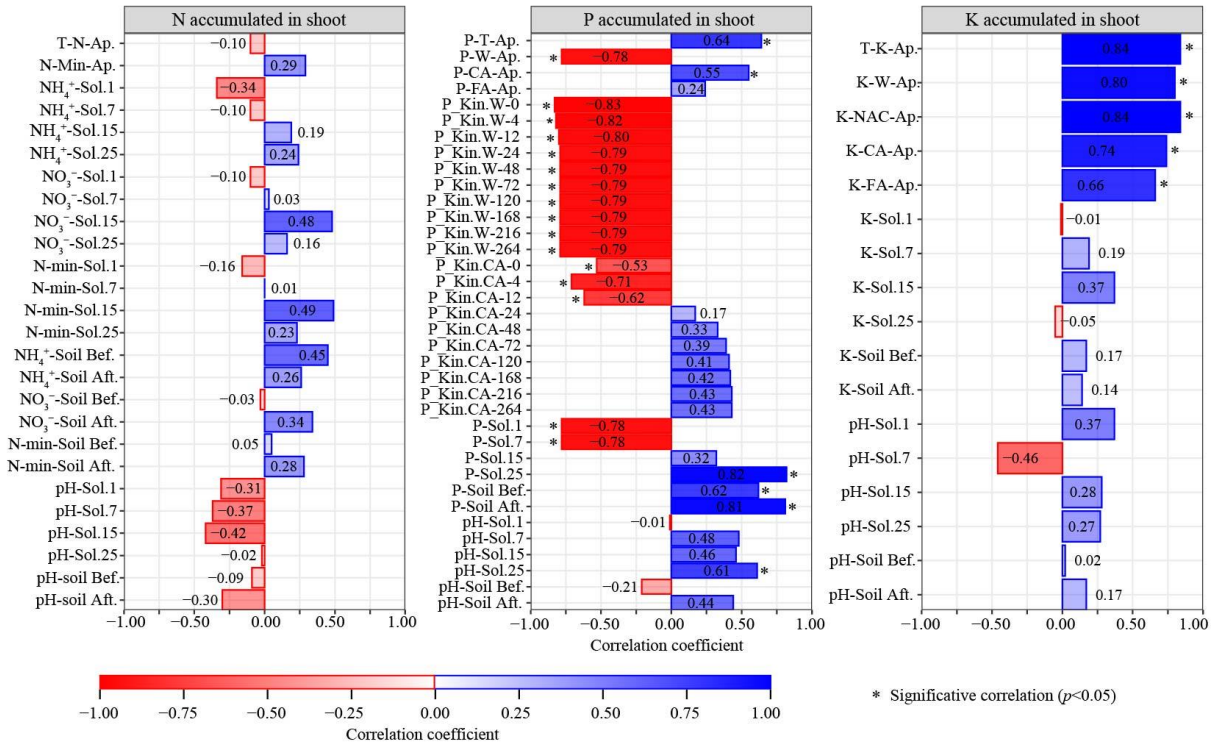

Figure 5. Correlation analysis between nitrogen (N) or phosphorus (P) or potassium (K) accumulated in the maize shoot and nutrients forms applied and availability in whole soil and soil solution. T-N-Ap. and N-Min-Ap.: amounts of total and mineral nitrogen forms applied during maize cultivation, respectively; NH_4^+-Sol.1, NH_4^+-Sol.7, NH_4^+-Sol.15 and NH_4^+-Sol.25: Ammonium content in soil solution at 1, 7, 15 and 25 days during maize cultivation, respectively; NO_3^--Sol.1, NO_3^--Sol.7, NO_3^--Sol.15 and NO_3^--Sol.25: nitrate content in soil solution at 1, 7, 15 and 25 days during maize cultivation, respectively; N-min-Sol.1, N-min-Sol.7, N-min-Sol.15 and N-min-Sol.25: mineral N content in soil solution at 1, 7, 15 and 25 days during maize cultivation, respectively; NH_4^+-Soil Bef. and NH_4^+-Soil Aft.: ammonium content in whole soil before and after maize cultivation, respectively; NO_3^--Soil Bef. and NO_3^--Soil Aft.: nitrate content in whole soil before and after maize cultivation, respectively; N-min-Soil Bef. and N-min-Soil Aft.: mineral N content in whole soil before and after maize cultivation, respectively; pH-Sol.1, pH-Sol.7, pH-Sol.15 and pH-Sol.25: pH in soil solution at 1, 7, 15 and 25 days during maize cultivation, respectively; pH-Soil Bef. and pH-Soil Aft.: pH in whole soil before and after maize cultivation, respectively; T-P-Ap., P-W-Ap., P-CA-Ap. and P-FA-Ap: amounts of total P and P soluble in water, citric acid and formic acid applied

during maize cultivation, respectively; P-Kin.W-0, P-Kin.W-4, P-Kin.W-12, P-Kin.W-24, P-Kin.W-48, P-Kin.W-72, P-Kin.W-120, P-Kin.W-168, P-Kin.W-216 and P-Kin.W-264: amounts of P release in water by the kinetics of P release at 0, 4, 12, 24, 48, 72, 120, 168, 216 and 264 hours, respectively; P-Kin.CA-0, P-Kin.CA-4, P-Kin.CA-12, P-Kin.CA-24, P-Kin.CA-48, P-Kin.CA-72, P-Kin.CA-120, P-Kin.CA-168, P-Kin.CA-216 and P-Kin.CA-264: amounts of P release in citric acid by the kinetics of P release at 0, 4, 12, 24, 48, 72, 120, 168, 216 and 264 hours, respectively; P-Sol.1, P-Sol.7, P-Sol.15 and P-Sol.25: P content in soil solution at 1, 7, 15 and 25 days during maize cultivation, respectively; P-Soil Bef. and P-Soil Aft.: P content available in whole soil before and after maize cultivation, respectively; T-K-Ap., K-W-Ap., K-NAC-Ap., K-CA-Ap. and K-FA-Ap: amounts of total K and K soluble in water, neutral ammonium citrate plus water, citric acid and formic acid applied during maize cultivation, respectively; K-Sol.1, K-Sol.7, K-Sol.15 and K-Sol.25: K content in soil solution at 1, 7, 15 and 25 days during maize cultivation, respectively; K-Soil Bef. and K-Soil Aft.: K content available in whole soil before and after maize cultivation, respectively;

4 Discussion

4.1 BBF chemical properties and FTIR-spectral signature

Due to the acidulation process involved in the BBFs synthesis, the pH of BBFs were acid (pH between 2.32-3.52) (**Table 2**). As in our study, however, using another inorganic acid (phosphoric acid) during BBFs synthesis, the pH of BBFs was reduced by acidulation compared to producing biochar without acidulation (Lustosa Filho et al., 2017). The pH of fertilizer controls dissolution and reactions in the soil-fertilizer interface (Lombi et al., 2005). In general, residues such as post coffee harvest used in our BBFs synthesis, when pyrolyzed, create biochar with alkaline pH (Lago et al., 2021). Alkaline pH of biochar can be a problem for P-BBFs synthesis because when Ca is present as in the use of APR, the increase of pH favors the formation of chemical stability reactions and stable precipitates between P and Ca that is unavailable to plants (Maluf et al., 2018); however in our synthesis, by controlling the synthesis we create BBFs that do not favor this type of reaction due to acid pH of BBFs.

The control during the synthesis of the new BBFs provided new properties such as different proportions of N-mineral (47-90%) and N-organic (10-53) forms, depending on the synthesis route (**Tables 2 and 3**). The main source in BBFs synthesis is N added via mineral forms; however, it was observed that part of N added was incorporated into biochar structure, transforming it into N-organic evaluated by chemical analysis and confirmed by the appearance of peaks in the FTIR spectrum of BBFs related to flexural N-H (acid amides) (**Figure 1**). Amides from biochar can generate NH_4^+ from amine and amide hydrolysis through the mineralization process (Wang et al., 2012). Part of N added remained in mineral forms as observed by chemical analysis and peaks related to NO_3 asymmetric stretching in the FTIR spectrum of BBFs. The N in materials based on biochar was founded in N-mineral and N-organic forms, and N-forms controlled the release of N (Wang et al., 2012). The different pools in organomineral fertilizers are essential to improve the efficiency of nitrogen fertilization because N-mineral supplies the N for the rapid growth of plants, while N-organic, when mineralized, supplies the N throughout the other phases of cultivation (Antille et al., 2014).

Highly soluble free forms of P in mineral fertilizers are prone to P losses in the soil, mainly in tropical soils due to specifically P adsorbed in Fe and Al oxides and low-activity mineral colloids, such as kaolinite (Fink et al., 2016; McLaughlin et al., 2011; Withers et al., 2018). Two strategies in OMFs are promising for increasing the agronomic efficiency of this class of fertilizers; one strategy is the reduction of readily available P evaluated by water solubility with the maintenance of the amount released in the long term evaluated by other methods such as CA, NAC+H_2O or FA (Maluf et al., 2018; Urrutia et al., 2014). In our BBFs, through the controls of the synthesis, it was possible to reduce the proportion of soluble P in water (11-76 %) compared to TSP, maintaining high levels of soluble P in NAC+H_2O (61-99 %), CA (65-85 %) and FA (56-79 %) (**Tables 2 and 3**).

The effect of P solubility occurs because the P is solubilized from the APR during the synthesis step, and the P is incorporated into the biochar matrix, forming organic P as observed in the FTIR spectrum by the appearance of peaks related to P-H organophosphorus and ionic bond P^{+}-O^{-} in acid phosphate esters (**Figure 1**), peaks already found in P-BBFs (Lustosa Filho et al., 2017). The reactions of P added via mineral forms and C from biochar promoting differences in solubility of P evaluated by different extractors such as water, FA, CA, and NAC+H_2O, were demonstrated using different sources of P as TSP or monoammonium phosphate or phosphoric acid mixed with biochar (Lustosa Filho et al., 2019, 2017; Suwanree et al., 2022). Besides, these effects of the interaction of C and P are related to the second strategy that includes a reaction between P and C, forming complexes with higher agronomic performance in plants (Erro et al., 2012).

The synthesis of NPK-BBFs on mineral sources has a more gradual release of K that can increase crop nutrient use efficiency, an effect related to the interaction of K and biochar (Piash et al., 2022). In our BBFs over the mineral source of K (KCl), the interaction of K and biochar was observed in the solubility of K in different extractors; according to the content of total K, BBFs over KCl reduced the proportion of K soluble in water (72-81 %), maintaining the high levels of K soluble in NAC+H_2O (89-99 %), indicating a more gradual release of K (**Tables 2 and 3**). In biochar, similar to what happens in the soil, there is the development of negative charges biochar, responsible for promoting the cation exchange capacity (CEC); CEC able to retain nutrients such as K in electrostatic adsorption bonds (Domingues et al., 2017; Lago et al., 2021; Munera-Echeverri et al., 2018).

4.2 Agronomic performance and the kinetics of P release of BBFs

Once the amount of N from the BBFs was applied fully at planting and the mineral fertilization with N (ammonium nitrate) was split (10% planting and 90% splitting at 13 days),

there were higher contents of N-mineral in whole soil before cultivation and in the soil solution at 1 and 7 days by BBFs over mineral fertilization, (**Figure 2**) with BBF4 having the higher values between BBFs due to the higher amounts of N-mineral by BBF4 fertilizer (**Supplementary material 3**). From the mineral split-fertilization at 13 days, and evaluating the N in the soil solution at 15 days, only the BBF4 had higher values over mineral fertilization. At the end of the maize cultivation, in the whole soil and soil solution (25 days), BBF4 and mineral fertilization had similar and higher values over others BBFs.

The effects on N availability in the whole soil and its solution from BBFs did not modify the N accumulation in the maize shoot since the N accumulation was similar for the BBFs and mineral fertilization, and the N forms applied and contents of N-mineral in the whole soil and its solution were not correlated with N accumulated in the maize shoot (**Figures 3 and 5**). Similar to our results, evaluating the mixture of N-urea with biochar and confirming its interaction by the formation of primary amides and amide carbonyl in the FTIR spectrum, the N-BBF produced did not increase N accumulation in the shoot in the first cultivation using beans as plant test; however, in successive cultivation in the same pots using maize, the N-BBFs increased the accumulation of N in the shoot over isolated application of urea, showing a residual effect of N fertilization with BBFs (Barbosa et al., 2022).

Where N interacts with biochar, N is retained by the biochar surfaces, decreases the release rate of N, and consequently may increase plant growth and efficiency of N by plants over mineral fertilization (Shi et al., 2020). Since in addition to this interaction, N in biochar can be found in different organic forms, more or less be mineralized over time according to the soil type (Wang et al., 2012), and taking into account the short time of our experiment (25 days) and the higher amounts of N-organic applied by BBFs (**Supplementary material 3**), there is a higher potential for BBFs over mineral fertilizers to mineralizer this N, so subsequent

incubation studies should be done to assess the potential of BBFs to mineralizer N, and the plants use this N.

When K is applied at the same amounts and phase of cultivation, in BBFs over mineral fertilizers, due to the gradual release of K, it is expected that the use efficiency of K by plants is increased since this more gradual release reduces K losses by leaching in the soil, which consequently increases the availability of K in the soil and can reduce the need to split the K fertilization (Fachini et al., 2022, 2021; Gwenzi et al., 2018; Piash et al., 2022). The more gradual release of K in BBFs involve the mechanisms as: i) K retention due to electrostatic attraction in negatively charged functional groups in biochar, such as carboxyl and phenolic; ii) physical protection of K inside the biochar pores; iii) hydrophobic nature of biochar that makes it difficult to water diffusion and consequently the dissolution of K (Fachini et al., 2022; Mukherjee et al., 2011). However, in our study due to splitting of K in mineral fertilization these effects of more gradual release on K availability and K nutrition of maize were not observed. Applying all the K of the BBFs at planting and the splitting used when the K was added via mineral fertilizers (KCl); initially, the soil K-Mehlich and K in the soil solution at 1 and 7 days were higher for the BBFs over KCl (**Figure 2**). Among the BBFs, the higher soil K-Mehlich was found to BBF3>BBF4>BBF1>BB2, increments related to higher amount of K applied (total K and K soluble in FA, CA, water, and NAC+H_2O) (**Supplementary material 3**).

The accumulation of K in the shoot was more affected by the amounts applied than by the availability of K in the soil and the solution, as observed by the correlation analysis (**Figure 5**); however, this higher accumulation of K was not factor that limited the production of biomass of maize, since there was no correlation between the accumulation of K in the shoot and the production of maize biomass. The lack of relationship between K accumulation in the maize shoot and biomass production is due to the relationship between K content and plant production,

where if and K is found in concentrations in the luxury range (above 50 g of K by kg of shoot tissue)(Marschner, 2012), increasing K concentration in the leaf does not increase biomass despite proportionally increasing K accumulation, as observed by the concentration of K in the maize shoot in our experiment, ranging from 88-174 g of K by kg of maize shoot tissue.

Although the availability of K does not explain the accumulation of K, after maize cultivation, the soil K-Mehlich contents were higher for mineral fertilization over BBFs, so an accumulation similar to BBFs (BBF3 and BBF4) by mineral fertilization (**Figures 2 and 3**). Thus, the splitting practice effectively supplied the K to the plant and promoted a higher residual effect over K incorporated in BBFs and fully applied in the planting fertilization. The practice of splitting K improves the use efficiency of K by plants; as part of this, K is applied when there is greater root development, which promotes favorable conditions for better K uptake (Torabian et al., 2021).

In tropical soils, there is a generalized natural deficiency of NPK, nutrients that limit crop production (Lopes and Guilherme, 2016), an effect found in our study where cultivation without the application of NPK is either by mineral fertilizers or BBFs limited the plant growth and NPK nutrition (**Figure 3**). In the use of fertilization with NPK, among the main effects of the applied forms and availability of nutrients on maize production, P was the nutrient that influenced the production of maize biomass since SDM, RDM and TDM were positively correlated with P accumulated in the maize shoot (**Figure 5**). Compared to NPK added via mineral fertilizers over BBFs, all BBFs increased TDM, RDM and P accumulated in the shoot, and SDM was increased by BBF1, BBF3 and BBF4 over mineral fertilizers.

In relation to P dynamics, the BBFs increased the accumulation of P in the shoot through different mechanisms; evaluating the soil P-resin, the BBFs over mineral fertilization increased the soil P-resin, with greater values found for BBF1 and BBF3 (**Figure 2**). The main effects of BBFs on P available include: i) the complexation of P in organic forms; ii) reduction

the P sorption and precipitation with cations in the soil solution; ii) reduction of P-specific adsorption in sites of tropical soils; iii) competitive reactions between P and C organic molecules from biochar by adsorption sites in the soil, thus blocking P adsorption sites; iv) a more gradual release of P from BBFs (An et al., 2021; Bai et al., 2022; Carneiro et al., 2021; Ghodszad et al., 2021; Johan et al., 2021). Since the availability of P is increased by the use of biochar, consequently the uptake and use efficiency of P is increased by the crops (Bai et al., 2022). Similarly, our results showed that the increase of soil P-resin was positively correlated with P accumulated in the shoot (**Figure 5**).

A more gradual release of P in P-BBFs may promote a higher residual effect in plants successively cultivated compared to mineral phosphate fertilizers (Carneiro et al., 2021) as verified in our study, where, besides the higher accumulation of P in maize shoot (**Figure 3**) by the BBFs, related to the increase in the initial soil P-resin, it was possible to verify a higher residual of fertilization with BBF1, BBF2 and BBF3, increasing the soil P-resin after maize cultivation (**Figure 2**). A more gradual release of P in BBFs is related to the reduction of amounts of P soluble in water, whether in traditional methods or studies of the kinetics of P release in water (Carneiro et al., 2021; Lustosa Filho et al., 2017; Suwanree et al., 2022)..

Compared to TSP, BBFs had a more gradual release of P reducing readily available P in water (**Table 2**), evaluating the standard method used in Brazil and studying the kinetics of release using water (**Figure 4**). The reduction in the amounts of readily available and soluble P in water, the reduction in the amount of P released in water throughout the study period (0 to 264 hours) of the kinetics of P release, and the reduction in the amount of P released in CA in the kinetics of P release study from 0 to 12 hours, showed a positive correlation with the accumulation of P in the shoot (**Figure 5**). The slow release from organomineral fertilizers as BBFs, may reduce P losses by adsorption reactions on the surface of the soil mineral and

consequently improve the P availability in soil and P uptake for plants (Bai et al., 2022; Frazão et al., 2019; Ghodszad et al., 2021; Sakurada et al., 2016), effect found in our study.

A more gradual release of P from BBFs reduced initial P contents in soil solution at 1 and 7 days (**Figure 2**). TSP rapidly released P into the soil solution, increasing P in the soil solution over BBFs; however, the amount of P in the soil solution at 1 and 7 days was negatively correlated with P accumulated in the shoot (**Figure 5**). Unlike TSP, BBFs gradually released P into the soil solution. At the time of higher plant growth in the study (25 days), the gradual release of P from the BBFs increased the solution P overt TSP. The amounts of P in the soil solution at 25 days were positively correlated with the P accumulated in the shoot. Highly soluble forms of P applied to the soil in the form of fertilizers promote a rapid increase in P concentration in the soil solution, and over time this P chemically reacts through precipitation or adsorption processes, which decreases its solubility (Johan et al., 2021), the effect observed by the application of TSP.

Among the BBFs, the BBF that provided the higher accumulation of P in the shoot was the one that had the lowest release of P in water but with the higher release of P when using CA as an extractor solution (**Figures 3 and 4**). Extractors such as water extract the P readily available and soluble P, while extractors such as CA extract P can be used by plants (Binh and Zapata, 2002; Erro et al., 2007). Thus, a strategy to ensure and evaluate adequate P supply would be the combination of low amounts of P released in release kinetics using water with high proportions released using CA, as observed in our study. Organic acids such as CA can dissolve phosphate in mineral compounds, and plant roots naturally secrete citrate into the soil to improve their P acquisition by the roots. In addition, di- and tricarboxylic acid anions, mainly by citrate and oxalate, can dissolve organic molecules to which P is bound, resulting in the release of inorganic P (Johan et al., 2021). Thus, using CA in P-release kinetics in BBFs is

promising as there is both mineral and organic P, where CA can access this P compared to kinetics performed only using water.

Besides, the pH of soil solution evaluated at 25 days (**Supplementary material 4**) increased by BBFs over TSP correlated with P accumulated in the shoot (**Figure 5**). The effect of BBFs over TSP increasing soil pH before cultivation was demonstrated by Lustosa Filho et al., (2019); however, this effect did not improve P nutrition in maize plants, contrary to what was observed in our study. Pyrolysis usually results in biochar with a pH in the alkaline range, so the soil pH is increased as a result of this effect (Bai et al., 2022; Domingues et al., 2017; Ghodszad et al., 2021; Johan et al., 2021); however, in our BBFs, the pH was in the acid range (**Table 2**). Furthermore, biochar can act as a buffer in the culture medium due to the presence of organic radicals (Domingues et al., 2017; Ghodszad et al., 2021; Johan et al., 2021). Comparing the initial and final pH (25 days) of the soil solution, the BBFs had lower variation in the values over TSP, indicating a possible buffering due to the use of BBFs. The effect of BBFs on the pH of the soil solution has a direct effect on the availability of P because as the pH decreases, there is a reduction in the availability of P by specific adsorption and formation of stable compounds between P and Fe and P and Al in tropical soils (Fink et al., 2016).

Thus, it was possible to observe that the synthesized BBFs influenced P nutrition and consequently maize biomass production through different mechanisms such as i) interaction between P and the pyrolyzed organic matrix forming complexes verified in the infrared; ii) reduction of readily available and water-soluble forms of P with the maintenance of P in forms released during cultivation; iii) gradual release of P contained in BBFs; iv) reduction of the initial levels of P in the soil solution with the release of this P in times of greater demand for the maize crop; v) increase in the initial availability of P in the whole soil; vi) Higher buffering of the pH of the soil solution at the time of higher vegetative growth, contributing to the increase

of P availability. In addition, BBFs promoted an increase in the residual effect of fertilization with P compared to TSP.

4.3 Study limitations and prospects

The new proposed cultivation method (**Supplementary material 2**) collecting the soil solution throughout the cultivation is promising for other experiments because, with a sampling of soil solution throughout crop cultivation, the release of NPK can be determined in soil solution throughout plant growth. Overall, soil solution is the compartment from which plants acquire nutrients. Furthermore, since one of the main characteristics of BBFs is the gradual release of NPK, in this new approach to assessing nutrient pools readily available to corps, it is possible to observe and measure nutrient release in real-time. However, the approach was developed for a short time for grown plants; thus, adaptations must be made to long-term plant growth in different cultivation scenarios.

The new synthesized BBFs are promising either to reduce N and K topdressing with all N and K added to soil at crop planting with the same efficiency of total N and K fertilization over splitting N and K mineral sources. In addition, BBFs have properties that ensure higher efficiency in using P than P soluble mineral sources. Therefore, it is necessary to test BBFs agronomic value crop fields in different cultivation scenarios to determine the most promising scenarios to promote more sustainable use of non-renewable NPK inputs.

According to BBF spectral signatures, the presence of C groups in the aliphatic form predominates in the formulated fertilizers, which favors plant growth, considering that these organic functional groups act as plant biostimulants. The role played by C-aliphatic groups as biostimulants trigger the activity of plasma membrane H^+-ATPase in response to the application of humic substances-based materials (Aguiar et al., 2013). H^+-ATPase is a proton pump in the plant cell that improves nutrient uptake (Marschner, 2012); thus, further studies must be carried

out on the role played by the organic matrix of BBFs on plant physiology and metabolites synthesis processes.

5 Conclusion

The production of biochar-based fertilizers (BBFs) promoted the interaction of N and P with the biochar matrix forming N and P organic forms, while K was retained in the negative charges of the biochar; consequently, NPK has a gradual release. The gradual release of N and K had the same effect as the mineral fertilization split applied to N and K nutrition in maize. The increased of P nutrition in maize by applying BBFs with gradual P release led to increased maize biomass production. P nutrition dynamics was the main factor affecting maize biomass production. The synthesized BBFs reduced the readily soluble and available P but maintained high levels of available P for a long time. P having a gradual release initially reduced the P levels in the soil solution; however, in times of higher requirements, this P was released with a high relation with the absorption of P. In addition, the gradual release of P promoted a higher availability of P in the whole soil, factors that increased P uptake by maize. In addition to improving P nutrition, BBFs on mineral sources hada higher residual effect on P fertilization.

6 Acknowledgments

Many thanks to the Coordination for the Improvement of Higher Education Personnel (CAPES) (CAPES-PROEX/AUXPE 593/2018), National Council for Scientific and Technological Development (CNPq) (303899/2015-8 and 307447/2019-7 grants), and the Foundation for Research of the State of Minas Gerais (FAPEMIG) for financial support and scholarships provided. UFLA is an equal opportunity provider and employer.

7 References

Aguiar, N.O., Novotny, E.H., Oliveira, A.L., Rumjanek, V.M., Olivares, F.L., Canellas, L.P., 2013. Prediction of humic acids bioactivity using spectroscopy and multivariate analysis. J. Geochemical Explor. 129, 95–102. https://doi.org/10.1016/j.gexplo.2012.10.005

An, X., Wu, Z., Liu, X., Shi, W., Tian, F., Yu, B., 2021. A new class of biochar-based slow-release phosphorus fertilizers with high water retention based on integrated co-pyrolysis and co-polymerization. Chemosphere 285, 131481. https://doi.org/10.1016/j.chemosphere.2021.131481

Antille, D.L., Sakrabani, R., Godwin, R.J., 2014. Nitrogen Release Characteristics from Biosolids-Derived Organomineral Fertilizers. Commun. Soil Sci. Plant Anal. 45, 1687–1698. https://doi.org/10.1080/00103624.2014.907915

Bai, S.H., Omidvar, N., Gallart, M., Kämper, W., Tahmasbian, I., Farrar, M.B., Singh, K., Zhou, G., Muqadass, B., Xu, C.-Y., Koech, R., Li, Y., Nguyen, T.T.N., van Zwieten, L., 2022. Combined effects of biochar and fertilizer applications on yield: A review and meta-analysis. Sci. Total Environ. 808, 152073. https://doi.org/10.1016/j.scitotenv.2021.152073

Barbosa, C.F., Correa, D.A., Carneiro, J.S. da S., Melo, L.C.A., 2022. Biochar Phosphate Fertilizer Loaded with Urea Preserves Available Nitrogen Longer than Conventional Urea. Sustainability 14, 686. https://doi.org/10.3390/su14020686

Baty, F., Ritz, C., Charles, S., Brutsche, M., Flandrois, J.-P., Delignette-Muller, M.-L., 2015. A Toolbox for Nonlinear Regression in R : The Package nlstools. J. Stat. Softw. 66. https://doi.org/10.18637/jss.v066.i05

Binh, T., Zapata, F., 2002. Standard characterization of phosphate rock samples from the FAO/IAEA phosphate project, in: Assessment of Soil Phosphorus Status and Management of Phosphatic Fertilizers to Optimize Crop Production. IAEA-TECDOC-1272, Vienna, pp. 9–23.

Brazil, 2017. Manual de métodos analíticos oficiais para fertilizantes e corretivos. MAPA, Brasília.

Bremner, J.M., Keeney, D.R., 1966. Determination and Isotope-Ratio Analysis of Different Forms of Nitrogen in Soils: 3. Exchangeable Ammonium, Nitrate, and Nitrite by Extraction-Distillation Methods. Soil Sci. Soc. Am. J. 30, 577–582. https://doi.org/10.2136/sssaj1966.03615995003000050015x

Carneiro, J.S.S., Andrade Ribeiro, I.C., Nardis, B.O., Barbosa, C.F., Lustosa Filho, J.F., Azevedo Melo, L.C., 2021. Long-term effect of biochar-based fertilizers application in

tropical soil: Agronomic efficiency and phosphorus availability. Sci. Total Environ. 760. https://doi.org/10.1016/j.scitotenv.2020.143955

Domingues, R.R., Trugilho, P.F., Silva, C.A., De Melo, I.C.N.A., Melo, L.C.A., Magriotis, Z.M., Sánchez-Monedero, M.A., 2017. Properties of biochar derived from wood and high-nutrient biomasses with the aim of agronomic and environmental benefits. PLoS One 12. https://doi.org/10.1371/journal.pone.0176884

Dou, Z., Toth, J.D., Jabro, J.D., Fox, R.H., Fritton, D.D., 1996. Soil nitrogen mineralization during laboratory incubation: Dynamics and model fitting. Soil Biol. Biochem. 28, 625–632. https://doi.org/10.1016/0038-0717(95)00184-0

Enders, A., Lehmann, J., 2012. Comparison of Wet-Digestion and Dry-Ashing Methods for Total Elemental Analysis of Biochar. Commun. Soil Sci. Plant Anal. 43, 1042–1052. https://doi.org/10.1080/00103624.2012.656167

Erro, J., Urrutia, O., Baigorri, R., Aparicio-Tejo, P., Irigoyen, I., Torino, F., Mandado, M., Yvin, J.C., Garcia-Mina, J.M., 2012. Organic Complexed Superphosphates (CSP): Physicochemical characterization and agronomical properties. J. Agric. Food Chem. 60, 2008–2017. https://doi.org/10.1021/jf204821j

Erro, J., Urrutia, O., San Francisco, S., Garcia-Mina, J.M., 2007. Development and agronomical validation of new fertilizer compositions of high bioavailability and reduced potential nutrient losses. J. Agric. Food Chem. 55, 7831–7839. https://doi.org/10.1021/jf0708490

Everaert, M., Warrinnier, R., Baken, S., Gustafsson, J.P., De Vos, D., Smolders, E., 2016. Phosphate-Exchanged Mg-Al Layered Double Hydroxides: A New Slow Release Phosphate Fertilizer. ACS Sustain. Chem. Eng. 4, 4280–4287. https://doi.org/10.1021/acssuschemeng.6b00778

Fachini, J., Figueiredo, C.C. de, Frazão, J.J., Rosa, S.D., da Silva, J., Vale, A.T. do, 2021. Novel K-enriched organomineral fertilizer from sewage sludge-biochar: Chemical, physical and mineralogical characterization. Waste Manag. 135, 98–108. https://doi.org/10.1016/j.wasman.2021.08.027

Fachini, J., Figueiredo, C.C. de, Vale, A.T. do, 2022. Assessing potassium release in natural silica sand from novel K-enriched sewage sludge biochar fertilizers. J. Environ. Manage. 314. https://doi.org/10.1016/j.jenvman.2022.115080

FAO, 2017. World fertilizer trends and outlook to 2020: Summary report. Food Agric. Organ. United Nations 38.

Fink, J.R., Inda, A.V., Tiecher, T., Barrón, V., 2016. Iron oxides and organic matter on soil phosphorus availability. Ciência e Agrotecnologia 40, 369–379.

https://doi.org/10.1590/1413-70542016404023016

Fox, C.L., 1951. Stable Internal Standard Flame Photometer for Potassium and Sodium Analyses. Anal. Chem. 23, 137–142. https://doi.org/10.1021/ac60049a028

Frazão, J.J., Benites, V. de M., Ribeiro, J.V.S., Pierobon, V.M., Lavres, J., 2019. Agronomic effectiveness of a granular poultry litter-derived organomineral phosphate fertilizer in tropical soils: Soil phosphorus fractionation and plant responses. Geoderma 337, 582–593. https://doi.org/10.1016/j.geoderma.2018.10.003

Gautam, R., Vanga, S., Ariese, F., Umapathy, S., 2015. Review of multidimensional data processing approaches for Raman and infrared spectroscopy. EPJ Tech. Instrum. 2, 1–8. https://doi.org/10.1140/epjti/s40485-015-0018-6

Ghodszad, L., Reyhanitabar, A., Maghsoodi, M.R., Asgari Lajayer, B., Chang, S.X., 2021. Biochar affects the fate of phosphorus in soil and water: A critical review. Chemosphere 283, 131176. https://doi.org/10.1016/j.chemosphere.2021.131176

Gmach, M.R., Cherubin, M.R., Kaiser, K., Cerri, C.E.P., 2020. Processes that influence dissolved organic matter in the soil: a review. Sci. Agric. 77. https://doi.org/10.1590/1678-992x-2018-0164

Gwenzi, W., Nyambishi, T.J., Chaukura, N., Mapope, N., 2018. Synthesis and nutrient release patterns of a biochar-based N–P–K slow-release fertilizer. Int. J. Environ. Sci. Technol. 15, 405–414. https://doi.org/10.1007/s13762-017-1399-7

Hamner, B., Frasco, M., 2018. Metrics: Evaluation Metrics for Machine Learning.

Johan, P.D., Ahmed, O.H., Omar, L., Hasbullah, N.A., 2021. Phosphorus Transformation in Soils Following Co-Application of Charcoal and Wood Ash. Agronomy 11, 2010. https://doi.org/10.3390/agronomy11102010

Kennedy, L.J., Vijaya, J.J., Sekaran, G., 2004. Effect of Two-Stage Process on the Preparation and Characterization of Porous Carbon Composite from Rice Husk by Phosphoric Acid Activation. Ind. Eng. Chem. Res. 43, 1832–1838. https://doi.org/10.1021/ie034093f

Kitson, R.E., Mellon, M.G., 1944. Colorimetric Determination of Phosphorus as Molybdivanadophosphoric Acid. Ind. Eng. Chem. Anal. Ed. 16, 379–383. https://doi.org/10.1021/i560130a017

Lago, B.C., Silva, C.A., Melo, L.C.A., Morais, E.G. de, 2021. Predicting biochar cation exchange capacity using Fourier transform infrared spectroscopy combined with partial least square regression. Sci. Total Environ. 794, 148762. https://doi.org/10.1016/j.scitotenv.2021.148762

Liang, Y., Cao, X., Zhao, L., Xu, X., Harris, W., 2014. Phosphorus Release from Dairy Manure,

the Manure-Derived Biochar, and Their Amended Soil: Effects of Phosphorus Nature and Soil Property. J. Environ. Qual. 43, 1504–1509. https://doi.org/10.2134/jeq2014.01.0021

Lombi, E., McLaughlin, M.J., Johnston, C., Armstrong, R.D., Holloway, R.E., 2005. Mobility, solubility and lability of fluid and granular forms of P fertiliser in calcareous and non-calcareous soils under laboratory conditions. Plant Soil 269, 25–34. https://doi.org/10.1007/s11104-004-0558-z

Lopes, A.S., Guilherme, L.R.G., 2016. A career perspective on soil management in the Cerrado region of Brazil, Advances in Agronomy. Elsevier Inc. https://doi.org/10.1016/bs.agron.2015.12.004

Lustosa Filho, J.F., Barbosa, C.F., Carneiro, J.S.D.S., Melo, L.C.A., 2019. Diffusion and phosphorus solubility of biochar-based fertilizer: Visualization, chemical assessment and availability to plants. Soil Tillage Res. 194. https://doi.org/10.1016/j.still.2019.104298

Lustosa Filho, J.F., Penido, E.S., Castro, P.P., Silva, C.A., Melo, L.C.A., 2017. Co-Pyrolysis of Poultry Litter and Phosphate and Magnesium Generates Alternative Slow-Release Fertilizer Suitable for Tropical Soils. ACS Sustain. Chem. Eng. 5, 9043–9052. https://doi.org/10.1021/acssuschemeng.7b01935

Maluf, H.J.G.M., Silva, C.A., Morais, E.G. de, Paula, L.H.D. de, 2018. Is Composting a Route to Solubilize Low-Grade Phosphate Rocks and Improve MAP-Based Composts? Rev. Bras. Ciência do Solo 42. https://doi.org/10.1590/18069657rbcs20170079

Marschner, P., 2012. Marschner's Mineral Nutrition of Higher Plants. Elsevier, Oxford. https://doi.org/10.1016/C2009-0-63043-9

McLaughlin, M.J., McBeath, T.M., Smernik, R., Stacey, S.P., Ajiboye, B., Guppy, C., 2011. The chemical nature of P accumulation in agricultural soils-implications for fertiliser management and design: An Australian perspective. Plant Soil 349, 69–87. https://doi.org/10.1007/s11104-011-0907-7

Mukherjee, A., Zimmerman, A.R., Harris, W., 2011. Surface chemistry variations among a series of laboratory-produced biochars. Geoderma 163, 247–255. https://doi.org/10.1016/j.geoderma.2011.04.021

Mumbach, G.L., Gatiboni, L.C., de Bona, F.D., Schmitt, D.E., Corrêa, J.C., Gabriel, C.A., Dall'Orsoletta, D.J., Iochims, D.A., 2020. Agronomic efficiency of organomineral fertilizer in sequential grain crops in southern Brazil. Agron. J. 112, 3037–3049. https://doi.org/10.1002/agj2.20238

Munera-Echeverri, J.L., Martinsen, V., Strand, L.T., Zivanovic, V., Cornelissen, G., Mulder, J., 2018. Cation exchange capacity of biochar: An urgent method modification. Sci. Total

Environ. 642, 190–197. https://doi.org/10.1016/j.scitotenv.2018.06.017

Murphy, J., Riley, J.P., 1962. A modified single solution method for the determination of phosphate in natural waters. Anal. Chim. Acta 27, 31–36. https://doi.org/10.1016/S0003-2670(00)88444-5

Novais, R.F.., Neves, J.C.L.., Barros, N.F., 1991. Ensaio em ambiente controlado, in: Oliveira, A.J.., Garrido, W.E.., Araújo, J.D.., Lourenço, S. (Eds.), Métodos de Pesquisa Em Fertilidade Do Solo. Embrapa-SEA, Brasília, p. 189−253.

Phares, C.A., Atiah, K., Frimpong, K.A., Danquah, A., Asare, A.T., Aggor-Woananu, S., 2020. Application of biochar and inorganic phosphorus fertilizer influenced rhizosphere soil characteristics, nodule formation and phytoconstituents of cowpea grown on tropical soil. Heliyon 6, e05255. https://doi.org/10.1016/j.heliyon.2020.e05255

Piash, M.I., Iwabuchi, K., Itoh, T., 2022. Synthesizing biochar-based fertilizer with sustained phosphorus and potassium release: Co-pyrolysis of nutrient-rich chicken manure and Ca-bentonite. Sci. Total Environ. 822, 153509. https://doi.org/10.1016/j.scitotenv.2022.153509

R Core Team, 2020. R: A language and environment for statistical computing.

Raij, B. V., Quaggio, J.A., da Silva, N.M., 1986. Extraction of phosphorus, potassium, calcium, and magnesium from soils by an ion-exchange resin procedure. Commun. Soil Sci. Plant Anal. 17, 547–566. https://doi.org/10.1080/00103628609367733

Russel, V.L., 2021. emmeans: Estimated Marginal Means, aka Least-Squares Means.

Sakurada, R., Batista, L.M.A., Inoue, T.T., Muniz, A.S., Pagliar, P.H., 2016. Organomineral phosphate fertilizers: Agronomic efficiency and residual effect on initial corn development. Agron. J. 108, 2050–2059. https://doi.org/10.2134/agronj2015.0543

Shi, W., Ju, Y., Bian, R., Li, L., Joseph, S., Mitchell, D.R.G., Munroe, P., Taherymoosavi, S., Pan, G., 2020. Biochar bound urea boosts plant growth and reduces nitrogen leaching. Sci. Total Environ. 701, 134424. https://doi.org/10.1016/j.scitotenv.2019.134424

Silva, C.A., Morais, E.G., 2022. Fertilizante organomineral NPK de liberação controlada produzido a partir de compósito de rocha fosfatada-biocarvão. BR1020220127840.

Silva, F.C. (Ed.), 2009. Manual de análises químicas de solos, plantas e fertilizantes, 2. ed. ed. Embrapa Informação Tecnológica, Brasília.

Singh, B., Camps-Arbestain, M., Lehmann, J., CSIRO (Australia), 2017. Biochar: A Guide to Analytical Methods, Csiro publishing.

Suwanree, S., Knijnenburg, J.T.N., Kasemsiri, P., Kraithong, W., Chindaprasirt, P., Jetsrisuparb, K., 2022. Engineered biochar from sugarcane leaves with slow phosphorus

release kinetics. Biomass and Bioenergy 156, 106304. https://doi.org/10.1016/j.biombioe.2021.106304

Teixeira, P.C., Donagemma, G.K., Fontana, A., Teixeira, W.G. (Eds.), 2017. Manual de métodos de análise de solo, 3rd ed. Embrapa, Brasília.

Torabian, S., Farhangi-Abriz, S., Qin, R., Noulas, C., Sathuvalli, V., Charlton, B., Loka, D.A., 2021. Potassium: A Vital Macronutrient in Potato Production—A Review. Agronomy 11, 543. https://doi.org/10.3390/agronomy11030543

Trivedi, M.K., Dahryn Trivedi, A.B., 2015. Spectroscopic Characterization of Disodium Hydrogen Orthophosphate and Sodium Nitrate after Biofield Treatment. J. Chromatogr. Sep. Tech. 06. https://doi.org/10.4172/2157-7064.1000282

Tumbure, A., Bishop, P., Bretherton, M., Hedley, M., 2020. Co-Pyrolysis of Maize Stover and Igneous Phosphate Rock to Produce Potential Biochar-Based Phosphate Fertilizer with Improved Carbon Retention and Liming Value. ACS Sustain. Chem. Eng. 8, 4178–4184. https://doi.org/10.1021/acssuschemeng.9b06958

UNIDO, IFDC, 1998. Fertilizer manual, 1st ed. Kluwer Academic Publishers, Dordrecht.

Urrutia, O., Erro, J., Guardado, I., San Francisco, S., Mandado, M., Baigorri, R., Claude Yvin, J., Ma Garcia-Mina, J., 2014. Physico-chemical characterization of humic-metal-phosphate complexes and their potential application to the manufacture of new types of phosphate-based fertilizers. J. Plant Nutr. Soil Sci. 177, 128–136. https://doi.org/10.1002/jpln.201200651

Wang, T., Camps Arbestain, M., Hedley, M., Bishop, P., 2012. Chemical and bioassay characterisation of nitrogen availability in biochar produced from dairy manure and biosolids. Org. Geochem. 51, 45–54. https://doi.org/10.1016/j.orggeochem.2012.07.009

Wang, Y., Yin, R., Liu, R., 2014. Characterization of biochar from fast pyrolysis and its effect on chemical properties of the tea garden soil. J. Anal. Appl. Pyrolysis 110, 375–381. https://doi.org/10.1016/j.jaap.2014.10.006

Wei, T., Simko, V., 2017. R package “corrplot”: Visualization of a Correlation Matrix.

Wickham, H., Averick, M., Bryan, J., Chang, W., McGowan, L., François, R., Grolemund, G., Hayes, A., Henry, L., Hester, J., Kuhn, M., Pedersen, T., Miller, E., Bache, S., Müller, K., Ooms, J., Robinson, D., Seidel, D., Spinu, V., Takahashi, K., Vaughan, D., Wilke, C., Woo, K., Yutani, H., 2019. Welcome to the Tidyverse. J. Open Source Softw. 4, 1686. https://doi.org/10.21105/joss.01686

Withers, P.J.A., Rodrigues, M., Soltangheisi, A., de Carvalho, T.S., Guilherme, L.R.G., Benites, V. de M., Gatiboni, L.C., de Sousa, D.M.G., Nunes, R. de S., Rosolem, C.A.,

Andreote, F.D., Oliveira, A. de, Coutinho, E.L.M., Pavinato, P.S., 2018. Transitions to sustainable management of phosphorus in Brazilian agriculture. Sci. Rep. 8, 2537. https://doi.org/10.1038/s41598-018-20887-z

Supplementary material 1. ATR-FTIR spectra of biochars (A) and Araxá phosphate rock (B) used in the biochar-based fertilizers synthesis.

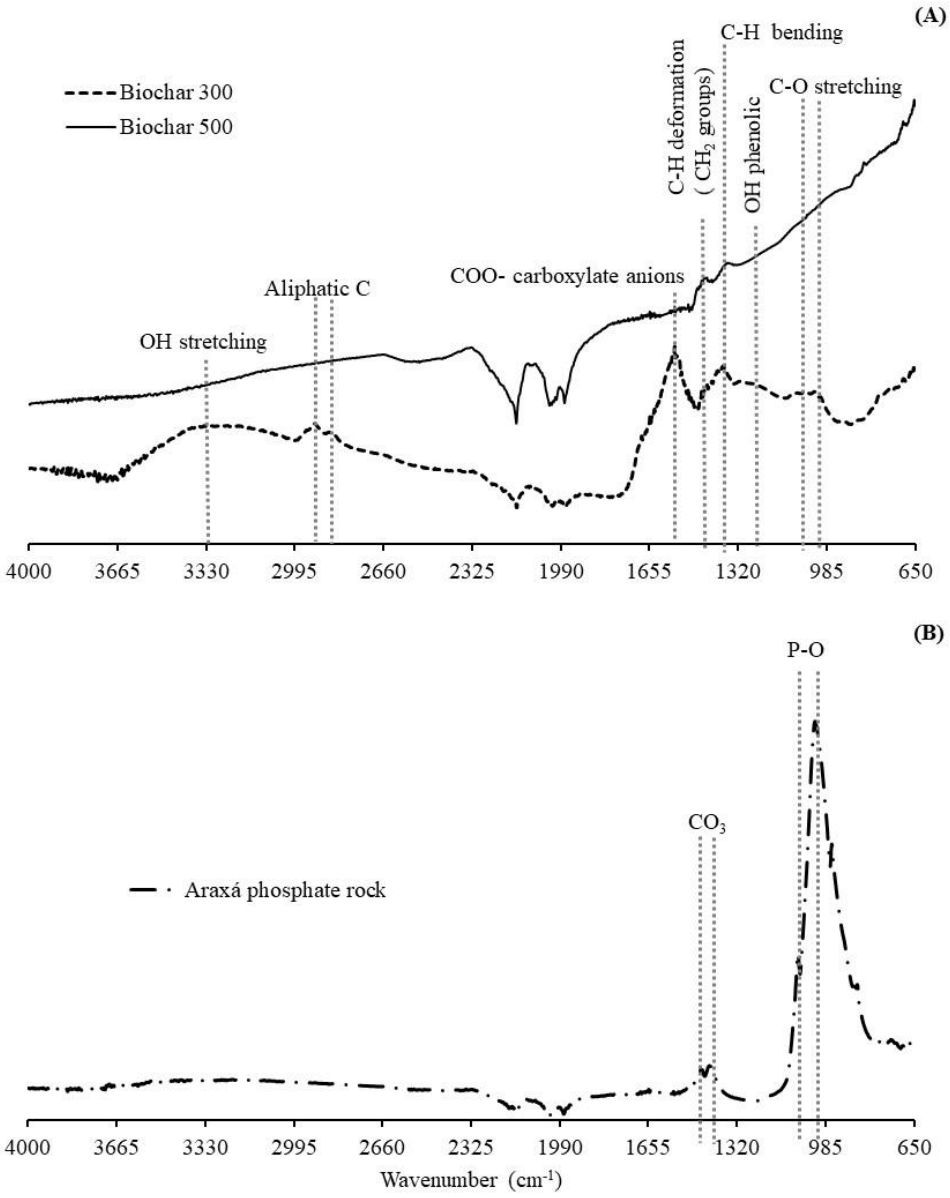

Supplementary material 2. Scheme of the mini-lysimeter package used for maize growth, and the process of vacuum used to collect and sampling soil solution.

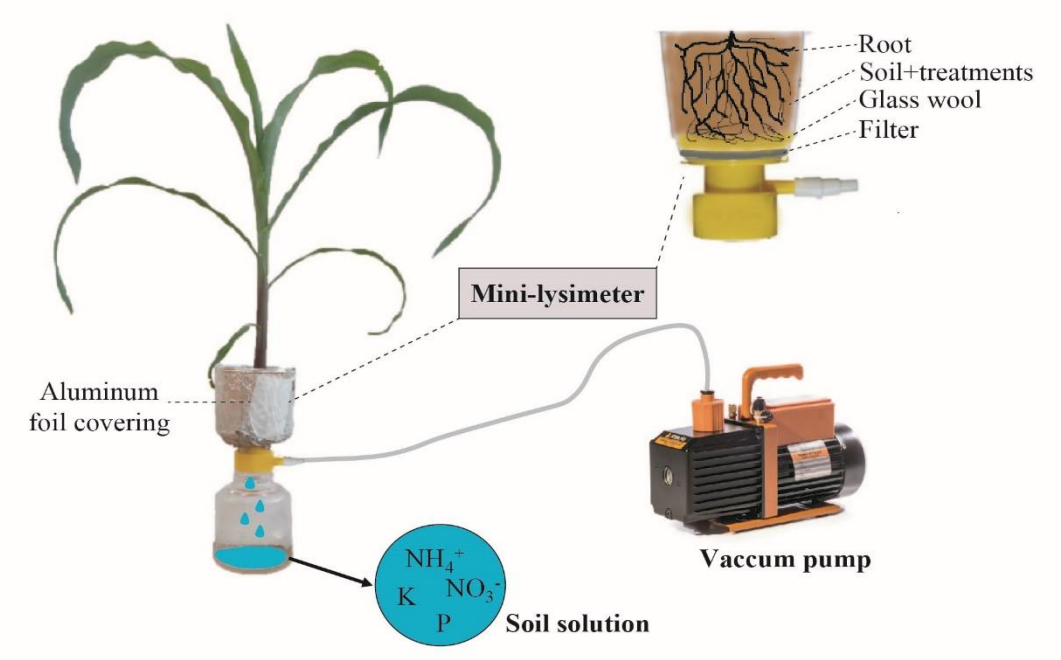

Supplementary material 3. Amounts of NPK forms and available applied by biochar-based fertilizers (BBFs) and mineral fertilizers for maize growing.

Treatments	Amount applied (mg kg^{-1})				
	N^{Total}	$N\text{-}NH_4^+$	$N\text{-}NO_3^-$	N-mineral	$N^{organic}$
BBF1	406	2	189	191	214
BBF2	384	3	215	218	165
BBF3	274	1	212	213	61
BBF4	324	0	291	291	33
+NPK	200*	100	100	200	0

Treatments	Amount applied (mg kg^{-1})				
	P^{Total}	P^{H_2O}	P^{CA}	P^{NAC+H_2O}	P^{FA}
BBF1	275	53	201	200	187
BBF2	202	154	172	200	160
BBF3	326	36	215	200	204
BBF4	271	144	175	200	152
+NPK	208	189	186	200	192

Treatments	Amount applied (mg kg^{-1})				
	K^{Total}	K^{H_2O}	K^{CA}	K^{NAC+H_2O}	K^{FA}
BBF1	140	105	106	133	110
BBF2	109	89	84	106	86
BBF3	185	146	146	184	125
BBF4	159	115	105	142	118
+NPK	150*	105	106	133	110

*: the amounts were divided, 20% of the amount applied at the planting fertilization and 80% applied after 13 days of maize planting. +NPK: NPK is added via ammonium nitrate, triple superphosphate, and potassium chloride. N^{Total}, $N\text{-}NH_4^+$, $N\text{-}NO_3^-$, $N^{mineral}$, and $N^{organic}$: respectively amount added in the soil of N total, ammonium, nitrate, mineral (ammonium+nitrate); P^{Total}, P^{H_2O}, P^{CA}, P^{NAC+H_2O}, and P^{FA}: respectively amount added in the soil of P total, soluble in water, in citric acid, in neutral ammonium citrate plus water and in formic acid; K^{Total}, K^{H_2O}, K^{CA}, K^{NAC+H_2O}, and K^{FA}: respectively amount added in the soil of K total, soluble in water, in citric acid, in neutral ammonium citrate plus water and in formic acid.

Supplementary material 4. pH of whole soil before and after maize cultivation; and N-pH in the soil solution according to biochar-based fertilizers at different times of planting (BBFs), NPK added via mineral fertilizers (+NPK) and maize cultivation without NPK application (-NPK).

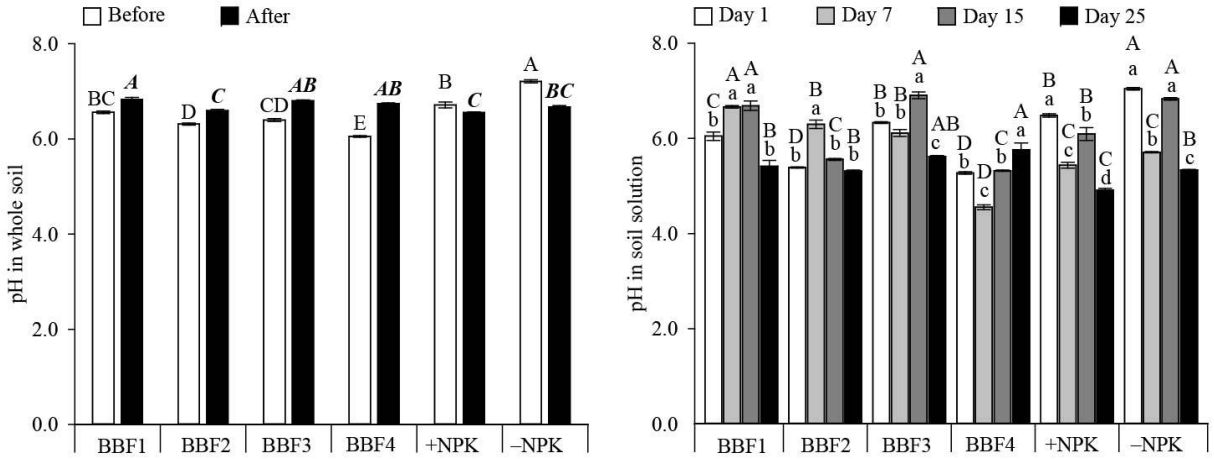

The bars with standard error followed by the same capital letter did not differ fertilizer treatment in each time evaluated (before or after cultivation or day 1, 7, 15, and 25) according to the Duncan test (p<0.05). The bars with standard error followed the same minuscule letter and did not differ the time evaluated in each fertilizer treatment tested according to the Duncan test (p<0.05).

Supplementary material 5. Coefficients of the kinetics of P release in water or citric acid of each fertilizer studied.

Kinetics of P release in water																		
Fertilizer	Linear			Elovich			Exponential			Power			Parabolic			Hyperbolic		
	R^2	Rmse	AIC	R^2	rmse	AIC	R^2	rmse	AIC	R^2	Rmse	AIC	R^2	rmse	AIC	R^2	rmse	AIC
BBF1	0.73	4.75	185	0.71	4.88	186	0.95	2.74	152	0.97	1.69	123	0.91	2.68	150	0.97	1.90	130
BBF2	0.40	12.36	242	0.88	5.42	193	0.93	8.39	219	0.92	4.48	181	0.63	9.69	227	0.95	8.00	216
BBF3	0.72	4.01	174	0.71	4.05	175	0.95	2.28	141	0.96	1.51	116	0.91	2.30	141	0.98	1.63	121
BBF4	0.39	6.45	203	0.93	2.15	137	0.86	14.72	252	0.95	1.89	129	0.63	5.08	189	0.88	14.61	252
TSP	0.27	7.49	212	0.91	2.63	149	0.87	20.19	271	0.91	2.65	150	0.48	6.35	202	0.87	20.15	271

Kinetics of P release in citric acid 2%																		
Fertilizer	Linear			Elovich			Exponential			Power			Parabolic			Hyperbolic		
	R^2	Rmse	AIC	R^2	rmse	AIC	R^2	rmse	AIC	R^2	Rmse	AIC	R^2	rmse	AIC	R^2	rmse	AIC
BBF1	0.59	24.35	283	0.77	18.08	265	0.96	8.85	222	0.94	9.19	224	0.81	16.41	259	0.99	5.89	198
BBF2	0.42	9.11	224	0.92	3.48	166	0.83	17.65	263	0.94	2.95	156	0.66	6.99	208	0.88	17.36	262
BBF3	0.58	25.47	285	0.80	17.52	263	0.96	9.07	223	0.95	8.68	221	0.81	17.28	262	0.99	5.74	196
BBF4	0.65	12.14	241	0.82	8.68	221	0.77	15.64	256	0.92	5.83	197	0.86	7.77	214	0.87	13.87	249
TSP	0.44	15.18	254	0.97	3.46	166	0.89	14.74	253	0.99	2.13	136	0.66	11.85	239	0.94	13.99	249

FINAL REMARKS

Different routes of synthesis of organomineral fertilizers containing N or P or K or Zn or fertilizers containing NPK promote properties in OMFs that can improve plant nutrition, as well as soil and solution nutrient availability. When humic acid (HA) was mixed with zinc sulfate, Zn was complexed in the organic matrix of organic radicals in HA. These molecules increase Zn contents in soil solution over the exclusive use of zinc sulfate to nourish crops; consequently, maize biomass production can be increased in the first crop. Subsequent cultivation of brachiaria after maize increased Zn availability in soil solution was also verified. In addition, during the cultivation of brachiaria in soil with a lower organic matter content, the application of HA+ Zinc sulfate promotes a higher buffering effect of the pH of the soil solution. Increased availability of Zn in the soil solution with a greater buffering of soil solution pH enhanced biomass production and Zn accumulation in brachiaria shoot (**Manuscript 1**).

Based on the interaction between HA and Zn, new routes of synthesis of organomineral fertilizers (OMFs) containing Zn complexed in the humic matrix were proposed and verified by infrared spectroscopy analysis. Consequently, the Zn from the Zn-OMFs was gradually released, and its diffusion in soil decreased, besides increasing the agronomic value of the Zn-OMFs over Zn sulfate. When Zn-OMFs are applied in Oxisoisl with contrasting soil organic matter levels and texture, there are different effects on the whole soil and its solution, considering the Zn-OMFs agronomic performance relies on soil type; these better agronomic performance of Zn-OMFs increased the biomass production of maize in the first cultivation, and the brachiaria biomass successively cultivated after maize (Zn residual effect). In addition, in Zn-OMFs, Zn-phosphate precipitates are less prone to be formed in soils; consequently, a positive secondary effect of Zn-OMFs on maize and brachiaria P nutrition was verified (**Manuscript 2**). The route of fertilizers synthesis was patented at INPI-Brazil (BR1020210079568).

Many positive effects are related to the forms and availability of nutrients contained in OMFs. Infrared analysis is used to qualitatively identify some of these forms in OMFs through a non-invasive mode. The quantitative determination of these forms and availability of nutrients are laboratory methodologies that are expensive, time-consuming, and generate laboratory residues. However, the partial least square regression based on infrared analysis is the approach for determining forms and pools of available nutrients found in OMFs in laboratory conditions. In compost-based OMFs, different mixtures of variable proportions of coffee husk, chicken manure and P sources (low-grade and soluble P sources) with different agronomic values, the

infrared analysis showed promise to quickly predict the forms and availability of nutrients evaluated in conventional lab methods by partial least square regression models based on infrared spectroscopy. Besides, amongst the routes used in OMFs synthesis, composting of monoammonium phosphate, coffee husk, and chicken manure is the most effective in generating with OMFs of high agronomic efficiency (**Manuscript 3**).

When OMFs are synthesized using composting, and piles of mixtures of monoammonium phosphate, coffee husk and chicken manure, the forms and nutrients readily available in OMFs in water are reduced, mainly for the kinetics of P release. In the OMFs, there is a lower release of P in water compared to the mineral soluble P source (monoammonium phosphate), as was shown by different methods of the kinetics of P release. When OMFs were added to Oxisols, with contrasting soil organic matter levels and texture, a reduction of initial P content in soil solution was noted, and an increase in the P available in the whole soil was verified in a soil type-dependent way. Thus, higher production of maize biomass improved NPK nutrition, and a higher residual effect of P was observed. In addition, OMFs have a different pattern in the release of NPK due to mineralization of N and P (OMF organic matrix) and leaching of K contained in OMFs, in addition to N and P mineralized and released by the SOM (**Manuscript 4**).

Compared to composting, pyrolysis is a new route that can be used faster in synthesizing OMFs. The mineral sources and feedstock can be treated before or after biochar production. When post-harvest coffee residue was mixed with low-grade phosphate sources, OMFs had a lower high agronomic value than TSP. However, when the acidulation process is used correctly, there is an increase in OMF agronomic value. Biochar-based fertilizers (BBFs), when synthesized through acidulation of phosphate rock and mixing of biochar with post-harvest coffee residue, is the suitable route t produce NPK fertilizers with gradual release of P. In addition, when Mg is added during the fertilizer synthesis process, P release becomes even slower. The agronomic value of BBFs produced and added to Oxisols to evaluate maize h grown before brachiaria is highly dependent on the soluble P-fertilizer index contents, such as P in neutral ammonium citrate plus water (NAC+H2O), citric acid or formic acid, being NAC+H2O the best P-fertilizer solubility index. Among the acids during phosphate rock acidulation and BBFs synthesis, nitric acid was the most effective in solubilizing apatite; however, when it is used before pyrolysis, a high amount of N is volatilized (**Manuscript 5**).

Using a new synthesis route where N losses are decreased and standardizing the amount of P applied via BBFs by its solubility in NAC+H2O are suitable for improving the agronomic performance of BBFs in Oxisol. The new BBFs increased the P use efficiency for maize

cultivated in the Sand Loam Oxisol (YO). The improved P nutrition increased maize biomass production. An increase in P use efficiency is related to different mechanisms and BBFs properties, including P bound to the OMF organic matrix and the gradual release of P by the organomineral fertilizers. Gradual release of P and the high P levels available in the long term was observed by the reduction of the P amounts released in the kinetics study in which water was used to leachate sand-fertilizer mixtures. However, when citric acid was the extractant solution, the BBFs showed a higher P release over water leachates, though P was gradually released. The BBFs initially reduced P levels in soil solution; however, in plant stages of high P demand, P was released and capable of attending to and efficiently nourishing maize plants. In addition, BBFs increased the initial availability of P in whole soil, besides having a higher residual effect for brachiaria plants grown after maize cultivation (**Manuscript 6**). Thus, different routes of the OMF produce OMFs with different properties, nutrient pools, rate of nutrient release and infrared spectral signatures, and these factors combined determine the OMFs effects on nutrient availability in whole soil and its solution, consequently affecting the biomass production, nutrient uptake and residual effects positively. The route of fertilizers synthesis was patented at INPI-Brazil (BR1020220127840).

Thus, the present thesis shows that different synthesis routes can produce new and efficient OMFs, characterized by the gradual release of nutrients and higher agronomic values that efficiently meet the supply of N, P, K and Zn to crops. In addition, a higher residual effect of P and Zn from OMFs was observed, and these effects are highly dependent on OMFs properties and synthesis routes. However, further studies must be carried out to determine the agronomic value of these OMFs synthesized under field conditions for different soil types and crops to validate these promising new technologies. In addition, due to the organic matrix present in OMFs, they may have a biostimulant role on plants, so this effect must be better elucidated in future studies.